

**$^{210}\text{POLONIUM AND } ^{210}\text{LEAD RADIONUCIDLES IN THE DELAWARE AND
CHESAPEAKE ESTUARINE AND COASTAL REGIONS}$**

by

David W. Marsan

A thesis submitted to the Faculty of the University of Delaware in partial fulfillment
of the requirements for the degree of Master of Science in Marine Studies

Summer 2013

Copyright 2013 David W. Marsan
All Rights Reserved

**²¹⁰POLONIUM AND ²¹⁰LEAD RADIONUCIDLES IN THE DELAWARE AND
CHESAPEAKE ESTUARINE AND COASTAL REGIONS**

by

David Marsan

Approved:

Thomas M. Church, Ph.D.
Professor in charge of thesis on behalf of the Advisory Committee

Approved:

Mark A. Moline, Ph.D.
Director of the School of Marine Science and Policy

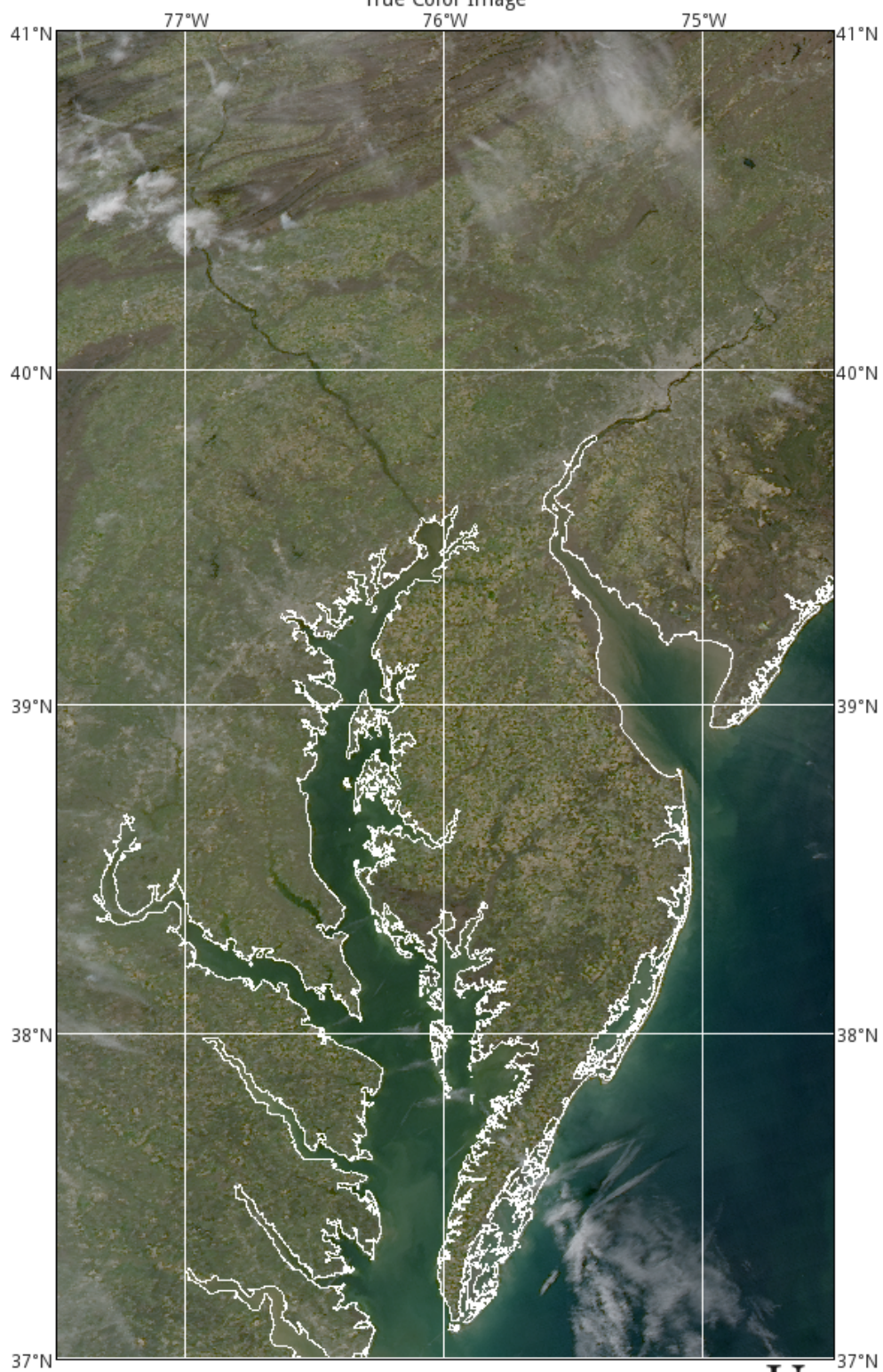
Approved:

Nancy M. Targett, Ph.D.
Dean of the College of Earth, Ocean, and Environment

Approved:

James G. Richards, Ph.D.
Vice Provost for Graduate and Professional Education

The Delmarva Region taken from the MODIS-AQUA satellite.
aqua.2012094.0403.173715.D.L3.hmodis.DEL.v09.250mTue Apr 3 17:37:15 2012
True Color Image



true_color
Delaware Area Map (HMODIS-AQUA-PM)
Version 9 (APS v4.2.5)

University of Delaware
College of Earth, Ocean, and Environment
www.ceoe.udel.edu



Acknowledgements

A M.S. thesis is an important stepping-stone on the way to become an accomplished, independent and productive researcher. The knowledge developed between the student and the main advisor during the M.S. are essential. That is why I am especially indebted to Thomas Church, without whose inalterable trust this work would not have emerged. Tom, you also always provided great support, feedback, and for introducing me to the field of radiochemistry, thank you! I would like to thank the members of my thesis committee for valuable discussion during the presentations of my work and especially for reviewing this thesis. I would like to acknowledge the great support, training and collaborative atmosphere provided by the Marine Studies school at the University of Delaware.

A special thanks to my lab mates and those who have aided this thesis: to Sylvain, thank you for the many revisions and help guiding me to be a better researcher; Ella for her assistance processing the hundreds of samples; to Nuria for helping in the early days of my research into radiochemistry; and to Maria for helping to guide me when I first joined the lab as an undergraduate. Funding was provided by the National Science Foundation Bridge to the Doctorate program. Finally, I couldn't have completed this thesis without the support and encouragements my family, my friends, and my closest colleagues provided all along, thank you so very much!

TABLE OF CONTENTS

| | |
|-----------------------|-------|
| LIST OF TABLES | viii |
| LIST OF FIGURES | x |
| PREFACE..... | xv |
| ABSTRACT..... | xviii |

Chapter

| | | |
|-------|------------------------------------------------------------------------------------------------------------------------------------------|----|
| 1 | SCAVENGING METHOD COMPARISON ASSOCIATED WITH THE ANALYSIS OF ^{210}Po AND ^{210}Pb IN ESTUARINE AND COASTAL WATER..... | 1 |
| 1.1 | Abstract | 2 |
| 1.2 | Introduction..... | 3 |
| 1.3 | Methods..... | 4 |
| 1.3.1 | Sample Collection and General Procedure | 4 |
| 1.3.2 | $\text{Fe}(\text{OH})_3$ Extraction Method (Sarin, et al., 1992)..... | 5 |
| 1.3.3 | Co-APDC Co-precipitation Method (Fleer and Bacon, 1984)..... | 6 |
| 1.3.4 | MnO_2 Scavenging Method (Bojanowski et al., 1983)..... | 6 |
| 1.3.5 | Plating Process..... | 6 |
| 1.3.6 | Processing/storage time..... | 7 |
| 1.4 | Results | 7 |
| 1.4.1 | Preferential Scavenging of ^{210}Po and ^{210}Pb | 8 |
| 1.4.2 | Comparison of Extraction Efficiency between $\text{Fe}(\text{OH})_3$ and Co-APDC..... | 8 |
| 1.4.3 | Comparison of Final Activity and Activity Ratios Between $\text{Fe}(\text{OH})_3$ and Co-APDC..... | 9 |
| 1.5 | Discussion | 10 |
| 1.5.1 | Po Speciation..... | 10 |
| 1.5.2 | Influence of Chemical Environment on Po and Pb Extraction Efficiencies and Activities..... | 12 |
| 1.5.3 | Recommendations..... | 15 |
| 1.6 | Conclusion | 16 |

| | |
|-----------------|----|
| REFERENCES..... | 18 |
| TABLES..... | 20 |
| FIGURES..... | 23 |

| | |
|------------------------------------------------------------------------------------------------------------------------------------------|----|
| 2 ESTUARINE AND COASTAL BIOGEOCHEMISTRY OF THE NATURAL RADIONUCILDES 210PO AND 210PB IN THE DELAWARE AND CHESAPEAKE ESTUARIES..... | 32 |
|------------------------------------------------------------------------------------------------------------------------------------------|----|

| | |
|--------------------------------|----|
| 2.1 Abstract | 33 |
| 2.2 Introduction | 34 |
| 2.3 Material and Methods | 36 |
| 2.4 Results | 38 |

| | |
|------------------------------------------------------|----|
| 2.4.1 Delaware Estuary | 38 |
| 2.4.2 Lower Delaware Salt Marsh (Canary Creek) | 39 |
| 2.4.3 Chesapeake Bay | 40 |

| | |
|----------------------|----|
| 2.5 Discussion | 41 |
|----------------------|----|

| | |
|--------------------------------------------------------------------------------------------------------------------------------|----|
| 2.5.1 Identification of Processes Controlling ²¹⁰ Po and ²¹⁰ Pb cycle in the Delaware Estuary..... | 42 |
| 2.5.2 Identification of Processes Controlling ²¹⁰ Po and ²¹⁰ Pb in the Lower Delaware Salt Marsh..... | 42 |
| 2.5.3 Identification of Processes Controlling ²¹⁰ Po and ²¹⁰ Pb in the Chesapeake Bay..... | 43 |
| 2.5.4 Residence Times..... | 45 |

| | |
|-----------------------|----|
| 2.6 Conclusions | 48 |
|-----------------------|----|

| | |
|-----------------|----|
| REFERENCES..... | 50 |
| TABLES..... | 53 |
| FIGURES..... | 56 |

| | |
|------------------------------------------------------------------------------------------------------------------------------------------------|----|
| 3 TWO-LAYER TIME VARIABLE MODEL OF THE DELAWARE AND CHESAPEAKEESTUARY TO GAUGE THE FATE OF TRACE METALS USING NATURAL RADIONUCLIDES..... | 61 |
|------------------------------------------------------------------------------------------------------------------------------------------------|----|

| | |
|---------------------------------------------|----|
| 3.1 Abstract | 62 |
| 3.2 Introduction | 63 |
| 3.3 Data Collection and Previous Work | 64 |
| 3.4 Description of Modeling Framework | 65 |
| 3.5 Model Parameters | 69 |
| 3.6 Conclusion | 72 |

| | |
|-----------------|----|
| REFERENCES..... | 74 |
| TABLES..... | 75 |
| FIGURES..... | 79 |

| | |
|------------------|----|
| CONCLUSIONS..... | 82 |
|------------------|----|

Appendix

| | |
|-------------------------------|----|
| A CHAPTER 1 | 84 |
| B CHAPTER 2 | 86 |
| C GRAZ, AUSTRIA RESULTS | 91 |

LIST OF TABLES

| | | |
|-------------------|-----------------------------------------------------------------------------------------------------------------------------------------------------------------------------------------------------------------------------------------------------------------------------------------------------------------------------------------------------------------------|----|
| Table 1.1: | The dissolved ^{210}Po and ^{210}Pb activities (dpm 100L ⁻¹) for the Delaware Estuary (DB and DBSMS) and Chesapeake Bay (CB) with associated errors for the Fe(OH) ₃ and Co-APDC scavenging methods..... | 20 |
| Table 1.2: | The dissolved ^{210}Po and ^{210}Pb activities (dpm 100L ⁻¹) for Canary Creek salt marsh (RI and CC) and the North Atlantic offshore station with associated errors for the Fe(OH) ₃ and Co-APDC scavenging methods..... | 21 |
| Table 1.3: | Scavenging efficiencies of ^{209}Po and associated errors for Fe(OH) ₃ , Co-APDC and Mn in the Delaware Bay(DB), Chesapeake Bay(CB), Intertidal salt marsh(DSM) and North Atlantic (NA). Note that Co-APDC consistently has higher ^{209}Po scavenging efficiency but is also associated with a larger relative standard deviation. | 22 |
| Table 2.1: | The dissolved and particulate ^{210}Po and ^{210}Pb activities (dpm 100L ⁻¹) for Delaware Estuary (DB and DBSMS) and Chesapeake Bay (CB)..... | 53 |
| Table 2.2: | The dissolved ^{210}Po and ^{210}Pb activities (dpm 100L ⁻¹) for Roosevelt Inlet (RI) and Canary Creek (CC) lower Delaware Bay salt marsh..... | 54 |
| Table 2.3: | Box model units and rates for the Delaware and Chesapeake Bay estuaries..... | 55 |
| Table 3.1: | Two-Layer Model Terminology..... | 75 |
| Table 3.2: | Magnitudes and Parameters used to solve for the partition coefficient (K_{p2}) in the Delaware and Chesapeake estuaries..... | 76 |
| Table 3.3: | Summary of chemical and physical parameters used in analysis of ^{210}Po and ^{210}Pb in the Delaware and Chesapeake estuaries..... | 77 |
| Table 3.4: | Partition Coefficients and residual Half-lives (d) of trace elements estimated in the Delaware and Chesapeake estuaries by the two-layer model. This not only shows the variation between estuarine regions (upper, mid, lower) but how radionuclides can be used as proxies to determine their residence times..... | 78 |

| | | |
|------------------|------------------------------------------------------------------------------------------------------------------------------------------------------------------------------------------------------------|-----|
| Table A1: | ^{210}Po and ^{210}Pb dissolved activities using the $\text{Fe}(\text{OH})_3$, Co-APDC scavenging methods collected during six estuarine and coastal research cruises..... | 84 |
| Table A2: | ^{210}Po and ^{210}Pb dissolved activities using the $\text{Fe}(\text{OH})_3$, Co-APDC scavenging methods collected during six estuarine and coastal research cruises..... | 85 |
| Table C1: | Dolt-3 (Dogfish Liver) and Dorm-2 (Dogfish Muscle) were used at reference standards throughout the experiments. | 105 |
| Table C2: | Total trace metal analysis for <i>Geukensia demissa</i> , and <i>Mytilus edulis</i> . Elements with “*” mean that sample concentration was outside of calibration curve range and cannot be confirmed..... | 106 |
| Table C3: | Total trace metal analysis for <i>Spartina alterniflora</i> and core samples. | 107 |
| Table C4: | Total trace metal analysis for the SML (mg/kg)..... | 108 |
| Table C5: | Flow Injection results compared with expected concentrations in extraction samples. | 109 |
| Table C6: | Ionosphere 5C species and sum results from extracts..... | 110 |
| Table C7: | Results from the anion exchange column Dionex As14..... | 111 |

LIST OF FIGURES

| | | |
|--------------------|-----------------------------------------------------------------------------------------------------------------------------------------------------------------------------------------------------------------------------------------------------------------------------------------------------------------------------------------------------------------------------------------------------------------------------------------------------------------------------------------------------------------------------------------------------------------|----|
| Figure 1.1: | Samples for this study were collected at each station as numbered with corresponding data in Tables 1 & 2. Samples were collected as follows: Delaware estuary 2012 April 1-3, Delaware salt marsh two locations over a 12hr tidal cycle 2012 June 1, Chesapeake estuary 2012 August 20-25 and single North Atlantic site sampled three times (Aug. 2011, Nov. 2011 and Aug. 2012). | 23 |
| Figure 1.2: | Protocol for ^{210}Po and ^{210}Pb activity measurement in dissolved seawater samples with different scavenging method up to the first plating..... | 24 |
| Figure 1.3: | The activities (dpm/100L) of $\text{Fe}(\text{OH})_3$ vs Co-APDC scavenging methods for ^{210}Po with a 1:1 line A) Delaware Bay, B) Chesapeake Bay; C) Intertidal Marsh; D) Offshore. Note that methods agree well in panels A and B but less so in C and D. Offshore samples are unique because Co-APDC reports higher ^{210}Po final activities than $\text{Fe}(\text{OH})_3$ | 25 |
| Figure 1.4: | The activities (dpm/100L) of $\text{Fe}(\text{OH})_3$ vs Co-APDC scavenging methods for ^{210}Pb with a 1:1 line A) Delaware Bay; B) Chesapeake Bay; C) Intertidal Marsh; D) Offshore. The data shows ^{210}Pb results are comparable through most regions, but differences occur offshore..... | 26 |
| Figure 1.5: | The activities (dpm/100L) of $\text{Fe}(\text{OH})_3$ and Co-APDC vs. MnO_2 scavenging methods for ^{210}Po and ^{210}Pb with a 1:1 line for only offshore samples. The data shows MnO_2 agrees more with $\text{Fe}(\text{OH})_3$ than Co-APDC for both ^{210}Po and ^{210}Pb | 27 |
| Figure 1.6: | Histogram of ^{210}Po and ^{210}Pb dissolved activity in the Delaware estuary compared between the $\text{Fe}(\text{OH})_3$ and Co-APDC scavenging methods. Sample station numbers are in order of those found in Table 1. The \star denotes the turbidity maximum and likely highest concentration of humic acid compounds. The \vee denotes the two locations where a phytoplankton bloom was observed. The ^{210}Pb results show that the methods agree within the calculated error through the entire Delaware estuary. | 28 |
| Figure 1.7: | Histogram of ^{210}Po and ^{210}Pb dissolved activity in the Canary Creek salt marsh compared between the $\text{Fe}(\text{OH})_3$ and Co-APDC scavenging methods. Sample station numbers are in order of those found in Table 1. The u denotes lowest observed dissolved oxygen and highest suspended particulate concentration..... | 29 |

Figure 1.8: Histogram of ^{210}Po and ^{210}Pb dissolved activity in the upper Chesapeake Bay compared between the $\text{Fe}(\text{OH})_3$ and Co-APDC scavenging methods. Sample station numbers are in order of those found in Table 2. The \oplus denotes lowest observed dissolved oxygen concentrations. The ^{210}Pb scavenging by each method shows agreement within the calculated error throughout the Chesapeake Bay.....30

Figure 1.9: Histogram of ^{210}Po and ^{210}Pb dissolved activity at the North Atlantic offshore site compared between the $\text{Fe}(\text{OH})_3$ and Co-APDC scavenging methods. Sample station numbers are in order of those found in Table 2. The \oplus denotes lowest observed dissolved oxygen concentrations. The \odot denotes surface waters at 1 to 15 meters.....31

Figure 2.1: Samples for this study were collected at each dot. Samples were collected as follows: Delaware estuary 2012 April 1-3, Delaware salt marsh two locations over a 12hr tidal cycle 2012 June 1, and Chesapeake estuary 2012 August 20-25.....56

Figure 2.2: Dissolved and particulate ^{210}Po and ^{210}Pb activities ($\text{dpm } 100\text{L}^{-1}$) presented as an ODV transect plot in the Delaware estuary.....57

Figure 2.3: Delaware Bay lower salt marsh dissolved ^{210}Po and ^{210}Pb activities ($\text{dpm } 100\text{L}^{-1}$) in Roosevelt inlet and Canary Creek over a 12-hr tidal cycle.....58

Figure 2.4: Dissolved and particulate ^{210}Po and ^{210}Pb activities ($\text{dpm } 100\text{L}^{-1}$) presented as an ODV transect plot in the upper Chesapeake estuary.....59

Figure 2.5: Box model depiction and symbol notation for dissolved ^{210}Po in the Delaware and upper Chesapeake estuary. The Delaware estuary utilized a regional (3 box-model) estuary model, while the Chesapeake used a single box model for the entire upper estuary.....60

Figure 3.1: Altered two-layer model for a river or estuarine system. Panel 1 depicts the processes affecting a chemical in a single region two-layer region. The next panel (2) combines n^{th} number of two-layer regions to simulate the processes moving seaward.....79

Figure 3.2: Chemical concentration on particulate sediment and on particulate in the water column (r_2/r_1) for the Delaware estuary. If r_2/r_1 is

| | | |
|--------------------|-------------------------------------------------------------------------------------------------------------------------------------------------------------------------------------------------------------------------------------------------------------------------------------------------------------------------------------------------------------------------------------------------------------------------------------------------------------------|-----|
| | greater than 1 more partitioning is occurring in the water column rather than the sediment. | 80 |
| Figure 3.3: | Chemical concentration on particulate sediment and on particulate in the water column (r_2/r_1) for the Chesapeake estuary. It is important to note that the ^{210}Po and ^{210}Pb data only includes the upper Chesapeake while the other elements include the entire Bay area. If r_2/r_1 is greater than 1 more partitioning is occurring in the water column rather than the sediment, while the opposite is true if less than 1..... | 81 |
| Figure B1: | Chemical parameters presented as ODV transect plot in the upper Chesapeake estuary..... | 86 |
| Figure B2: | Nutrient concentrations presented as ODV transect plot in the upper Chesapeake estuary..... | 87 |
| Figure B3: | Particulate concentrations presented as ODV transect plot in the upper Chesapeake estuary..... | 88 |
| Figure B4: | Chemical parameters presented as ODV transect plot in the Delaware estuary..... | 89 |
| Figure B5: | Nutrient concentrations presented as ODV transect plot in the Delaware estuary..... | 90 |
| Figure C1: | Canary Creek Delaware intertidal marsh sampling area. Samples were collected at two sites (Roosevelt Inlet and Canary Creek) over a 12 hour tidal cycle..... | 112 |
| Figure C2: | Depth distribution of trace metal content measured from the Canary creek core sample. Trace metal concentrations are normalized to Al to account for the accumulation affected by the variation in the mobility of different trace metals..... | 113 |
| Figure C3: | Depth profiles of elements from various Delaware Salt marshes... | 114 |
| Figure C4: | Depth profiles of elements from sediment cores from two Delaware Salt Marshes. | 115 |
| Figure C5: | Extraction of As and Se compounds from freeze dried sea surface microlayer..... | 116 |
| Figure C6: | Full time range chromatogram for Arsenic Dry MeOH Direct (a) and Dry MeOH with 10% H ₂ O ₂ (b) added..... | 117 |

| | | |
|--------------------|----------------------------------------------------------------------------------------------------------------------------------------------------------|-----|
| Figure C7: | Full time range chromatogram for Arsenic Wet H ₂ O Direct (a) and Wet H ₂ O with 10% H ₂ O ₂ (b) added..... | 118 |
| Figure C8: | Full Time range chromatogram for Arsenic Wet MeOH Direct (a) and Wet MeOH with 10% H ₂ O ₂ (b) added..... | 119 |
| Figure C9: | Full time range chromatogram for Arsenic Dry MeOH evaporate direct (a) and Dry MeOH evaporate with 10% H ₂ O ₂ (b) added..... | 120 |
| Figure C10: | Full time range chromatogram for Arsenic Residue 0.1M TFA direct (a) and Residue 0.1M TFA with 10% H ₂ O ₂ (b) added..... | 121 |
| Figure C11: | Full time range chromatogram for Arsenic Dry MeOH Direct (a) and Dry MeOH with 10% H ₂ O ₂ (b) added..... | 122 |
| Figure C12: | Full time range chromatogram for Arsenic Wet H ₂ O Direct (a) and Wet H ₂ O with 10% H ₂ O ₂ (b) added..... | 123 |
| Figure C13: | Full Time range chromatogram for Arsenic Wet MeOH Direct (a) and Wet MeOH with 10% H ₂ O ₂ (b) added. | 124 |
| Figure C14: | Full time range chromatogram for Arsenic Dry MeOH evaporate direct (a) and Dry MeOH evaporate with 10% H ₂ O ₂ (b) added..... | 125 |
| Figure C15: | Full time range chromatogram for Arsenic Residue 0.1M TFA direct (a) and Residue 0.1M TFA with 10% H ₂ O ₂ (b) added..... | 126 |
| Figure C16: | Full time range chromatogram for Selenium Dry MeOH Direct (a) and Dry MeOH with 10% H ₂ O ₂ (b) added. | 127 |
| Figure C17: | Full time range chromatogram for Selenium Wet H ₂ O Direct (a) and Wet H ₂ O with 10% H ₂ O ₂ (b) added..... | 128 |
| Figure C18: | Full Time range chromatogram for Selenium Wet MeOH Direct (a) and Wet MeOH with 10% H ₂ O ₂ (b) added. | 129 |
| Figure C19: | Full time range chromatogram for Selenium Dry MeOH evaporate direct (a) and Dry MeOH evaporate with 10% H ₂ O ₂ (b) added..... | 130 |
| Figure C20: | Full time range chromatogram for Selenium Residue 0.1M TFA direct (a) and Residue 0.1M TFA with 10% H ₂ O ₂ (b) added..... | 131 |
| Figure C21: | Full time range chromatogram for Selenium Dry MeOH Direct (a) and Dry MeOH with 10% H ₂ O ₂ (b) added..... | 132 |

Figure C22: Full time range chromatogram for Selenium Wet H2O Direct (a) and Wet H2O with 10% H2O2 (b) added.....133

Figure C23: Full Time range chromatogram for Selenium Wet MeOH Direct (a) and Wet MeOH with 10% H2O2 (b) added.....134

Figure C24: Full time range chromatogram for Selenium Dry MeOH evaporate direct (a) and Dry MeOH evaporate with 10% H2O2 (b) added.....135

Figure C25: Full time range chromatogram for Selenium Residue 0.1M TFA direct (a) and Residue 0.1M TFA with 10% H2O2 (b) added.....136

PREFACE

1.1 Context of the study

The oceans continuously receive inputs of virtually all chemical elements from a number of sources such as rivers, rain, dry deposition, hydrothermal vents, submarine groundwater discharge and marine sediments. A major source, and focus of this thesis, is that of estuaries. Elements and chemical species have been accumulating over time in seawater to high concentrations (e.g. sodium), while others are found only in trace amounts. This is due to differences in their biogeochemical behavior, specifically the degree of their particle reactivity, a property through which elements are prone to uptake by particles (both biogenic and detrital). These particles are continuously sinking or being resuspended through the estuarine and coastal water column, thus removing the associated elements to sediments or transporting them to coastal oceans. The scavenging behavior of elements is readily observed from their vertical distribution in the oceans, but is much more difficult in shallow and dynamic estuarine systems. To understand the uptake and removal process by particles, it is necessary to follow or “trace” these estuarine constituents.

Trace elements and their isotopes play a useful role in tracing processes in the marine environment. The use of naturally occurring radioactive tracers in the estuarine and ocean environment indirectly allow on to estimate particle fluxes. Radionuclides are produced and decayed at well-known fixed rates; this allows for measurement of time-dependent processes. If the radionuclide is also biogeochemically reactive, it is prone to associate with and/or adsorb onto those particles, which can then be tracked throughout the water column. A combination of these two characteristics (lithogenic vs. biogenic) is needed in order for these tracers to be a well-resolved tool for measuring biogeochemical fluxes. For example, surface and upper ocean studies utilize the short-lived particle reactive isotopes of the ^{238}U decay series such as ^{234}Th (Coale and Bruland, 1985).

Naturally occurring radon daughter radionuclides in the U-Th decay series are introduced to estuaries along with stable trace elements via the atmosphere

and freshwater sources. However, these series include elements that have very different aquatic chemical properties and half-lives of decay. As such, different parent-daughter pairs can become distributed between dissolved and particulate phases. Nuclide disequilibria is imposed along the estuarine chemical gradient according to rates of scavenging versus radioactive decay of a soluble parent and the particle reactive nature of daughter nuclide, as demonstrated in estuaries and salt marshes (Church and Sarin, 1987).

Two such naturally occurring radionuclides ^{210}Po ($t_{1/2} = 138.4$ d) and ^{210}Pb ($t_{1/2} = 22.3$ y) have been widely used to study dissolved and particle fluxes throughout ocean and estuarine marine environments (Bacon et al., 1976; Nozaki, et al. 1976; Thomson and Turekian, 1976; Cochran and Masque, 2003). In seawater, both nuclides are particle-reactive, while ^{210}Po is also bioactive and concentrates within organic tissues (Stewart and Fisher, 2003a,b; Stewart et al. 2005). Due to such different particle-reactive characteristics, the nuclide disequilibrium produced is able to define scavenging and particle fluxes, including organic matter.

In estuarine and salt marsh waters, the main source of ^{210}Pb and ^{210}Po includes the following; atmospheric deposition, rock leaching, groundwater discharge, and river flow. Soon after introduction to estuarine watersheds, the ^{222}Rn daughter products, namely ^{210}Pb and ^{210}Po , get quickly associated with suspended particles. The radionuclide ^{210}Pb has a short residence time in the atmosphere ranging from a few days to a couple weeks, after deposition on land or ocean surface by dry and wet deposition respectively (Moore et al., 1974). In the estuarine marine system ^{210}Pb is produced not only by atmospheric deposition but also *in situ* by decay of ^{226}Ra found in sediment pore waters (Broecker et al., 1967). *In situ* ^{210}Pb production (<0.1 dpm/100L) in shallow coastal waters is almost negligible compared to the atmospheric flux, while the opposite is true in the open ocean (Cochran, 1992). In estuarine and coastal waters the main source of ^{210}Po is from the *in situ* decay of ^{210}Pb , which can be found in concentrations between 10-20 dpm per 100L (Lambert et al., 1982). From the measurement of

^{210}Po and ^{210}Pb disequilibria in the estuarine environment the nuclides can be used as proxies for estimating trace element residence times.

A simple one-box model of the material balance equation for a daughter nuclide produced continuously by the radioactive decay of its parent can be used to produce scavenging residence times. Although simple box models provide useful information on the scavenging residence times of elements, more detailed models of increasing complexity are needed to define specific processes associated with particle dynamics of the estuarine system. As such, this thesis will enhance the understanding of the estuarine biogeochemical cycles for ^{210}Po and ^{210}Pb , which is intimately linked to the understanding of the cycling of particle-reactive radionuclides.

ABSTRACT

One of the primary objectives of this thesis is to present an integrated study of the ^{210}Pb and ^{210}Po radioactive tracers, and assess their use as tracers for particle and trace element export from different estuarine and coastal environments. In order to achieve this main objective, the thesis was split into three sections, each enhancing the understanding of the natural radionuclides ^{210}Pb and ^{210}Po in the estuarine and coastal system.

Chapter 1 is dedicated to testing the sampling and analytical methods of ^{210}Po and ^{210}Pb extraction from estuarine and coastal waters, specifically comparing the two most widely used scavenging methods, $\text{Fe}(\text{OH})_3$ and Co-APDC. The chapter describes experiments conducted on about 100 samples collected from the Delaware estuary, Chesapeake estuary, Delaware intertidal marsh and an offshore continental slope site. Data in the chapter clarifies the accuracy and reliability of each method and includes suggestions to enhance them. Other details include results of calculations, error propagation, spike calibration, plating efficiency and the MnO_2 scavenging method.

Chapter 2 presents a synthesis of the estuarine and coastal biogeochemistry of ^{210}Po and ^{210}Pb in the Delaware and Chesapeake estuaries. A single box model is presented using steady state equations to determine residence times of the radionuclides. This chapter presents five highlights: 1) How ^{210}Pb and ^{210}Po dissolved and particulate data can reveal key biogeochemical processes and rates in estuaries; 2) Are regional differences in estuaries dominated by a single or compilation of biogeochemical process; 3) Do sub-oxic bottom waters affect the distribution of ^{210}Po and ^{210}Pb ; 4) Can disequilibria between parent (^{210}Pb) and grand-daughter (^{210}Po) be used to identify and quantify principle processes; 5) Will a simple mass balance model result in reliable net scavenging residence times for the Delaware and Chesapeake estuaries.

Chapter 3 will advance the simple single box-model from chapter 2 to a more complex two-layer model. The model will include evaluations of the fate of not only ^{210}Po and ^{210}Pb in the Delaware and Chesapeake estuaries but also the

trace elements Fe, Cu, Cd, Ni, Zn, Pb, Cr, Co and Mn. Residences times, presented as half-lives along with rates and partition coefficients will be identified for the water column including at the sediment water interface.

The thesis will revisit the major conclusions obtained from the work presented along with suggestions for future work. Appendix sections include supporting hydrographic data and a compilation of salt marsh trace metal results conducted in Graz, Austria. Trace metal work included a suite of 26 elements measured in a core, two species of mussels, *Spartina alterniflora* marsh plant and the sea surface microlayer (SML) from an intertidal Delaware salt marsh.

Chapter 1

SCAVENGING METHOD COMPARISON ASSOCIATED WITH THE ANALYSIS OF 210Po AND 210Pb IN ESTUARINE AND COASTAL WATERS

Marsan¹, D., Rigaud¹, S. and Church¹, T.

¹School of Marine Science and Policy, University of Delaware, Newark, DE 19716
USA.

Highlights:

- Two widely used scavenging methods (Fe(OH)₃ and Co-APDC) for ²¹⁰Po and ²¹⁰Pb compared
- No statistical difference was found to support the preferential uptake of spike (²⁰⁹Po) or natural (²¹⁰Po) by any of the scavenging methods
- Fe(OH)₃ and Co-APDC methods display statistically comparable ²¹⁰Pb activities but Fe(OH)₃ yields more precise and consistent ²¹⁰Po activities in estuarine and coastal waters
- MnO₂ is as accurate and consistent alternative scavenging technique for ²¹⁰Po and ²¹⁰Pb extraction from open ocean seawater

Acknowledgements

- Dr. Luther for providing research cruise time in the Delaware and Chesapeake supported by NSF/OCE grants 1031272 and 1059892.
- Graduate support for D. Marsan was provided by NSF Grant- HRD-1139870- Greater Philadelphia Region LSAMP Bridge to the Doctorate (Cohort IX)
- Dr. Baskaran for counting salt marsh samples
- Ella McDougal for assisting in sample collection

1.1 Abstract

Documented is a study of the two most widely utilized extraction techniques ($\text{Fe}(\text{OH})_3$, Co-APDC, and MnO_2) for the extraction of the naturally occurring radionuclide pair ^{210}Po and ^{210}Pb in estuarine and coastal seawater. Included are >100 individual samples collected during six samplings in the Delaware Bay, Canary Creek salt marsh, Chesapeake Bay and a coastal North Atlantic Ocean station. Surface and deep dissolved samples were collected at each site, plus auxiliary samples for chemical parameters. The $\text{Fe}(\text{OH})_3$ and Co-APDC scavenging methods do not preferentially uptake the natural (^{210}Po) or spike (^{209}Po) polonium isotopes over the other elevated spike added to coastal seawater. Generally the scavenging methods agree quite well but more so for ^{210}Pb final activities with a <5% relative variation. On the other hand ^{210}Po activities agree as a whole between the methods but less so in areas of high suspended particles, high biological production and low oxygen. We hypothesize that the discrepancies arise because polonium acts as a sulfur analog. We also hypothesize that under conditions of low pH (2-5), low dissolved oxygen and high levels of sulfur humic acids, which are typical of salt marsh and estuarine environments, promotes differences between the scavenging methods. It is also hypothesized that the formal charge ($\text{Po}(0)$ or $\text{Po}(\text{II})$) and compounds (ligand or chelate) being formed by ^{210}Po leads to Co-APDC scavenging yielding lower final ^{210}Po activities. On the other hand ^{210}Pb discrepancy is not seen because the predominant charge is Pb^{2+} and it is associated mostly with chelate compounds that allow ^{210}Pb to be assessable by both methods.

It is suggested that the $\text{Fe}(\text{OH})_3$ scavenging method be utilized as the preferred method for extraction of ^{210}Po and ^{210}Pb from estuarine and coastal waters. The Co-APDC method appears less consistent, yet in the open ocean it is operationally as reliable as $\text{Fe}(\text{OH})_3$ and takes less processing time. Here the MnO_2 scavenging method displayed reliable scavenging of ^{210}Po and ^{210}Pb . As such it should be considered as an alternative scavenging method for the extraction of ^{210}Po and ^{210}Pb from seawater.

Keywords

^{210}Po ; ^{210}Pb ; $\text{Fe}(\text{OH})_3$; Co-APDC; method comparison; estuaries; coastal

1.2 Introduction

Accurate and consistent techniques to examine dissolved and particle dynamics in marine eco-systems have been investigated for the past several decades. One such technique is the naturally occurring ^{210}Pb ($t_{1/2}=22.3\text{y}$) and ^{210}Po ($t_{1/2}=138\text{d}$) radionuclide pair (Bacon et al., 1976; Nozaki, et al. 1976; Thomson and Turekian, 1976; Cochran and Masque, 2003; Rutgers van der Loeff and Geiber, 2007). Both nuclides are included within the ^{238}U decay chain, with ^{210}Po produced from the decay of ^{210}Pb via ^{210}Bi ($t_{1/2}=5.0\text{d}$). In seawater, both nuclides are particle-reactive, while ^{210}Po is also bioactive and concentrates within organic tissues (Stewart and Fisher, 2003a,b; Stewart et al. 2005). Due to different particle-reactive characteristics, the nuclide disequilibrium produced is able to define scavenging rates and particle fluxes, including organic matter with depth (Sarin et al., 1999; Stewart et al., 2007; Verdeny et al., 2009). Therefore accurate and consistent results for scavenging methods are needed to quantify the ^{210}Po and ^{210}Pb activities in seawater.

A recent assessment of the precision and accuracy of the current procedures for ^{210}Po and ^{210}Pb measurement was conducted as part of an intercalibration study using dissolved and particulate seawater samples (Church et al., 2012). A major conclusion found that results reported by laboratories agree well (relative standard deviation, RSD <50%) for samples with relatively high ^{210}Po and ^{210}Pb activities (>0.1dpm), but became rather poor (RSD up to 200%) for lower activity samples. As a follow-up on the intercalibration work, an assessment of the calculations and uncertainties for determining ^{210}Po and ^{210}Pb in seawater was conducted (Rigaud et al., in revision). This study found that for ^{210}Po activities the final relative uncertainty is more variable than ^{210}Pb and depends on the $^{210}\text{Po} / ^{210}\text{Pb}$ activity ratio in the sample and the time elapsed between sampling and sample processing. A key step not reported by each group was that of scavenging technique used, specifically either the widely used ($\text{Fe}(\text{OH})_3$ and Co-APDC) co-precipitation methods. Another method using MnO_2 followed by Sr-resin separation has not been widely adopted or tested in seawater (Bojanowski et al., 1983).

In the context of this paper, over a hundred samples were collected throughout the Delaware Bay, including an intertidal marsh, upper Chesapeake Bay, and offshore coastal waters in order to test the accuracy and consistency of the $\text{Fe}(\text{OH})_3$ and Co-APDC scavenging techniques (Figure 1.1). The aims of the present paper are: 1) review extraction protocols used for ^{210}Po and ^{210}Pb measurement in seawater, 2) evaluate extraction efficiency results from biogeochemically diverse estuarine and coastal regions, 3) statistically compare accuracy and precision of the $\text{Fe}(\text{OH})_3$ and Co-APDC scavenging methods 4) recommend improvements for the scavenging methods.

1.3 Methods

1.3.1 Sample Collection and General Procedure

Water samples were collected during six cruises from 2011-12 throughout the Delaware Bay, Chesapeake Bay and a North Atlantic Ocean station (Figure 1.1). The seawater was collected using Niskin bottles deployed at designated depths. The 20 L Cubitainers® were filled with filtered ($0.45\mu\text{m}$) seawater using Gelman Sciences sterilized Mini Capsule Filter membranes, and acidified to pH 2 using HCl. The cubitainers were sealed and stored in a dark room until being transferred to cold storage once ashore. The filtered and acidified seawater samples were assumed to be isolated from storage artifacts based on earlier findings (Chung et al., 1983). During the cruises, samples were also collected for particulate ^{210}Po and ^{210}Pb , along with nutrient, POC, PON, and other hydrographic parameters (salinity, temperature, conductivity, fluorometer and dissolved oxygen).

Upon arriving ashore the dissolved seawater samples were promptly split into 10L aliquots and several documented protocols were used (Figure 1.2). Duplicate samples were processed following modified co-precipitation methods $\text{Fe}(\text{OH})_3$ (Nozaki 1986; Sarin et al., 1992), Co-APDC (Fleer and Bacon, 1984) and for some offshore samples using MnO_2 precipitation (Bojanowski et al., 1983). Recovery of the co-precipitate is conducted using a peristaltic pump with a $0.45\mu\text{m}$ nucleopore filter. The precipitate is then dissolved in an acid solution (1M HCl for $\text{Fe}(\text{OH})_3$, 1M HCl and 1% H_2O_2 mix for MnO_2 , and 6M HNO_3 for Co-APDC),

evaporated to near dryness and recovered in 0.5M HCl solution. The samples are plated by spontaneous deposition onto a silver disc (Flynn, 1968), and their activities measured by alpha spectroscopy. A small aliquot is taken for lead yield and then the remaining Po in solution is removed using AG-1X8 anion exchange resin as described by Sarin et al., (1992). After separation, another small aliquot is taken from the final eluate solution containing the ^{210}Pb and both small aliquots measured using flame atomic absorption to determine Pb yields. The final eluate solution is re-spiked with ^{209}Po and stored for 6 months to allow in-growth of ^{210}Po from ^{210}Pb . After 6 months the ^{210}Pb activity of the samples is determined by plating Po nuclides present in the eluate solution on a new silver disc thus measuring the in-growth of ^{210}Po (Figure 1.1). Ultimately the determination of the initial activities of ^{210}Po and ^{210}Pb at the time of collection is calculated using the equations and corrections that account for decay, ingrowth and recovery of each nuclide with accumulative error (Rigaud et al., in revision).

1.3.2 Fe(OH)₃ Extraction Method (Sarin, et al., 1992)

Once the 10-liter seawater sample is spiked with ^{209}Po and Pb carrier, 100 mg of FeCl_3 is added (Figure 1.2). The sample is allowed to equilibrate for 24 hours; then 4M ammonium (NH_4OH) is slowly added to obtain a pH=4.0, at which point 1mL of 10% sodium chromate solution is added to aid in Pb extraction and stirred vigorously. Next, more ammonium is added to obtain a final pH=8.5 and allowed to precipitate out for 12-24 hours. To aid in the precipitation of Fe(OH)_3 , a “seed” solution (Fe(OH)_3 already precipitated in a separate container) of FeCl_3 and ammonium can be added.

After the sample settles, the supernatant water is siphoned and the precipitate recovered by filtration using a Geotech peristaltic pump with Nucleopore 0.45 μm polycarbonate filter placed in a Savillex Teflon holder. Filtration is complete within 20 minutes. The Nucleopore filter is then placed in a 50ml Teflon container with 30ml of 0.5M HCl solution to dissolve the precipitate. Once the precipitate is

dissolved the filter is rinsed with 0.5M HCl and removed. The solution is then ready for plating.

1.3.3 Co-APDC Co-precipitation Method (Fleer and Bacon, 1984)

A solution of 20 mg of Co is added to the 10-liter sample. The sample equilibrates for 24 hours, at which point 25ml of a 2g/100ml solution of APDC is slowly added drop wise for 30 minutes, while stirring vigorously (Figure 1.2). The entire sample is then filtered after 1 hour using the same filtration apparatus as described earlier. Typical filtration times are between 20 minutes to 4 hours depending on sample type (i.e open ocean, salt marsh or estuary). Once filtered the Nuclepore filter is rinsed with 6M nitric acid into a 50ml teflon container. The precipitate is then digested and the nitric acid transformed into a HCl solution at (90°C) by being evaporated to near dryness and brought up three times in 9M HCl. Once the precipitate is fully digested and transformed, it is diluted in 40ml of 0.5M HCl solution before plating.

1.3.4 MnO₂ Scavenging Method (Bojanowski et al., 1983)

Manganese is added to a 10-liter sample using solutions 1.5mL of 0.2 mol L⁻¹ KMnO₄ and 1.5mL of 0.3 mol L⁻¹ MnCl₂. KMnO₄ is added first as an organic oxidant and allowed to equilibrate for 15 minutes, then stirred vigorously for 30-60 minutes in order to attain equilibrium of the complexes between the Mn (VI) and Mn(III) species. Adjust the pH to 8.5 using NH₄OH and allow the MnO₂ precipitate to settle overnight. The supernatant water is then siphoned and the precipitate recovered by filtration within 1 hour following steps outlined in Figure 2. The precipitate is then digested by adding a 1% H₂O₂ in 1M HCl solution at constant temperature (90°C) for 30 minutes and is then ready for plating.

1.3.5 Plating Process

The spontaneous deposition of ²¹⁰Po onto a polished disc can result in highly variable results depending on the temperature, time, pH, agitation and additions of ascorbic acid. A comparative analysis of Po plating conditions was conducted using experimental water taken from Indian River Inlet in order to identify a procedure

that maximizes plating efficiency. The ideal conditions were observed to occur when plating for 12 hours in a capped Teflon beaker with a 40ml solution of 0.5 M HCl using a 12mm disc, at 90°C with constant stirring with the addition of 250-500mg of ascorbic acid. Maximum yields of $98 \pm 5\%$ were obtained (Marsan, unpublished results). For this work the silver disc is attached to a modified circular magnetic stir disc using rubber cement and allowed to dry before being added to solution. Utilizing these plating conditions will limit the loss of Po and Pb as had been previously observed (Garcia-Orellana and Garcia-Leon 2002; Baskaran et al., 2009).

1.3.6 Processing/storage time

Rapid separation and processing of nuclides such as ^{210}Po and ^{210}Pb are important because the methodology requires that the in-situ ^{210}Po be assayed (or at least separated from ^{210}Pb) as quickly as possible after the sample collection to limit decay and in-growth. When a large number of samples are collected in the field, processing and quick separation of the ^{210}Po and ^{210}Pb from seawater needs to be completed in order to limit radionuclide decay and increased error. Hence the storage times need to be constrained over a period of about a week to limit the loss of Po and Pb. Shortening processing time while maintaining a high recovery efficiency of ^{210}Po and ^{210}Pb was accomplished with the use of a peristaltic pump and encapsulated filters. Example experiments using this combination decreased processing time, from spike addition to plating, for $\text{Fe}(\text{OH})_3$ from 7 to 5 days and from 6 to 3 days for Co-APDC, while increasing extraction efficiency of ^{209}Po from $72 \pm 11\%$ to $89 \pm 10\%$. Although processing time decreased the major factor resulting in increased error propagation is a prolonged sampling to separation time often seen during extended length cruises. As such onboard processing is suggested if possible.

1.4 Results

The two most widely used scavenging methods $\text{Fe}(\text{OH})_3$ and Co-APDC were tested ($n=104$) using estuarine and coastal water samples. Scavenging methods were compared using regression analysis and focused on two comparisons, the

extraction efficiency and final activity precision. Dissolved activities and errors of ^{210}Po and ^{210}Pb can be found in Table 1 and Table 2. Extraction efficiencies are reported in Table 3.

1.4.1 Preferential Scavenging of ^{210}Po and ^{209}Po

Preferential scavenging efficiency of natural (^{210}Po) and spike (^{209}Po) were tested for $\text{Fe}(\text{OH})_3$ and Co-APDC. Using experimental water collected from Indian River Inlet, 6 sets of triplicates were run for each method using standard additions of both nuclides including supplementing the natural ^{210}Po by 100 fold. The experimental water salinity was 34ppt, fully oxygenated and filtered by $0.45\mu\text{m}$ nucleopore filter before processing. Scavenging ratios between ^{209}Po and ^{210}Po for $\text{Fe}(\text{OH})_3$ were found to not differ statistically ($\pm 4.2\%$). As for Co-APDC the scavenging ratio was also found to not differ statistically ($\pm 4.5\%$). It is important to note that only the ratios of each elevated isotope spike differed in these tests, while the chemical properties of the water as aliquots were constant.

1.4.2 Comparison of Extraction Efficiency between $\text{Fe}(\text{OH})_3$ and Co-APDC

Average scavenging efficiencies of spike ^{209}Po for 1st plating from samples located around the Delaware region are reported in Table 3. Maximum scavenging efficiencies for each method has been evidenced up to 98% recovery. $\text{Fe}(\text{OH})_3$ often exhibited lower scavenging efficiencies than Co-APDC. Samples from the Delaware Bay, Chesapeake Bay and intertidal marsh indicate that Co-APDC scavenges ^{209}Po at a higher rate (60-73%) than $\text{Fe}(\text{OH})_3$ (36-68%). Relative standard deviation for Co-APDC extraction efficiency ranged from 33-45% while $\text{Fe}(\text{OH})_3$ was 24-52%. Offshore $\text{Fe}(\text{OH})_3$, Co-APDC, and MnO_2 scavenging efficiencies differed slightly from 60-68% with a relative standard deviation of 20%. Low scavenging efficiencies for each method were related to areas of high particulate (DB) and low oxygen (CB) contents (Table 1.1 and Table 1.2)

1.4.3 Comparison of Final Activity and Activity Ratios Between Fe(OH)₃ and Co-APDC

Comparing ²¹⁰Po final activity over the estuarine and coastal regions found reasonable agreement between methods but also show some differences depending on the origin of the samples (Figure 3). Samples in the Delaware Bay (Figure 1.3 panel A) agreed quite well with a mean difference of 8% for all samples, which is within the average error of each sample. The Delaware estuary as a whole showed good agreement, but deviations between methods occurred in the upper estuary. The upper estuary discrepancy is exhibited by Fe(OH)₃ yielding higher ²¹⁰Po activities than Co-APDC. Similar to the Delaware, the Chesapeake Bay (Figure 1.2 panel B) ²¹⁰Po activities as a whole agree quite well between methods with a mean difference of 11%, which is slightly greater than the average error of each sample. The Chesapeake Bay during the summer of 2012 was dominated by a sub-oxic water mass at depth and seaward of Baltimore Harbor, where a phytoplankton bloom was observed (Appendix A). Discrepancies between methods occur within regions of sub-oxic and phytoplankton bloom with Fe(OH)₃ showing higher ²¹⁰Po activities than Co-APDC.

Intertidal marsh (Figure 1.3 panel C) samples were collected over a 12-hour tidal cycle from two locations within Canary Creek marsh. Temperature and oxygen over the tidal cycle did not vary, while particulate concentrations were largest during ebbing and low tide. Mean differences between scavenging methods were similar at both locations within 13%. Maximum mean differences were observed during ebbing and low tide (75%) as a result of higher Fe(OH)₃ ²¹⁰Po activities compared to Co-APDC. Seasonal offshore samples (Figure 1.3 panel D) displayed the greatest mean difference between scavenging methods 19%. Unlike the Delaware, Chesapeake and intertidal marsh Co-APDC consistently showed higher ²¹⁰Po activities than Fe(OH)₃. The greatest discrepancy between methods occurred at 200m during the winter sampling, with Co-APDC being 50% greater. Water chemistry at this depth coincided with an oxygen minimum zone.

Comparing ²¹⁰Pb activities between methods in the same samples showed that both methods display similar activities (Figure 1.4). The Delaware and

Chesapeake (Figure 1.4 panel A and B) mean scavenging differences between methods were both 4%. This value is far less than the average error (10%) associated with the ^{210}Po samples. As for the intertidal marsh and offshore (Figure 1.4 panel C and D) the mean scavenging difference of ^{210}Pb between methods was 8% and 15% for $\text{Fe}(\text{OH})_3$ and for Co-APDC respectively. The Intertidal marsh mean difference is below the average error associated with the individual samples (<10%). The offshore mean difference is driven by one high ^{210}Pb activity difference, Co-APDC at 50% greater than $\text{Fe}(\text{OH})_3$ activity reported during the winter 2011 sampling at 200m depth. A small set of samples collected in the North Atlantic was tested using the MnO_2 scavenging method. MnO_2 data gave comparable results to $\text{Fe}(\text{OH})_3$ with a mean difference of <15% for ^{210}Po and ^{210}Pb .

1.5 Discussion

Scavenging efficiencies from 1st plating of ^{209}Po show that Co-APDC is generally more efficient than $\text{Fe}(\text{OH})_3$. Experiments were ran using Indian River Inlet water to test if either $\text{Fe}(\text{OH})_3$, Co-APDC or MnO_2 preferentially extracts detailed spikes of ^{209}Po or ^{210}Po to a greater extent but found no statistical evidence of such a difference. The results comparing $\text{Fe}(\text{OH})_3$ and Co-APDC scavenging methods taken as a whole were statistically equivalent for extracting elevated amounts of ^{210}Po and ^{210}Pb from estuarine and coastal seawater (Figure 1.2 and 3). However, certain biogeochemical processes occurring in estuarine waters appear to have led to some discrepancies between methods with $\text{Fe}(\text{OH})_3$ displaying higher ^{210}Po activities versus Co-APDC. Results for the MnO_2 co-precipitation method indicate it is just as reliable of an option for ^{210}Po and ^{210}Pb extraction from coastal seawater samples.

1.5.1 Po speciation

The preferential extraction of one polonium isotope of, (^{209}Po or ^{210}Po), over the other is important because the chemical state of each in seawater is unknown, and thus isotopic equilibrium needs to be known to determine if they extract differently. The experimental water experiments used known amounts of standard

^{209}Po and ^{210}Po in a standard additions manner to see if $\text{Fe}(\text{OH})_3$, Co-APDC or MnO_2 preferentially extracted the spike (^{209}Po) or natural (^{210}Po) polonium isotope. It was found that there is no statistical (within 1 standard deviation) difference between extraction efficiencies. It is important to note that this experiment was conducted only using coastal experimental water which could include lower levels of humic acids. Though isotopic equilibrium was observed, it cannot be confirmed by this study alone under natural concentrations of ^{210}Po and with the natural speciation of ^{210}Po in seawater being unknown. Further experiments should be conducted using standard additions with natural levels of spike. Some indication of equivalent species of natural (^{210}Po) and spike (^{209}Po) are needed to confirm that isotopic equilibrium occurs. Another experiment should include such additions as using filtered seawater with different biogeochemical properties such as varied humic acids, dissolved oxygen and pH concentrations.

As reported there is not a preferential extraction of polonium isotopes in restricted experiments using coastal waters, thus the scavenging methods were directly compared for extraction efficiency of ^{209}Po and final ^{210}Po and ^{210}Pb activities. Extraction efficiencies of ^{209}Po were greater for Co-APDC than that of either $\text{Fe}(\text{OH})_3$ or MnO_2 . The likely reason lies in the chemical nature of scavenging which occurs differently for each method. Co-APDC utilizes APDC that is a water-soluble compound that forms insoluble uncharged chelates as solid precipitates with a variety of metals. At the low metal concentration levels found in natural waters, the dithiocarbamate chelates form complexes, but at higher carrier (e.g. Co) concentration levels the chelates co-precipitate. Since the metal ion in the chelate is effectively shielded by hydrophobic groups, precipitation in a multi-metal system is relatively nonselective; the chelates of several metals precipitate together rather than as separate phases. If one transition metal (e.g. Co) is present in sufficient excess concentration to act as a carrier and forms the precipitate, other metals (e.g. ^{210}Po and ^{210}Pb) should be effectively incorporated into the precipitate regardless of their concentration. Addition of Co^{2+} to the sample as a carrier produces filterable particles upon mixing with APDC. As for $\text{Fe}(\text{OH})_3$ and MnO_2 co-precipitation method, FeCl_3 or MnCl_2 and KMnO_4 (to act as an oxidant) added to an

acidic solution hydrolyze when ammonium is added, increasing the pH forming the $\text{Fe}(\text{OH})_3$ or MnO_2 colloidal solid precipitates which flocculate out of solution. The likely cause of higher ^{209}Po efficiencies from Co-APDC scavenged samples are that co-precipitate, rather than colloidal aggregates occur, allowing the ^{209}Po and ^{210}Po to be scavenged more efficiently. Increased scavenging efficiency has the added importance of lower counting times, due to higher activities, thus decreasing uncertainties and errors, which become compounded. As presented by Rigaud et al., (in revision) when low activities (<0.1 dpm/100L) of ^{210}Po and ^{210}Pb are observed, the calculated results become increasingly difficult to accurately measure. By limiting loss of ^{210}Po and ^{210}Pb during the scavenging step, higher activities can be achieved.

1.5.2 Influence of Chemical Environment on Po and Pb Extraction Efficiencies and Activities

Histograms of $\text{Fe}(\text{OH})_3$ and Co-APDC ^{210}Po and ^{210}Pb activities with associated errors allows for more insight into how biogeochemical processes may affect scavenging (Figure 6-9). Final activities of ^{210}Po compared between the two methods agree as a whole but conditions such as high particulate concentrations, low oxygen and increased biological activity can cause discrepancies to occur. Here particulate concentrations in the Delaware and Chesapeake can reach up to 50 mg/L. It is generally observed that discrepancies between $\text{Fe}(\text{OH})_3$, (higher) and Co-APDC (lower) final activities occur at concentrations of >30 mg/L. Within the Delaware estuary two processes cause the greatest discrepancy between scavenging methods for ^{210}Po , high-suspended particulate matter at the turbidity maximum and a phytoplankton bloom (Figure 1.6). Only three samples display differences outside of the calculated error for ^{210}Po , while for ^{210}Pb all samples agree. As discussed earlier an increase in suspended particulate matter likely involves an increase in humic acid compounds, which may compete with the scavenging methods during extraction from seawater. Possible explanations could involve increased sulfur containing humic acids from salt marshes and non-extracted colloids that are able to pass through 0.45 μm filters. As such the phytoplankton bloom could also cause a

discrepancy because polonium associated within very small organic compounds leading to a method (Co-APDC in this case) not being capable of scavenging all of the natural ^{210}Po .

The Canary Creek salt marsh samples show how a combination of low dissolved oxygen and high suspended particulate concentration can promote discrepancy between scavenging methods (Figure 1.7). Five samples of ^{210}Po and one of ^{210}Pb show scavenging method difference outside of the calculated error range. Salt marshes are known to have pH levels as low as 3-5 and are abundant in sulfur containing organic compounds (Luther et al., 1991). Lower pH levels promote humic acid precipitation, while binding of either ^{210}Po or ^{210}Pb to sulfur compounds creates very strong complexes, which are competitively difficult to co-extract. Building upon a low oxygen discrepancy trend the upper Chesapeake Bay fits with its sub-oxic to anoxic conditions (Figure 1.8). Four samples located at the lowest dissolved oxygen depths show that Co-APDC does not extract the same amount of ^{210}Po as $\text{Fe}(\text{OH})_3$. Low oxygen or sub-oxic zones are prevalent in near bottom waters during summer months in the Chesapeake Bay and offshore between stratified water masses. Thus lower concentrations of dissolved oxygen can create a chemical environment, which allows for less oxidizing potential and greater sulfur binding compounds. The North Atlantic offshore site displayed the largest $\text{Fe}(\text{OH})_3$ and Co-APDC discrepancy but unlike the estuarine environments Co-APDC produced better extraction of both ^{210}Po and ^{210}Pb (Figure 1.9). Sample 20 from Figure 1.9 is located at a depth of 200 meters and is associated with the isopycnal zone stabilizing two water masses. The other differences seen occur at surface depths from 1 to 15 meters and are likely associated with higher organic compound concentration. As a whole the $\text{Fe}(\text{OH})_3$, Co-APDC, and MnO_2 scavenging methods used in estuarine and coastal waters scavenge ^{210}Pb generally to the same extent.

The estuarine and salt marsh ecosystem is a dynamic biogeochemical system, which is poised between reducing and oxidizing conditions. We hypothesize that polonium acts in a similar way to sulfur under these estuarine conditions in such a way that it binds with oxygen, nitrogen, and sulfur ligands creating a charged $\text{Po}(\text{II})$ compounds. While in the open ocean polonium is likely bound by carbon and has a

formal charge of Po(0). On the other hand Pb has a formal charge of Pb^{2+} and forms carboxylic chelates with carbon and oxygen. By understanding the formal charge and compounds (i.e. chelates or ligands) that ^{210}Po and ^{210}Pb form under different biogeochemical conditions discrepancies between scavenging methods can be solved. The order of ease of oxidation of Po^{2-} could be to Po(0) or Po (II) and depends on pH for Po(II) and H_2Po . For Po (II) oxidation, the oxidation is slower at lower pH (as seen in salt marshes and after acidification of samples). However, in the presence of organic ligands containing carboxylate groups or on adsorption of Po(II) to clays, Po(II) oxidation is significantly enhanced at low pH values 3-5. This enhanced oxidation competes with the Co-APDC scavenging method in order to precipitate ^{210}Po . On the other hand the $Fe(OH)_3$ method is not affected due to the pH being raised to pH=8.5.

Polonium species and oxidation states are poorly understood in the marine environment. On the other hand dissolved ^{210}Pb associates largely with dissolved carbonates and its predominate state is Pb(II). Dissolved Po appears to act as an S analogue or binding to S ligands, but is primarily understood to associate with protein in living organisms (Stewart and Fisher, 2003a). It is believed that polonium acts as a Class B metal ion, which readily bind with sulphhydryl (-SH), disulphide(-S-S-), thioether (-SR) and amino (-NH₂) functional groups; with borderline metals (such as Pb) exhibiting an intermediate behavior between class B and class A metals. These preferentially bind with phosphates, carboxylic and carbonyl functional groups (ligands with oxygen as the donor atom).

The differences seen in scavenging methods throughout the estuarine and coastal system seem to be linked to sub-oxic and high particulate concentration regions. We hypothesize that the lower ^{210}Po activities found using the Co-APDC scavenging method is linked to how polonium associates and reacts with humic acids in seawater. Non-volatile reduced organic sulfur materials are expected of the types R-S-H (thiols), R-S₂-R (organic sulfides), R-S-S-R (organic disulfides) with R being alkyl groups, or sulfur containing humic or fulvic compounds in salt marshes (Francois, 1987a). Generally, such organic sulfur compounds could be digenetic products of reactions under reducing conditions between high molecular weight

lignin type materials and inorganic reduced sulfur (SH-, FeS, FeS₂ and S_{x-2}). Luther et al.,(1991) observed that when oxidizing conditions are extreme as evidence by low porewater pH(<5) or in the case of this study by acidifying the samples after filtration, negligible alkalinity concentrations are present, and enhanced sulfate reduction rates over sulfide oxidation rates are likely. When the rate of oxidation of reduced sulfur compounds is competitive with or less than the rate of sulfate reduction (i.e. pH values nearer to 6) and reasonable alkalinity concentration, tidal flooding can promote reduced sulfur oxidation (Ferdelman et al., 1990).

1.5.3 Recommendations

Suggestions on which method to utilize should be based not only on accuracy and consistency but also on processing time. For estuarine and coastal waters we suggest the utilization of Fe(OH)₃ over Co-APDC. The accuracy and precision of Fe(OH)₃ extraction in high suspended matter, high productivity, and low oxygen zones appears superior than that of Co-APDC. Another important factor is time of processing, where estuarine and coastal waters are high in humic acids and could present competitive complexes with Co-APDC thus impeding precipitation and slowing filtering to days instead of minutes. Extended time (days) after the precipitation for Co-APDC can lead to dissolution and degradation of the Co-APDC complex, thus causing a loss in ²¹⁰Po and ²¹⁰Pb activity in the sample. The major step where loss of ²¹⁰Po and ²¹⁰Pb activity occurs with all methods is the precipitation and filtering of the sample; limiting this loss will result in lower compounded errors.

The Fe(OH)₃ method is the preferred method for estuarine and coastal waters. Though it is suggested that Co-APDC scavenging not be preferred in estuarine and coastal systems, it is just as consistent as Fe(OH)₃ in the open ocean and has shorter processing times. Another method for future consideration is MnO₂, which showed equivalent results to Fe(OH)₃ for the extraction of ²¹⁰Po and ²¹⁰Pb from open ocean seawater.

1.6 Conclusions

The $\text{Fe}(\text{OH})_3$ and Co-APDC scavenging methods were tested on 104 samples from estuarine and coastal water to evaluate their accuracy and consistency. The ^{209}Po and ^{210}Po scavenging experiment using coastal waters found no preferential uptake of one isotope over the other for the $\text{Fe}(\text{OH})_3$ and Co-APDC methods. More studies should be conducted to determine if different water chemistries (humic acid, pH etc.) could affect the differential scavenging of each isotope and if a state of isotopic equilibrium in natural waters is achieved. An interesting way to test isotopic equilibrium would include expanded standard addition experiments and the use of oxidizing agents such as UV- H_2O_2 oxidation to determine if significant species degradation increases the extraction efficiency and consistency.

The ^{210}Pb activities for both methods agree and no statistical difference between scavenging methods is evident between estuarine and coastal waters. The ^{210}Po activities as a whole agree but differences are present in areas of high-suspended particles, high biological activity and low oxygen concentrations. The likely cause for discrepancy between methods is the formal charge of Po (Po(0) or Po(II)) in the extracted sample and whether it is impeded in being bound by ligands (oxygen, nitrogen or sulfur) or carbon molecules. The acidification of samples after filtration during storage may be a hindrance for the Co-APDC method when sulfur and humic acid compounds are present in high concentration and can compete for the chelated precipitate. The $\text{Fe}(\text{OH})_3$ method is not affected because in order to promote co-precipitation the pH is raised to 8.5. Interestingly the ^{210}Pb activities do not display a discrepancy between methods because Pb likely forms chelates and colloids with a formal charge of Pb^{2+} allowing it to be easily assessable by either method regardless of the biogeochemical conditions. Further work should be conducted to confirm the speciation and oxidation states of ^{210}Po in seawater to promote conversation on more consistent extraction.

The $\text{Fe}(\text{OH})_3$ scavenging produces consistent and more reliable ^{210}Po and ^{210}Pb activity results under a variety of biogeochemical conditions tested in estuarine and coastal waters. It is suggested that the $\text{Fe}(\text{OH})_3$ scavenging method be utilized as the preferred method for extraction of ^{210}Po and ^{210}Pb from estuarine and coastal

waters. Although Co-APDC is less reliable in estuarine and coastal waters compared to $\text{Fe}(\text{OH})_3$, in the open ocean it has the added advantage of faster processing times. Future studies should focus on validating the hypothesis that $\text{Fe}(\text{OH})_3$ and Co-APDC scavenging differences are affected by chemical properties in the seawater such that the presence of DOC material such as sulfur humic acid, low oxygen and biological levels of production can be remediated for maximum extraction of both ^{210}Po and ^{210}Pb natural nuclides.

REFERENCES

Bacon, M. P., D. W. Spencer, and P. G. Brewer. 1976. $^{210}\text{Pb}/^{226}\text{Ra}$ and $^{210}\text{Po}/^{210}\text{Pb}$ disequilibria in seawater and suspended particulate matter. *Earth and Planetary Science Letters* **32**: 277-296.

Baskaran, M., G. H. Hong, and P. H. Santschi. 2009. Radionuclide analyses in seawater. p. 259-304. In O. Wurl (ed.), *Practical guidelines for the analysis of seawater*. CRC Press, Boca Raton.

Bojanowski, R., R. Fukai, S. Ballestra, and H. Asari. 1983. Determination of natural radioactive elements in marine environmental materials by ion exchange and alpha spectrometry, p. 1-13. *In* I.A.E.A. [ed.].

Chung, T., and H. Craig. 1983. ^{210}Pb in the Pacific: the GEOSECS measurements of particulate and dissolved concentrations. *Earth Planet. Sci. Lett.* 65(2):406-432

Church, T., Sarin, M. 1995. Natural U-Th series radionuclide studies of estuarine processes. *Changes in Fluxes in Estuaries: Implication From Science to Management*. (Eds. K.R. Dyer and R.J. Orth), *Proceedings of the ECSA22/ERF Symposium*, Plymouth England, September 13-18, 1992. Pp.91-95.

Cochran, J. K., and P. Masqué. 2003. Short-lived U/Th Series Radionuclides in the Ocean: Tracers for Scavenging Rates, Export Fluxes and Particle Dynamics. *Reviews in Mineralogy and Geochemistry* **52**: 461-492.

Ferdelman, T., Church, T., Luther, G. 1990. Sulfur enrichment of humic substances in a Delaware Salt marsh core. *Geochimica Vol. 55*, pp. 979-988.

Fleer, A. P., and M. P. Bacon. 1984. Determination of ^{210}Pb and ^{210}Po in seawater and marine particulate matter. *Nuclear Instruments and Methods in Physics Research* **223**: 243-249.

Flynn, W. W. 1968. The determination of low levels of polonium-210 in environmental materials. *Anal. Chim. Acta* **43**: 221-227.

Francois R. 1987a. A study of sulfur enrichment in the humic fraction of marine sediment during early diagenesis. *Geochim. Cosmochim. Acta* 51, 17-27.

García-Orellana, I., and M. García-León. 2002. An easy method to determine ^{210}Po and ^{210}Pb by alpha spectrometry in marine environmental samples. *Appl. Radiat. Isot.* 56:633-636.

Luther, G., Ferdelman, T., Kostka, J., Tsamakis, E., Church, T. 1991. Temporal and

spatial variability of reduced sulfur species (FeS_2 , S_2O_3) and porewater parameters in salt marsh sediments. *Biogeochemistry* 14: 57-88.

Nozaki, Y. 1986. ^{226}Ra - ^{222}Rn - ^{210}Pb systematics in seawater near the bottom of the ocean. *Earth and Planetary Science Letters* **80**: 36-40.

Nozaki, Y., J. Thomson, and K. K. Turekian. 1976. The distribution of ^{210}Pb and ^{210}Po in the surface waters of the Pacific Ocean. *Earth and Planetary Science Letters* **32**: 304-312.

Rigaud, S., Puigcorb , V., Camara-Mor, P., Casacuberta, N., Roca-Mart , M., Garcia-Orellana, J., Benitez-Nelson, C.R., Masque, P., and Church, T. An assessment of the methods, calculation and uncertainties in the determination of ^{210}Po and ^{210}Pb activities in seawater.

Rutgers van Der Loeff, M. M., and W. S. Moore. 2007. Determination of natural radioactive tracers, p. 365-397. *Methods of Seawater Analysis*. Wiley-VCH Verlag GmbH.

Sarin, M. M., R. Bhushan, R. Rengarajan, and D. N. Yadav. 1992. The simultaneous determination of ^{238}U series nuclides in seawater: results from the Arabian Sea and Bay of Bengal. *Indian J. Mar. Sci.* **21**: 121-127.

Stewart, G. M., and N. S. Fisher. (2003a). Experimental studies on the accumulation of polonium-210 by marine phytoplankton. *Limnology and Oceanography*, 48, 1193-1201.

Thomson, J., and K. K. Turekian. 1976. ^{210}Po and ^{210}Pb distributions in ocean water profiles from the Eastern South Pacific. *Earth and Planetary Science Letters* **32**: 297-303.

TABLES

Table 1.1: The dissolved ^{210}Po and ^{210}Pb activities (dpm 100L^{-1}) for the Delaware Estuary (DB and DBSMS) and Chesapeake Bay (CB) with associated errors for the Fe(OH)₃ and Co-APDC scavenging methods.

| Station | Salinity | Depth (m) | Oxygen (umol/l) | Particulate (mg/L) | Fe(OH) ₃ Co-Precipitation Method | | | | | Co-APDC Co-Precipitation Method | | | | |
|-----------------------|----------|-----------|-----------------|--------------------|-----------------------------------------------------------|-----------------------------------------------------------|---------------------------------------------|-----------------------------------------------------------|-----------------------------------------------------------|---------------------------------------------|--|--|--|--|
| | | | | | $^{210}\text{Po}_{\text{diss}}$ (dpm 100L^{-1}) | $^{210}\text{Pb}_{\text{diss}}$ (dpm 100L^{-1}) | $^{210}\text{Po}/^{210}\text{Pb}$ dissolved | $^{210}\text{Po}_{\text{diss}}$ (dpm 100L^{-1}) | $^{210}\text{Pb}_{\text{diss}}$ (dpm 100L^{-1}) | $^{210}\text{Po}/^{210}\text{Pb}$ dissolved | | | | |
| Delaware Bay | | | | | | | | | | | | | | |
| 1 | 0.1 | 11.8 | 323 | 7.2 | 1.76 ± 0.19 | 1.85 ± 0.32 | 0.95 ± 0.19 | 1.89 ± 0.24 | 1.81 ± 0.36 | 1.04 ± 0.27 | | | | |
| 1 | 0.1 | 2.4 | 325 | 3.9 | 1.43 ± 0.18 | 2.19 ± 0.35 | 0.65 ± 0.13 | 1.35 ± 0.26 | 1.95 ± 0.52 | 0.69 ± 0.15 | | | | |
| 3 | 2.0 | 10.4 | 319 | 21.1 | 1.56 ± 0.14 | 3.02 ± 0.21 | 0.52 ± 0.11 | 1.44 ± 0.23 | 3.10 ± 0.20 | 0.46 ± 0.13 | | | | |
| 3 | 2.0 | 2.8 | 321 | 18.0 | 1.70 ± 0.22 | 3.23 ± 0.39 | 0.53 ± 0.09 | 1.93 ± 0.27 | 3.19 ± 0.42 | 0.61 ± 0.13 | | | | |
| 5 | 7.2 | 2.0 | 320 | 31.3 | 2.58 ± 0.23 | 1.37 ± 0.28 | 1.89 ± 0.43 | 2.29 ± 0.22 | 1.39 ± 0.30 | 1.65 ± 0.35 | | | | |
| 10 | 6.7 | 1.8 | 327 | 21.7 | 1.92 ± 0.20 | 2.10 ± 0.33 | 0.92 ± 0.17 | 1.63 ± 0.31 | 2.27 ± 0.42 | 0.72 ± 0.14 | | | | |
| 10 | 8.5 | 9.1 | 319 | 34.1 | 1.96 ± 0.22 | 2.10 ± 0.40 | 0.93 ± 0.21 | 1.55 ± 0.41 | 2.15 ± 0.42 | 0.72 ± 0.16 | | | | |
| 11 | 8.2 | 2.0 | 337 | 17.1 | 2.27 ± 0.22 | 3.23 ± 0.40 | 0.70 ± 0.11 | 2.19 ± 0.25 | 3.28 ± 0.36 | 0.67 ± 0.38 | | | | |
| 11 | 12.4 | 10.0 | 315 | 24.5 | 2.04 ± 0.20 | 1.70 ± 0.28 | 1.20 ± 0.23 | 1.95 ± 0.37 | 2.03 ± 0.45 | 0.96 ± 0.52 | | | | |
| 12 | 16.5 | 12.9 | 315 | 26.5 | 2.47 ± 0.23 | 3.79 ± 0.40 | 0.65 ± 0.09 | 2.30 ± 0.28 | 3.61 ± 0.34 | 0.64 ± 0.66 | | | | |
| 12 | 10.9 | 2.2 | 342 | 26.4 | 1.77 ± 0.20 | 0.98 ± 0.30 | 1.80 ± 0.59 | 1.84 ± 0.30 | 1.01 ± 0.35 | 1.82 ± 0.51 | | | | |
| 13 | 12.3 | 2.2 | 353 | 19.4 | 2.21 ± 0.21 | 1.32 ± 0.29 | 1.68 ± 0.40 | 1.95 ± 0.24 | 1.41 ± 0.29 | 1.38 ± 0.28 | | | | |
| 13 | 15.4 | 10.1 | 300 | 21.3 | 2.30 ± 0.22 | 1.27 ± 0.30 | 1.82 ± 0.47 | 2.09 ± 0.26 | 1.31 ± 0.25 | 1.60 ± 0.36 | | | | |
| 14 | 21.5 | 2.1 | 308 | 22.8 | 2.54 ± 0.24 | 1.62 ± 0.30 | 1.57 ± 0.33 | 2.30 ± 0.30 | 1.71 ± 0.29 | 1.35 ± 0.31 | | | | |
| 14 | 16.2 | 15.4 | 347 | 21.9 | 2.17 ± 0.21 | 2.42 ± 0.35 | 0.89 ± 0.15 | 2.30 ± 0.27 | 2.54 ± 0.33 | 0.91 ± 0.20 | | | | |
| 15 | 18.8 | 2.0 | 330 | 10.4 | 4.73 ± 0.36 | 3.88 ± 0.41 | 1.22 ± 0.16 | 3.73 ± 0.37 | 3.78 ± 0.32 | 0.99 ± 0.12 | | | | |
| 15 | 23.7 | 14.3 | 307 | 12.2 | 2.12 ± 0.21 | 1.96 ± 0.32 | 1.08 ± 0.21 | 1.88 ± 0.20 | 2.07 ± 0.21 | 0.91 ± 0.13 | | | | |
| 16 | 25.5 | 2.1 | 306 | 12.0 | 3.90 ± 0.34 | 2.83 ± 0.35 | 1.38 ± 0.21 | 2.48 ± 0.23 | 2.86 ± 0.33 | 0.87 ± 0.26 | | | | |
| 16 | 21.5 | 11.7 | 318 | 10.6 | 2.59 ± 0.23 | 1.58 ± 0.30 | 1.64 ± 0.35 | 2.51 ± 0.19 | 1.62 ± 0.30 | 1.55 ± 0.24 | | | | |
| 17 | 24.1 | 1.9 | 310 | 10.6 | 3.16 ± 0.28 | 3.05 ± 0.38 | 1.03 ± 0.16 | 3.11 ± 0.25 | 3.25 ± 0.32 | 0.96 ± 0.11 | | | | |
| 17 | 26.0 | 12.1 | 301 | 10.9 | 3.36 ± 0.28 | 2.85 ± 0.37 | 1.18 ± 0.18 | 3.33 ± 0.22 | 2.89 ± 0.21 | 1.15 ± 0.15 | | | | |
| 18 | 26.3 | 2.0 | 306 | 10.6 | 4.45 ± 0.35 | 2.16 ± 0.32 | 2.06 ± 0.35 | 3.58 ± 0.31 | 2.37 ± 0.50 | 1.51 ± 0.12 | | | | |
| 19 | 28.2 | 2.0 | 297 | 11.1 | 3.29 ± 0.28 | 1.63 ± 0.29 | 2.02 ± 0.40 | 3.04 ± 0.22 | 1.69 ± 0.23 | 1.79 ± 0.20 | | | | |
| 20 | 31.8 | 1.6 | 297 | 17.0 | 2.48 ± 0.21 | 2.16 ± 0.31 | 1.15 ± 0.19 | 2.18 ± 0.27 | 2.22 ± 0.33 | 0.98 ± 0.21 | | | | |
| 21 | 30.4 | 2.0 | 295 | 8.0 | 2.21 ± 0.22 | 1.75 ± 0.23 | 1.26 ± 0.11 | 2.16 ± 0.31 | 1.89 ± 0.31 | 1.15 ± 0.17 | | | | |
| 21 | 31.0 | 15.3 | 292 | 7.0 | 2.68 ± 0.24 | 1.23 ± 0.29 | 2.18 ± 0.54 | 2.73 ± 0.28 | 1.24 ± 0.23 | 2.20 ± 0.34 | | | | |
| SMS 1 | 5.2 | 2.0 | - | - | 1.46 ± 0.17 | 1.29 ± 0.29 | 1.13 ± 0.29 | 1.41 ± 0.32 | 1.21 ± 0.41 | 1.17 ± 0.11 | | | | |
| SMS 2 | 10.3 | 2.0 | - | - | 1.96 ± 0.19 | 1.64 ± 0.34 | 1.20 ± 0.27 | 1.61 ± 0.27 | 1.52 ± 0.21 | 1.06 ± 0.14 | | | | |
| SMS 3 | 13.2 | 2.0 | - | - | 2.44 ± 0.23 | 1.28 ± 0.30 | 1.90 ± 0.48 | 1.90 ± 0.24 | 1.29 ± 0.25 | 1.47 ± 0.15 | | | | |
| SMS 4 | 15.1 | 2.0 | - | - | 1.34 ± 0.16 | 1.03 ± 0.29 | 1.30 ± 0.40 | 1.40 ± 0.22 | 1.09 ± 0.34 | 1.28 ± 0.31 | | | | |
| SMS 5 | 17.6 | 2.0 | - | - | 2.48 ± 0.26 | 3.83 ± 0.48 | 0.65 ± 0.11 | 2.53 ± 0.26 | 3.79 ± 0.32 | 0.67 ± 0.20 | | | | |
| SMS 6 | 21.2 | 2.0 | - | - | 1.53 ± 0.17 | 1.68 ± 0.32 | 0.91 ± 0.20 | 1.65 ± 0.25 | 1.60 ± 0.32 | 1.03 ± 0.21 | | | | |
| SMS 7 | 23.3 | 2.0 | - | - | 4.26 ± 0.31 | 2.14 ± 0.35 | 1.99 ± 0.36 | 4.35 ± 0.22 | 2.14 ± 0.29 | 2.03 ± 0.21 | | | | |
| SMS 8 | 25.9 | 2.0 | - | - | 3.93 ± 0.33 | 2.00 ± 0.32 | 1.96 ± 0.35 | 4.13 ± 0.37 | 2.11 ± 0.75 | 1.95 ± 0.06 | | | | |
| Chesapeake Bay | | | | | | | | | | | | | | |
| CB 01 | 12.70 | 4.8 | 27 | 188 | 2.10 ± 0.23 | 1.17 ± 0.29 | 1.79 ± 0.48 | 2.20 ± 0.22 | 1.20 ± 0.15 | 1.84 ± 0.30 | | | | |
| CB 01 | 14.20 | 10.4 | 130 | 10.2 | 1.37 ± 0.21 | 0.61 ± 0.30 | 2.23 ± 1.14 | 1.40 ± 0.42 | 0.74 ± 0.34 | 1.90 ± 0.57 | | | | |
| CB 01 | 15.90 | 17.7 | 34 | 11.8 | 2.83 ± 0.25 | 0.89 ± 0.33 | 3.18 ± 1.20 | 2.20 ± 0.21 | 0.91 ± 0.20 | 2.42 ± 0.20 | | | | |
| CB 01 | 17.10 | 22.0 | 2 | 14.4 | 2.18 ± 0.19 | 0.73 ± 0.30 | 2.97 ± 1.24 | 1.98 ± 0.19 | 0.78 ± 0.23 | 2.54 ± 0.24 | | | | |
| CB 02 | 13.08 | 3.0 | 153 | 19.1 | 1.51 ± 0.19 | 0.60 ± 0.29 | 2.51 ± 1.23 | 1.39 ± 0.23 | 0.57 ± 0.17 | 2.44 ± 0.29 | | | | |
| CB 02 | 14.19 | 8.2 | 71 | 16.1 | 4.44 ± 0.36 | 3.01 ± 0.50 | 1.48 ± 0.28 | 3.03 ± 0.34 | 3.04 ± 0.42 | 1.00 ± 0.12 | | | | |
| CB 02 | 15.50 | 13.9 | 41 | 13.6 | 2.70 ± 0.29 | 1.04 ± 0.50 | 2.60 ± 1.29 | 2.11 ± 0.22 | 1.06 ± 0.13 | 1.99 ± 0.18 | | | | |
| CB 02 | 17.03 | 21.9 | 1 | 15.7 | 1.07 ± 0.21 | 4.33 ± 1.00 | 0.25 ± 0.07 | 0.55 ± 0.20 | 4.25 ± 0.61 | 0.13 ± 0.11 | | | | |
| CB 02 | 17.03 | 21.5 | 1 | 11.4 | 1.27 ± 0.31 | 0.39 ± 0.32 | 3.22 ± 2.74 | 1.09 ± 0.26 | 0.38 ± 0.47 | 2.86 ± 0.23 | | | | |
| CB 03 | 10.80 | 0.8 | 142 | 37.1 | 1.65 ± 0.24 | 2.69 ± 0.40 | 0.61 ± 0.13 | 1.37 ± 0.28 | 2.68 ± 0.45 | 0.51 ± 0.12 | | | | |
| CB 03 | 13.30 | 9.1 | 23 | 26.7 | 2.48 ± 0.23 | 0.53 ± 0.30 | 4.70 ± 2.70 | 2.13 ± 0.22 | 0.60 ± 0.14 | 3.57 ± 0.27 | | | | |
| CB 04 | 8.01 | 1.1 | 188 | 31.6 | 1.40 ± 0.18 | 0.71 ± 0.31 | 1.97 ± 0.90 | 1.58 ± 0.25 | 0.76 ± 0.18 | 2.08 ± 0.35 | | | | |
| CB 04 | 6.60 | 1.9 | 177 | 27.7 | 1.95 ± 0.26 | 2.42 ± 0.46 | 0.81 ± 0.18 | 1.85 ± 0.25 | 2.64 ± 0.32 | 0.70 ± 0.22 | | | | |
| CB 05 | 10.02 | 9.1 | 96 | 41.5 | 2.00 ± 0.32 | 0.95 ± 0.46 | 2.11 ± 1.07 | 1.77 ± 0.36 | 0.94 ± 0.81 | 1.88 ± 0.15 | | | | |
| CB 05 | 3.20 | 0.5 | 175 | 25.0 | 0.83 ± 0.16 | 0.44 ± 0.28 | 1.90 ± 1.29 | 0.72 ± 0.19 | 0.50 ± 0.16 | 1.44 ± 0.14 | | | | |
| CB 06 | 2.06 | 0.5 | 172 | 30.0 | 2.55 ± 0.38 | 1.10 ± 0.49 | 2.32 ± 1.08 | 2.00 ± 0.34 | 1.15 ± 0.24 | 1.74 ± 0.26 | | | | |
| CB 06 | 3.14 | 9.0 | 155 | 51.9 | 2.09 ± 0.22 | 0.92 ± 0.35 | 2.27 ± 0.88 | 1.89 ± 0.19 | 1.07 ± 0.26 | 1.77 ± 0.34 | | | | |

Table 1.2: The dissolved ^{210}Po and ^{210}Pb activities ($\text{dpm } 100\text{L}^{-1}$) for Canary Creek salt marsh (RI and CC) and the North Atlantic offshore station with associated errors for the $\text{Fe}(\text{OH})_3$ and Co-APDC scavenging methods.

| Station | Salinity | Tidal Height | Oxygen ($\mu\text{mol/l}$) | Fe(OH) ₃ Co-Precipitation Method | | | | | Co-APDC Co-Precipitation Method | | | | |
|--------------------------------|----------|--------------|------------------------------|----------------------------------------------------------------------|----------------------------------------------------------------------|---------------------------------------------|--------------|--------------|----------------------------------------------------------------------|----------------------------------------------------------------------|---------------------------------------------|--|--|
| | | | | $^{210}\text{Po}_{\text{diss}}$ ($\text{dpm } 100 \text{ l}^{-1}$) | $^{210}\text{Pb}_{\text{diss}}$ ($\text{dpm } 100 \text{ l}^{-1}$) | $^{210}\text{Po}/^{210}\text{Pb}$ dissolved | | | $^{210}\text{Po}_{\text{diss}}$ ($\text{dpm } 100 \text{ l}^{-1}$) | $^{210}\text{Pb}_{\text{diss}}$ ($\text{dpm } 100 \text{ l}^{-1}$) | $^{210}\text{Po}/^{210}\text{Pb}$ dissolved | | |
| RI01 | 26.8 | flooding | 5.3 | 4.33 ± 0.33 | 1.74 ± 0.35 | 2.48 ± 0.54 | 1.63 ± 0.49 | 1.57 ± 0.19 | 1.03 ± 0.05 | | | | |
| RI02 | 27.4 | ebbing | 4.9 | 3.51 ± 0.31 | 1.24 ± 0.39 | 2.84 ± 0.53 | 3.55 ± 0.34 | 1.10 ± 0.26 | 3.22 ± 0.31 | | | | |
| RI03 | 27.6 | ebbing | 2.2 | 5.79 ± 0.49 | 3.84 ± 0.45 | 1.51 ± 0.22 | 4.83 ± 0.64 | 3.71 ± 0.37 | 1.30 ± 0.35 | | | | |
| RI04 | 27.4 | ebbing | 3.4 | 2.79 ± 0.25 | 1.91 ± 0.36 | 1.46 ± 0.30 | 2.43 ± 0.38 | 2.05 ± 0.35 | 1.18 ± 0.28 | | | | |
| RI05 | 25.8 | ebbing | 2.0 | 9.95 ± 0.82 | 11.57 ± 1.05 | 0.86 ± 0.11 | 3.75 ± 0.34 | 12.49 ± 1.08 | 0.30 ± 0.06 | | | | |
| RI06 | 25.7 | slack low | 2.1 | 5.03 ± 0.40 | 4.20 ± 0.48 | 1.20 ± 0.17 | 2.46 ± 0.67 | 4.16 ± 0.72 | 0.59 ± 0.09 | | | | |
| RI07 | 27.9 | flooding | 2.1 | 3.46 ± 0.29 | 2.45 ± 0.55 | 1.41 ± 0.34 | 1.25 ± 0.45 | 2.18 ± 0.46 | 0.57 ± 0.09 | | | | |
| RI08 | 28.1 | flooding | 1.1 | 3.27 ± 0.31 | 2.63 ± 0.73 | 1.25 ± 0.37 | 3.79 ± 0.37 | 2.61 ± 0.37 | 1.45 ± 0.38 | | | | |
| CC01 | 21.7 | flooding | 2.7 | 6.68 ± 0.58 | 6.36 ± 0.68 | 1.05 ± 0.14 | 6.62 ± 0.18 | 6.49 ± 0.16 | 1.02 ± 0.17 | | | | |
| CC02 | 23.2 | ebbing | 3.6 | 3.87 ± 0.42 | 7.21 ± 0.83 | 0.54 ± 0.08 | 3.04 ± 0.14 | 7.33 ± 0.24 | 0.41 ± 0.09 | | | | |
| CC03 | 21.2 | ebbing | 1.7 | 6.13 ± 0.69 | 6.35 ± 0.69 | 0.96 ± 0.15 | 5.85 ± 0.65 | 6.48 ± 1.34 | 0.90 ± 0.23 | | | | |
| CC04 | 20.2 | ebbing | 3.0 | 6.69 ± 1.06 | 13.82 ± 1.52 | 0.48 ± 0.09 | 3.61 ± 0.93 | 8.35 ± 0.97 | 0.43 ± 0.12 | | | | |
| CC05 | 19.5 | ebbing | 2.2 | 4.78 ± 0.65 | 5.54 ± 0.70 | 0.86 ± 0.16 | 6.30 ± 0.98 | 5.65 ± 0.90 | 1.11 ± 0.14 | | | | |
| CC06 | 18.2 | slack low | 1.9 | 8.28 ± 0.73 | 4.62 ± 0.65 | 1.79 ± 0.30 | 6.92 ± 1.10 | 4.84 ± 0.56 | 1.43 ± 0.32 | | | | |
| RI11 | 27.3 | flooding | 1.1 | 2.00 ± 0.23 | 13.11 ± 1.09 | 0.15 ± 0.02 | 1.25 ± 0.21 | 13.22 ± 1.48 | 0.09 ± 0.01 | | | | |
| RI13 | 26.5 | slack low | 3.6 | 3.66 ± 0.30 | 2.07 ± 0.33 | 1.77 ± 0.32 | 3.19 ± 0.38 | 2.19 ± 0.20 | 1.46 ± 0.24 | | | | |
| RI13 | 26.5 | flooding | 1.7 | 3.56 ± 0.31 | 2.01 ± 0.23 | 1.77 ± 0.21 | 3.11 ± 0.31 | 2.06 ± 0.27 | 1.51 ± 0.28 | | | | |
| RI14 | 25.6 | slack low | 3.0 | 4.14 ± 0.34 | 2.62 ± 0.34 | 1.58 ± 0.24 | 4.02 ± 0.40 | 2.59 ± 0.36 | 1.55 ± 0.36 | | | | |
| RI15 | 26.7 | slack low | 5.3 | 3.60 ± 0.30 | 2.90 ± 0.37 | 1.24 ± 0.19 | 3.27 ± 0.25 | 2.98 ± 0.29 | 1.10 ± 0.20 | | | | |
| RI16 | 30.1 | flooding | 4.9 | 3.23 ± 0.26 | 1.81 ± 0.34 | 1.79 ± 0.37 | 3.38 ± 0.37 | 1.74 ± 0.31 | 1.95 ± 0.31 | | | | |
| North Atlantic Offshore | | | | | | | | | | | | | |
| 8/2/11 | 33.5 | 1.0 | 200 | 1.74 ± 1.77 | 9.63 ± 0.77 | 0.18 ± 0.18 | 1.67 ± 1.72 | 10.42 ± 0.83 | 0.16 ± 0.17 | | | | |
| | 33.5 | 1.0 | 200 | 6.36 ± 1.06 | 9.55 ± 0.80 | 0.67 ± 0.12 | 5.74 ± 1.10 | 9.79 ± 0.82 | 0.59 ± 0.12 | | | | |
| | 33.5 | 1.0 | 200 | 3.32 ± 1.04 | 9.42 ± 0.81 | 0.35 ± 0.11 | 5.45 ± 1.11 | 9.72 ± 0.83 | 0.56 ± 0.12 | | | | |
| | 33.5 | 1.0 | 200 | 4.44 ± 1.28 | 13.95 ± 1.11 | 0.32 ± 0.10 | 5.51 ± 1.07 | 9.50 ± 0.82 | 0.58 ± 0.12 | | | | |
| | 33.9 | 15.0 | 198 | 4.28 ± 0.31 | 9.01 ± 0.78 | 0.47 ± 0.05 | 5.23 ± 0.37 | 9.55 ± 0.82 | 0.55 ± 0.06 | | | | |
| | 33.9 | 15.0 | 198 | 4.43 ± 0.31 | 8.19 ± 0.72 | 0.54 ± 0.06 | 5.20 ± 0.37 | 9.47 ± 0.83 | 0.55 ± 0.06 | | | | |
| | 33.9 | 15.0 | 198 | 4.51 ± 0.32 | 8.65 ± 0.76 | 0.52 ± 0.06 | 5.78 ± 0.39 | 8.75 ± 0.77 | 0.66 ± 0.07 | | | | |
| | 34.9 | 2000.0 | 252 | 4.51 ± 0.32 | 5.19 ± 0.50 | 0.87 ± 0.10 | 4.83 ± 0.41 | 4.29 ± 0.46 | 1.12 ± 0.15 | | | | |
| | 34.9 | 2000.0 | 252 | 4.05 ± 0.30 | 4.49 ± 0.46 | 0.90 ± 0.11 | 5.60 ± 0.41 | 5.13 ± 0.52 | 1.09 ± 0.14 | | | | |
| | 34.9 | 2000.0 | 252 | 4.33 ± 0.32 | 5.46 ± 0.52 | 0.79 ± 0.10 | 5.90 ± 0.41 | 4.99 ± 0.51 | 1.18 ± 0.15 | | | | |
| 11/3/11 | 33.4 | 1.0 | 200 | 2.73 ± 1.63 | 16.60 ± 1.29 | 0.16 ± 0.10 | 4.54 ± 1.50 | 18.65 ± 1.45 | 0.24 ± 0.08 | | | | |
| | 33.4 | 1.0 | 200 | 3.01 ± 1.36 | 17.45 ± 1.40 | 0.17 ± 0.08 | 2.88 ± 0.63 | 6.07 ± 0.53 | 0.47 ± 0.11 | | | | |
| | 33.4 | 1.0 | 200 | 1.11 ± 0.53 | 5.95 ± 0.52 | 0.19 ± 0.09 | 8.91 ± 1.52 | 12.70 ± 1.07 | 0.70 ± 0.13 | | | | |
| | 34.1 | 15.0 | 227 | 2.55 ± 0.39 | 2.29 ± 0.33 | 1.11 ± 0.24 | 2.51 ± 0.41 | 3.47 ± 0.37 | 0.72 ± 0.14 | | | | |
| | 34.5 | 15.0 | 225 | 3.04 ± 0.48 | 3.00 ± 0.41 | 1.01 ± 0.21 | 3.72 ± 0.44 | 2.01 ± 0.31 | 1.85 ± 0.36 | | | | |
| | 35.6 | 30.0 | 153 | 5.63 ± 0.78 | 4.92 ± 0.60 | 1.14 ± 0.21 | 4.59 ± 0.68 | 4.81 ± 0.59 | 0.95 ± 0.18 | | | | |
| | 35.5 | 50.0 | 163 | 3.73 ± 0.67 | 5.05 ± 0.54 | 0.74 ± 0.15 | 3.05 ± 0.66 | 5.67 ± 0.58 | 0.54 ± 0.13 | | | | |
| | 35.5 | 100.0 | 143 | 4.32 ± 0.61 | 3.98 ± 0.47 | 1.09 ± 0.20 | 11.51 ± 0.86 | 0.62 ± 0.35 | 18.61 ± 10.71 | | | | |
| | 35.6 | 150.0 | 181 | 2.47 ± 0.69 | 6.37 ± 0.64 | 0.39 ± 0.11 | 5.89 ± 0.87 | 7.47 ± 0.73 | 0.79 ± 0.14 | | | | |
| | 35.6 | 200.0 | 209 | 24.24 ± 2.63 | 27.52 ± 1.84 | 0.88 ± 0.11 | 55.44 ± 7.43 | 65.11 ± 3.96 | 0.85 ± 0.13 | | | | |
| 8/21/13 | 35.1 | 5.8 | 181 | 3.97 ± 0.41 | 9.31 ± 0.78 | 0.43 ± 0.06 | 2.50 ± 0.34 | 10.84 ± 1.40 | 0.23 ± 0.04 | | | | |
| | 36.1 | 77.0 | 132 | 9.24 ± 0.70 | 5.76 ± 0.60 | 1.60 ± 0.21 | 8.24 ± 0.72 | 7.91 ± 1.23 | 1.04 ± 0.19 | | | | |
| | 35.3 | 150.0 | 118 | 5.21 ± 0.36 | 2.19 ± 0.34 | 2.38 ± 0.40 | 6.15 ± 0.41 | 4.28 ± 0.52 | 1.44 ± 0.20 | | | | |
| | 35.3 | 199.0 | 127 | 4.82 ± 0.39 | 4.42 ± 0.53 | 1.09 ± 0.16 | 4.91 ± 0.38 | 4.06 ± 0.45 | 1.21 ± 0.17 | | | | |
| | 35.1 | 272.0 | 151 | 3.83 ± 0.36 | 5.77 ± 0.75 | 0.66 ± 0.11 | 4.94 ± 0.39 | 5.37 ± 0.67 | 0.92 ± 0.14 | | | | |
| | 35.0 | 350.0 | 187 | 6.54 ± 0.56 | 10.14 ± 0.93 | 0.64 ± 0.08 | 7.94 ± 0.67 | 7.96 ± 0.82 | 1.00 ± 0.13 | | | | |
| | 35.0 | 386.0 | 203 | 4.70 ± 0.38 | 7.47 ± 0.69 | 0.63 ± 0.08 | 4.65 ± 0.39 | 5.32 ± 0.66 | 0.87 ± 0.13 | | | | |
| | 35.0 | 503.0 | 216 | 4.10 ± 0.34 | 5.09 ± 0.54 | 0.81 ± 0.11 | 6.23 ± 0.45 | 6.29 ± 0.79 | 0.99 ± 0.14 | | | | |

Table 1.3: Scavenging efficiencies of ^{209}Po and associated errors for $\text{Fe}(\text{OH})_3$, Co-APDC and MnO_2 methods used with filtered water samples from the Delaware Bay(DB), Chesapeake Bay(CB), Intertidal salt marsh(DSM) and North Atlantic (NA).

| Scavenging Method | Location | n | Average ^{209}Po Scavenging Efficiency | Counting Error \pm | Scaveneing Efficiency Standard Deviation | Relative Standard Deviation |
|--------------------------|----------|----|-------------------------------------------------|----------------------|------------------------------------------|-----------------------------|
| $\text{Fe}(\text{OH})_3$ | DB | 37 | 46% | 2% | 11% | 24% |
| Co-APDC | DB | 37 | 60% | 3% | 25% | 41% |
| $\text{Fe}(\text{OH})_3$ | CB | 17 | 40% | 2% | 19% | 47% |
| Co-APDC | CB | 17 | 73% | 4% | 25% | 35% |
| $\text{Fe}(\text{OH})_3$ | DSM | 24 | 36% | 2% | 19% | 52% |
| Co-APDC | DSM | 24 | 61% | 5% | 27% | 45% |
| $\text{Fe}(\text{OH})_3$ | NA | 29 | 68% | 3% | 21% | 31% |
| Co-APDC | NA | 29 | 66% | 3% | 22% | 33% |
| $\text{Mn}(\text{O}_2)$ | NA | 22 | 60% | 2% | 18% | 31% |

FIGURES

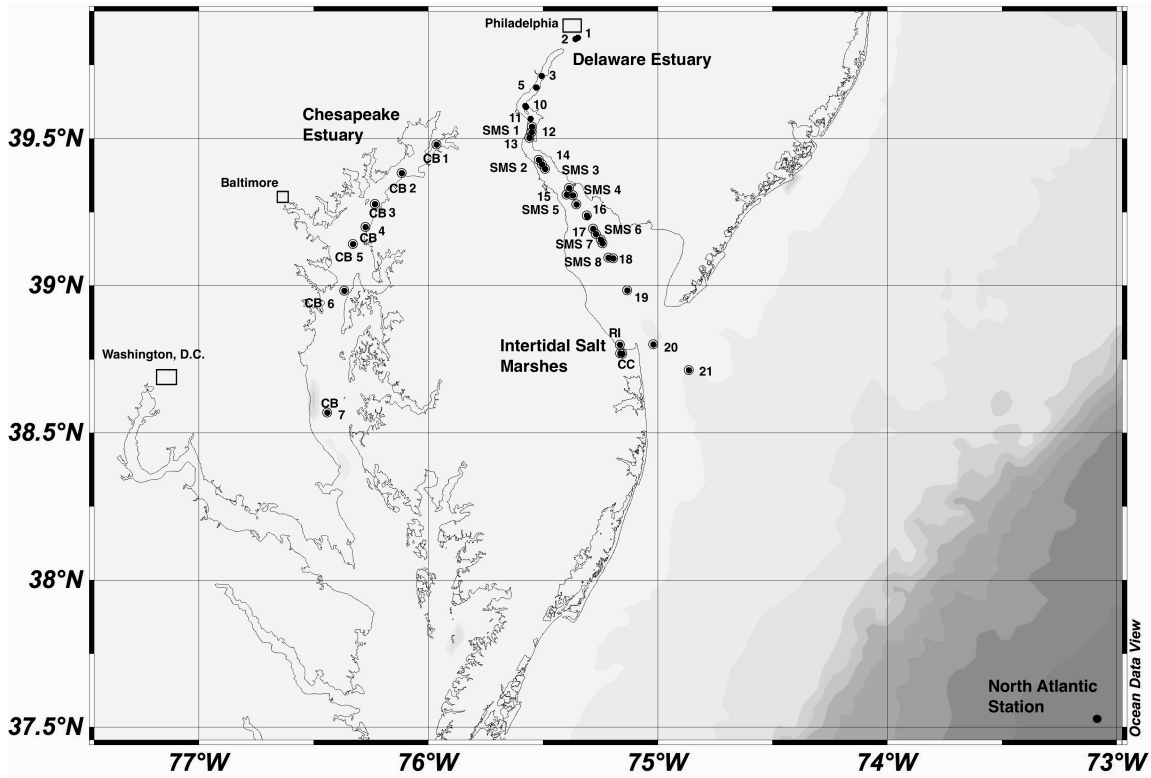


Figure 1.1: Samples for this study were collected at each station as numbered with corresponding data in Tables 1 & 2. Samples were collected as follows: Delaware estuary 2012 April 1-3, Delaware salt marsh two locations over a 12hr tidal cycle 2012 June 1, Chesapeake estuary 2012 August 20-25 and single North Atlantic site sampled three times (Aug. 2011, Nov. 2011 and Aug. 2012).

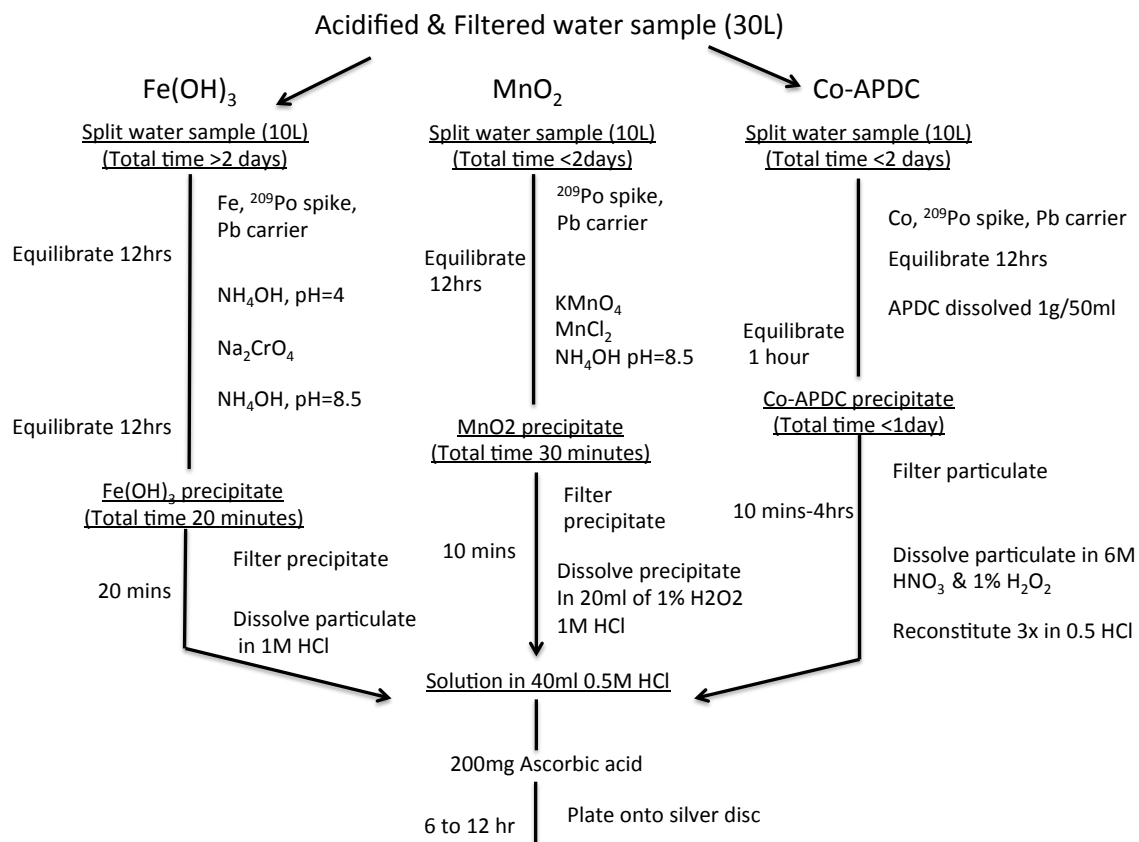


Figure 1.2: Protocol for ^{210}Po and ^{210}Pb activity measurement in dissolved seawater samples with different scavenging method up to the first plating

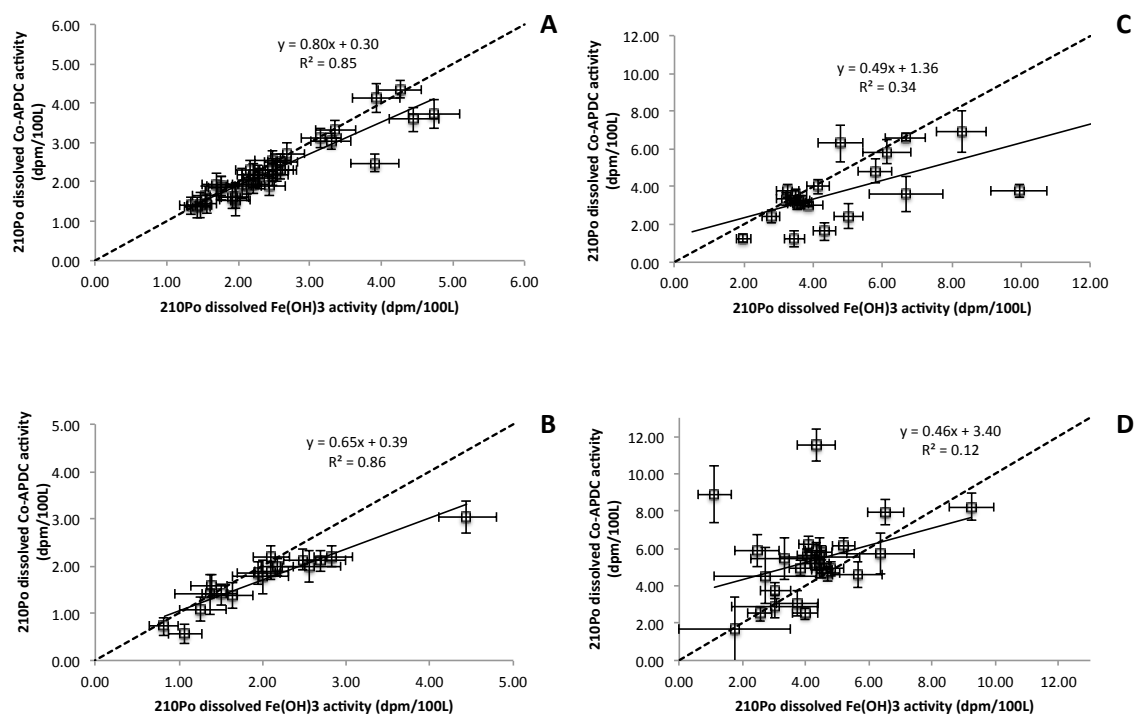


Figure 1.3: The activities (dpm/100L) of $\text{Fe}(\text{OH})_3$ vs Co-APDC scavenging methods for ^{210}Po . A 1:1 line (dashed) and linear regression (solid) for A) Delaware Bay, B) Chesapeake Bay; C) Delaware Intertidal Marsh; D) Offshore. Note that methods agree well in panels A and B but less so in C and D. Offshore samples are unique because Co-APDC yields higher ^{210}Po final activities than $\text{Fe}(\text{OH})_3$.

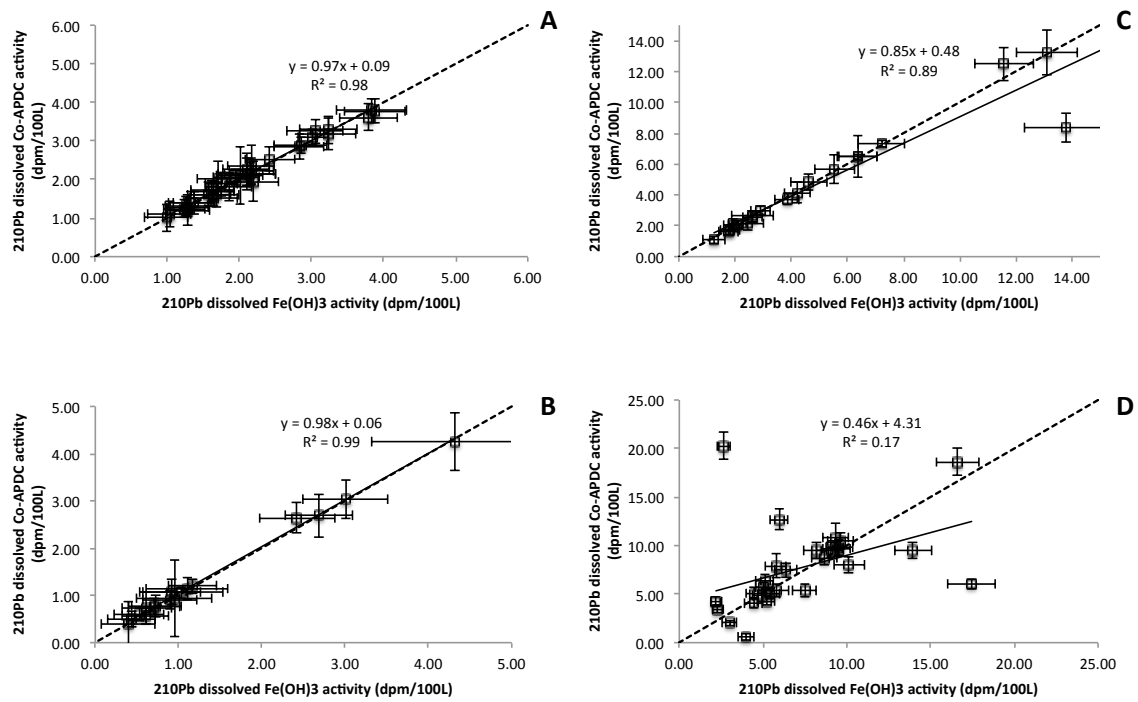


Figure 1.4 The activities (dpm/100L) of $\text{Fe}(\text{OH})_3$ vs Co-APDC scavenging methods for ^{210}Pb . A 1:1 line (dashed) and linear regression (solid) for A) Delaware Bay, B) Chesapeake Bay; C) Intertidal Marsh; D) Offshore. The data shows ^{210}Pb results are comparable through most regions, but some differences can occur offshore.

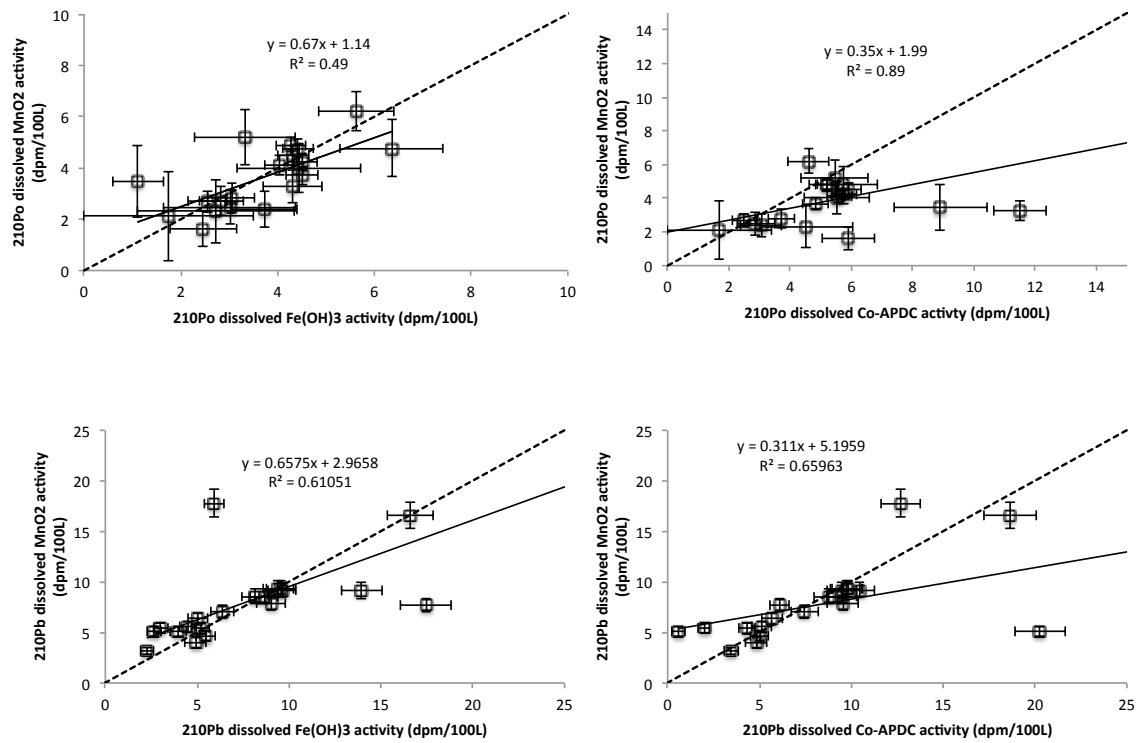


Figure 1.5: The activities (dpm/100L) of Fe(OH)₃ and Co-APDC vs. MnO₂ scavenging methods for ²¹⁰Po and ²¹⁰Pb with A 1:1 line (dashed) and linear regression (solid) for offshore samples. The data shows MnO₂ agrees more with Fe(OH)₃ than Co-APDC for both ²¹⁰Po and ²¹⁰Pb.

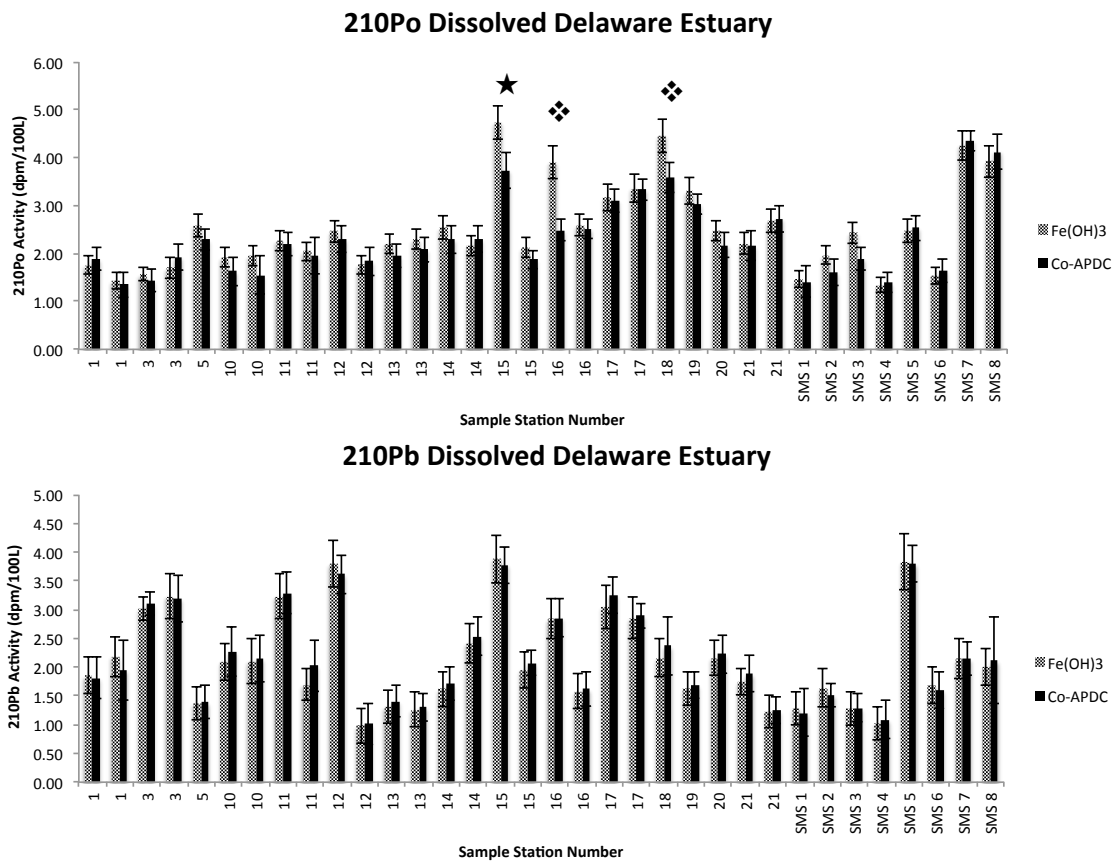
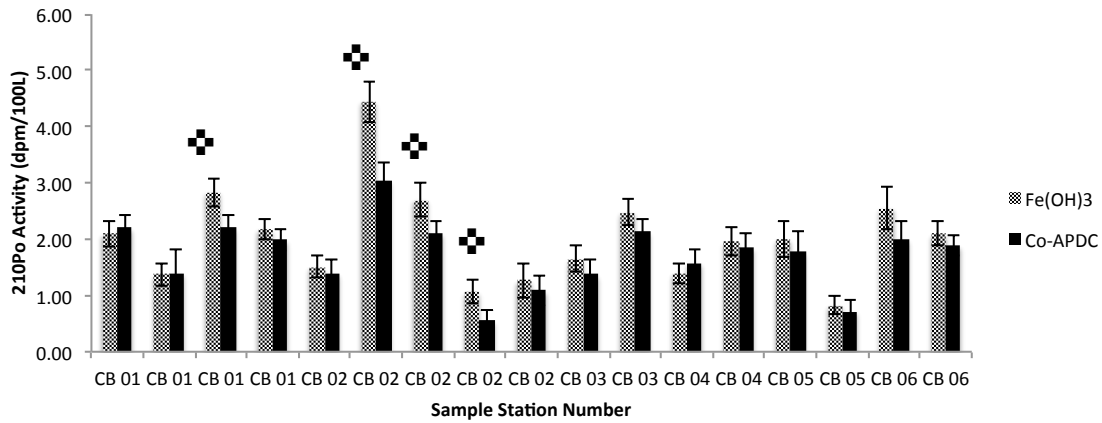


Figure 1.6: Histogram of ²¹⁰Po and ²¹⁰Pb dissolved activity in the Delaware estuary compared between the Fe(OH)₃ and Co-APDC scavenging methods. Sample station numbers are in order of those found in Table 1. The ★ denotes the turbidity maximum and likely highest concentration of humic acid compounds. The ❖ denotes the two locations where a phytoplankton bloom was observed. The ²¹⁰Pb results show that the methods agree within the calculated error through the entire Delaware estuary.

210Po Dissolved Chesapeake Bay



210Pb Dissolved Chesapeake Bay

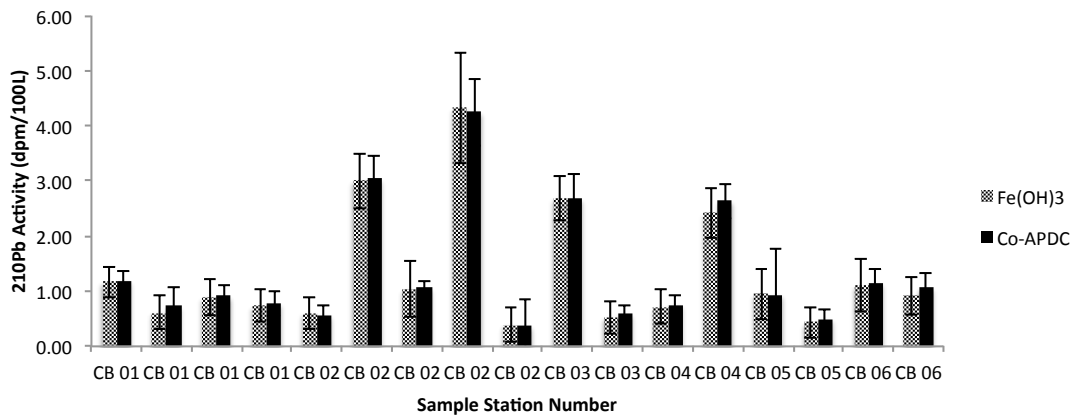


Figure 1.7: Histogram of ²¹⁰Po and ²¹⁰Pb dissolved activity in the Canary Creek salt marsh compared between the Fe(OH)₃ and Co-APDC scavenging methods. Sample station numbers are in order of those found in Table 1. The ◆ denotes lowest observed dissolved oxygen and highest suspended particulate concentration.

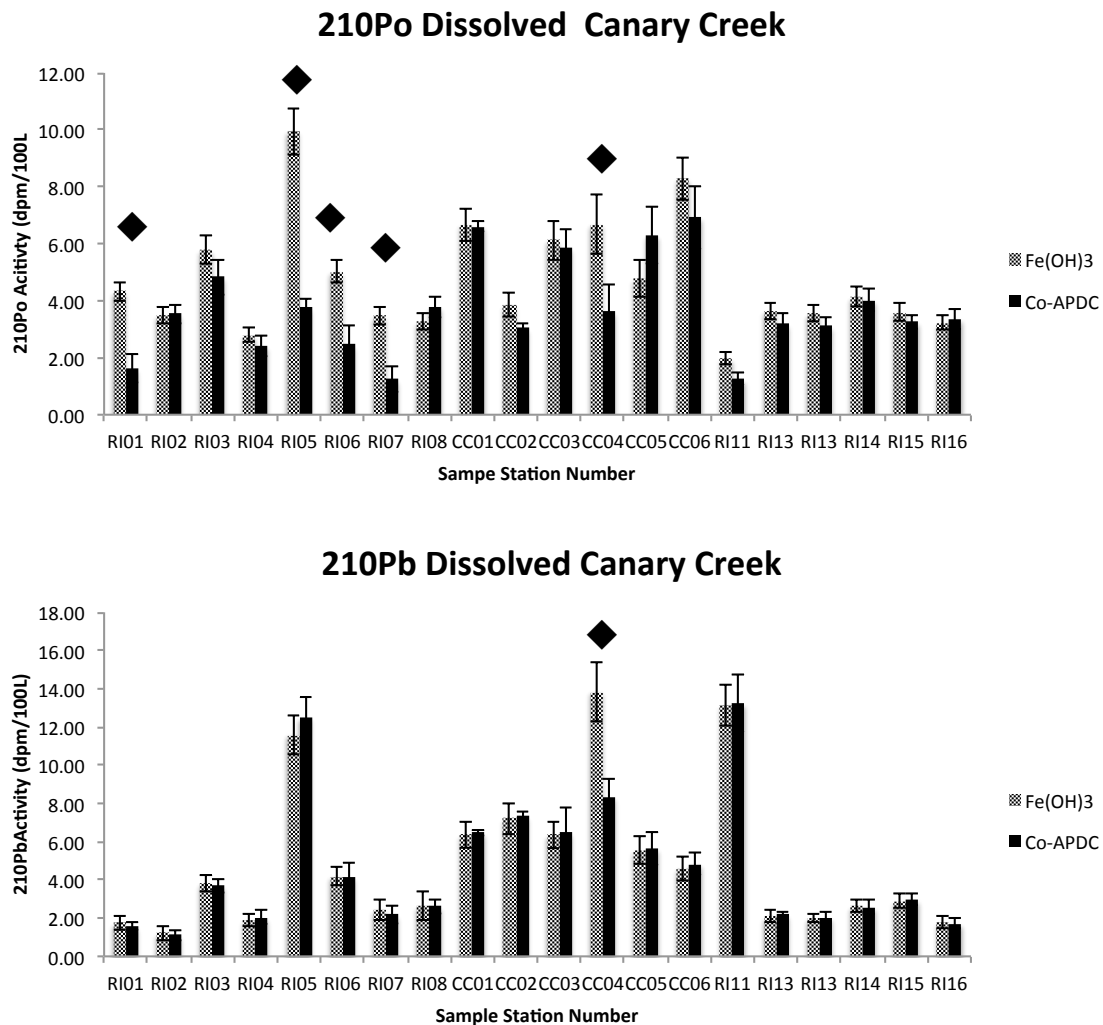
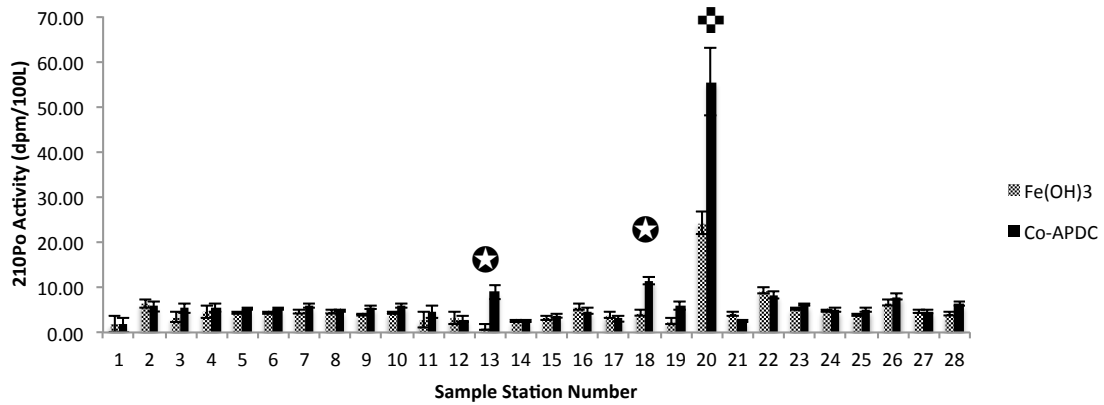


Figure 1.8: Histogram of ^{210}Po and ^{210}Pb dissolved activity in the upper Chesapeake Bay compared between the $\text{Fe}(\text{OH})_3$ and Co-APDC scavenging methods. Sample station numbers are in order of those found in Table 2. The \blacklozenge denotes lowest observed dissolved oxygen concentrations. The ^{210}Pb scavenging by each method shows agreement within the calculated error throughout the Chesapeake Bay.

210Po Dissolved North Atlantic



210Pb Dissolved North Atlantic

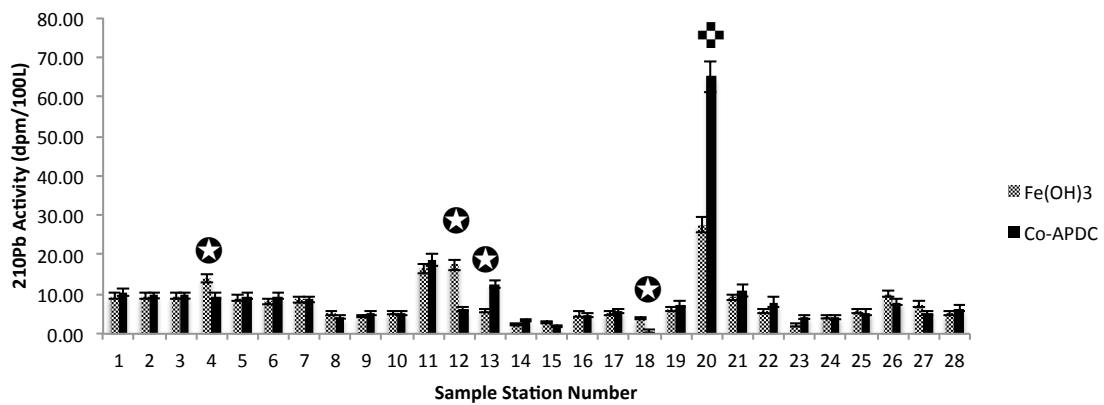


Figure 1.9: Histogram of ²¹⁰Po and ²¹⁰Pb dissolved activity at the North Atlantic offshore site compared between the Fe(OH)₃ and Co-APDC scavenging methods. Sample station numbers are in order of those found in Table 2. The ✚ denotes lowest observed dissolved oxygen concentrations. The ★ denotes surface waters at 1 to 15 meters.

Chapter 2

ESTUARINE AND COASTAL BIOGEOCHEMISTRY OF THE NATURAL RADIONUCILDES ^{210}Po AND ^{210}Pb IN THE DELAWARE AND CHESAPEAKE ESTUARIES

Highlights

- 1) Estuarine ^{210}Pb and ^{210}Po data reveal key biogeochemical processes and rates
- 2) Delaware Bay displays regional differentiation due to dominant particle reactions
- 3) Chesapeake Bay displays vertical differentiation from deep sub-oxic redox cycling
- 4) Parent (^{210}Pb) grand-daughter (^{210}Po) disequilibria evidence principle processes
- 5) Net scavenging residence times calculated weeks (Delaware) to months (Chesapeake)

Acknowledgements

-Dr. Luther for providing research cruise time in the Delaware and Chesapeake supported by NSF/OCE grants 1031272 and 1059892.

-Graduate support for D. Marsan was provided by NSF Grant- HRD-1139870- Greater Philadelphia Region LSAMP Bridge to the Doctorate (Cohort IX)

-Post-Doctoral support for S. Rigaud was provided by NSF/OCE grant 0961653.

2.1 Abstract

The natural radionuclides ^{210}Po and ^{210}Pb may be used to identify and quantify the processes by which trace elements are transferred, removed and cycled in the marine environment including coastal and estuarine waters. The Delaware and Chesapeake Bays are two of the largest and most utilized estuaries of the United States with flushing times on the order of months to years, hosting key biogeochemical reactions. The isotopes ^{210}Po and ^{210}Pb were measured in the dissolved and particulate water phases of the Delaware and upper Chesapeake estuaries during the spring and summer of 2012 covering the salinity gradient. The $^{210}\text{Po}/^{210}\text{Pb}$ activity ratio fluctuated from upper to lower estuary from 0.3 to 5. The upper Delaware estuary, near the headwaters, was characterized by suspended particles that scavenged both dissolved ^{210}Po and ^{210}Pb . The Delaware estuary turbidity maximum appears to be the dominant biogeochemical force effecting ^{210}Po and ^{210}Pb distribution between dissolved-particulate phases as reflected in their activity ratios. Surrounding intertidal marshes act as a source for dissolved ^{210}Pb to the estuary. A consecutively sectioned (upper, mid, lower estuary) box-model of the Delaware estuary calculated the dissolved mean scavenging residence time of ^{210}Po to be on the order of 3 weeks. However, for dissolved ^{210}Pb mean scavenging residence times is calculated to decrease from 3 weeks to 10 days from upper to lower estuary. This is also evidenced in parent (^{210}Pb), granddaughter (^{210}Po) disequilibria during biogeochemical processing. On the other hand the upper Chesapeake Bay during summer months was dominated by a $^{210}\text{Po}/^{210}\text{Pb}$ activity ratio of two or greater. The sub-oxic bottom waters of the upper Chesapeake contained larger concentrations of solubilized ^{210}Po and ^{210}Pb , likely due to redox cycling of manganese. A single box-model found mean scavenging residence times in the upper Chesapeake on the order of months for both radionuclides, with ^{210}Po being twice as great as ^{210}Pb .

Keywords

^{210}Po ; ^{210}Pb ; estuaries; salt marsh; Chesapeake Bay; Delaware Bay

2.2 Introduction

Estuaries are among the most important marine systems for the transport of continental materials, including trace elements, to the oceans. The sources of material include natural weathering of continental trace elements, plus anthropogenic discharges from urban areas, which are often located within estuaries. Dissolved and particulate material can enter the estuarine system from rivers, groundwater or atmospheric fallout and radioactive production. Both dissolved and particulate elements are subjected to a series of biogeochemical processes, which can result in significant transfers between the biotic and abiotic phases. Estuaries host biogeochemical processes such as nutrient and carbon cycling along the salinity gradient. Processes associated within the river and seawater mixing zone are well recognized (Church, 1986) but the rates are difficult to establish.

The naturally occurring ^{210}Po and ^{210}Pb radionuclide pair has been widely used to examine dissolved and particle dynamics in marine eco-systems over the past several decades (Bacon et al., 1976; Nozaki, et al. 1976; Thomson and Turekian, 1976; Cochran and Masque, 2003; Rutgers van der Loeff and Moore, 2007). Although the primary use of the radionuclide pair has been in the open ocean, there have been a few studies and applications involving ^{210}Pb and ^{210}Po in the coastal marine environment (Santschi et al., 1979; Church, 1986; Carvalho, 1997). The mechanism for removal includes adsorption (^{210}Po and ^{210}Pb) and absorption (^{210}Po) by suspended particles and organisms respectively. The particulate activities inversely follow the concentration of suspended particles in the estuary including areas of greater biological mass (Church, 1986). Thus the utility of the ^{210}Po and ^{210}Pb radionuclide method is evident, although some limitations exist. Notably that of time-scales, as ^{210}Po is capable of accurately estimating rates only on the order of weeks to months commensurate with its half-life (138d). Also the radionuclide pair is unique in that the major source of the parent ^{210}Pb is from atmospheric deposition, such that the rate of this input must be accurately gauged to estimate ^{210}Pb input to quantify scavenging rates.

This paper presents a comprehensive estuarine data set on the radionuclides ^{210}Po and ^{210}Pb for the two largest U.S. estuaries, the Chesapeake and Delaware estuaries. The Delaware and upper Chesapeake estuaries are unique among major east coast estuaries in the U.S. and can be compared (Figure 2.1). Both are characterized by a single major input, the Delaware and Susquehanna Rivers, respectively. Both host major metropolitan cities of Philadelphia, and Baltimore in the upper estuary region, which can cause significant impact due to anthropogenic industrial impacts. The Delaware estuary is a shallow (10m average depth) single estuary bordered by numerous small intertidal creeks and salt marshes. In contrast the Chesapeake Bay is a composite of several river-estuarine systems, each with individual lithologies and drainage characteristics. It has distinct upper and lower sections, such that its upper part above the Potomac ($38^{\circ} 1'11.8 \text{ N}$; $76^{\circ} 20'8.7 \text{ W}$) is a deep drowned river channel sided by clay cliffs that have the tendency to become sub- to anoxic at depth during the summer time. On average, the Delaware estuary has a flushing time of about 100 days while the Chesapeake can range from 6-12 months, both of which is compatible with the $^{210}\text{Po}/^{210}\text{Pb}$ radionuclide parent-daughter pair (Church and Sarin, 1995). Thus, these two estuaries present two different biogeochemical systems and an overall rationale to use the ^{210}Po and ^{210}Pb radionuclides to study their processes.

Earlier papers summarized the U-Th radionuclides in the Delaware (Church and Sarin, 1995) but only included dissolved surface concentrations of the ^{210}Po and ^{210}Pb isotopes. Here we present surface and depth data of ^{210}Po and ^{210}Pb in the dissolved and particulate phases throughout the salinity gradients of the Delaware and upper Chesapeake estuary. This is supported by physiochemical water parameters including temperature, salinity, dissolved oxygen, fluorescence, suspended mater, particulate organic carbon and nitrogen (POC, PON), and major nutrients (NO_3^- , NH_4^+ , PO_4^{3-} and Si) concentrations.

The main objectives of this paper are to 1) identify the main biogeochemical processes controlling ^{210}Po and ^{210}Pb cycling in the estuarine environment and 2) use the radionuclide pair to quantify biogeochemical processes and dissolved-particulate exchange rates 3) assess the role of pervasive intertidal salt marshes in

affecting the radionuclide chemistry of the lower Delaware Bay. Quantitatively, this study uses mass balance calculations in order to model the mean scavenging residence time, defined as the mean dissolved ^{210}Po and ^{210}Pb adsorption by particles. The results are compared between the two estuaries and regionally for the Delaware estuary. Also calculated are the reaction sorption rates, λ_s , defined as the scavenging rate constant for dissolved ^{210}Po and ^{210}Pb onto suspended particles. These rates can by proxy be applicable for other trace elements with similar biogeochemical behavior.

2.3 Material and Methods

Water samples for ^{210}Po and ^{210}Pb analyses were collected during spring (April 2012) and summer (August 2012) for the Delaware and Chesapeake estuaries, respectively (Table 2.1). The samples were collected aboard the R/V Sharp along the entire Delaware salinity gradient (0-31psu) and upper Chesapeake (2-17psu) with a surface (2m) and bottom depth sample collected using Niskin bottles, supplemented by the surface ship pump (SMS). Water samples were also collected from intertidal waters of a lower Delaware (Canary Creek) salt marsh (Table 2.2) over a 12-hour tidal cycle on 01 June 2012 at two sites, near the Roosevelt Inlet and within Canary Creek (1 mile from Delaware Bay). A single end member sample of the system was collected from Red Mill Pond, a primary freshwater source for the marsh.

A total of 34 Delaware, 17 intertidal Delaware Salt marsh and 17 Chesapeake dissolved and particulate samples were collected. In 20L Cubitainers® dissolved samples were filtered using Gelman Sciences sterilized Mini Capsule Filter membranes ($<0.45\mu\text{m}$), and acidified to pH 2 using HCl. The cubitainers were sealed and stored in the dark until being transferred to cold dark storage once ashore. The filtered and acidified seawater samples were assumed to be isolated from storage artifacts based on earlier findings (Chung and Craig, 1983). Separate particulate subsamples were filtered through pre-weighed $0.45\mu\text{m}$ polycarbonate membrane filters ($^{210}\text{Po}/^{210}\text{Pb}$ particulate) and ashed glass fiber filters (POC and PON). Filters were placed in an -80°C freezer until processing. Polycarbonate membrane filters

were processed by HNO₃ digestion at 90°C for a day. Separate filtered samples were collected and stored using acid cleaned vials in order to analyze bay nutrients (NO₃⁻, NH₄⁺, PO₄³⁻ and Si). Physiochemical parameter such as temperature, salinity, dissolved oxygen, conductivity, productivity, suspended matter were measured in-situ using a CTD probe (YSI, Inc.).

Dissolved seawater samples were processed for ²¹⁰Po and ²¹⁰Pb using an established protocol (Fleer and Bacon 1984). Weighed additions of ²⁰⁹Po isotope spike and stable Pb, made from lead mineral (“dead lead”), carrier were added to each sample for isotopic dilution analysis and chemical yield, respectively. The ²⁰⁹Po spike was calibrated using two certified reference materials (IAEA-RGU-1 and MIST-SRM983) and found to be 2.12±0.05 dpm/g (35.3 ±0.8 mBq/g), averaging 1dpm per sample. Stable Pb carrier was calibrated using atomic absorption and a pre-weighed amount averaging 20mg of Pb was added to each sample. Nuclides were extracted by co-precipitation with Fe(OH)₃ (Thomson and Turekian, 1976; Nozaki, 1986). The precipitate was recovered by filtration (0.45µm polycarbonate Nuclepore) and then dissolved in a 0.5M HCl solution. In the case of particulate samples, the solid phase is dried, weighed and spiked with ²⁰⁹Po and lead carrier before being completely dissolved using a mixture of strong acids (including HF). The solution digest is evaporated to near-dryness and recovered in 0.5M HCl solution. The ²¹⁰Po and ²⁰⁹Po are plated by spontaneous deposition onto a silver disc (Flynn, 1968) and their activities measured by alpha spectroscopy. The remaining Po in solution is removed using AG-1X8 anion exchange resin as described by Sarin et al., (1992). A small aliquot of the solution is taken in order to measure Pb recovery before anion column separation. After separation, another small aliquot is taken from the final eluate solution containing the ²¹⁰Pb and both were measured using Flame atomic absorption to determine Pb carrier concentration. The final eluate solution is re-spiked with ²⁰⁹Po and stored at least 6 months to allow in-growth of ²¹⁰Po from ²¹⁰Pb. Then the ²¹⁰Pb activity of the samples is determined by plating the eluate solution on another silver disc thus measuring the in-growth of ²¹⁰Po. Finally, the determination of the initial activities of ²¹⁰Po and ²¹⁰Pb at the time of collection is calculated using the equations and corrections accounting for decay and ingrowth of

both nuclides detailed in Rigaud et al., (submitted). Duplicate blanks were determined by processing a liter of distilled water in the same way as the samples to correct the calculated activities (<4% sample activity). Detector background was individually subtracted from each sample activity (<3%). The reproducibility of the method was tested based on duplicate analysis of five different stations with the mean relative standard deviations, between duplicate analyses found to be 3.3%.

2.4 Results

The radionuclide activities are presented in Table 1 for the Delaware and the Chesapeake Bays, and in Table 2.2 for the Delaware salt marsh. Oceanographic standard units (dpm/100L) are used. Transect figures for the Chesapeake and Delaware estuaries were created using Ocean Data View (ODV)(Schlitzer, 2013). ODV figures utilized the data collected and gridded field function in order to represent water column trends over the entire transect. All physiochemistry data which includes temperature, salinity, dissolved oxygen, conductivity, suspended mater, POC, PON, NO_3^- , NH_4^+ , PO_4^{3-} and Si are located in the Supplemental Materials.

2.4.1 Delaware Estuary

Throughout the Delaware estuary the salinity and temperature gradient are well mixed from surface to within a few meters of the bottom. Higher temperatures were measured in the upper estuary and gradually decreased seaward towards higher salinity coastal waters. Dissolved oxygen concentrations were constant (320 $\mu\text{mol/L}$) in the upper estuary, reached 360 $\mu\text{mol/L}$ in the mid estuary and 290 $\mu\text{mol/L}$ in the lower estuary. Freshwater in the upper estuary is low in suspended particulate matter (3.91mg/L), increasing in the turbidity maximum (40-60km transect distance) to 35mg/L and then decreasing in higher salinity waters. Dissolved nutrient concentrations for NO_3^- , NH_4^+ , PO_4^{3-} and Si, while POC and PON concentrations increase moving from low to higher salinity waters. The decrease of nutrients and increase in POC and PON are likely indicative of a phytoplankton spring bloom in the mid to lower estuary (Supplemental Materials).

Dissolved ^{210}Po concentrations in the Delaware estuary ranged from 1.34 to 4.73 dpm/100L, with lower dissolved ^{210}Pb concentrations varying from 0.98 to 3.88 dpm/100L (Figure 2). Upper estuary dissolved concentrations of ^{210}Po were low and increased moving into high salinity waters. Mid to lower estuary concentrations of dissolved ^{210}Po increased to a maximum of 4.73 dpm/100L, as did POC (1.5mg/L) and PON (5.5 mg/L) concentrations. Dissolved ^{210}Pb concentrations in surface waters were relatively constant (≈ 2 dpm/100L) from low to high salinities, with the only major variation occurring at bottom depths of the lower estuary (0.98dpm/100L). Mid-estuary dissolved ^{210}Pb decreased from 2.5 to 1.0 dpm/100L where increased dissolved oxygen occurred. In the spring, the dissolved $^{210}\text{Po}/^{210}\text{Pb}$ activity ratios in the upper estuary (0-50km section distance) were generally less than one while an excess (>1) was present in the mid to lower estuary.

Particulate concentrations of ^{210}Po and ^{210}Pb ranged from 1.11 to 18.41 and 0.41 to 60.05 dpm/100L respectively. In lower the salinity upper estuary both particulate ^{210}Po and ^{210}Pb are highest in the turbidity maximum (25-75km transect distance). Towards the mid-estuary ^{210}Po and ^{210}Pb activities drop to <1 dpm/100L as the salinity increases and the suspended particulate decreases. The $^{210}\text{Po}/^{210}\text{Pb}$ activity ratio is deficient (<1) in the upper estuary and increases to an excess (3) from mid to lower estuary.

2.4.2 Lower Delaware Salt Marsh (Canary Creek)

Intertidal sampling occurred at two locations in, Roosevelt Inlet (entrance) and Canary Creek (upstream). The salinity concentrations over the tidal cycle ranged between 27-29 and 20-24 psu respectively, while there was no difference between temperature, dissolved oxygen, and NO_3^- concentrations between the sampling sites. However, POC, PON, Si and PO_4^{3-} concentrations were maximum at high tide in Canary Creek while they were relatively constant at Roosevelt Inlet (Supplemental Materials).

Dissolved ^{210}Po ranged from 2.79 to 9.95 dpm/100L at Roosevelt Inlet and 3.87 to 13.9 dpm/100L at Canary Creek with the marsh end member at Red Mill

pond at 9.0 dpm/100L (Figure 2.3). Over the tidal cycle ^{210}Po in Canary Creek increased during flooding tide, while the closer to Delaware Bay (Roosevelt Inlet) is generally constant with a highest concentration at low tide. Dissolved ^{210}Pb ranged from 1.2 to 11.6 dpm/100L at Roosevelt Inlet and from 4.6 to 13.8 dpm/100L at Canary Creek with the end member of 18.9 dpm/100L at Red Mill pond. The maximum dissolved ^{210}Pb at both sites occurred during the ebbing tide. However, the ^{210}Pb dissolved activity versus tides at Canary Creek were similar to Roosevelt Inlet but with a slight delay caused by distance from intertidal waters (Figure 2.3). Dissolved activity ratios, ($^{210}\text{Po}/^{210}\text{Pb}$), at Canary Creek were measured to be close to equilibrium until low tide. From low to flooding tide dissolved $^{210}\text{Po}/^{210}\text{Pb}$ at Canary Creek was in excess of 2.5. Throughout the tidal cycle, excess dissolved $^{210}\text{Po}/^{210}\text{Pb}$ at Roosevelt Inlet was observed, with a maximum during high tide of 2.8.

2.4.3 Chesapeake Bay

During late summer, the upper more shallow regions of the estuary were represented by a well-mixed region, which persisted for 60km seaward. The upper Chesapeake Bay water column at higher salinities was well defined with a sub-oxic interface separating surface and bottom waters. Here two distinct water masses were separated by a well-developed thermocline and oxygen deficient zone below 12m (Table 2.1). A turbidity maximum was present in the upper shallow regions represented by a suspended particulate matter concentration greater than 60mg/L. Suspended particulate concentrations were constant until midway down the estuary when it dropped to <10 mg/L. The POC concentrations were constant (0.4mg/L) above 10m throughout the upper Chesapeake estuary. Below 10m and within the sub-oxic zone, POC concentrations of 1.2mg/L were observed decreasing to near zero at bottom. Dissolved nutrient concentrations of NO_3^- and Si at the mouth of the Susquehanna are at maximum and decrease down the estuary, while the opposite trend is observed by NH_4^+ and PO_4^{3-} . In sub-oxic waters below 12m (55 to 125km transect distance) increases in NH_4^+ , PO_4^{3-} and Si were observed (Supplemental Materials).

Dissolved radionuclide concentrations along the upper Chesapeake estuary ranged from 0.83 to 4.44 dpm/100L and 0.39 to 4.33 dpm/100L for ^{210}Po and ^{210}Pb respectively. The upper Chesapeake estuary dissolved ^{210}Po activity was high (4 dpm/100L) at the mouth of the Susquehanna River and decreased to 2-2.5dpm/100L seaward. The dissolved ^{210}Pb activity was constant at 1.0 dpm/100L throughout the entire upper Chesapeake estuary other than at two points, 60km and 120km. At 60km distance an enrichment of 4.0 dpm/100L of dissolved ^{210}Pb is associated with the mouth of Baltimore Harbor. North of the Potomac at depth, a sub-oxic zone is associated with an increased dissolved ^{210}Pb and ^{210}Po activity. Between 7 and 12 meters the dissolved ^{210}Po concentration (4.4 dpm/100L) and ^{210}Pb (3.0 dpm/100L) were maximum but then decreased to 1 dpm/100L in more sub-oxic deep waters (below 12 meters). An excess dissolved $^{210}\text{Po}/^{210}\text{Pb}$ activity ratio is observed over most of the Chesapeake estuary and in some regions reached as high as 5.

Particulate concentrations of both radionuclides were more enriched than dissolved concentrations, 0.34 to 31.28 dpm/100L and 0.31 to 67.09 dpm/100L for ^{210}Po and ^{210}Pb respectively. In the upper estuary the particulate concentrations of the radionuclides were correlated with suspended matter at the turbidity maximum (0-20 km). The highest particulate activity (120km) for both radionuclides was located at 15 meters down in the sub-oxic bottom waters, with activities of 67 dpm/100L and 11 dpm/100L for ^{210}Pb and ^{210}Po respectively.

2.5 Discussion

The distribution of dissolved and particulate ^{210}Po and ^{210}Pb in the Delaware and Chesapeake estuaries differ mainly due to biogeochemical characteristics. The Delaware estuary is dominated by high-suspended particulate concentration. The most unique aspect of the upper Chesapeake estuary is the prevalence of a deep sub-oxic zone during the summer months. Sub-oxic waters allow for distribution between dissolved and particulate ^{210}Po and ^{210}Pb concentrations that are dependent on associated redox chemistries. Finally, box-model calculations of scavenging residence times for both estuaries will be discussed to give insight into

scavenging residence times and dissolved-particulate sorption rates which can be analogous proxies for other trace elements.

2.5.1 Identification of Processes Controlling ^{210}Po and ^{210}Pb cycle in the Delaware Estuary

The distribution of dissolved and particulate ^{210}Po and ^{210}Pb throughout the estuarine regions of the Delaware Bay indicate that as the nuclides enter the estuary they are differentially removed from solution at the freshwater/salt water-mixing zone. This could include a combination of co-precipitation with humic substances, Fe-Mn hydroxides and by adsorption onto suspended particles. This is evident by particulate ^{210}Po and ^{210}Pb activities on suspended material, which are higher in the turbidity maximum. The distinctly higher concentration of dissolved ^{210}Pb observed in the upper Delaware estuary is attributed to the increased fresh water discharge to the estuary from the spring runoff. The higher ^{210}Po concentration observed in the mid to lower estuary is linked to a spring phytoplankton bloom. In the lower estuary near bottom a decrease in dissolved ^{210}Pb concentration is attributed to the influx of higher salinity coastal waters and suspended sediment scavenging.

During the Delaware spring transect, the $^{210}\text{Po}/^{210}\text{Pb}$ dissolved activity ratio in the surface waters were either one or slightly above, while throughout the bottom waters the ratio was two or greater. Such differential behavior of these two isotopes implies that the ^{210}Po is regenerated in the mid-salinity regions. Subsequently it is removed in the surface waters at higher salinities by biological activity. During the sinking of the particulate debris and the scavenged ^{210}Po is regenerated back to the bottom waters. Overall, the main removal of dissolved ^{210}Pb and ^{210}Po is by co-precipitation and adsorption onto suspended particulate matter in the turbidity maximum of the upper estuary.

2.5.2 Identification of Processes Controlling ^{210}Po and ^{210}Pb cycle in the Lower Delaware Salt Marsh (Canary Creek)

The dissolved concentrations for both radionuclides in the Delaware intertidal marsh are distinctly higher than those measured in the estuary and coastal waters

(Table 2). The lower salt marshes of the Delaware Bay could therefore act as a source of dissolved ^{210}Pb and ^{210}Po that may explain the constant concentration of both nuclides in the mid-lower Delaware estuary well seaward of the turbidity maximum that should have initially scavenged the fluvial radionuclides. Noteworthy is the $^{210}\text{Po}/^{210}\text{Pb}$ dissolved activity ratio in the upper salt marsh (Canary Creek) that remained at equilibrium from high to low tide, while the Roosevelt Inlet station was consistently greater than one. The difference between sites possibly indicates that excess dissolved ^{210}Po from the Bay inundates the marsh while dissolved ^{210}Pb from the marsh is exported to the Bay. A large concentration of ^{210}Po (versus ^{210}Pb) in the tidal waters suggests that marsh vegetation and increased biogeochemical reactivity on the marsh surface during the late spring acts as a source for dissolved ^{210}Pb . We hypothesize that the salt marsh acts as a source of dissolved ^{210}Pb due to higher intertidal scavenging from atmospheric deposition. Alternatively, dissolved ^{210}Po could be precipitated by the marsh sediments during reduction of sulfur, its elemental analogue (Luther and Church, 1988).

2.5.3 Identification of Processes Controlling ^{210}Po and ^{210}Pb cycle in the Chesapeake Bay

Unlike the Delaware estuary the Chesapeake is surrounded by a number of distinct rivers and tributaries, which influence ^{210}Po and ^{210}Pb distribution. The Susquehanna River is responsible for 87% of the freshwater influx in the upper estuary creating a turbidity maximum where both dissolved ^{210}Po and ^{210}Pb are scavenged onto suspended matter, similar to the Delaware estuary. Data shows an increase in particulate ^{210}Po (35 dpm/100L) and ^{210}Pb (75 dpm/100L) in the turbidity maximum, while particulate activity of both radionuclides decrease to <3 dpm/100L down the estuary. The suspended matter throughout the upper Chesapeake contains a significant amount of POC, which could break down and regenerate ^{210}Po , while ^{210}Pb is almost entirely removed as particles. High concentrations of dissolved ^{210}Po are likely due to a combination of river dissolved discharge and regeneration of organisms from the Susquehanna during the highly productive summer.

A characteristic of the Chesapeake Bay is the pervasive sub-oxic and anoxic zone, which can occur at depths as shallow as 5 to 10 meters. However, during the August 2012 cruise only sub-oxic waters were evident below 12m in the mid-estuary (75-120km). There are limited investigations on the aqueous geochemistry of ^{210}Po and ^{210}Pb at sub-oxic and anoxic interfaces such as those in the upper Chesapeake Bay. The surface waters of the upper Chesapeake between 80km and 120km show depleted dissolved ^{210}Po and ^{210}Pb that could rapidly be scavenged by biogenic particles (e.g., plankton, microbes) that settle out in the water column. A decrease in concentration of dissolved NO_3^- , PO_4^{3-} and Si and increase of NH_4^+ , POC, and PON nutrient concentrations indicate that a phytoplankton bloom likely occurred leading to scavenging of both dissolved ^{210}Po and ^{210}Pb from surface waters. Thus the particulate activity of ^{210}Po and ^{210}Pb in surface waters are twice that of the dissolved suggesting sorption or bioaccumulation. This sorption step is thought to be very fast (hours) and becomes evident during times of high productivity, such as during spring and summer months (McKee and Todd, 1993). There is much evidence to suggest that ^{210}Po , more so than ^{210}Pb , is closely tied to water column cycling of phytoplankton and zooplankton (Nozaki et al., 1976; Stewart et al., 2007). A strong biological link offers a mechanism for both dissolved ^{210}Po and ^{210}Pb depletion from surface water and increased particulate activities.

The removal of dissolved ^{210}Po and ^{210}Pb from oxygen rich surface waters to sub-oxic bottom waters at 120km allows for the regeneration of ^{210}Po (5 dpm/100L) and ^{210}Pb (4 dpm/100L) at 8 to 12m (pycnocline). In the water column deeper than 12 meters where the density is greatest particulate ^{210}Po and ^{210}Pb activity increased while dissolved ^{210}Po and ^{210}Pb decreased down to 20 meters. Nitrate as well was constant at 15 $\mu\text{mol/L}$ from surface waters down to the upper boundary of the suboxic zone and then decreased to near zero within the suboxic zone. Nitrate maxima were observed near the upper and lower boundaries of the nitrite maximum, corresponding to zones of nitrification and de-nitrification respectively. Dissolved NH_4^+ , PO_4^{3-} and Si all increase at the depth where nitrate is depleted.

Luther et al., (1994) showed evidence that dissolved manganese and iron also increase at the depth where nitrate is depleted, with increasing manganese. At the redox interface MnO_2 begins sub-oxic reduction and dissolution, bound ^{210}Po and ^{210}Pb can also become solubilized. We hypothesize that the solubilized ^{210}Po and ^{210}Pb seen at 12 meters depth is due to sub-oxic reduction and dissolution of MnO_2 . In contrast, FeOOH -bound ^{210}Po or ^{210}Pb would only be released to solution in this region, but does not appear to undergo reduction and dissolution, which did not occur during this study. The newly released dissolved ^{210}Po and ^{210}Pb can then diffuse either upward in the water column towards the sub-oxic boundary or downward into anoxic waters where ^{210}Pb and ^{210}Po could be permanently removed from the water column by sulfide co-precipitation in the bottom sediments.

Similarly, dissolved ^{210}Po removal from the surface and regeneration at depth are commensurate with a particulate maximum observed by Todd et al., (1986) and Canfield et al., (1995) in the Orca Basin, Gulf of Mexico and an Antarctic lake. An idealized model of ^{210}Po and ^{210}Pb behavior across an $\text{O}_2/\text{H}_2\text{S}$ interface was first proposed by Bacon et al. (1980) in anoxic ocean basins. The model can be utilized to describe the fate of many redox-sensitive, particulate reactive species within other oxic/anoxic systems, including a redox sensitive estuary such as the Chesapeake estuary. Thus, in the upper Chesapeake Bay, the water column profiles of ^{210}Po and ^{210}Pb in sub-oxic areas are hypothesized to be influenced by the redox cycling of Fe/Mn oxides at the water column pycnocline.

2.5.4 Residence times

The radionuclide results can be used to estimate the net scavenging residence time, defined as the ^{210}Po and ^{210}Pb in solution relative to adsorption on sediment particles. As such the scavenging rate constant for dissolved ^{210}Po and ^{210}Pb onto suspended matter is based on a simple box model (Figure 2.5). The Delaware Bay geomorphology fits that of a typical estuary with a broad inner bay bounded by two cape entrances, with partially mixed characteristics. As such it meets the basic requirements of a box-model based on a mass balance of the radionuclides. For this, we assume that measured concentrations of radionuclides (Table 2.1) are

representative of yearly spring and summer concentrations. The estuaries may be represented by either a single (upper Chesapeake estuary) or three successive (upper, mid, and lower Delaware estuary) box-models, each with steady state conditions maintained for at least several months (Figure 2.5).

We start by considering the hydrology of Delaware estuary. The flux of fresh water to the Delaware estuary can vary greatly seasonally. On average, the freshwater inflow is $570\text{m}^3\text{s}^{-1}$, but during the spring months increases to $1100\text{m}^3\text{s}^{-1}$ with a direct rainfall into the estuary of $650\text{l m}^{-2}\text{a}^{-1}$ (Sharp et al., 1982). Taking into consideration the surface area of the estuary ($2,030\text{ km}^3$), direct rainfall contributes $2.21 \times 10^9\text{ m}^3\text{ a}^{-1}$ (Kim et al., 2000), which is a small (6%) fraction of the annual river discharge. The intertidal marshes surrounding the Delaware estuary are also a source of water $3.8 \times 10^{10}\text{ m}^3\text{ a}^{-1}$ (Church, 1986). The Delaware estuary is also highly influenced by higher salinity coastal waters and thus an outflow term, that takes into account the tidal influence, is calculated to be $2.52 \times 10^{10}\text{ m}^3\text{ a}^{-1}$. Therefore, the mean residence time of water in the estuary (R_w ,) is 0.337a (123 days) under average water flow conditions.

The balance of dissolved ^{210}Po in the estuary depends upon discharges of dissolved ^{210}Po into the estuary, ^{210}Po produced through radioactive decay of dissolved ^{210}Pb , ^{210}Po radioactive decay, ^{210}Po removal from solution, and ^{210}Po exported with the water discharged to the coastal sea. This is depicted in Figure 2.5 with data from Table 2.3 using standard units of Bq. Therefore, the mass balance equation for dissolved ^{210}Po in the estuary is

$$\lambda_{Po}A_{Pb} + I_r + I_{smPo} + \lambda_{Po}I_{smPb} + I_{aPo} + \lambda_{Po}I_{aPb} = \lambda_{Po}A_{Po} + \lambda_s A_{Po} + \lambda_w A_{Po} \quad (1)$$

Substituting the data into equation (1) and solving for λ_s , the scavenging rate constant for ^{210}Po onto suspended matter and sediment particles is 4.22 a^{-1} . Relative to adsorption on sediment particles, dissolved ^{210}Po mean residence time for the whole estuary is estimated at 0.24a or 86 days. The other mechanism contributing to the removal of dissolved ^{210}Po from the estuary is the outflow of water into the sea. As the input of dissolved ^{210}Po in the estuary is $1.45 \times 10^{10}\text{ Bq a}^{-1}$, the ^{210}Po is exported with a rate of $\lambda_w = 2.97\text{a}^{-1}$ is $4.29 \times 10^{10}\text{ Bq a}^{-1}$. This export corresponds to about 60% of the annual delivery of dissolved ^{210}Po to the estuary. Therefore, only

40% of the dissolved ^{210}Po entering the estuary is removed by sorption onto sedimenting particles and trapped, in the estuary and intertidal marshes. It must be noted that this is a net flux, as steady state cycling surely occurs in the estuary.

In the Delaware estuary sufficient data allows an upper, mid and lower region to be readily defined, the box-model can be zonally distributed to distinguish successive estuarine processes. As such the same equations can be abridged using values for each specific region of the Delaware. Using the concentration of dissolved ^{210}Po broken down by region (i.e. upper, mid and lower) results in scavenging residence times of 22 days, 20 days, and 25 days.

An identical mass balance equation may be written for dissolved ^{210}Pb with

$$\lambda_{Pb}A_{Ra} + I_r + I_{smPb} + \lambda_{Pb}I_{sm} + I_a + \lambda_{Pb} = \lambda_{Pb}A_{Pb} + \lambda_sA_{Pb} + \lambda_wA_{Pb} \quad (2)$$

where, λ_{Pb} is the radioactive decay constant ^{210}Pb , $\lambda_{Pb}A_{Ra}$ corresponds to the ^{210}Pb ingrowth from dissolved ^{226}Ra in the estuary, and the other variables similar to those already introduced. The contribution of ^{226}Ra from atmospheric deposition is assumed to be negligible. The contribution of dissolved ^{226}Ra through radioactive decay to total dissolved ^{210}Pb also is minimal, when compared with other ^{210}Pb sources. Solving equation (2), λ_s , defined as the scavenging rate constant for ^{210}Pb onto suspended sediment particles is equal to 5.47 a^{-1} , and the mean residence time of soluble ^{210}Pb in the whole Delaware estuary is 0.31a or 66.6 days. This discharge of soluble ^{210}Pb to coastal waters accounts for 55% of the annual input of soluble ^{210}Pb received by the estuary. Therefore, most of the ^{210}Pb entering the estuary in the soluble phase is either sorbed onto suspended particles and trapped in sediment accumulation zones of the estuary, such as intertidal marshes, or discharged bound to suspended matter into the coastal ocean. As with ^{210}Po , the ^{210}Pb residence time for the Delaware estuary is best differentiated by zonal region resulting in times of 21 days, 14 days and 10 days respectively.

Utilizing a similar approach, mean residence times for the upper estuary of the Chesapeake Bay in the summer were calculated utilizing only a single box-model. The sampling of the Chesapeake Bay focused on the upper Chesapeake and thus a zonal approach was not applied. The upper estuary of the Chesapeake is defined here as the region extending from the mouth of the Susquehanna River seaward to

the mouth of the Potomac Estuary. This region encompassing the upper bay includes the eastern and western tributaries, which includes 1484 km² and is 14% of the total Bay area (Ranasinghe et al., 1998). Unlike the Delaware estuary there are essentially no significant intertidal marshes surrounding the upper bay and thus no marsh flux is considered. Using the data from Table 1, λ_s , the scavenging rate constant for dissolved ²¹⁰Po onto suspended matter and sediment particles is 2.91a⁻¹. The mean residence time of ²¹⁰Po in solution relative to adsorption on sediment particles is estimated at 0.34a or 125 days, while for dissolved ²¹⁰Pb, λ_s is 6.61a⁻¹ and the mean residence time is 0.15a or 55 days.

Comparing the two single-box model λ_s scavenging rate constant results of ²¹⁰Po for the estuaries, Delaware (4.22 a⁻¹) and the Chesapeake (2.91a⁻¹), suggest that biogenic scavenging is greater in the upper Chesapeake estuary. However, ²¹⁰Pb the scavenging rates of the Delaware (5.47 a⁻¹) and the Chesapeake (6.61a⁻¹) suggests that the physicochemical adsorption on particles is somewhat greater in the Delaware. It is hypothesized that other trace elements with similar chemical characteristics as ²¹⁰Pb (Type A) and ²¹⁰Po (Type B) will have similar sorption rates. “Type A” trace metals tend to form cations, which react with negatively charged ions and suspended particles, and includes elements such as Fe, Mn, Co and Cr (Church, 1986). However “Type B” metals tend more to form stronger complexes or compounds with organic matter include elements such as Zn, Ni, Cu, Cd, Ag, and Hg.

2.6 Conclusions

The following conclusions can be drawn on the implications of geochemical cycling of ²¹⁰Po and ²¹⁰Pb in the estuarine waters of the Delaware and Chesapeake estuaries. The upper Delaware estuary, dominated by high turbidity, results in short mean residence times of ²¹⁰Po (22 days) and ²¹⁰Pb (20 days) due to their high affinity for particles. The mid-Delaware estuary largely deposits suspended particles, significantly decreasing the residence time of ²¹⁰Pb (14 days). Because of increased biological productivity and cycling, the more bioactive ²¹⁰Po (20 days) only slightly decreases in residence time. As a whole the lower estuary should be more influenced by particulate influx of coastal waters including, tidal salt marshes,

that is reflected in a low ^{210}Pb (10 days) residence time. As such, the intertidal marshes are a source of ^{210}Pb , while acting as a sink for ^{210}Po , leading to higher residence time (25 days) for ^{210}Po .

The mean residence time of the radionuclides in the upper Chesapeake is quite long, 125 and 55 days respectively for ^{210}Po and ^{210}Pb during the summer. The large mean residence time for ^{210}Po is likely linked to the higher productivity of the less turbid upper Chesapeake during the summer months, as ^{210}Po is being preferentially scavenged and regenerated by organisms. The turbidity maximum near the Susquehanna is the main sink of ^{210}Pb from the water column. The higher ^{210}Po mean residence time of the Chesapeake versus the Delaware is likely due to a larger productivity per volume over the upper Chesapeake versus the Delaware, leading to greater biological scavenging and regeneration. The large differences overall between residence times in the two estuaries likely is due to a higher scavenging rates in more turbid waters of the Delaware combined with different spring conditions of higher discharge and lower productivity. The estimated residence time for each nuclide in either estuary is applicable for estimating scavenging export of other bioactive elements to the coastal ocean.

REFERENCES

- Bacon, M.P., Spencer, D.W., Brewer, P.G. 1976. $^{210}\text{Pb}/^{226}\text{Ra}$ and $^{210}\text{Po}/^{210}\text{Pb}$ disequilibria in seawater and suspended particulate matter. *Earth Planet. Sci. Lett* 32, 277-296.
- Bacon, M.P., Brewer, P.G., Spencer, D.W., Murraray, J.W., 1980. Lead-210, polonium-210 manganese and iron in the Cariaco Trench. *Deep Sea Res.* 27, 119-135.
- Canfield, D.E., Green, W.J., Nixon, P., 1995. ^{210}Pb and stable lead through the redox transition zone of an Antarctic lake. *Geochim. Cosmochim. Acta* 59, 2459-2468.
- Carvalho, F., 1997. Distribution, cycling and mean residence time of ^{226}Ra , ^{210}Pb and ^{210}Po in the Tagus estuary. *The Science of the Total Environment* 196, 151-161.
- Chung, T., Craig, H. 1983. ^{210}Pb in the Pacific: the GEOSECS measurements of particulate and dissolved concentrations. *Earth Planet. Sci. Lett.* 65(2), 406-432
- Church, T.M., 1986. Biogeochemical factors influencing the residence time of microconstituents in a large tidal estuary, Delaware Bay. *Mar. Chem.* 18, 393-406.
- Church, T., Sarin, M.. 1995. Natural U-Th series radionuclide studies of estuarine processes, in: Dyer, K.R., Orth, R.J. (Eds.), *Changes in Fluxes in Estuaries: Implication From Science to Management*. Proceedings of the ECSA22/ERF Symposium, Plymouth, England, September 13-18, 1992, pp.91-95.
- Cochran, J.K., Masqué, P., 2003. Short-lived U/Th Series Radionuclides in the Ocean: Tracers for Scavenging Rates, Export Fluxes and Particle Dynamics. *Reviews in Mineralogy and Geochemistry* 52, 461-492.
- Fleer, A.P., Bacon, M.P., 1984. Determination of ^{210}Pb and ^{210}Po in seawater and marine particulate matter. *Nuclear Instruments and Methods in Physics Research* 223, 243-249.
- Flynn, W. W., 1968. The determination of low levels of polonium-210 in environmental materials. *Anal. Chim. Acta* 43, 221-227.
- Kim, G., Hussain, N. Church, T., 2000. Excess ^{210}Po in the coastal atmosphere. *Tellus.* 52B, 74-80.
- Luther, G.W. III, Church, T.M., 1988. Seasonal cycling of sulfur and iron in porewaters of a Delaware salt marsh. *Mar. Chem.* 23, 295-310.

- Luther, G.W. III, Nuzzio, D.B., Wu, J., 1994. Speciation of manganese in Chesapeake Bay waters by volumetric methods. *Anal. Chim. Acta* 284, 473-480.
- McKee, B.A., Todd, J.F., 1993. Uranium behavior in a permanently anoxic fjord: microbial control? *Limnol. Oceanogr.* 38, 408-414.
- Nozaki, Y., 1986. ^{226}Ra - ^{222}Rn - ^{210}Pb systematics in seawater near the bottom of the ocean. *Earth and Planetary Science Letters* 80, 36-40.
- Nozaki, Y., J. Thomson, and K. K. Turekian. 1976. The distribution of ^{210}Pb and ^{210}Po in the surface waters of the Pacific Ocean. *Earth Planet. Sci. Lett* 32, 304-312.
- Ranasinghe, J.A., Scott, L.C. Kelly, F.S., 1998. Chesapeake Bay Water Quality Monitoring Program Long-term benthic monitoring and assessment component. July 1984-Dec 1997. Versar, Inc., Columbia, MD.
- Rigaud, S., Puigcorbé, V., Camara-Mor, P., Casacuberta, N., Roca-Martí, M., Garcia-Orellana, J., Benitez-Nelson, C.R., Masque, P., Church, T. submitted, 2013. An assessment of the methods, calculation and uncertainties in the determination of ^{210}Po and ^{210}Pb activities in seawater. *Limnol. Oceanogr. Methods*.
- Rutgers van Der Loeff, M. M., Moore, W.S., 2007. Determination of natural radioactive tracers, p. 365-397, in: *Methods of Seawater Analysis*. Wiley-VCH Verlag GmbH.
- Santschi, P.H., Li, Y.H., Bell, J., 1979. Natural radionuclides in the water of Narragansett Bay. *Earth Planet. Sci. Lett.*, 45, 201-213.
- Sarin, M. M., Bhushan, R., Rengarajan, R., Yadav, D.N.. 1992. The simultaneous determination of ^{238}U series nuclides in seawater: results from the Arabian Sea and Bay of Bengal. *Indian J. Mar. Sci.* 21, 121-127.
- Schlitzer, R., 2013. Ocean Data View, <http://odv.awi.de>.
- Sharp, J. Coulberson, C. Church, T., 1982. The chemistry of the Delaware estuary. General Considerations. *Limnol. Oceanogr.*, 27(6), 1015-1028.
- Stewart, G., Cochran, J., Xue, J., Lee, C., Wakeham, S., Armstrong, R., Masque, P., Miquel, J. 2007. Exploring the connection between ^{210}Po and organic matter in the northwestern Mediterranean. *Deep Sea Research I.* 54, 415-427.
- Thomson, J., Turekian, K.K., 1976. ^{210}Po and ^{210}Pb distributions in ocean water profiles from the Eastern South Pacific. *Earth Planet. Sci. Lett* 32, 297-303.

Todd, J.F., Wong, G.T.F., Reid, D., 1986. The geochemistries of ^{210}Po and ^{210}Pb in waters overlying and within the Orca Basin, Gulf of Mexico. *Deep Sea Res.* 33, 1293-1306.

TABLES

Table 2.1: The dissolved and particulate ^{210}Po and ^{210}Pb activities (dpm 100L⁻¹) for Delaware Estuary (DB and DBSMS) and Chesapeake Bay (CB)

| Station | Salinity (psu) | Oxygen ($\mu\text{mol/L}$) | Depth (m) | $^{210}\text{Po}_{\text{diss}}$ | | $^{210}\text{Po}_{\text{part}}$ | | $^{210}\text{Pb}_{\text{diss}}$ | | $^{210}\text{Pb}_{\text{part}}$ | | $^{210}\text{Po}/^{210}\text{Pb}_{\text{diss}}$ | | $^{210}\text{Po}/^{210}\text{Pb}_{\text{part}}$ | |
|---------|-------------------|---------------------------------|--------------|---------------------------------|----------------------------|---------------------------------|----------------------------|---------------------------------|----------------------------|---------------------------------|----------------------------|-------------------------------------------------|--------|-------------------------------------------------|--------|
| | | | | (dpm 100 l ⁻¹) | (dpm 100 l ⁻¹) | (dpm 100 l ⁻¹) | (dpm 100 l ⁻¹) | (dpm 100 l ⁻¹) | (dpm 100 l ⁻¹) | (dpm 100 l ⁻¹) | (dpm 100 l ⁻¹) | | | | |
| DB 01 | 0.15 | 323 | 11.82 | 1.76 | ± 0.19 | 1.21 | ± 0.69 | 1.85 | ± 0.32 | 13.11 | ± 1.55 | 0.95 | ± 0.19 | 0.09 | ± 0.05 |
| DB 01 | 0.15 | 325 | 2.38 | 1.43 | ± 0.18 | 1.26 | ± 1.07 | 2.19 | ± 0.35 | 15.23 | ± 2.12 | 0.65 | ± 0.13 | 0.08 | ± 0.04 |
| DB 03 | 1.97 | 319 | 10.38 | 1.56 | ± 0.14 | 4.65 | ± 0.98 | 3.02 | ± 0.21 | 16.66 | ± 2.03 | 0.52 | ± 0.11 | 0.28 | ± 0.05 |
| DB 03 | 1.96 | 321 | 2.82 | 1.70 | ± 0.22 | 4.76 | ± 1.01 | 3.23 | ± 0.39 | 16.76 | ± 2.13 | 0.53 | ± 0.09 | 0.28 | ± 0.07 |
| DB 05 | 7.20 | 320 | 2.02 | 2.58 | ± 0.23 | 18.41 | ± 1.94 | 1.37 | ± 0.28 | 15.93 | ± 3.23 | 1.89 | ± 0.43 | 1.16 | ± 0.26 |
| DB 10 | 6.75 | 327 | 1.83 | 1.92 | ± 0.20 | 14.82 | ± 1.97 | 2.10 | ± 0.33 | 57.84 | ± 5.03 | 0.92 | ± 0.17 | 0.26 | ± 0.09 |
| DB 10 | 8.50 | 319 | 9.10 | 1.96 | ± 0.22 | 15.35 | ± 1.04 | 2.10 | ± 0.40 | 60.05 | ± 4.93 | 0.93 | ± 0.21 | 0.26 | ± 0.09 |
| DB 11 | 8.20 | 337 | 1.95 | 2.27 | ± 0.22 | 4.86 | ± 1.65 | 3.23 | ± 0.40 | 9.09 | ± 2.70 | 0.70 | ± 0.11 | 0.54 | ± 0.14 |
| DB 11 | 12.37 | 315 | 10.00 | 2.04 | ± 0.20 | 6.04 | ± 1.03 | 1.70 | ± 0.28 | 14.72 | ± 2.88 | 1.20 | ± 0.23 | 0.41 | ± 0.11 |
| DB 12 | 16.53 | 315 | 12.88 | 2.47 | ± 0.23 | 11.02 | ± 1.73 | 3.79 | ± 0.40 | 20.10 | ± 2.01 | 0.65 | ± 0.09 | 0.55 | ± 0.15 |
| DB 12 | 10.93 | 342 | 2.17 | 1.77 | ± 0.20 | 8.38 | ± 2.56 | 0.98 | ± 0.30 | 10.77 | ± 2.91 | 1.80 | ± 0.59 | 0.78 | ± 0.19 |
| DB 13 | 12.30 | 353 | 2.16 | 2.21 | ± 0.21 | 6.81 | ± 1.25 | 1.32 | ± 0.29 | 10.70 | ± 2.44 | 1.68 | ± 0.40 | 0.64 | ± 0.19 |
| DB 13 | 15.38 | 300 | 10.12 | 2.30 | ± 0.22 | 13.11 | ± 1.50 | 1.27 | ± 0.30 | 14.39 | ± 2.76 | 1.82 | ± 0.47 | 0.91 | ± 0.21 |
| DB 14 | 21.47 | 308 | 2.13 | 2.54 | ± 0.24 | 16.05 | ± 2.33 | 1.62 | ± 0.30 | 14.54 | ± 3.02 | 1.57 | ± 0.33 | 1.10 | ± 0.24 |
| DB 14 | 16.18 | 347 | 15.41 | 2.17 | ± 0.21 | 13.28 | ± 2.63 | 2.42 | ± 0.35 | 14.06 | ± 4.34 | 0.89 | ± 0.15 | 0.94 | ± 0.35 |
| DB 15 | 18.82 | 330 | 1.98 | 4.73 | ± 0.36 | 3.98 | ± 1.01 | 3.88 | ± 0.41 | 0.58 | ± 0.26 | 1.22 | ± 0.16 | 6.82 | ± 2.31 |
| DB 15 | 23.72 | 307 | 14.26 | 2.12 | ± 0.21 | 2.14 | ± 0.87 | 1.96 | ± 0.32 | 0.55 | ± 0.31 | 1.08 | ± 0.21 | 3.89 | ± 1.42 |
| DB 16 | 25.52 | 306 | 2.10 | 3.90 | ± 0.34 | 1.83 | ± 0.93 | 2.83 | ± 0.35 | 0.41 | ± 0.25 | 1.38 | ± 0.21 | 4.46 | ± 1.20 |
| DB 16 | 21.47 | 318 | 11.69 | 2.59 | ± 0.23 | 1.35 | ± 1.07 | 1.58 | ± 0.30 | 1.15 | ± 0.89 | 1.64 | ± 0.35 | 1.17 | ± 0.81 |
| DB 17 | 24.10 | 310 | 1.95 | 3.16 | ± 0.28 | 1.61 | ± 1.05 | 3.05 | ± 0.38 | 0.51 | ± 0.30 | 1.03 | ± 0.16 | 3.15 | ± 1.01 |
| DB 17 | 25.96 | 301 | 12.08 | 3.36 | ± 0.28 | 2.09 | ± 0.93 | 2.85 | ± 0.37 | 0.59 | ± 0.34 | 1.18 | ± 0.18 | 3.54 | ± 1.10 |
| DB 18 | 26.31 | 306 | 2.03 | 4.45 | ± 0.35 | 3.37 | ± 1.45 | 2.16 | ± 0.32 | 1.24 | ± 0.95 | 2.06 | ± 0.35 | 2.71 | ± 0.76 |
| DB 19 | 28.22 | 297 | 2.00 | 3.29 | ± 0.28 | 4.44 | ± 1.25 | 1.63 | ± 0.29 | 2.08 | ± 1.34 | 2.02 | ± 0.40 | 2.14 | ± 1.48 |
| DB 20 | 31.81 | 297 | 1.58 | 2.48 | ± 0.21 | 1.57 | ± 0.77 | 2.16 | ± 0.31 | 2.43 | ± 1.21 | 1.15 | ± 0.19 | 0.65 | ± 0.32 |
| DB 21 | 30.44 | 295 | 1.98 | 2.21 | ± 0.22 | 2.34 | ± 1.34 | 1.75 | ± 0.23 | 2.44 | ± 1.98 | 1.26 | ± 0.11 | 0.96 | ± 0.27 |
| DB 21 | 31.03 | 292 | 15.29 | 2.68 | ± 0.24 | 1.11 | ± 0.41 | 1.23 | ± 0.29 | 1.03 | ± 0.40 | 2.18 | ± 0.54 | 1.08 | ± 0.28 |
| DBSMS 1 | 5.17 | 326 | 2.00 | 1.46 | ± 0.17 | 15.13 | ± 1.84 | 1.29 | ± 0.29 | 14.22 | ± 2.33 | 1.13 | ± 0.29 | 1.06 | ± 0.11 |
| DBSMS 2 | 10.33 | 323 | 2.00 | 1.96 | ± 0.19 | 9.11 | ± 2.21 | 1.64 | ± 0.34 | 13.98 | ± 2.51 | 1.20 | ± 0.27 | 0.65 | ± 0.17 |
| DBSMS 3 | 13.19 | 315 | 2.00 | 2.44 | ± 0.23 | 10.02 | ± 1.97 | 1.28 | ± 0.30 | 11.76 | ± 1.78 | 1.90 | ± 0.48 | 0.85 | ± 0.2 |
| DBSMS 4 | 15.1 | 311 | 2.00 | 1.34 | ± 0.16 | 7.45 | ± 1.33 | 1.03 | ± 0.29 | 10.54 | ± 2.49 | 1.30 | ± 0.40 | 0.71 | ± 0.26 |
| DBSMS 5 | 17.63 | 308 | 2.00 | 2.48 | ± 0.26 | 3.73 | ± 1.11 | 3.83 | ± 0.48 | 0.78 | ± 0.23 | 0.65 | ± 0.11 | 4.78 | ± 1.87 |
| DBSMS 6 | 21.21 | 303 | 2.00 | 1.53 | ± 0.17 | 1.39 | ± 0.93 | 1.68 | ± 0.32 | 0.78 | ± 0.42 | 0.91 | ± 0.20 | 1.78 | ± 0.57 |
| DBSMS 7 | 23.32 | 302 | 2.00 | 4.26 | ± 0.31 | 1.71 | ± 0.87 | 2.14 | ± 0.35 | 0.58 | ± 0.21 | 1.99 | ± 0.36 | 2.95 | ± 0.99 |
| DBSMS 8 | 25.87 | 301 | 2.00 | 3.93 | ± 0.33 | 3.27 | ± 1.22 | 2.00 | ± 0.32 | 1.39 | ± 0.93 | 1.96 | ± 0.35 | 2.35 | ± 0.99 |
| | | | | | | | | | | | | | | | |
| CB 01 | 12.70 | 188 | 4.8 | 2.10 | ± 0.23 | 0.76 | ± 0.11 | 1.17 | ± 0.29 | 1.76 | ± 0.26 | 1.79 | ± 0.48 | 0.44 | ± 0.09 |
| CB 01 | 14.20 | 130 | 10.4 | 1.37 | ± 0.21 | 0.53 | ± 0.21 | 0.61 | ± 0.30 | 3.12 | ± 0.49 | 2.23 | ± 1.14 | 0.17 | ± 0.07 |
| CB 01 | 15.90 | 34 | 17.7 | 2.83 | ± 0.25 | 0.46 | ± 0.16 | 0.89 | ± 0.33 | 1.00 | ± 0.37 | 3.18 | ± 1.20 | 0.46 | ± 0.23 |
| CB 01 | 17.10 | 2 | 22.0 | 2.18 | ± 0.19 | 1.26 | ± 0.15 | 0.73 | ± 0.30 | 0.69 | ± 0.34 | 2.97 | ± 1.24 | 1.83 | ± 0.45 |
| CB 02 | 13.08 | 153 | 3.0 | 1.51 | ± 0.19 | 2.42 | ± 0.11 | 0.60 | ± 0.29 | 0.68 | ± 0.26 | 2.51 | ± 1.23 | 3.54 | ± 1.35 |
| CB 02 | 14.19 | 71 | 8.2 | 4.44 | ± 0.36 | 5.34 | ± 0.12 | 3.01 | ± 0.50 | 1.88 | ± 0.27 | 1.48 | ± 0.28 | 2.84 | ± 0.06 |
| CB 02 | 15.50 | 41 | 13.9 | 2.70 | ± 0.29 | 10.66 | ± 0.19 | 1.04 | ± 0.50 | 67.09 | ± 0.87 | 2.60 | ± 1.29 | 0.16 | ± 0.60 |
| CB 02 | 17.03 | 1 | 21.9 | 1.07 | ± 0.21 | 2.56 | ± 0.14 | 4.33 | ± 1.00 | 0.31 | ± 0.16 | 0.25 | ± 0.07 | 8.25 | ± 2.45 |
| CB 02 | 17.03 | 1 | 21.5 | 1.27 | ± 0.31 | 1.58 | ± 0.17 | 0.39 | ± 0.32 | 0.37 | ± 0.19 | 3.22 | ± 2.74 | 4.27 | ± 1.79 |
| CB 03 | 10.80 | 142 | 0.8 | 1.65 | ± 0.24 | 0.34 | ± 0.05 | 2.69 | ± 0.40 | 1.91 | ± 0.13 | 0.61 | ± 0.13 | 0.18 | ± 0.03 |
| CB 03 | 13.30 | 23 | 9.1 | 2.48 | ± 0.23 | 6.89 | ± 0.09 | 0.53 | ± 0.30 | 2.78 | ± 0.18 | 4.70 | ± 2.70 | 2.48 | ± 0.17 |
| CB 04 | 8.01 | 188 | 1.1 | 1.40 | ± 0.18 | 5.53 | ± 0.07 | 0.71 | ± 0.31 | 1.77 | ± 0.16 | 1.97 | ± 0.90 | 3.12 | ± 0.28 |
| CB 05 | 6.60 | 177 | 1.9 | 1.95 | ± 0.26 | 3.30 | ± 0.09 | 2.42 | ± 0.46 | 3.34 | ± 0.20 | 0.81 | ± 0.18 | 0.99 | ± 0.07 |
| CB 05 | 10.02 | 96 | 9.1 | 2.00 | ± 0.32 | 9.64 | ± 0.08 | 0.95 | ± 0.46 | 10.70 | ± 0.16 | 2.11 | ± 1.07 | 0.90 | ± 0.02 |
| CB 06 | 3.20 | 175 | 0.5 | 0.83 | ± 0.16 | 9.95 | ± 0.19 | 0.44 | ± 0.28 | 7.64 | ± 0.31 | 1.90 | ± 1.29 | 1.30 | ± 0.06 |
| CB 07 | 2.06 | 172 | 0.5 | 2.55 | ± 0.38 | 3.55 | ± 0.16 | 1.10 | ± 0.49 | 34.82 | ± 0.45 | 2.32 | ± 1.08 | 0.10 | ± 0.00 |
| CB 07 | 3.14 | 155 | 9.0 | 2.09 | ± 0.22 | 31.28 | ± 0.65 | 0.92 | ± 0.35 | 27.61 | ± 0.74 | 2.27 | ± 0.88 | 1.13 | ± 0.04 |

Table 2.2: The dissolved ^{210}Po and ^{210}Pb activities (dpm 100L⁻¹) for Roosevelt Inlet (RI) and Canary Creek (CC) lower Delaware Bay salt marsh.

| Station | Salinity (psu) | Tide Height (ft) | $^{210}\text{Po}_{\text{diss}}$ (dpm 100 l ⁻¹) | $^{210}\text{Pb}_{\text{diss}}$ (dpm 100 l ⁻¹) | $^{210}\text{Po}/^{210}\text{Pb}_{\text{diss}}$ |
|---------|-------------------|---------------------|---------------------------------------------------------------|---------------------------------------------------------------|-------------------------------------------------|
| RI 01 | 26.80 | high tide | 4.33 ± 0.33 | 1.74 ± 0.35 | 2.48 ± 0.54 |
| RI 02 | 27.40 | ebbing | 3.51 ± 0.31 | 1.24 ± 0.39 | 2.84 ± 0.53 |
| RI 03 | 27.60 | ebbing | 5.79 ± 0.49 | 3.84 ± 0.45 | 1.51 ± 0.22 |
| RI 04 | 27.40 | ebbing | 2.79 ± 0.25 | 1.91 ± 0.36 | 1.46 ± 0.30 |
| RI 05 | 25.80 | low tide | 9.95 ± 0.82 | 11.57 ± 1.05 | 0.86 ± 0.11 |
| RI 06 | 25.70 | flooding | 5.03 ± 0.40 | 4.20 ± 0.48 | 1.20 ± 0.17 |
| RI 07 | 27.90 | flooding | 3.46 ± 0.29 | 2.45 ± 0.55 | 1.41 ± 0.34 |
| RI 08 | 28.10 | flooding | 3.27 ± 0.31 | 2.63 ± 0.73 | 1.25 ± 0.37 |
| CC 01 | 21.70 | high tide | 6.68 ± 0.58 | 6.36 ± 0.68 | 1.05 ± 0.14 |
| CC 02 | 23.20 | ebbing | 3.87 ± 0.42 | 7.21 ± 0.83 | 0.54 ± 0.08 |
| CC 03 | 21.20 | ebbing | 6.13 ± 0.69 | 6.35 ± 0.69 | 0.96 ± 0.15 |
| CC 04 | 20.20 | ebbing | 6.69 ± 1.06 | 13.82 ± 1.52 | 0.48 ± 0.09 |
| CC 05 | 19.50 | low tide | 4.78 ± 0.65 | 5.54 ± 0.70 | 0.86 ± 0.16 |
| CC 06 | 18.20 | flooding | 8.28 ± 0.73 | 4.62 ± 0.65 | 1.79 ± 0.30 |
| CC 07 | 19.30 | flooding | 10.11 ± 0.88 | 8.73 ± 0.91 | 1.16 ± 0.16 |
| CC 08 | 20.50 | flooding | 13.90 ± 1.02 | 6.04 ± 0.69 | 2.30 ± 0.31 |
| RMP | 0.40 | low tide | 9.00 ± 1.39 | 18.85 ± 2.53 | 0.48 ± 0.10 |

Table 2.3: Box model units and rates for the Delaware and Chesapeake Bay estuaries

| | $\lambda(a^{-1})$ | $A(\text{Bq m}^{-3})$ | $I_r(\text{Bq m}^{-3})$ | $I_{sm}(\text{Bq m}^{-3})$ | $I_a(\text{Bq m}^{-3} \text{ per year})$ | $\lambda_s(a^{-1})$ | $\lambda_w(a^{-1})$ |
|-------------------|---------------------------------------------|----------------------------|----------------------------|----------------------------|---------------------------------------------|----------------------------|---------------------|
| | | 0.42 (^{210}Po) | 0.81 (^{210}Po) | 0.79 (^{210}Po) | | | |
| | 1.83 (^{210}Po) | 0.35 (^{210}Pb) | 0.43 (^{210}Pb) | 1.27 (^{210}Pb) | 8.00×10^{-5} (^{210}Po) | 4.22 (^{210}Po) | |
| Delaware | 3.11×10^{-2} (^{210}Pb) | 0.90 (^{226}Ra) | 0.28 (^{226}Ra) | 1.83 (^{226}Ra) | 0.075 (^{210}Pb) | 5.47 (^{210}Pb) | 2.97 |
| | | 0.34 (^{210}Po) | 0.39 (^{210}Po) | | | | |
| | 1.83 (^{210}Po) | 0.22 (^{210}Pb) | 0.17 (^{210}Pb) | | 8.00×10^{-5} (^{210}Po) | 2.91 (^{210}Po) | |
| Chesapeake | 3.11×10^{-2} (^{210}Pb) | 3.08 (^{226}Ra) | 0.96 (^{226}Ra) | - | 0.075 (^{210}Pb) | 6.61 (^{210}Pb) | 1.03 |

FIGURES

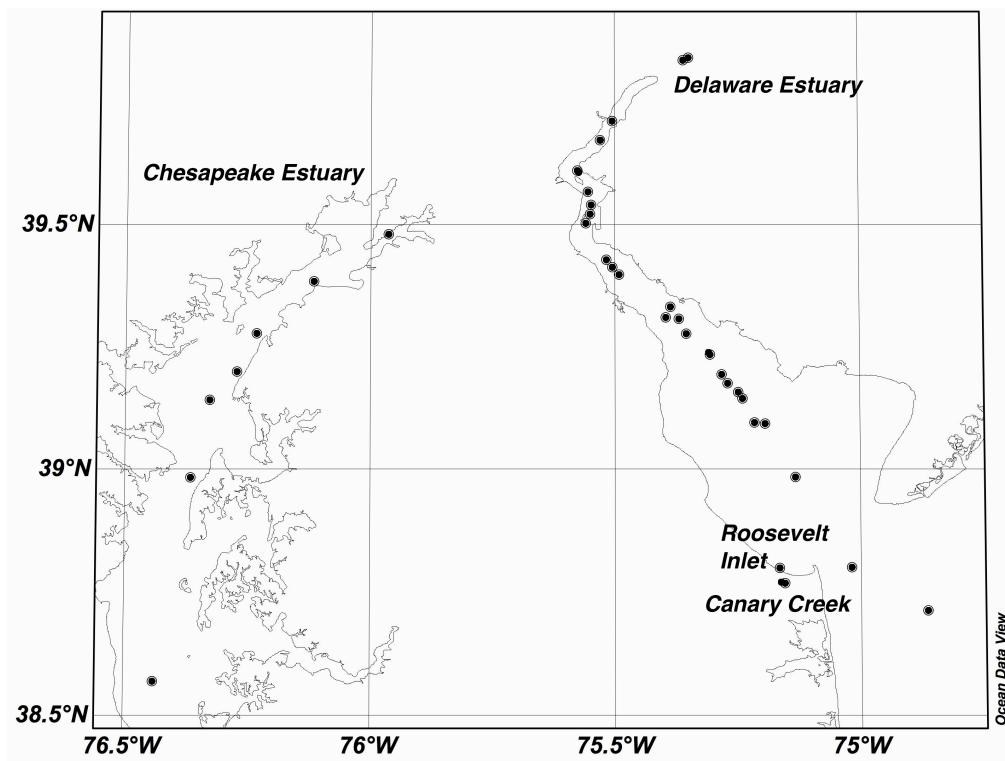


Figure 2.1: Samples for this study were collected at each dot. Samples were collected as follows: Delaware estuary 2012 April 1-3, Delaware salt marsh two locations over a 12hr tidal cycle 2012 June 1, and Chesapeake estuary 2012 August 20-25.

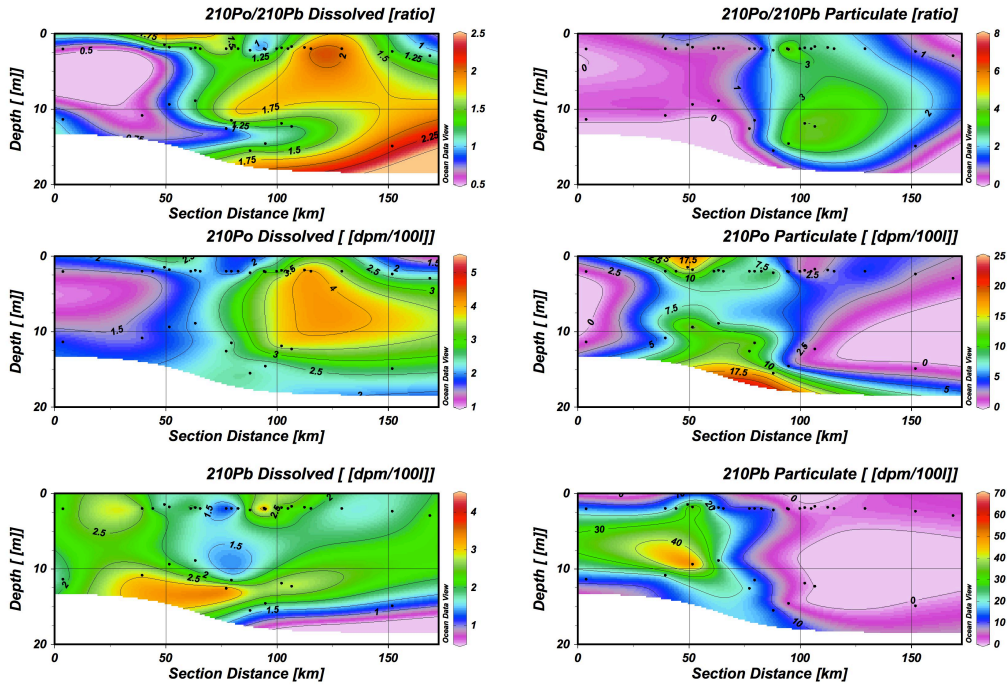


Figure 2.2: Dissolved and particulate ^{210}Po and ^{210}Pb activities (dpm 100L^{-1}) presented as an ODV transect plot in the Delaware estuary.

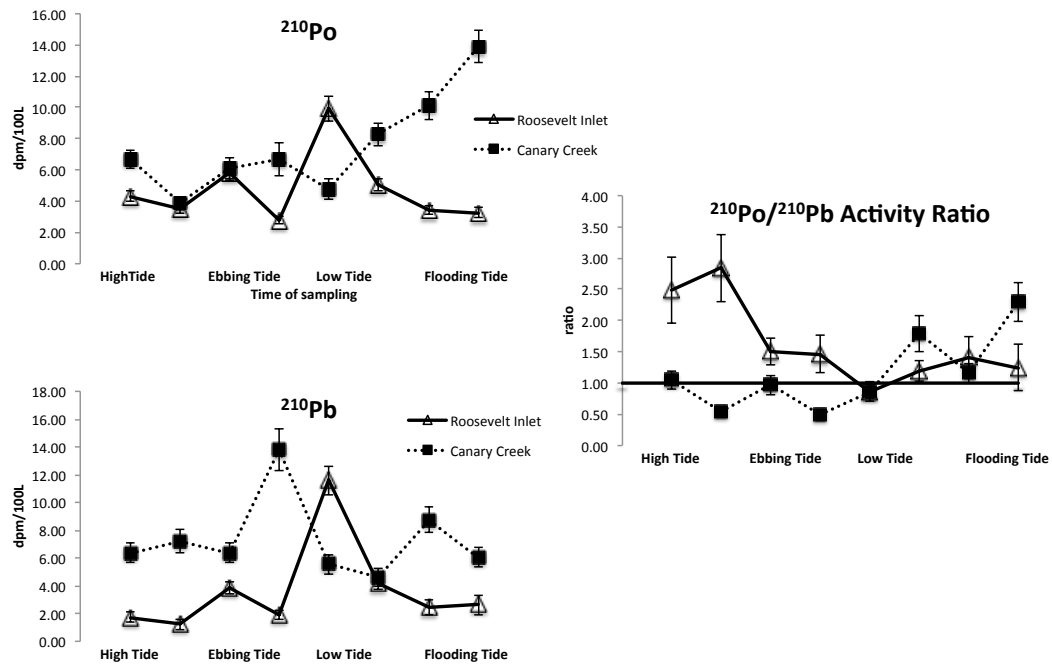


Figure 2.3: Delaware Bay lower salt marsh dissolved ^{210}Po and ^{210}Pb activities (dpm 100L^{-1}) in Roosevelt inlet and Canary Creek over a 12-hr tidal cycle.

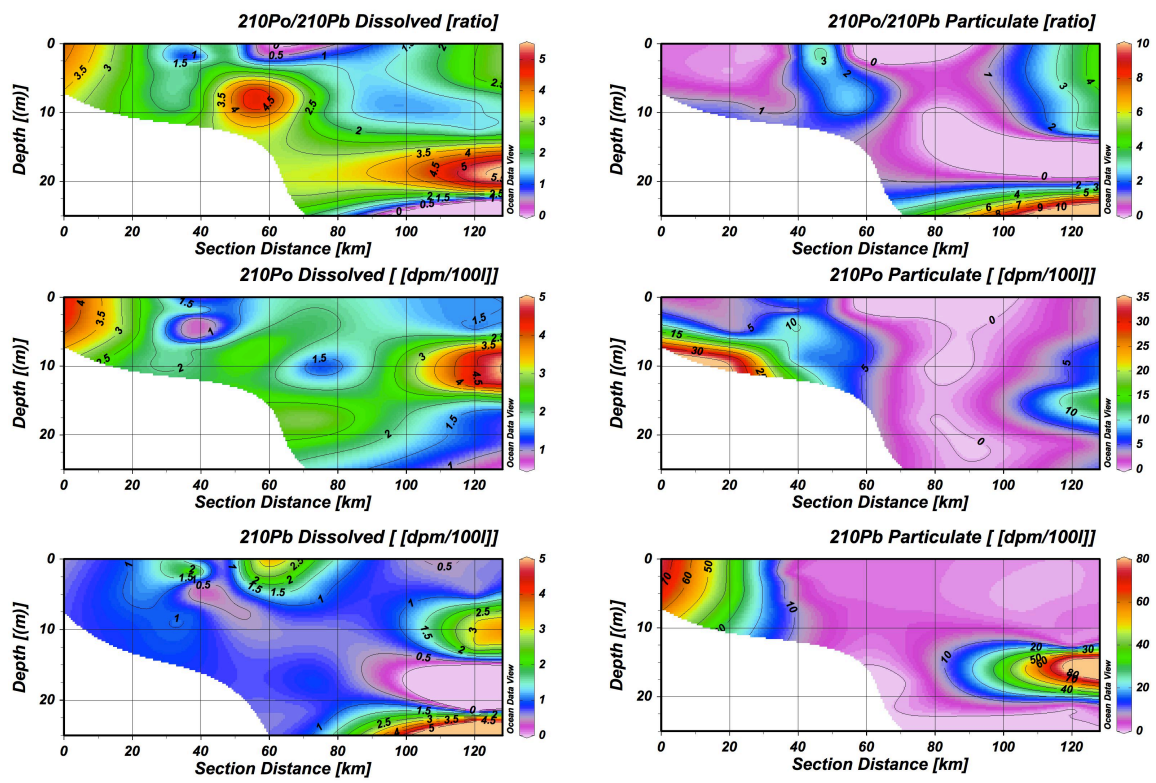


Figure 2.4: Dissolved and particulate ^{210}Po and ^{210}Pb activities (dpm 100L⁻¹) presented as an ODV transect plot in the upper Chesapeake estuary.

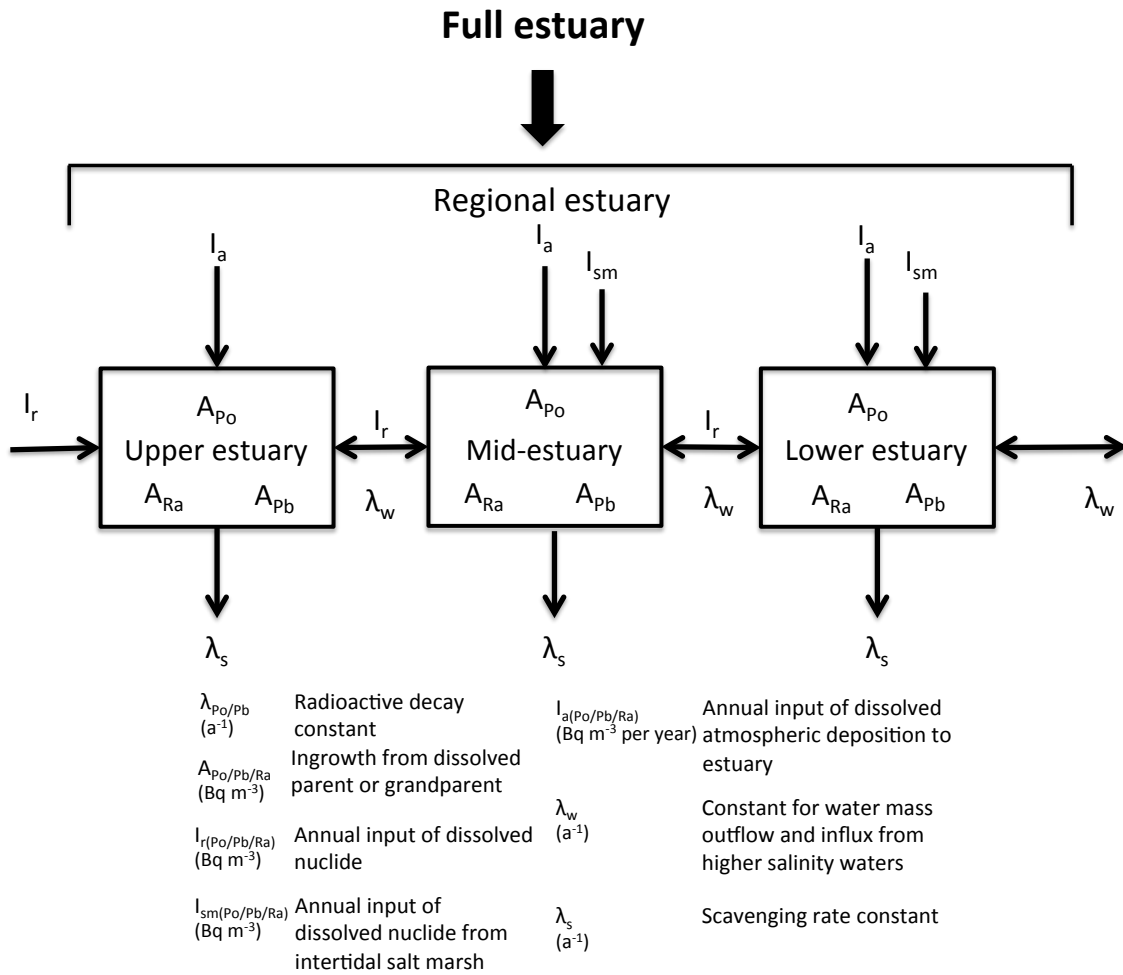


Figure 2.5: Box model depiction and symbol notation for dissolved ^{210}Po in the Delaware and upper Chesapeake estuary. The Delaware estuary utilized a regional (3 box-model) estuary model, while the Chesapeake used a single box model for the entire upper estuary.

Chapter 3

TWO-LAYER TIME VARIABLE MODEL OF THE DELAWARE AND CHESAPEAKE ESTUARY TO GAUGE THE FATE OF TRACE METALS USING NATURAL RADIONUCLIDES

Highlights:

- Modeling sediment-water systems to estimate estuarine dissolved and particulate chemical exchange
- Radionuclides ^{210}Po and ^{210}Pb are able to resolve the dissolved and particulate exchange between bioactive trace elements
- Two-layer model results estimate residence times of weeks (Delaware) and months (Chesapeake) for ^{210}Po and ^{210}Pb that are comparable to the simple box model results

Acknowledgements

- Dr. Luther for providing research cruise time in the Delaware and Chesapeake supported by NSF/OCE grants 1031272 and 1059892.
- Graduate support for D. Marsan was provided by NSF Grant- HRD-1139870- Greater Philadelphia Region LSAMP Bridge to the Doctorate (Cohort IX)
- Dr. Church and Dr. Sommerfield for providing sediment and water column trace element data

3.1 Abstract

A two-layer model has been developed that utilizes field data of trace elements (Fe, Mn, Co, Zn, Cr, Cd, Mn, Cu, Pb, Ni) and the radionuclides (^{210}Po and ^{210}Pb) from two large estuarine systems (Delaware and Chesapeake estuaries). A simplified time variable model of chemical partitioning is presented in the form of analytical solutions for the total, dissolved and particulate concentrations of chemicals in well mixed, interactive, water column and sediment compartments. The model formulation incorporates chemical decay and transport mechanisms of particulate and diffusive exchange between water column and sediment. Results reveal the significance of partitioning on chemical fate, and highlight the important utility of a modeling framework, which incorporates realistic mechanisms of water column and sediment interaction. The use of radionuclides ^{210}Po and ^{210}Pb allows for the tracing of elements with similar reaction chemistries in estuarine environments. Similar residence times, weeks (^{210}Pb) to months (^{210}Po) were estimated by the two-layer model and agree within a factor of 2 with those calculated in a simple box model (Chapter 2). It was also confirmed that trace elements can be grouped with ^{210}Pb (Fe, Pb, Mn, Co and Cr) and ^{210}Po (Cd, Cu, Zn and Ni) based on their residence times in each estuary. The behavior of these trace element groups is linked to their specific biogeochemical reactivity's as shown in other marine environments. For example, ^{210}Po chemical reactivity is similar to other bio-reactive trace elements such as Cu, Cd, Zn, Ni like S, which are mostly assimilated by carbon fixation and thus have similar residence half lives in the estuarine and coastal waters. While ^{210}Pb , which is similar to the physiochemical behavior of Fe, Mn, Co, Cr, and stable Pb displayed similar residence half lives.

Keywords: Partitioning; Model; ^{210}Po ; ^{210}Pb ; Trace Elements; Estuaries

3.2 Introduction

Quantifying the fate of trace elements in the aquatic environment requires the use of a modeling framework, which incorporates idealized transport and reaction mechanisms. Trace elements are associated, to a greater or less degree, with suspended and sedimented particles that are present in the water. Thus, particle transport mechanisms markedly affect the trace element fate in natural water, such as estuaries. The two-layer model that has been developed includes mechanisms of particle transport, as well as partitioning and reaction rates.

The methodology presented is based on the principle of conservation of mass. It has been expressed in mathematical form for application to lakes, impoundments and flowing streams (DiToro et., al. 1982: DiToro et., al. 1984) and here it will be applied to estuarine systems. The fate of chemicals in rivers and estuaries is similar in many ways to the situation in lakes. Whereas lakes can be represented, in many cases, by two completely mixed volumes, i.e., the water column and active sediment segments, the estuary also includes the distribution of trace elements and associated particles downstream from the point of discharge. The over all construct for an estuary is shown in Figure 3.1 along with symbol and dimensions in Table 3.1 as being represented by a sequence of completely mixed segments, each only influenced by inflow and outflow of water and sediment column trace elements.

A release of chemical, M_t is discharged to a completely mixed water volume V_1 with depth H_1 , where it undergoes dilution by water flow, Q_1 . The chemical is partitioned between the dissolved and particulate phases in the water column (denoted by subscript 1) and in the sediment (denoted by subscript 2) that has a solids concentration of m_1 and m_2 respectively. The chemical is then transferred between the water column and sediment layer by settling and re-suspension of particles and via diffusive exchange between the dissolved phases in the water and sediment. The chemical may also undergo first order decay in the water column and sediment or it may be removed from the system by sedimentation. The loading rate

of chemical W is the primary input to the water column. The reactions that remove the chemical (i.e. decay, resuspension, diffusion, volatilization, burial) are summed to yield the total decay rates (organic matter or radiometric decay) in the water column k_1 , and sediment k_2 .

Utilizing the radionuclide pair ^{210}Po and ^{210}Pb that are similarly particle reactive, presents an intrinsic metric to test such an adapted two-layer model for estuarine systems. The mechanism for removal includes adsorption (^{210}Po and ^{210}Pb) and absorption (^{210}Po) by suspended particles and organisms respectively, thus the radionuclides can be used to estimate the trace element transport and transfer rates throughout the estuary. This paper aims to 1) detail the calculations of a two-layer model to be applicable for estuarine systems, 2) apply the two-layer model in the Delaware and Chesapeake estuaries using radionuclides (^{210}Po and ^{210}Pb) to track other trace elements (Fe, Cd, Cu, Ni, Zn, Pb, Cr, Co and Mn), and specify residence half-lives and partitioning coefficients for trace elements and radionuclides.

3.3 Data Collection and Previous work

Data was collected over a number of years and by other researchers (Church et al., 1986 and 1988; Bopp et al., (1980); Sinex and Helz 1981). The Delaware estuary trace elements (Fe, Cd, Cu, Ni, Zn and stable Pb) water column data were collected by Church, (et., al 1986 and 1988) while sediment data was collected by Bopp, (MS thesis 1973) during the spring of 1979-1980. The ^{210}Po and ^{210}Pb water column data was collected by Marsan et al., (submitted) while upper estuary sediment cores were collected by Sommerfield (unpublished) during the spring of 2012. Sediment data for ^{210}Pb was not available in the mid to lower estuary due to very low concentrations of clay that prevented grab sampling. Instead sediment data was used from intertidal marshes surrounding the estuary where most of the deposition occurs in the Delaware estuary.

Chesapeake Bay water column trace elements (Cr, Co, Zn, Mn, Ni and stable Pb) were collected by Church et al., (unpublished) while sediment data was

collected by Sinex and Helz (1981). The ^{210}Po and ^{210}Pb water column data was collected by Marsan et al., (submitted) and detailed in chapter 2, while ^{210}Pb sediment data from Sinex and Helz (1981) was utilized. Detailed sample collection and procedures can be found in the previous chapters of this thesis and in Bopp et al., (1980), and Sinex and Helz (1981).

3.4 Description of Modeling Framework

The principle features of the modeling framework (DiToro et al., 1982) are two distinct layers (water column and sediment) whose only interaction with the adjacent downstream box is from water column transport (Figure 3.1). The original model framework was based on an instantaneous release of chemical while in an estuary system this fluctuates seasonally. The “instantaneous release” for each estuary system is determined by the concentration measured at the first station of each estuary, times an appropriately integrated time interval. Thus the initial water column concentration is simply $C_{T1(0)}=M_T/V_1$. The first step is to model the sediment-water column dissolved and particulate chemical exchange. A two-layer model can solve for the fate of partitioning trace elements in a predefined box split in two, water column (denoted by subscript 1) and sediment (denoted by subscript 2) (Figure 3.1 and described in Table 3.1). From the model K_{p1} and K_{p2} , chemical partitioning coefficients in liters per day, can be estimated and then be used to solve for the estuary divided into successive segments to account for re-distribution seaward.

The two-layer model takes into account two distinct areas, the water column:

$$V_1 \frac{dC_{T1}}{dt} = QC_{T_{in}} - QC_{T1} - v_s A f_{p1} C_{T1} + v_{rs} A f_{p2} C_{T2} - k_1 V_1 C_{T1} - v_v A f_{d1} C_{T1} + v_d A \left(\frac{f_{d2} C_{T2}}{\phi_2} - f_{d1} C_{T1} \right) \quad (1)$$

Equation (1) accounts for inflow-outflow of water, particle settling and resuspension, decay, volatilization and diffusion of the chemical. While in sediment:

$$V_2 \frac{dC_{T2}}{dt} = v_s A f_{p1} C_{T1} - v_{rs} A f_{p2} C_{T2} - v_b A f_{p2} C_{T2} - k_2 V_2 C_{T2} + v_d A (f_{d1} C_{T1} - \frac{f_{d2} C_{T2}}{\phi_2}) \quad (2)$$

Equation (2) accounts for particle settling, resuspension and burial along with decay and diffusion occurring in the sediment. The steady-state solution from equations (1) & (2) is:

$$\frac{C_{T2}}{C_{T1}} = \frac{(v_s f_{p1} + v_d f_{d1})}{(v_{rs} f_{p2} + v_b f_{p2} + k_2 H_2 + \frac{v_d f_{d2}}{\phi_2})} \quad (3)$$

Taking into account:

Particulate chemical in the water column and sediment= $C_{p1}, C_{p2} (\frac{\mu g}{L})$

Concentration on particles in water column and sediment= $r_1, r_2 (\frac{\mu g}{kg})$

Concentration ratio of chemical on particles in sediment/water column= r_2/r_1

And factoring into equation (3) yields:

$$\begin{aligned} \frac{r_2}{r_1} &= \frac{\frac{C_{p2}}{m_2}}{\frac{C_{p1}}{m_1}} = \frac{\frac{f_{p2} C_{T2}}{m_2}}{\frac{f_{p1} C_{T1}}{m_1}} = \left(\frac{f_{p2}}{f_{p1}} \right) \left(\frac{m_1}{m_2} \right) \left(\frac{C_{T2}}{C_{T1}} \right) \\ &= \left(\frac{f_{p2}}{f_{p1}} \right) \left(\frac{m_1}{m_2} \right) \left(\frac{v_s f_{p1} + v_d f_{d1}}{v_{rs} f_{p2} + v_b f_{p2} + v_d f_{d2} + k_2 H_2} \right) \\ \frac{f_{d1}}{f_{p1}} &= \frac{1/(1 + m_1 K_{p1})}{m_1 K_{p2}/(1 + m_1 K_{p1})} = \frac{1}{m_1 K_{p1}} \end{aligned} \quad (4)$$

The solids mass balance (equation 5) in terms of velocities of settling (s), resuspension (rs) and burial (b) can be expressed as:

$$0 = v_s m_1 - v_{rs} m_2 - v_b m_2 \quad (5)$$

Rearranging equation (5) to be equal to the solids concentration of the water column (m_1) and sediment layer (m_2):

$$\frac{m_1}{m_2} = \frac{v_{RS} + v_B}{v_S} \quad (6)$$

Resulting in a simplification of equation (4) by factoring in equation (5):

$$\frac{r_2}{r_1} = \frac{(v_{RS} + v_B)f_{p2} + v_D f_{d2} \left(\frac{K_{p2}}{K_{p1}}\right)}{(v_{RS} + v_B)f_{p2} + v_D f_{d2} + k_2 H_2} \quad (7)$$

From the final solution, equation (7), the r_2/r_1 defined as the ratio of chemical on particles in the sediment (r_2) and particulates in the water column (r_1), can be further simplified to three cases depending on the parameters used:

- (1) If $K_{p2}=K_{p1}$ and $k_2=0$ then $r_2=r_1$
- (2) If $v_{RS}+v_B \gg v_D$ (particle mixing \gg diffusive exchange) then $r_2=r_1$
- (3) If $v_{RS}+v_B \ll v_D$ (particle mixing \ll diffusive exchange)

Then equation (7) simplifies to:

$$\frac{r_2}{r_1} = \frac{K_{p2}}{K_{p1}} \text{ and } \frac{r_2/K_{p2}}{r_1/K_{p1}} = \frac{C_{d2}}{C_{d1}} = 1$$

As was shown above, equation (7) can be simplified to yield three cases. One can solve for the partition coefficients (K_{p1} and K_{p2}) by using the r_2/r_1 values as follows:

$$\frac{r_2}{r_1} = \frac{\frac{v_{RS}v_B}{v_D} + \frac{f_{p2}}{f_{d2}} + \left(\frac{K_{p2}}{K_{p1}}\right)}{\frac{v_{RS} + v_B}{v_D} + \frac{f_{p2}}{f_{d2}} + 1} \quad (8)$$

Solving for the mixing parameter (γ):

$$\gamma = \frac{v_{RS} + v_B}{v_D} m_2 \quad (9)$$

Then by factoring equation (9) into (8) reduces to:

$$\frac{r_2}{r_1} = \frac{\gamma K_{p2} + \left(\frac{K_{p2}}{K_{p1}}\right)}{\gamma K_{p2} + 1} \quad (10)$$

Finally, the partition coefficient for the sediment can be solved:

$$K_{p2} = \frac{r_2/r_1}{\gamma(1 - r_2/r_1) + \frac{1}{K_{p1}}} \quad (11)$$

If particle mixing >> diffusive mixing, such as in case (2) for the Delaware and Chesapeake estuaries, the K_{p1} term can be dropped out since it is much smaller than K_{p2} . Thus (11) can be simplified to equation (12):

$$K_{p2} = \frac{r_2/r_1}{\gamma(1 - r_2/r_1)} \quad (12)$$

We will now consider the seaward distribution of the model (Figure 1). For both estuaries we consider them to be represented by completely mixed and successive volume segments. The subscript denotes the segment being considered. Thus C_{T1} is the water column chemical concentration in segment 1; Q_1 is the water inflow; and so on for all other parameters. The first estuarine segment upstream receives a loading flux of chemical W_{T1} . Its outflow is Q_2 , the net flow rate of the estuary seaward and corrected for higher salinity intrusion. If the concentration of chemical from the seaward influx is neglected, then the first segment can be expressed by the equations 1 through 12 presented for a single section.

Consider the second completely mixed estuarine segment. Although vertical sediment and interstitial water mixing is still being considered, horizontal bed motion is assumed to be negligible. The reason for this assumption is that for the fixed-bed case, the second stream segment receives only a water column input of trace element as a result of water flow from the upstream segment. A similar argument applies to each successive estuarine volume element so that an estuary can be divided into n segments. Parameters used for water inflow-outflow, intertidal

marsh, atmospheric deposition, are the same described in chapter 2 and used for the single box-model.

3.5 Model Parameters

Based on a review of hydrological data from the Delaware and Chesapeake estuaries, parameters for each trace element (Fe, Cd, Cu, Ni, Zn, Pb, Cr, Co, and Mn) and radionuclides (^{210}Po and ^{210}Pb) were used (Table 2). The Delaware and Chesapeake estuaries were treated vertically as well mixed water column with a defined sediment layer. The depth of the active sediment layer is estimated from chemical diffusion into the sediment. Thus, a sediment grab deployed to a depth of 1-2cm was used to characterize each trace element respectively.

The mass loadings of interest are the chemical and solids flux rates to the estuaries. Each research group accurately measured inputs of trace elements and radionuclides. The analysis of particulate transport in the estuary was also accurately measured including suspended solids concentrations in the water column and sediment. For the Delaware estuary the main freshwater source is the Delaware River but another significant source of trace elements are the pervasive intertidal marshes surrounding the estuary, as described (Marsan et al., submitted). The model takes into account two sources, the Delaware River and intertidal marshes.

Solving for the ratio concentration of chemical on particulate in sediment and on particulate in the water column (r_2/r_1) for the trace elements in the Delaware and Chesapeake estuary one finds that in both estuaries particle mixing is much larger than diffusive exchange. In the Delaware estuary the r_2/r_1 value is 10-100 times greater, meaning more partitioning of particulate elements is occurring in the water column rather than the sediment (Figure 2). The trace elements with the greatest r_2/r_1 ratio to the least are $\text{Fe} \geq \text{Cu} \geq \text{Zn} \geq \text{Cd} \geq ^{210}\text{Pb} \geq \text{Pb} \geq ^{210}\text{Po} \geq \text{Ni}$. From upper to lower Delaware estuary each element distribution is quite uniform other than for ^{210}Po , ^{210}Pb , stable Pb and Ni. The latter group of elements follows a trend of higher r_2/r_1 ratios in the upper estuary that decrease seaward toward mid-estuary and then again increase in the lower estuary.

On the other hand the Chesapeake estuary (Figure 3.3) is rather different, four groups on elements can be made based of their r_2/r_1 ratio; first Co, Cr, and Zn; next Ni, Pb, ^{210}Pb and ^{210}Po ; and finally Mn. The first group (Co, Cr, and Zn) all display lower r_2/r_1 values in the upper Chesapeake then rapidly increase and stay constant seaward. The second group (Ni, Pb, ^{210}Pb , ^{210}Po) display r_2/r_1 values that never increase above 10 or below 0.1. This most likely indicates that the partitioning occurring in the water column is only somewhat greater than that in the sediment. Finally, the last element, Mn, displays an r_2/r_1 that is almost entirely below 1, meaning that most of the partitioning is occurring in the sediment rather than the water column.

The magnitudes and parameters are estimated by using yearly averages and by testing the log of the mixing parameter (γ) value that best fits a line equation for each element. The reason a best-fit line equation is used to determine the mixing parameter is because the burial velocity (v_B), resuspension velocity (v_{RS}) and diffusion mass transfer (v_D) are all estimated. The best-fit line of $\log \gamma$ can determine if the estimates are reasonable or need to be evaluated for each estuary. It was found that a $\log \gamma$ of -3 and -4 for the Delaware and Chesapeake Bay respectively best fits the line equation. This suggests that the parameters estimated in Table 2 are likely valid for each estuary.

The partitioning coefficient in the sediment (K_{p2}) is calculated in Table 3.3 using the estimated magnitudes and parameters found in Table 3.2. The negative K_{p2} term means that particle partitioning is not only much larger than diffusive mixing but that the mixing is occurring in the water column rather than the sediment. The use of ^{210}Po and ^{210}Pb in the model is important because their decay rates are well known and thus can be used as proxies to measure trace elements. Under this situation ^{210}Po and ^{210}Pb data is used in the two-layer model to determine residence half lives in the Delaware and Chesapeake estuary (Table 3.3).

The Delaware estuary is divided into upper, mid and lower estuary, while only the upper Chesapeake estuary is evaluated for the ^{210}Po and ^{210}Pb radionuclides. The calculated Delaware estuary residence half-life in the water column was for ^{210}Pb (31, 7, and 17 days) and ^{210}Po (36, 15, and 38 days) and in the

corresponding sediment fraction ^{210}Pb (180, 97, and 52 days) and ^{210}Po (171, 88, and 76 days) respectively. The difference observed between water column and sediment suggests that ^{210}Po and ^{210}Pb are being retained in the estuary by sedimentation. As discussed earlier the bottom sediment of the mid to lower Delaware estuary is mostly sand. Rather than not have a bottom sediment term, in the estuary a sediment concentration was determined by the surrounding intertidal salt marshes, which traps or filters most sediment from the estuary (Sharp, et al., 1984). If the marsh term were excluded from the calculation the residence half lives between the sediment and water column in the estuary for ^{210}Po and ^{210}Pb would be the same. Instead we observe that the marshes act as a sink of ^{210}Po and ^{210}Pb in the Delaware estuary.

The residence half-lives are calculated in the upper Chesapeake water column for ^{210}Pb (77 days) and ^{210}Po (183 days) and in the corresponding sediment layer ^{210}Pb (345 days) and ^{210}Po (394 days). This represents a greater sink of radionuclides in the Chesapeake bottom sediment than in the Delaware estuary. The Chesapeake does not have pervasive intertidal marshes as discussed in Chapter 2, instead the drowned river bottom is high in silt and clay sediment. The bottom sediment in the Chesapeake acts as the main sink for the ^{210}Pb and ^{210}Po radionuclides. Not only can the radionuclide residence times be compared to the previous single box model, here it can be compared as a proxy to other trace elements in order to determine their half-lives.

Using similar parameters and rates as Table 3.3, partition coefficients and residence half-lives were estimated for other trace elements (Table 3.4). Trace elements can be grouped with ^{210}Pb (Fe, Pb, Mn, Co and Cr) and ^{210}Po (Cd, Cu, Zn and Ni) based on their residence half-lives in each estuary. The ^{210}Pb and corresponding trace element residence half-lives in the Delaware are on the order of weeks, while the ^{210}Po group is on the order of months. Note that the behavior of ^{210}Po is similar to other bio-reactive trace elements such as Cu, Cd, Zn, Ni like S, and more assimilated by carbon fixation. This is in contrast to ^{210}Pb , which is associated with physicochemical processes as are Fe, Mn, Co, Cr and stable Pb.

Comparing the results from the previous single box model and the two-layer model we find generally a good deal of agreement. Both models predict that water column ^{210}Po and ^{210}Pb residence times are both on the order of weeks and months for the Delaware and Chesapeake Bay. The two-layer model has the increased capability of measuring the residence time of the radionuclides in bottom sediment and their sediment-water partitioning. As a whole the two-layer model creates a more realistic situation for modeling the dynamic mechanisms, partitioning coefficients, residence times and transport processes of an estuary, than possibly with a single box-model. There are some drawbacks to using the two-layer model in estuaries; a key provision of the model for example, there is no provision for lateral sediment movement while in reality there should be some occurring. Another exception is the estimation of terms used in the model such as re-suspension velocity, burial velocity, settling rate and diffusive exchange (Table 3.2), however these may be easily solved by a comprehensive sampling to measure there parameter. Nevertheless the results compare well, within a factor of 2, with the previous single box model and should be investigated more to aid in confirming and advancing the two-layer model for use in estuarine systems.

3.6 Conclusion

The two-layer model results for the Delaware and Chesapeake estuaries underscore the significance of chemical partitioning on determining rates and residence times. Along with determining partitioning, the two-layer model highlights the importance and utility of a modeling framework that incorporates realistic mechanisms of water column and sediment interaction. Trace elements and radionuclides are capable of being modeled using such an adapted two-layer model for estuaries. Using the two-layer model with the radionuclides ^{210}Po and ^{210}Pb allows for estimates of trace element residence times and partitioning in the estuarine sediment-water. This paper identified two distinct groups of trace elements, which can be associated with ^{210}Pb (Fe, stable Pb, Mn, Co and Cr) and ^{210}Po (Cd, Cu, Zn and Ni) as proxies. Knowing how trace elements partition in estuarine systems will allow for more defined estimates of the rate of transport and

particle fate of radionuclides and trace elements within estuaries. Future experiments should be conducted to include samples of trace elements collected from the water column and sediment concurrently. By collecting samples at once the factor of 2 difference between the two models should help reduce the uncertainty between the two models and lead to a more viable tool for evaluating the fate of trace elements and radionuclides. Other work should focus on expanding the list of trace elements to understand if they too would be capable of being modeled using radionuclides as proxies.

REFERENCES

Bopp, F. (1980). Trace Metal Geochemistry of Upper Delaware Bay. Master Thesis-University of Delaware.

Church, T. M., J. M. Tramontano, J. R. Scudlark and S. L. Murray. 1988. Trace metals in the waters of the Delaware estuary. (In:) Ecology and Restoration of the Delaware River Basin. (ed. S.K. Majumdar, E.W. Miller and L. E. Sage), The Philadelphia Academy of Sciences.

Church, T. M., J. M. Tramontano and S. Murray. 1986. Trace metal fluxes through the Delaware estuary. (In:) Proc. of Int'l. Council for Exploration of the Sea (ICES) Symposium. "Contaminant Fluxes through the Coastal Zone," Nantes, France, May 1984. Rapp. P.v Reun. Cons. Int. Explor. Merc., 186:271-276.

DiToro, D.M., D.J. O'Connor, R.V. Thomann and J.P. St. John. 1982. Simplified model of the fate of partitioning chemical in lakes and streams. In K.L. Dickson, A.W. Maki, and J.Cairns, Jr., eds., Modeling the Fate of Chemicals in the Environment. Ann Arbor Science Publications, Ann Arbor, MI, pp. 165-190.

DiToro, D.M. and P.R. Paquin (1984). Time variable model of the fate of DDE and Lindane in a quarry. Environ. Toxicol. Chem. 3: 335-353.

Sharp, J. H., J. R. Pennock, T. M. Church, J. M. Tramontano and L. A. Cifuentes. 1984. The estuarine interaction of nutrients, organics, and metals: A case study in the Delaware Estuary. (In:) The Estuary as a Filter, (ed. V. S. Kennedy), Academic Press, pp. 241-257.

TABLES

Table 3.1: Two-Layer model terminology

| Water Column | | Sediment | |
|-------------------------------------------|-----------------------------|-------------------------------------------|-----------------------------|
| C_{T1} | Total Chemical(mg/L) | C_{T2} | Total Chemical(mg/L) |
| f_{d1} | Fraction dissolved | f_{d2} | Fraction dissolved |
| $f_{d1}=1/(1+m_1K_{p1})$ | | $f_{d2}=1/(1+m_2K_{p2})$ | |
| m_1 | Solids Concentration(kg/L) | m_2 | Solids Concentration(kg/L) |
| $C_{d1}=f_{d1}C_{T1}$ | Dissolved Chemical(mg/L) | $C_{d2}=f_{d2}C_{T2}$ | Dissolved Chemical(mg/L) |
| f_{p1} | Fraction particulate | f_{p2} | Fraction particulate |
| $f_{p1}=m_1K_{p1}/(1+m_1K_{p1})=1-f_{d1}$ | | $f_{p2}=m_2K_{p2}/(1+m_2K_{p2})=1-f_{d2}$ | |
| $C_{p1}=f_{p1}C_{T1}$ | Particulate Chemical(mg/kg) | $C_{p2}=f_{p2}C_{T2}$ | Particulate Chemical(mg/kg) |
| K_{p1} | Partition Coefficient | K_{p2} | Partition Coefficient |
| k_1 | Decay | k_2 | Decay |

Table 3.2: Magnitudes and parameters used to solve for the partition coefficient (K_{p2}) in the Delaware and Chesapeake estuaries

| <u>Magnitudes and Parameters</u> | | <u>Delaware Bay</u> | <u>Chesapeake Bay</u> |
|----------------------------------|-----------------------------------------|------------------------------------|------------------------------------|
| Burial velocity | v_B | 0.5 cm/yr | 1 cm/yr |
| Resuspension velocity | v_{RS} | 5 cm/yr | 5 cm/yr |
| Diffusion Coefficient | D | 1 cm ² /d | 1 cm ² /d |
| Diffusion Depth | H | 1 cm | 1 cm |
| Diffusion Mass Transfer Coeff | v_D | 1 cm/d | 1 cm/d |
| Sediment Solids Concentration | m_2 | 0.01 kg/L | 0.1 kg/L |
| Mixing Parameter | $\gamma = \frac{v_{RS} + v_B}{v_D} m_2$ | 10 ⁻² -10 ⁻³ | 10 ⁻³ -10 ⁻⁴ |

Table 3.3: Summary of chemical and physical parameters used and calculated by the two-layer model for ²¹⁰Po and ²¹⁰Pb in the Delaware and Chesapeake estuaries

| Chemical/Physical Parameters | Units | Delaware Bay | | | | Chesapeake Bay | | | |
|---------------------------------|-------|-------------------|-------------------|-------------------|-------------------|-------------------|-------------------|-------------------|-------------------|
| | | Water Column | | Sediment Layer | | Water Column | | Sediment Layer | |
| | | ²¹⁰ Pb | ²¹⁰ Po |
| Depth | m | 11 | 11 | 0.02 | 0.02 | 15 | 15 | 0.02 | 0.02 |
| Suspended Solids | mg/L | 30 | 30 | 7.5E+05 | 7.5E+05 | 20 | 20 | 7.5E+05 | 7.5E+05 |
| Particle Velocities | | | | | | | | | |
| Settling | m/d | 0.005 | 0.005 | - | - | 0.005 | 0.005 | - | - |
| Resuspension | mm/yr | - | - | 50 | 50 | - | - | 50 | 50 |
| Sedimentation | mm/yr | - | - | 5 | 5 | - | - | 10 | 10 |
| Diffusive Exchange | cm/d | 1 | 1 | - | - | 1 | 1 | - | - |
| Dissolved Fraction | | | | | | | | | |
| upper | | 0.076 | 0.195 | 0.004 | 0.004 | 0.119 | 0.264 | 0.004 | 0.004 |
| mid | | 0.156 | 0.172 | 0.004 | 0.004 | - | - | - | - |
| lower | | 0.630 | 0.575 | 0.004 | 0.004 | - | - | - | - |
| Particulate Fraction | | | | | | | | | |
| upper | | 0.924 | 0.805 | 0.996 | 0.996 | 0.881 | 0.736 | 0.996 | 0.996 |
| mid | | 0.844 | 0.828 | 0.996 | 0.996 | - | - | - | - |
| lower | | 0.370 | 0.425 | 0.996 | 0.996 | - | - | - | - |
| Total Removal Rate | L/d | 0.015 | 0.012 | 0.001 | 0.001 | 0.018 | 0.008 | 0.0004 | 0.0004 |
| Model Related Parameters | | | | | | | | | |
| Particulate concentration | | | | | | | | | |
| Ratio, r2/r1 | upper | | 15.73/11.01 | | | 16.38/50.65 | | | |
| | mid | | 1.69/3.055 | | | | | | |
| | lower | | 16.53/7.12 | | | | | | |
| Total Apparent Removal Rate | L/d | | 0.0029/0.0083 | | | 0.0029/0.0083 | | | |
| Total Transfer-Decay Rates | | | | | | | | | |
| Water Colum | L/d | | 0.0051/8.64e-6 | | | 0.0051/8.64e-6 | | | |
| Sediment | L/d | | 0.0051/8.64e-6 | | | 0.0051/8.64e-6 | | | |
| Partition Coefficient, Kp2 | | | | | | | | | |
| upper | | | 77.23/55.09 | | | 62.90/628.70 | | | |
| mid | | | 0.38/3.14 | | | | | | |
| lower | | | 85.57/21.76 | | | | | | |
| Half Life | | | | | | | | | |
| upper | d | 31 | 36 | 180 | 171 | 77 | 183 | 345 | 394 |
| mid | d | 7 | 15 | 97 | 88 | | | | |
| lower | d | 17 | 38 | 52 | 76 | | | | |

Table 3.4: Partition coefficients of trace elements and residual half-lives (d) estimated in the Delaware and Chesapeake estuaries by the two-layer model. This not only shows the trends between estuarine regions (upper, mid, lower) but how radionuclides can be used as proxies to determine their residence half-lives.

| Trace element | Model Parameters | Delaware Bay Water Column | | | Chesapeake Bay Water Column | |
|---------------|----------------------------|---------------------------|-----|-------|-----------------------------|-------|
| | | upper | mid | Lower | upper | lower |
| Fe | Partition Coefficient, Kp2 | 66 | 91 | 3282 | | |
| | Half Life, d | 37 | 11 | 15 | | |
| Cu | Partition Coefficient, Kp2 | 274 | 299 | 1617 | 6 | 26 |
| | Half Life, d | 40 | 29 | 45 | 157 | 112 |
| Zn | Partition Coefficient, Kp2 | 54 | 24 | 274 | 9 | 270 |
| | Half Life, d | 35 | 20 | 41 | 173 | 199 |
| Cd | Partition Coefficient, Kp2 | 192 | 29 | 136 | | |
| | Half Life, d | 42 | 19 | 38 | | |
| Ni | Partition Coefficient, Kp2 | 8 | 1 | 13 | 2 | 45 |
| | Half Life, d | 21 | 7 | 12 | 141 | 117 |
| Pb | Partition Coefficient, Kp2 | 35 | 1 | 23 | 7 | 2 |
| | Half Life, d | 30 | 5 | 14 | 89 | 57 |
| Cr | Partition Coefficient, Kp2 | | | | 18 | 243 |
| | Half Life, d | | | | 82 | 74 |
| Co | Partition Coefficient, Kp2 | | | | 25 | 358 |
| | Half Life, d | | | | 88 | 92 |
| Mn | Partition Coefficient, Kp2 | | | | 0 | 1 |
| | Half Life, d | | | | 51 | 55 |

FIGURES

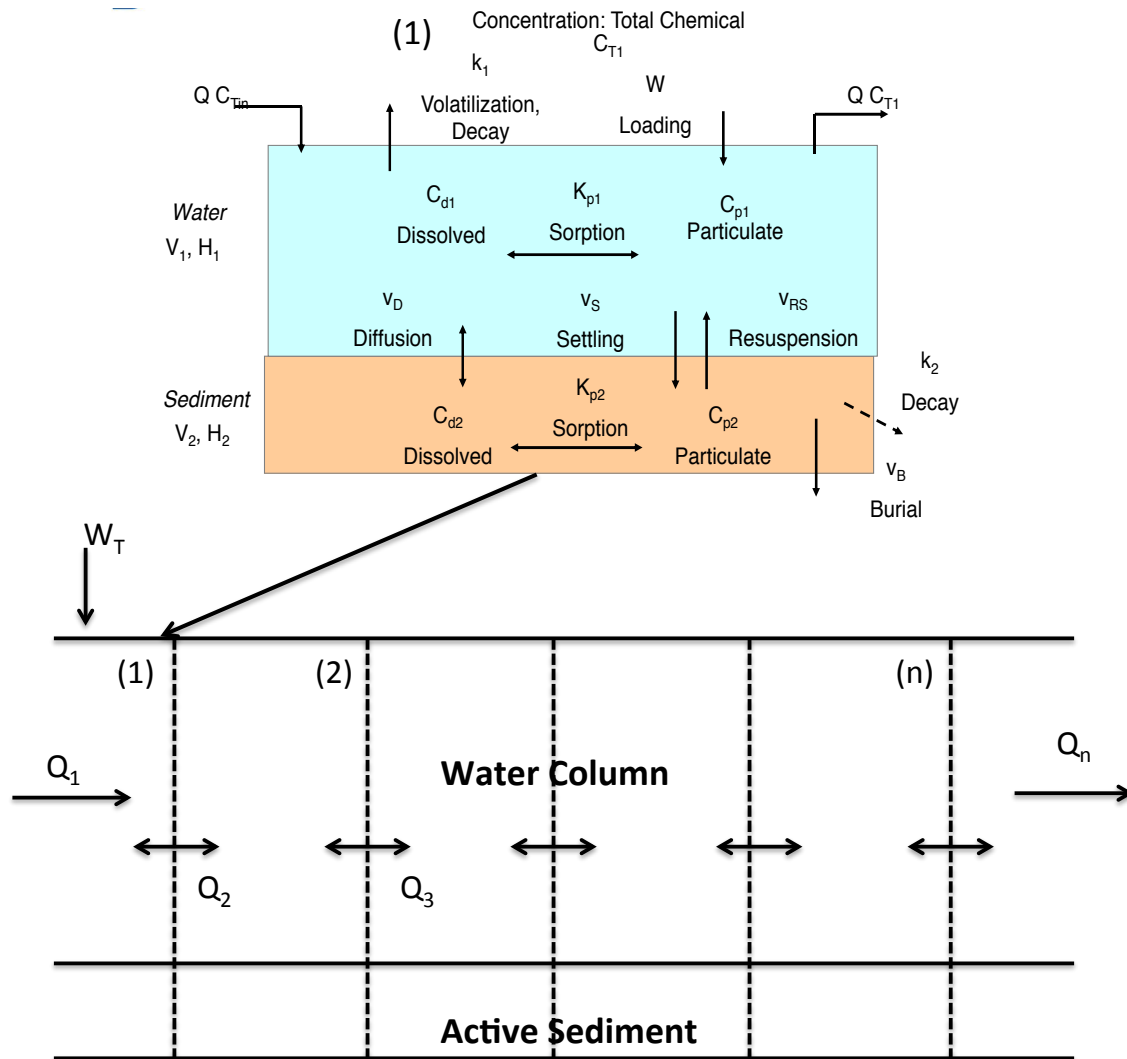


Figure 3.1: Altered two-layer model for a river or estuarine system. Panel 1 depicts the processes affecting a chemical in a single region two-layer region. The next panel (2) combines n^{th} number of two-layer regions to simulate the processes moving seaward.

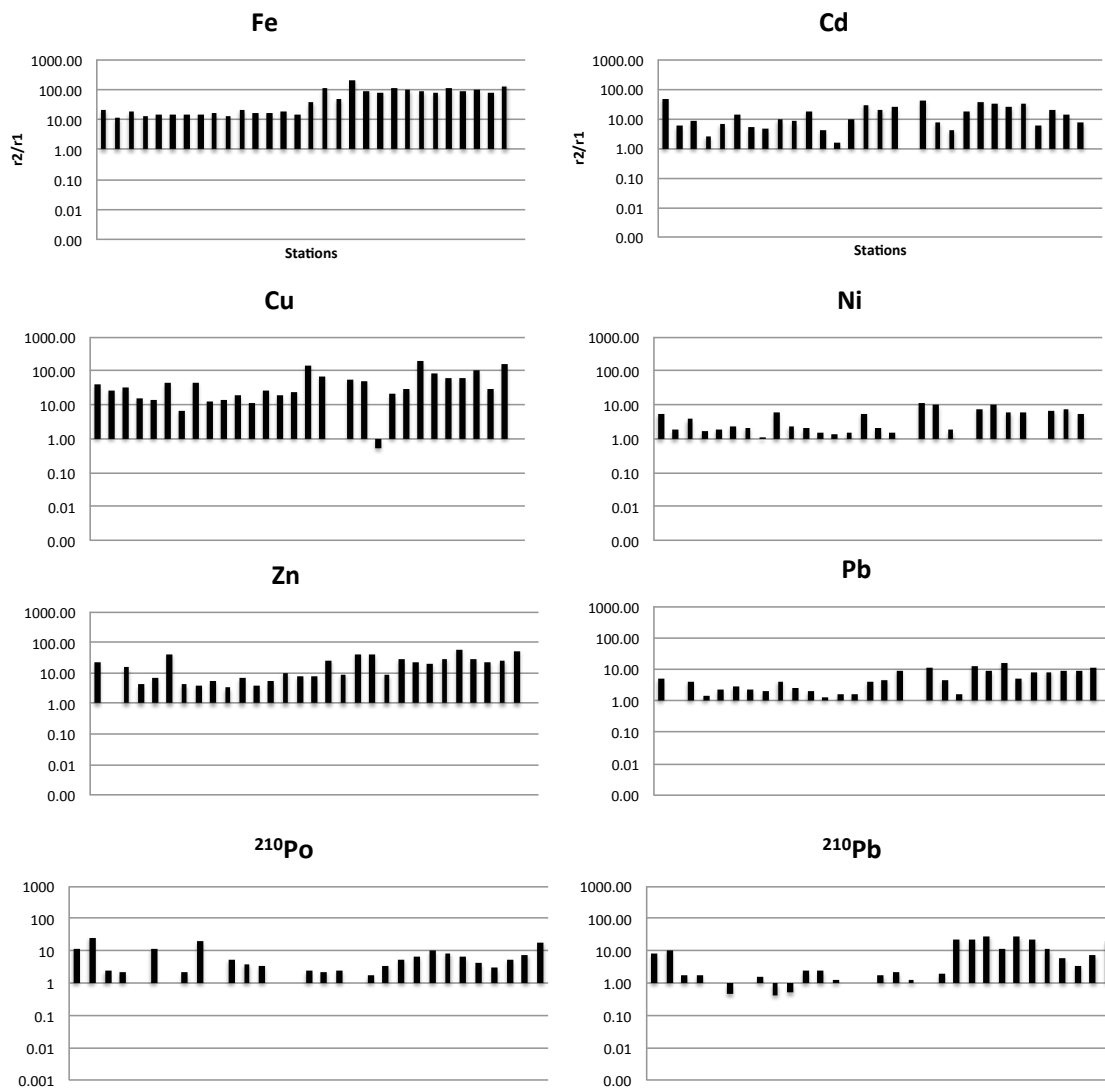


Figure 3.2: Chemical concentration ratio on particles in the sediment to that on particulate in the water column (r_2/r_1) for the Delaware estuary. If r_2/r_1 is greater than 1, more partitioning is occurring in the water column rather than the sediment.

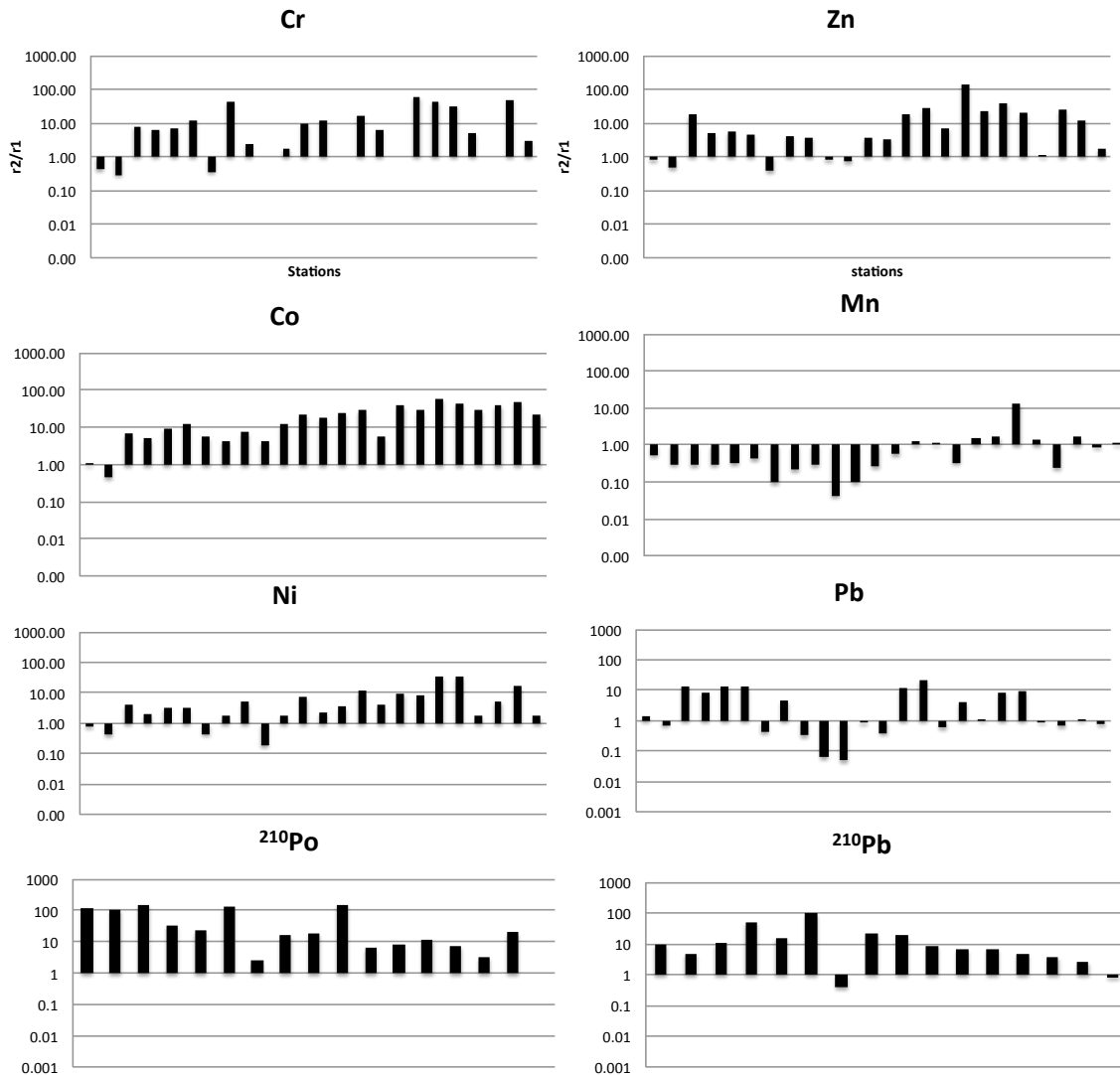


Figure 3.3: Chemical concentration ratio on particles in the sediment to that on particulate in the water column (r_2/r_1) for the Chesapeake estuary. It is important to note that the ^{210}Po and ^{210}Pb data only includes the upper Chesapeake while the other elements include the entire Bay. If r_2/r_1 is greater than 1 more partitioning is occurring in the water column rather than the sediment, while the opposite is true if less than 1.

CONCLUSIONS

This thesis is based on the study of ^{210}Po and ^{210}Pb as tracers for biogeochemical processes that affect the distribution of the trace elements in estuarine and coastal environments. The ^{210}Po and ^{210}Pb are two naturally occurring particle-reactive radionuclides that can be used to provide a direct approach for estimating rates of biogeochemical processes and trace element transfers by means of their measured disequilibrium. The work presented in this thesis was conceived according to three principal objectives. The first was to thoroughly test the two widely used scavenging methods, $\text{Fe}(\text{OH})_3$ and Co-APDC to ascertain their reliability and accuracy in extracting ^{210}Po and ^{210}Pb from estuarine and coastal waters. The second objective was to provide for the practical application of ^{210}Po and ^{210}Pb as tracers of biogeochemical processes in the estuarine and coastal systems. The third objective was to apply both a simple one box and more complex two-layer model calculation for the radionuclide pair to estimate the distribution and residence times of trace elements in estuaries.

Chapter 1 confirmed that the extraction technique $\text{Fe}(\text{OH})_3$ is the more reliable and accurate scavenging method for the extraction of ^{210}Po and ^{210}Pb from estuarine waters. The Co-APDC extraction technique was affected by certain biogeochemical conditions in the estuary such as high particulate concentrations, low oxygen and high biological production. However, it is still a viable option for use in the open ocean environment, as is an alternative scavenging method using MnO_2 , both of which produced reliable and accurate results at the offshore North Atlantic site. Future work should focus on the study of ^{210}Po speciation in seawater in order to understand its aqueous chemical reactions so that more consistent scavenging techniques can be applied. Other projects in process include an expanded suite of scavenging methods conducted throughout the North Atlantic and Mediterranean, which will greatly expand such understanding throughout the estuary.

Chapter 2 described that ^{210}Po and ^{210}Pb clearly identified and differentiated biogeochemical processes occurring in the Delaware and Chesapeake estuaries. The Delaware estuary displayed regional differentiation due to dominant particle reactions. The upper Chesapeake estuary displayed vertical differentiation of ^{210}Po and ^{210}Pb attributed to deep sub-oxic redox cycling. A simple one-box scavenging model was developed based on the ^{210}Po and ^{210}Pb disequilibrium and found that net scavenging residence times were weeks (Delaware) to months (Chesapeake). Future work should focus on the sub-oxic and anoxic basins such as in the deeper Chesapeake estuary and on what redox cycles may affect ^{210}Po and ^{210}Pb disequilibria.

Chapter 3 further developed a more expansive two-layer model to estimate sediment-water partition coefficients as well as residence half-lives of ^{210}Po and ^{210}Pb and by proxy associated trace elements. As such the ^{210}Po and ^{210}Pb could be used to accurately estimate similar residence half-lives and distribution of trace elements of similar particle reactivity within a few days to weeks. Future work should collect and measure ^{210}Po and ^{210}Pb waters and sediment concurrently along with a suite of bioactive trace elements to further develop this two-layer model.

During the course of this thesis other opportunities arose where we were able to test the radionuclide pair ^{210}Po and ^{210}Pb . These include the GEOTRACES study conducted throughout the North Atlantic Ocean displaying diverse oceanic, biogeochemical, and atmospheric regimes. The results from this work will be presented in the near future. Another such opportunity included research in Graz, Austria with Dr. Kevin Francesconi where an ecosystem study was conducted in a Delaware intertidal marsh for not only ^{210}Po and ^{210}Pb but also a suite of 24 trace elements. This work was completed on a number of samples such as, marsh core, marsh grass, two species of mussel and the surface microlayer. The work was presented in Maastricht, Netherlands and a short review of the work can be found in Appendix 3. In light of the research undertaken for this thesis we are hopeful that our results will further contribute to our knowledge of ^{210}Po and ^{210}Pb as tracers in estuarine and coastal systems.

Appendix A

Table A1: ^{210}Po and ^{210}Pb dissolved activities using the $\text{Fe}(\text{OH})_3$, Co-APDC scavenging methods collected during six estuarine and coastal research cruises.

| Station | Salinity | Depth (m) | Oxygen (umol/l) | Particulate (mg/L) | Fe(OH) ₃ Co-Precipitation Method | | | | Co-APDC Co-Precipitation Method | | | |
|---------|----------|-----------|-----------------|--------------------|------------------------------------------------------------|------------------------------------------------------------|---------------------------------------------|-------------|------------------------------------------------------------|------------------------------------------------------------|---------------------------------------------|--|
| | | | | | $^{210}\text{Po}_{\text{diss}}$ (dpm 100 l ⁻¹) | $^{210}\text{Pb}_{\text{diss}}$ (dpm 100 l ⁻¹) | $^{210}\text{Po}/^{210}\text{Pb}$ dissolved | | $^{210}\text{Po}_{\text{diss}}$ (dpm 100 l ⁻¹) | $^{210}\text{Pb}_{\text{diss}}$ (dpm 100 l ⁻¹) | $^{210}\text{Po}/^{210}\text{Pb}$ dissolved | |
| 1 | 0.1 | 11.8 | 323 | 7.2 | 1.76 ± 0.19 | 1.85 ± 0.32 | 0.95 ± 0.19 | 1.89 ± 0.24 | 1.81 ± 0.36 | 1.04 ± 0.27 | | |
| 1 | 0.1 | 2.4 | 325 | 3.9 | 1.43 ± 0.18 | 2.19 ± 0.35 | 0.65 ± 0.13 | 1.35 ± 0.26 | 1.95 ± 0.52 | 0.69 ± 0.15 | | |
| 3 | 2.0 | 10.4 | 319 | 21.1 | 1.56 ± 0.14 | 3.02 ± 0.21 | 0.52 ± 0.11 | 1.44 ± 0.23 | 3.10 ± 0.20 | 0.46 ± 0.13 | | |
| 3 | 2.0 | 2.8 | 321 | 18.0 | 1.70 ± 0.22 | 3.23 ± 0.39 | 0.53 ± 0.09 | 1.93 ± 0.27 | 3.19 ± 0.42 | 0.61 ± 0.13 | | |
| 5 | 7.2 | 2.0 | 320 | 31.3 | 2.58 ± 0.23 | 1.37 ± 0.28 | 1.89 ± 0.43 | 2.29 ± 0.22 | 1.39 ± 0.30 | 1.65 ± 0.35 | | |
| 10 | 6.7 | 1.8 | 327 | 21.7 | 1.92 ± 0.20 | 2.10 ± 0.33 | 0.92 ± 0.17 | 1.63 ± 0.31 | 2.27 ± 0.42 | 0.72 ± 0.14 | | |
| 10 | 8.5 | 9.1 | 319 | 34.1 | 1.96 ± 0.22 | 2.10 ± 0.40 | 0.93 ± 0.21 | 1.55 ± 0.41 | 2.15 ± 0.42 | 0.72 ± 0.16 | | |
| 11 | 8.2 | 2.0 | 337 | 17.1 | 2.27 ± 0.22 | 3.23 ± 0.40 | 0.70 ± 0.11 | 2.19 ± 0.25 | 3.28 ± 0.36 | 0.67 ± 0.38 | | |
| 11 | 12.4 | 10.0 | 315 | 24.5 | 2.04 ± 0.20 | 1.70 ± 0.28 | 1.20 ± 0.23 | 1.95 ± 0.37 | 2.03 ± 0.45 | 0.96 ± 0.52 | | |
| 12 | 16.5 | 12.9 | 315 | 26.5 | 2.47 ± 0.23 | 3.79 ± 0.40 | 0.65 ± 0.09 | 2.30 ± 0.28 | 3.61 ± 0.34 | 0.64 ± 0.66 | | |
| 12 | 10.9 | 2.2 | 342 | 26.4 | 1.77 ± 0.20 | 0.98 ± 0.30 | 1.80 ± 0.59 | 1.84 ± 0.30 | 1.01 ± 0.35 | 1.82 ± 0.51 | | |
| 13 | 12.3 | 2.2 | 353 | 19.4 | 2.21 ± 0.21 | 1.32 ± 0.29 | 1.68 ± 0.40 | 1.95 ± 0.24 | 1.41 ± 0.29 | 1.38 ± 0.28 | | |
| 13 | 15.4 | 10.1 | 300 | 21.3 | 2.30 ± 0.22 | 1.27 ± 0.30 | 1.82 ± 0.47 | 2.09 ± 0.26 | 1.31 ± 0.25 | 1.60 ± 0.36 | | |
| 14 | 21.5 | 2.1 | 308 | 22.8 | 2.54 ± 0.24 | 1.62 ± 0.30 | 1.57 ± 0.33 | 2.30 ± 0.30 | 1.71 ± 0.29 | 1.35 ± 0.31 | | |
| 14 | 16.2 | 15.4 | 347 | 21.9 | 2.17 ± 0.21 | 2.42 ± 0.35 | 0.89 ± 0.15 | 2.30 ± 0.27 | 2.54 ± 0.33 | 0.91 ± 0.20 | | |
| 15 | 18.8 | 2.0 | 330 | 10.4 | 4.73 ± 0.36 | 3.88 ± 0.41 | 1.22 ± 0.16 | 3.73 ± 0.37 | 3.78 ± 0.32 | 0.99 ± 0.12 | | |
| 15 | 23.7 | 14.3 | 307 | 12.2 | 2.12 ± 0.21 | 1.96 ± 0.32 | 1.08 ± 0.21 | 1.88 ± 0.20 | 2.07 ± 0.21 | 0.91 ± 0.13 | | |
| 16 | 25.5 | 2.1 | 306 | 12.0 | 3.90 ± 0.34 | 2.83 ± 0.35 | 1.38 ± 0.21 | 2.48 ± 0.23 | 2.86 ± 0.33 | 0.87 ± 0.26 | | |
| 16 | 21.5 | 11.7 | 318 | 10.6 | 2.59 ± 0.23 | 1.58 ± 0.30 | 1.64 ± 0.35 | 2.51 ± 0.19 | 1.62 ± 0.30 | 1.55 ± 0.24 | | |
| 17 | 24.1 | 1.9 | 310 | 10.6 | 3.16 ± 0.28 | 3.05 ± 0.38 | 1.03 ± 0.16 | 3.11 ± 0.25 | 3.25 ± 0.32 | 0.96 ± 0.11 | | |
| 17 | 26.0 | 12.1 | 301 | 10.9 | 3.36 ± 0.28 | 2.85 ± 0.37 | 1.18 ± 0.18 | 3.33 ± 0.22 | 2.89 ± 0.21 | 1.15 ± 0.15 | | |
| 18 | 26.3 | 2.0 | 306 | 10.6 | 4.45 ± 0.35 | 2.16 ± 0.32 | 2.06 ± 0.35 | 3.58 ± 0.31 | 2.37 ± 0.50 | 1.51 ± 0.12 | | |
| 19 | 28.2 | 2.0 | 297 | 11.1 | 3.29 ± 0.28 | 1.63 ± 0.29 | 2.02 ± 0.40 | 3.04 ± 0.22 | 1.69 ± 0.23 | 1.79 ± 0.20 | | |
| 20 | 31.8 | 1.6 | 297 | 17.0 | 2.48 ± 0.21 | 2.16 ± 0.31 | 1.15 ± 0.19 | 2.18 ± 0.27 | 2.22 ± 0.33 | 0.98 ± 0.21 | | |
| 21 | 30.4 | 2.0 | 295 | 8.0 | 2.21 ± 0.22 | 1.75 ± 0.23 | 1.26 ± 0.11 | 2.16 ± 0.31 | 1.89 ± 0.31 | 1.15 ± 0.17 | | |
| 21 | 31.0 | 15.3 | 292 | 7.0 | 2.68 ± 0.24 | 1.23 ± 0.29 | 2.18 ± 0.54 | 2.73 ± 0.28 | 1.24 ± 0.23 | 2.20 ± 0.34 | | |
| SMS 1 | 5.2 | 2.0 | - | - | 1.46 ± 0.17 | 1.29 ± 0.29 | 1.13 ± 0.29 | 1.41 ± 0.32 | 1.21 ± 0.41 | 1.17 ± 0.11 | | |
| SMS 2 | 10.3 | 2.0 | - | - | 1.96 ± 0.19 | 1.64 ± 0.34 | 1.20 ± 0.27 | 1.61 ± 0.27 | 1.52 ± 0.21 | 1.06 ± 0.14 | | |
| SMS 3 | 13.2 | 2.0 | - | - | 2.44 ± 0.23 | 1.28 ± 0.30 | 1.90 ± 0.48 | 1.90 ± 0.24 | 1.29 ± 0.25 | 1.47 ± 0.15 | | |
| SMS 4 | 15.1 | 2.0 | - | - | 1.34 ± 0.16 | 1.03 ± 0.29 | 1.30 ± 0.40 | 1.40 ± 0.22 | 1.09 ± 0.34 | 1.28 ± 0.31 | | |
| SMS 5 | 17.6 | 2.0 | - | - | 2.48 ± 0.26 | 3.83 ± 0.48 | 0.65 ± 0.11 | 2.53 ± 0.26 | 3.79 ± 0.32 | 0.67 ± 0.20 | | |
| SMS 6 | 21.2 | 2.0 | - | - | 1.53 ± 0.17 | 1.68 ± 0.32 | 0.91 ± 0.20 | 1.65 ± 0.25 | 1.60 ± 0.32 | 1.03 ± 0.21 | | |
| SMS 7 | 23.3 | 2.0 | - | - | 4.26 ± 0.31 | 2.14 ± 0.35 | 1.99 ± 0.36 | 4.35 ± 0.22 | 2.14 ± 0.29 | 2.03 ± 0.21 | | |
| SMS 8 | 25.9 | 2.0 | - | - | 3.93 ± 0.33 | 2.00 ± 0.32 | 1.96 ± 0.35 | 4.13 ± 0.37 | 2.11 ± 0.75 | 1.95 ± 0.06 | | |
| CB 01 | 12.70 | 4.8 | 27 | 188 | 2.10 ± 0.23 | 1.17 ± 0.29 | 1.79 ± 0.48 | 2.20 ± 0.22 | 1.20 ± 0.15 | 1.84 ± 0.30 | | |
| CB 01 | 14.20 | 10.4 | 130 | 10.2 | 1.37 ± 0.21 | 0.61 ± 0.30 | 2.23 ± 1.14 | 1.40 ± 0.42 | 0.74 ± 0.34 | 1.90 ± 0.57 | | |
| CB 01 | 15.90 | 17.7 | 34 | 11.8 | 2.83 ± 0.25 | 0.89 ± 0.33 | 3.18 ± 1.20 | 2.20 ± 0.21 | 0.91 ± 0.20 | 2.42 ± 0.20 | | |
| CB 01 | 17.10 | 22.0 | 2 | 14.4 | 2.18 ± 0.19 | 0.73 ± 0.30 | 2.97 ± 1.24 | 1.98 ± 0.19 | 0.78 ± 0.23 | 2.54 ± 0.24 | | |
| CB 02 | 13.08 | 3.0 | 153 | 19.1 | 1.51 ± 0.19 | 0.60 ± 0.29 | 2.51 ± 1.23 | 1.39 ± 0.23 | 0.57 ± 0.17 | 2.44 ± 0.29 | | |
| CB 02 | 14.19 | 8.2 | 71 | 16.1 | 4.44 ± 0.36 | 3.01 ± 0.50 | 1.48 ± 0.28 | 3.03 ± 0.34 | 3.04 ± 0.42 | 1.00 ± 0.12 | | |
| CB 02 | 15.50 | 13.9 | 41 | 13.6 | 2.70 ± 0.29 | 1.04 ± 0.50 | 2.60 ± 1.29 | 2.11 ± 0.22 | 1.06 ± 0.13 | 1.99 ± 0.18 | | |
| CB 02 | 17.03 | 21.9 | 1 | 15.7 | 1.07 ± 0.21 | 4.33 ± 1.00 | 0.25 ± 0.07 | 0.55 ± 0.20 | 4.25 ± 0.61 | 0.13 ± 0.11 | | |
| CB 02 | 17.03 | 21.5 | 1 | 11.4 | 1.27 ± 0.31 | 0.39 ± 0.32 | 3.22 ± 2.74 | 1.09 ± 0.26 | 0.38 ± 0.47 | 2.86 ± 0.23 | | |
| CB 03 | 10.80 | 0.8 | 142 | 37.1 | 1.65 ± 0.24 | 2.69 ± 0.40 | 0.61 ± 0.13 | 1.37 ± 0.28 | 2.68 ± 0.45 | 0.51 ± 0.12 | | |
| CB 03 | 13.30 | 9.1 | 23 | 26.7 | 2.48 ± 0.23 | 0.53 ± 0.30 | 4.70 ± 2.70 | 2.13 ± 0.22 | 0.60 ± 0.14 | 3.57 ± 0.27 | | |
| CB 04 | 8.01 | 1.1 | 188 | 31.6 | 1.40 ± 0.18 | 0.71 ± 0.31 | 1.97 ± 0.90 | 1.58 ± 0.25 | 0.76 ± 0.18 | 2.08 ± 0.35 | | |
| CB 04 | 6.60 | 1.9 | 177 | 27.7 | 1.95 ± 0.26 | 2.42 ± 0.46 | 0.81 ± 0.18 | 1.85 ± 0.25 | 2.64 ± 0.32 | 0.70 ± 0.22 | | |
| CB 05 | 10.02 | 9.1 | 96 | 41.5 | 2.00 ± 0.32 | 0.95 ± 0.46 | 2.11 ± 1.07 | 1.77 ± 0.36 | 0.94 ± 0.81 | 1.88 ± 0.15 | | |
| CB 05 | 3.20 | 0.5 | 175 | 25.0 | 0.83 ± 0.16 | 0.44 ± 0.28 | 1.90 ± 1.29 | 0.72 ± 0.19 | 0.50 ± 0.16 | 1.44 ± 0.14 | | |
| CB 06 | 2.06 | 0.5 | 172 | 30.0 | 2.55 ± 0.38 | 1.10 ± 0.49 | 2.32 ± 1.08 | 2.00 ± 0.34 | 1.15 ± 0.24 | 1.74 ± 0.26 | | |
| CB 06 | 3.14 | 9.0 | 155 | 51.9 | 2.09 ± 0.22 | 0.92 ± 0.35 | 2.27 ± 0.88 | 1.89 ± 0.19 | 1.07 ± 0.26 | 1.77 ± 0.34 | | |

Table A2: ^{210}Po and ^{210}Pb dissolved activities using the $\text{Fe}(\text{OH})_3$, Co-APDC scavenging methods collected during six estuarine and coastal research cruises.

| Station | Salinity | Depth (m) | Oxygen (umol/l) | Fe(OH) ₃ Co-Precipitation Method | | | Co-APDC Co-Precipitation Method | | |
|--------------------------------|----------|-----------|-----------------|------------------------------------------------------------|------------------------------------------------------------|---------------------------------------------|------------------------------------------------------------|------------------------------------------------------------|---------------------------------------------|
| | | | | $^{210}\text{Po}_{\text{diss}}$ (dpm 100 l ⁻¹) | $^{210}\text{Pb}_{\text{diss}}$ (dpm 100 l ⁻¹) | $^{210}\text{Po}/^{210}\text{Pb}$ dissolved | $^{210}\text{Po}_{\text{diss}}$ (dpm 100 l ⁻¹) | $^{210}\text{Pb}_{\text{diss}}$ (dpm 100 l ⁻¹) | $^{210}\text{Po}/^{210}\text{Pb}$ dissolved |
| RI01 | 26.8 | 0.1 | 5.3 | 4.33 ± 0.33 | 1.74 ± 0.35 | 2.48 ± 0.54 | 1.63 ± 0.49 | 1.57 ± 0.19 | 1.03 ± 0.05 |
| RI02 | 27.4 | 0.1 | 4.9 | 3.51 ± 0.31 | 1.24 ± 0.39 | 2.84 ± 0.53 | 3.55 ± 0.34 | 1.10 ± 0.26 | 3.22 ± 0.31 |
| RI03 | 27.6 | 0.1 | 2.2 | 5.79 ± 0.49 | 3.84 ± 0.45 | 1.51 ± 0.22 | 4.83 ± 0.64 | 3.71 ± 0.37 | 1.30 ± 0.35 |
| RI04 | 27.4 | 0.1 | 3.4 | 2.79 ± 0.25 | 1.91 ± 0.36 | 1.46 ± 0.30 | 2.43 ± 0.38 | 2.05 ± 0.35 | 1.18 ± 0.28 |
| RI05 | 25.8 | 0.1 | 2.0 | 9.95 ± 0.82 | 11.57 ± 1.05 | 0.86 ± 0.11 | 3.75 ± 0.34 | 12.49 ± 1.08 | 0.30 ± 0.06 |
| RI06 | 25.7 | 0.1 | 2.1 | 5.03 ± 0.40 | 4.20 ± 0.48 | 1.20 ± 0.17 | 2.46 ± 0.67 | 4.16 ± 0.72 | 0.59 ± 0.09 |
| RI07 | 27.9 | 0.1 | 2.1 | 3.46 ± 0.29 | 2.45 ± 0.55 | 1.41 ± 0.34 | 1.25 ± 0.45 | 2.18 ± 0.46 | 0.57 ± 0.09 |
| RI08 | 28.1 | 0.1 | 1.1 | 3.27 ± 0.31 | 2.63 ± 0.73 | 1.25 ± 0.37 | 3.79 ± 0.37 | 2.61 ± 0.37 | 1.45 ± 0.38 |
| CC01 | 21.7 | 0.1 | 2.7 | 6.68 ± 0.58 | 6.36 ± 0.68 | 1.05 ± 0.14 | 6.62 ± 0.18 | 6.49 ± 0.16 | 1.02 ± 0.17 |
| CC02 | 23.2 | 0.1 | 3.6 | 3.87 ± 0.42 | 7.21 ± 0.83 | 0.54 ± 0.08 | 3.04 ± 0.14 | 7.33 ± 0.24 | 0.41 ± 0.09 |
| CC03 | 21.2 | 0.1 | 1.7 | 6.13 ± 0.69 | 6.35 ± 0.69 | 0.96 ± 0.15 | 5.85 ± 0.65 | 6.48 ± 1.34 | 0.90 ± 0.23 |
| CC04 | 20.2 | 0.1 | 3.0 | 6.69 ± 1.06 | 13.82 ± 1.52 | 0.48 ± 0.09 | 3.61 ± 0.93 | 8.35 ± 0.97 | 0.43 ± 0.12 |
| CC05 | 19.5 | 0.1 | 2.2 | 4.78 ± 0.65 | 5.54 ± 0.70 | 0.86 ± 0.16 | 6.30 ± 0.98 | 5.65 ± 0.90 | 1.11 ± 0.14 |
| CC06 | 18.2 | 0.1 | 1.9 | 8.28 ± 0.73 | 4.62 ± 0.65 | 1.79 ± 0.30 | 6.92 ± 1.10 | 4.84 ± 0.56 | 1.43 ± 0.32 |
| CC07 | 19.3 | 0.1 | 2.6 | 10.11 ± 0.88 | 8.73 ± 0.91 | 1.16 ± 0.16 | - ± - | - ± - | - ± - |
| CC08 | 20.5 | 0.1 | 1.1 | 13.90 ± 1.02 | 6.04 ± 0.69 | 2.30 ± 0.31 | - ± - | - ± - | - ± - |
| RMP | 0.4 | 0.1 | 3.4 | 9.00 ± 1.39 | 18.85 ± 2.53 | 0.48 ± 0.10 | - ± - | - ± - | - ± - |
| RI11 | 27.3 | 0.1 | 1.1 | 2.00 ± 0.23 | 13.11 ± 1.09 | 0.15 ± 0.02 | 1.25 ± 0.21 | 13.22 ± 1.48 | 0.09 ± 0.01 |
| RI12 | 26.2 | 0.1 | 2.7 | 0.51 ± 0.26 | 27.13 ± 2.13 | 0.00 ± 0.01 | - ± - | - ± - | - ± - |
| RI13 | 26.5 | 0.1 | 3.6 | 3.66 ± 0.30 | 2.07 ± 0.33 | 1.77 ± 0.32 | 3.19 ± 0.38 | 2.19 ± 0.20 | 1.46 ± 0.24 |
| RI13 | 26.5 | 0.1 | 1.7 | 3.56 ± 0.31 | 2.01 ± 0.23 | 1.77 ± 0.21 | 3.11 ± 0.31 | 2.06 ± 0.27 | 1.51 ± 0.28 |
| RI14 | 25.6 | 0.1 | 3.0 | 4.14 ± 0.34 | 2.62 ± 0.34 | 1.58 ± 0.24 | 4.02 ± 0.40 | 2.59 ± 0.36 | 1.55 ± 0.36 |
| RI15 | 26.7 | 0.1 | 5.3 | 3.60 ± 0.30 | 2.90 ± 0.37 | 1.24 ± 0.19 | 3.27 ± 0.25 | 2.98 ± 0.29 | 1.10 ± 0.20 |
| RI16 | 30.1 | 0.1 | 4.9 | 3.23 ± 0.26 | 1.81 ± 0.34 | 1.79 ± 0.37 | 3.38 ± 0.37 | 1.74 ± 0.31 | 1.95 ± 0.31 |
| North Atlantic Offshore | | | | | | | | | |
| 8/2/11 | 33.5 | 1.0 | 200 | 1.74 ± 1.77 | 9.63 ± 0.77 | 0.18 ± 0.18 | 1.67 ± 1.72 | 10.42 ± 0.83 | 0.16 ± 0.17 |
| | 33.5 | 1.0 | 200 | 6.36 ± 1.06 | 9.55 ± 0.80 | 0.67 ± 0.12 | 5.74 ± 1.10 | 9.79 ± 0.82 | 0.59 ± 0.12 |
| | 33.5 | 1.0 | 200 | 3.32 ± 1.04 | 9.42 ± 0.81 | 0.35 ± 0.11 | 5.45 ± 1.11 | 9.72 ± 0.83 | 0.56 ± 0.12 |
| | 33.5 | 1.0 | 200 | 4.44 ± 1.28 | 13.95 ± 1.11 | 0.32 ± 0.10 | 5.51 ± 1.07 | 9.50 ± 0.82 | 0.58 ± 0.12 |
| | 33.9 | 15.0 | 198 | 4.28 ± 0.31 | 9.01 ± 0.78 | 0.47 ± 0.05 | 5.23 ± 0.37 | 9.55 ± 0.82 | 0.55 ± 0.06 |
| | 33.9 | 15.0 | 198 | 4.43 ± 0.31 | 8.19 ± 0.72 | 0.54 ± 0.06 | 5.20 ± 0.37 | 9.47 ± 0.83 | 0.55 ± 0.06 |
| | 33.9 | 15.0 | 198 | 4.51 ± 0.32 | 8.65 ± 0.76 | 0.52 ± 0.06 | 5.78 ± 0.39 | 8.75 ± 0.77 | 0.66 ± 0.07 |
| | 34.9 | 2000.0 | 252 | 4.51 ± 0.32 | 5.19 ± 0.50 | 0.87 ± 0.10 | 4.83 ± 0.41 | 4.29 ± 0.46 | 1.12 ± 0.15 |
| | 34.9 | 2000.0 | 252 | 4.05 ± 0.30 | 4.49 ± 0.46 | 0.90 ± 0.11 | 5.60 ± 0.41 | 5.13 ± 0.52 | 1.09 ± 0.14 |
| | 34.9 | 2000.0 | 252 | 4.33 ± 0.32 | 5.46 ± 0.52 | 0.79 ± 0.10 | 5.90 ± 0.41 | 4.99 ± 0.51 | 1.18 ± 0.15 |
| 11/3/11 | 33.4 | 1.0 | 200 | 2.73 ± 1.63 | 16.60 ± 1.29 | 0.16 ± 0.10 | 4.54 ± 1.50 | 18.65 ± 1.45 | 0.24 ± 0.08 |
| | 33.4 | 1.0 | 200 | 3.01 ± 1.36 | 17.45 ± 1.40 | 0.17 ± 0.08 | 2.88 ± 0.63 | 6.07 ± 0.53 | 0.47 ± 0.11 |
| | 33.4 | 1.0 | 200 | 1.11 ± 0.53 | 5.95 ± 0.52 | 0.19 ± 0.09 | 8.91 ± 1.52 | 12.70 ± 1.07 | 0.70 ± 0.13 |
| | 33.7 | 15.0 | 235 | 2.83 ± 0.46 | 2.64 ± 0.40 | 1.07 ± 0.24 | - ± - | - ± - | - ± - |
| | 34.1 | 15.0 | 227 | 2.55 ± 0.39 | 2.29 ± 0.33 | 1.11 ± 0.24 | 2.51 ± 0.41 | 3.47 ± 0.37 | 0.72 ± 0.14 |
| | 34.5 | 15.0 | 225 | 3.04 ± 0.48 | 3.00 ± 0.41 | 1.01 ± 0.21 | 3.72 ± 0.44 | 2.01 ± 0.31 | 1.85 ± 0.36 |
| | 35.6 | 30.0 | 153 | 5.63 ± 0.78 | 4.92 ± 0.60 | 1.14 ± 0.21 | 4.59 ± 0.68 | 4.81 ± 0.59 | 0.95 ± 0.18 |
| | 35.5 | 50.0 | 163 | 3.73 ± 0.67 | 5.05 ± 0.54 | 0.74 ± 0.15 | 3.05 ± 0.66 | 5.67 ± 0.58 | 0.54 ± 0.13 |
| | 35.5 | 100.0 | 143 | 4.32 ± 0.61 | 3.98 ± 0.47 | 1.09 ± 0.20 | 11.51 ± 0.86 | 0.62 ± 0.35 | 18.61 ± 10.71 |
| | 35.6 | 150.0 | 181 | 2.47 ± 0.69 | 6.37 ± 0.64 | 0.39 ± 0.11 | 5.89 ± 0.87 | 7.47 ± 0.73 | 0.79 ± 0.14 |
| | 35.6 | 200.0 | 209 | 24.24 ± 2.63 | 27.52 ± 1.84 | 0.88 ± 0.11 | 55.44 ± 7.43 | 65.11 ± 3.96 | 0.85 ± 0.13 |
| 8/21/13 | 35.1 | 5.8 | 181 | 3.97 ± 0.41 | 9.31 ± 0.78 | 0.43 ± 0.06 | 2.50 ± 0.34 | 10.84 ± 1.40 | 0.23 ± 0.04 |
| | 36.1 | 77.0 | 132 | 9.24 ± 0.70 | 5.76 ± 0.60 | 1.60 ± 0.21 | 8.24 ± 0.72 | 7.91 ± 1.23 | 1.04 ± 0.19 |
| | 35.3 | 150.0 | 118 | 5.21 ± 0.36 | 2.19 ± 0.34 | 2.38 ± 0.40 | 6.15 ± 0.41 | 4.28 ± 0.52 | 1.44 ± 0.20 |
| | 35.3 | 199.0 | 127 | 4.82 ± 0.39 | 4.42 ± 0.53 | 1.09 ± 0.16 | 4.91 ± 0.38 | 4.06 ± 0.45 | 1.21 ± 0.17 |
| | 35.1 | 272.0 | 151 | 3.83 ± 0.36 | 5.77 ± 0.75 | 0.66 ± 0.11 | 4.94 ± 0.39 | 5.37 ± 0.67 | 0.92 ± 0.14 |
| | 35.0 | 350.0 | 187 | 6.54 ± 0.56 | 10.14 ± 0.93 | 0.64 ± 0.08 | 7.94 ± 0.67 | 7.96 ± 0.82 | 1.00 ± 0.13 |
| | 35.0 | 386.0 | 203 | 4.70 ± 0.38 | 7.47 ± 0.69 | 0.63 ± 0.08 | 4.65 ± 0.39 | 5.32 ± 0.66 | 0.87 ± 0.13 |
| | 35.0 | 503.0 | 216 | 4.10 ± 0.34 | 5.09 ± 0.54 | 0.81 ± 0.11 | 6.23 ± 0.45 | 6.29 ± 0.79 | 0.99 ± 0.14 |

Appendix B

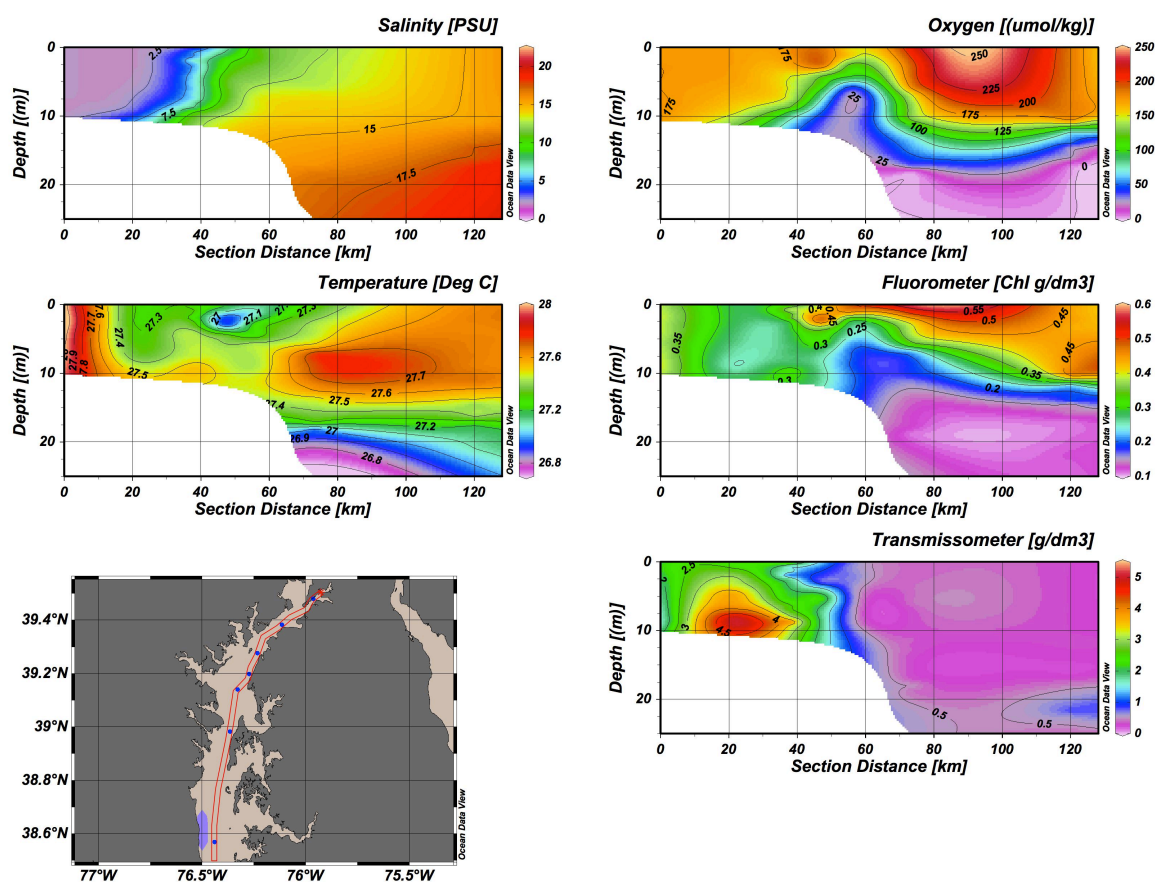


Figure B1: Chemical parameters presented as ODV transect plot in the upper Chesapeake estuary.

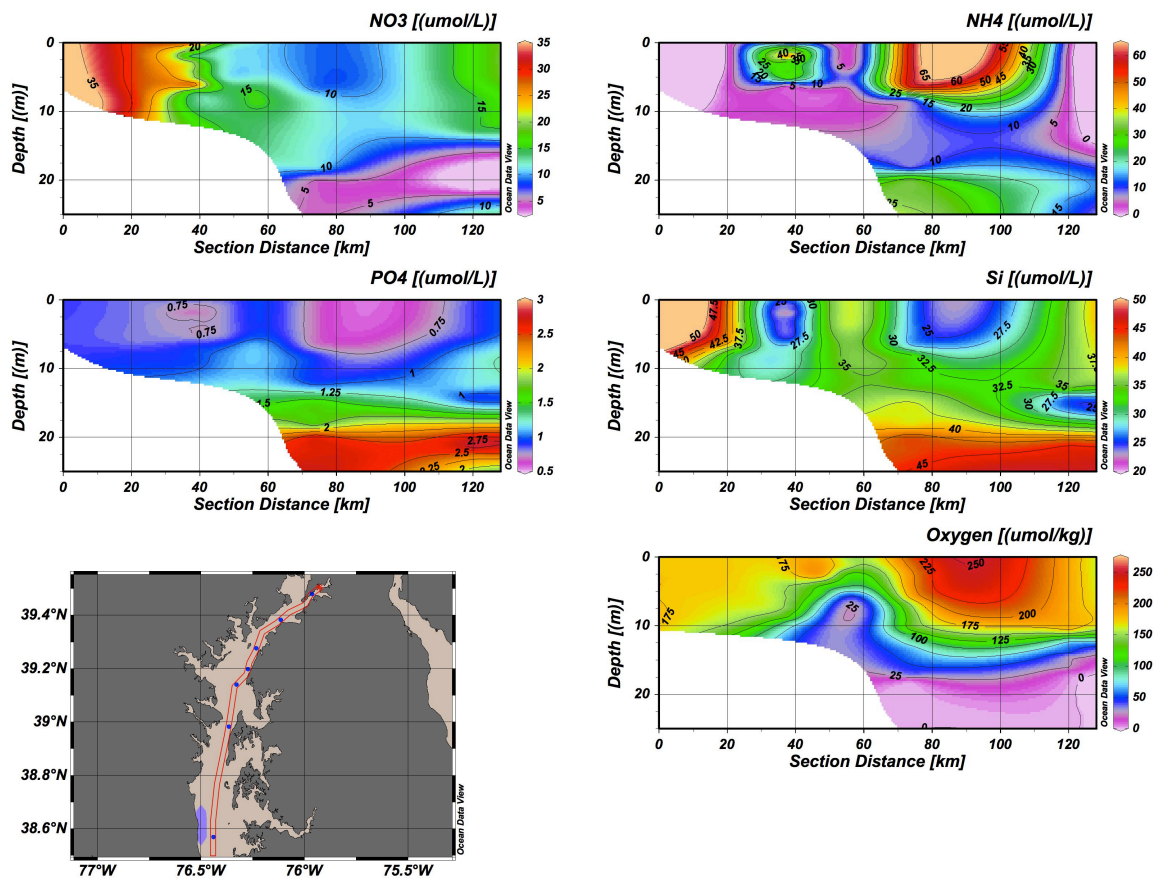


Figure B2: Nutrient concentrations presented as ODV transect plot in the upper Chesapeake estuary.

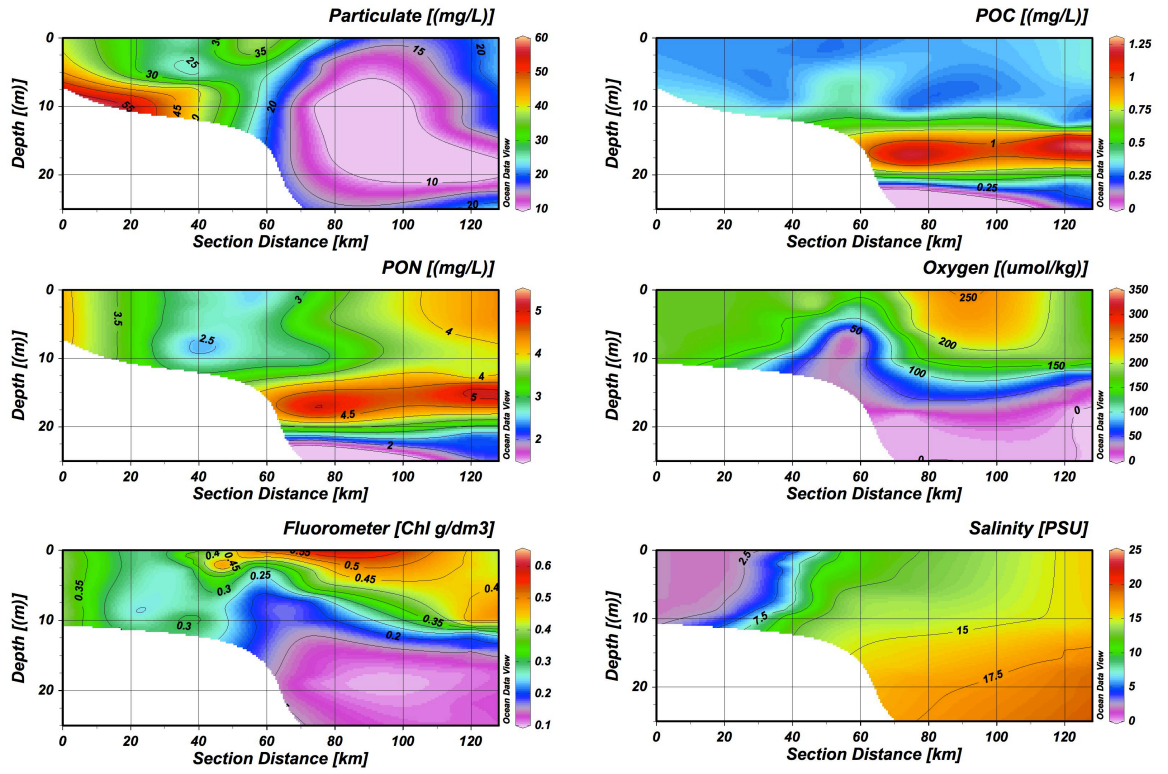


Figure B3: Particulate concentrations presented as ODV transect plot in the upper Chesapeake estuary.

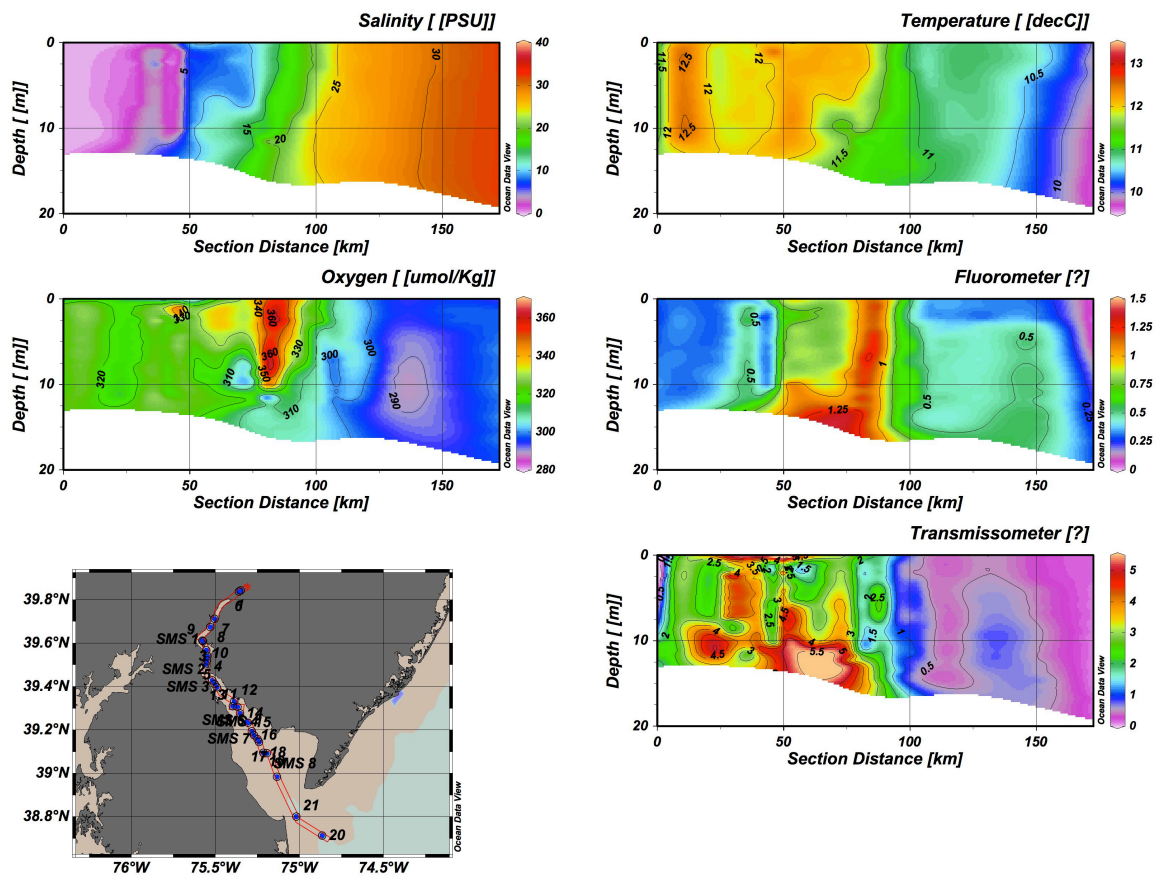


Figure B4: Chemical parameters presented as ODV transect plot in the Delaware estuary.

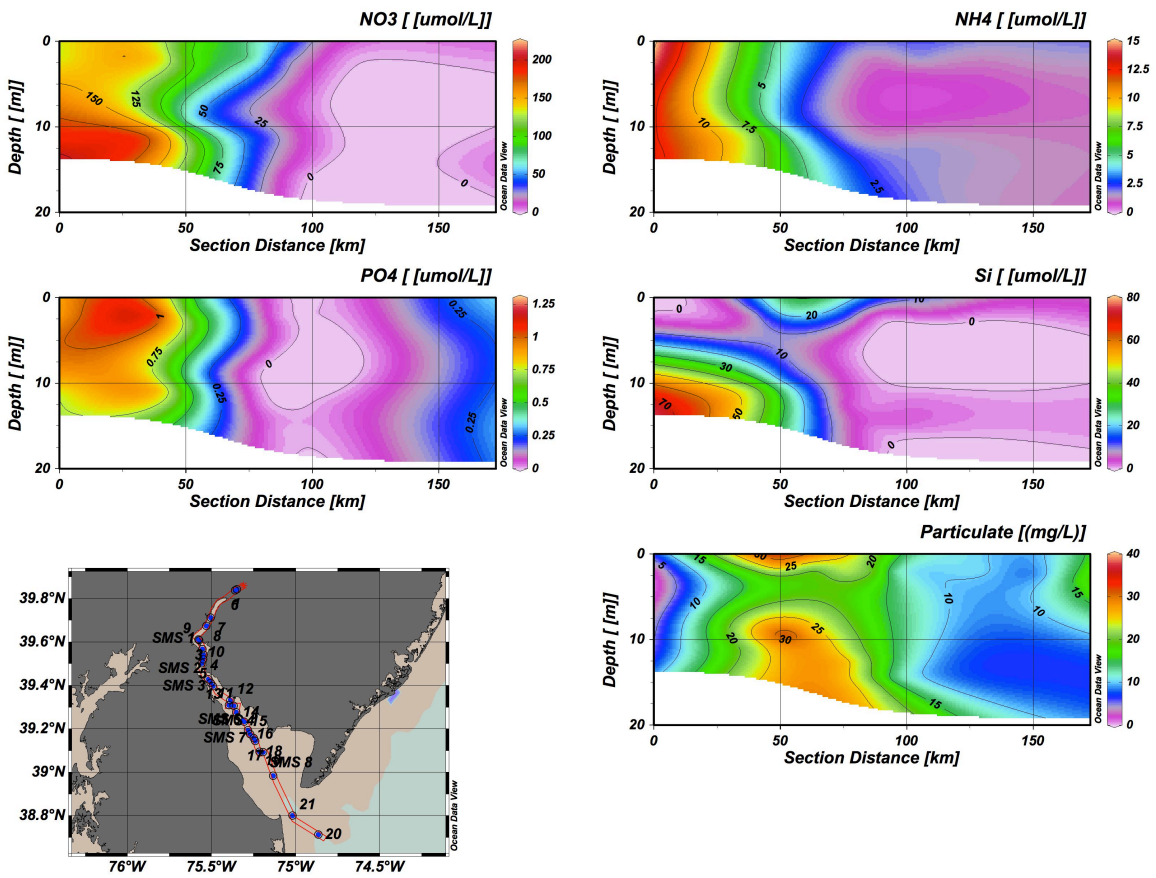


Figure B5: Nutrient concentrations presented as ODV transect plot in the Delaware estuary.

Appendix C

Selenium and Arsenic Species Determination in the Sea Surface Microlayer

Marsan, D.¹, Francesconi, K., Church, T.¹

¹School of Marine Science and Policy, University of Delaware, Newark, DE 19716-3501
USA.

² Department of Analytical Chemistry, Graz University of Technology, Graz, Austria

Abstract:

The pathways by which polonium species are accumulated and transferred in aquatic ecosystems are relatively unknown. Examination of whole marine ecosystems rather than individual organisms provides greater insights into the biogeochemical cycling of trace metals, like polonium. This study focused on the sea surface microlayer, which is the top 100 micrometers of the ocean surface where all exchange occurs between the atmosphere and ocean. It is unique in chemical, physical, and biological properties due to the high concentrations of organic compounds such as amino acids, carbohydrates, fatty acids, and lipids. Knowledge of speciation of elements is important due to their toxicity in high concentrations and how that speciation affects interactions at the air-sea interface. Utilizing the lack of knowledge in this layer concerning Se and As species ICPMS/HPLC was utilized to help answer this question. The speciation experiments of Se in the surface microlayer would also complement previous research conducted by Bahrou, Church et al. (2012) and will allow for the prospect of future research into Po speciation based assumption it acts as a sulfur-analogue like Se.

Identification of arsenic and selenium species including total element concentrations (Ag, Al, As, B, Ba, Be, Bi, Ca, Cd, Co, Cr, Cu, Fe, Ga, K, Li, Mg, Mn, Mo, Na, Ni, Pb, Po, Rb, Se, Sr, Te, Tl, U, V and Zn) was completed on specimens of the marsh mussel, *Geukensia demissa* and *Mytilus edulis*, the saltmarsh plant *Spartina alterniflora*, surface micro-layer (SML) and a sediment core taken from a Delaware estuarine salt marsh. Identification of major arsenic and selenium species was successful, the predominant As species are anionic while the Se speciation concentrations were too low to establish reliable results. The species identified include arsenate, arsenite, dimethylarsinate, dimethylarsinoyethanol, arseonbetaine, selenate and selenite. I also report data that the amount of non-extractable or recalcitrant arsenic and selenium (i.e. insoluble after sequential extractions with water/methanol, acetone, and hexane; 13% As and 13% Se yield) did not increase with time, but treatment of the pellet with 0.1M trifluoroacetic acid at 95°C solubilizes 25% of the recalcitrant arsenic while only 2% Se is extracted. This recalcitrant arsenic is predominately inorganic arsenic.

Introduction:

Polonium (^{210}Po) and radioactive lead (^{210}Pb) in marine organisms have attracted the attention of scientists due to their relatively high concentrations in marine biota and also because ^{210}Po constitutes the major source of natural radiation received by humans through the consumption of seafood (Cherry and Shannon, 1974; Parfenov, 1974). ^{210}Po ($t_{1/2}=138.39\text{d}$) is the final alpha-emitting daughter nuclide in the natural ^{238}U decay series. It enters the marine environment through the natural radioactive decay of ^{222}Rn gas from the surface of the land, ^{226}Ra dissolved in solution, and via wet and dry atmospheric deposition of ^{210}Bi , ^{210}Pb and ^{210}Po (Turekian et al. 1977).

There is a great deal of information about the concentrations of ^{210}Po and ^{210}Pb in marine organisms mostly completed by Cherry and Heyraud and their colleagues in the 70's. Recently there has been investigations into the behavior of ^{210}Po in marine organisms and food chains (Bulamn et al., 1995; Dahlgaard, 1996). It has also been shown that ^{210}Po concentration in *Mytilus*, *Littorina*, and *Ulva* are highly correlated with class B (sulfur-seeking) metals, suggesting that metallothioneins may affect the uptake and loss of ^{210}Po in marine organisms (Wildgust et al., 1998).

Preferential assimilation of ^{210}Po over ^{210}Pb in the soft tissues of marine organisms results in $^{210}\text{Po}/^{210}\text{Pb}$ ratios $\gg 1$ in marine biota. For example the reported concentrations of ^{210}Po are up to 700 Bqkg^{-1} ($2.4 \times 10^3\text{ dpmkg}^{-1}$) in mussel soft tissues (Germain et al., 1995). ^{210}Po , ^{210}Pb and ^{238}Th , all of which speciate as cations in seawater, display very strong binding affinities to particle surfaces, including organisms. ^{210}Pb associates largely with dissolved carbonates (Brulan, 1983), ^{238}Th is primarily associated with hydroxides (Turner et al., 1981), while the speciation of Po in seawater remains unknown. Po appears to behave similarly to Se, either acting as an S analogue or binding to S ligands, but is primarily understood to associate with protein in living organisms (Cherry and Heyraud, 1981; Fisher et al., 1983; Cherrier et al., 1995; Stewart and Fisher, 2003a).

Despite the numerous studies on ^{210}Po accumulation in marine organisms the specific mechanism of uptake remain unclear. Because there is no known biological requirement for polonium, it appears that it is taken up inadvertently as an analogue of some needed element. Due to its position in-group VI of the periods table and its known association with protein, it has been suggested that Po acts as a sulfur-analogue like Se (Schwarz, 1976; Cherrier et al., 1995, Church and Sarin, 2008). Other studies have found high concentrations of Po associated with metallothionein and cysteine in invertebrate and vertebrate livers (Durand et al., 1999), and a link between Po- an S- containing amino acids in sinking organic matter has also been seen (Stewart et al., 2007).

Metallothioneins are low molecular weight (6 to 8 kdaltons), cysteine-rich (20 to 30%), metal binding proteins whose synthesis represents a specific response of an organism to exposure of Class B and/or Borderline metals such as Cd, Cu, Hg and Zn (Engel and Roesijadi 1987; Viarengo 1989). As the concentration of Class B and Borderline metals increase in cells, they stimulate de novo synthesis of

apothioneins that bind metal cations in a non-toxic/available form (Roesijadi, 1992; Viarengo and Nott 1993).

Predominantly class B and borderline metals (Nieboer and Richardson, 1980) displayed correlations with ^{210}Po in the digestive gland of *M. edulis*. Class B metal ions readily bind with sulphhydryl (-SH), disulphide (-S-S-), thioether (-SR) and amino (-NH₂) functional groups; with borderline metals exhibiting an intermediate behavior between class B and class A metals, which preferentially bind with phosphates, carboxylic and carbonyl functional groups (ligands with oxygen as the donor atom) (Nieboer and Richardson, 1980; Rainbow, 1997). If ^{210}Po behaves as a class B metal then other class B metals may affect the accumulation of ^{210}Po by marine organisms. Exposure to a class B metal such as cadmium induces metal-binding proteins called metallothioneins (Lambot, 1976). Metallothioneins, rich in -SH groups, are potentially important binding sites for ^{210}Po and could result in an enhanced accumulation of the radioisotope.

Mytilus edulis and *Geukensia demissa* feed by filtering suspended particulates, which are sorted by size and density using grooves on the gill (Atkins, 1936, 1937) and adsorbed to the mucus covering of the gill surface (MacGinitie, 1941). Suspended particulates greater than 3-6 μm are retained and further sorted by the labial palps (Newel, 1979). The correlation between the inorganic suspended particle weight and the digestive gland ^{210}Po specific activity probably reflects a direct relationship suggesting that the majority of ^{210}Po from *M. edulis* is from inorganically-bound ^{210}Po .

One of the primary uptake routes of metals by mussels is across the gill. Cadmium, for example, is adsorbed initially onto the gill surface mucus or directly onto the cell membrane and subsequently crosses the plasma membrane by passive diffusion or via a membrane-carrier (Viarengo, 1989). Sulphydryl-rich soluble proteins within the cell bind the metal, facilitating a continuous removal process by creating a permanent gradient across the cell (Viarengo, 1989).

Surface Microlayer

At the air-sea interface, the sea surface microlayer is the physical boundary between the ocean and the atmosphere. It is roughly considered to be the upper most 1mm of the ocean, the SML is physically and chemically distinct compared with the subsurface water and is characteristically enriched with biogenic organic compounds such as lipids, proteins and polysaccharides (Liss and Duce, 2005). The presence of the surface film and surface tension properties means the SML is a unique habitat that is often referred to as the neuston. Surface films occur on all water bodies, marine, estuarine and freshwater, sometimes as visible slicks, and are rapidly reformed after mixing by wind or waves. The structure of the SML is of great importance for understanding the exchange of chemicals between the oceans and the atmosphere.

Selenium Background

Selenium is a ubiquitous trace element, which exists in multiple chemical forms in seawater, including different oxidation states and organic metalloids compounds. Selenium is essential for the growth of various photosynthetic species at natural levels (Price and Thompson, 1987), but becomes toxic to fish and birds at elevated concentrations (Ohlendorf, 1989). The toxicity and physiological effects of selenium are affected by its chemical form (Shamberger, 1983). A literature review shows that selenite is more bioavailable to phytoplankton growth, selenate; however, can be more toxic (Wrench and Measures, 1982). The physiological behavior of selenium has fostered considerable interest in biogeochemical cycle studies over the last several decades (Measures and Burton, 1980; Cutter and Bruland, 1984; Cutter et al., 1995; and Cutter and Cutter, 2001).

Dissolved Se in seawater exists as selenate (Se VI), selenite (Se IV), and dissolved organic selenide (Se II). Data of speciation, distribution and behavior of dissolved selenium have been reported in estuary, coastal and open ocean waters, though none on the SML. Selenium is removed from the water column by uptake of aquatic organisms and by accumulation in cells, the biomethylation into dimethyl selenide (Cooke and Bruland, 1987). It can also be regenerated from organic selenides in deep waters via biodegradation (Cutter and Cutter, 2001). Selenite and selenate have been reported to have a nutrient type depth profile in the ocean, displaying surface water depletion and deep water enrichment (Cutter and Cutter, 2001). Though all of this data is present including biogeochemical cycles of selenium in the marine environment have been formulated (Measures and Burton, 1980; Cutter and Bruland, 1984) there is no mention of Se speciation in the SML region.

Arsenic background

Arsenic is widely distributed in the environment occurring naturally in air, soil, water, plants and animals. Arsenic can enter the environment through natural activities such as volcanic actions, erosion of rocks and forest fires, or through human actions such as mining activity, combustion of fossil fuels, and use of arsenical pesticides, herbicides and wood preservatives (Zhang et al., 2002). Humans are unavoidably exposed to arsenic through water sources and the food chain. The two inorganic arsenicals, arsenate (V) and arsenite (III), both of which are highly toxic, are major arsenic species in drinking water. Food products have a very broad range of arsenic levels, with the highest level being associated with seafood. Two reviews have comprehensively covered the types of arsenic compounds and occurrence of arsenic in the environment (Cullen and Reimer, 1989) and the methods and analytical techniques for the determination of different arsenic species (Francesconi and Kuehnelt, 2004).

The majority of arsenicals that have been discovered are associated with seafood such as fish, shellfish and seaweeds, which contain relatively high concentrations of arsenic (Francesconi and Edmond, 1997; Schmeisser et al., 2004). Inorganic arsenicals typically constitute $<0.2 \mu\text{g As g}^{-1}$ dry mass (Sirot et al., 2009). Arsenosugars are also found at significant concentrations in animals feeding on algae (mussels and oysters; typically $0.5\text{-}5 \mu\text{g As g}^{-1}$ dry mass) (Francesconi and Kuehnelt 2002). There are other arsenicals that can be found but in much smaller

concentrations, namely methylarsonate, dimethylarsinate, arsenocholine, trimethylarsine oxide, and tetramethylarsonium ion.

The arsenic compounds discussed above are classified in the water-soluble group, and more than 40 species have been reported. Even though these compounds were found their structures in the sea surface microlayer remain unknown. The limited data available for As and Se species in the SML make this an important piece in understanding the unique environment.

Procedure

Sample Collection and Preparation

Samples were collected from three locations along the Canary Creek saltmarsh in Lewes, Delaware (Figure C1). Gastropod species collected were *Geukensia demissa* and *Mytilus edulis* (commonly known as the ribbed and blue mussel respectively), were collected near the Roosevelt Inlet Bridge area. Plant and associated core samples collected was the common *Spartina alterniflora*, which was also collected near the Roosevelt Inlet Bridge. The surface microlayer sample was collected from near the Canary Creek bridge on New Road.

Plant samples were collected whole, including roots and associated sediment, and placed into acid-washed plastic zip-lock bags and then placed on dry ice. Gastropods were collected by hand and placed in an acid-washed plastic jar, which was then placed on dry ice. The surface microlayer was collected using an acid washed polyethylene bucket lid then placed in an acid washed plastic container and placed on dry ice. Samples were transported back to the laboratory and split for travel to Graz, Austria for total trace metal and speciation analysis while the other half were placed in -80°C freezer for analysis of Po and Pb upon return. Plant samples were separated into sediment, root, and leaf tissue. Gastropods were cracked open gently and extracted whole. The Gastropod tissue was then rinsed using Milli-Q water to clean off shell grit and placed in individual acid washed vials. All samples were then freeze dried for about 48 hours to a constant mass.

Sample Analysis

Analytical techniques used

Determination of arsenic species by coupling high performance liquid chromatography (HPLC) with mass spectrometry (MS) has commonly been used for arsenic speciation (Goessler and Kuehnelt 2002; Francesconi and Kuehnelt 2004). In this proposal selenium and arsenic speciation was done with HPLC coupled to an inductively coupled plasma mass spectrometric.

Inductively coupled plasma mass spectrometry (ICPMS)

ICPMS is an analytical technique that performs elemental analysis with a great deal of sensitivity and is capable of simultaneous determination of a large range of elements. When ICPMS is coupled to HPLC, it can be used for quantification

of species at levels down to about $0.1 \mu\text{g L}^{-1}$. The ICPMS instrument utilizes plasma as an atmospheric pressure ion source and a mass analyzer as a detection system for ions. The sample is pumped into a nebulizer, where it is converted to an aerosol. The small droplets of the aerosol are separated from larger droplets using a spray chamber and then transported into the ICP torch. A high-energy argon plasma is generated inside the torch under the influence of radiofrequency power. At which point the sample aerosol is simultaneously decomposed and ionized in the plasma (plasma temperature is in the order of 6,000 to 10,000 K). The ions produced are extracted from the plasma into the mass analyzer region. The ions are separated and detected based on their mass/charge ration (m/z).

Determination of Selenium and Arsenic species by HPLC/ICPMS

The mobile phases for HPLC measurements will be prepared by dissolving an appropriate amount of buffer in water. The pH of the mobile phase was adjusted to the desired pH, and the water was added to give a final volume of 1L. Standard and sample solutions were transferred to 1mL polypropylene vials and closed with a crimp cap before analysis. The outlet of the HPLC column will be directly connected to an Agilent 7500ce ICPMS, equipped with a Babington nebulizer, by 0.125 mm PEEK (polyetheretherketone) tubing (Upchurch Scientific, Oak Harbour, USA). The ICPMS system will be tuned with a solution of $10 \mu\text{g L}^{-1}$, which was introduced directly to the ICPMS (i.e. by passing the HPLC column). The torch position, gas flows and lens voltages was adjusted to give maximum response for As and Se signal.

Before the measurements, the analytical column was conditioned with the mobile phase at the flow rate to be used for analysis for at least 30min. The intensity of the arsenic and selenium ion was monitored using the “time-resolved” analysis software. Additionally, for As the ion intensity at m/z 77 ($^{40}\text{Ar}^{37}\text{Cl}$) was monitored to detect possible argon chloride ($^{40}\text{Ar}^{35}\text{Cl}$) manually with ICPMS chromatographic software C.01.00 (Agilent Technologies). Quantification of selenium and arsenic species was performed with external calibration against the standard solutions of relevant species.

Data

Total Trace Metal Concentration Analysis

Total trace metal concentrations were determined by ICPMS after mineralization of the samples with microwave assisted acid digestion. Specified portions of samples, extracted solutions (fractions), and certified reference materials were weighed into quartz tubes (12ml) and concentrated nitric acid (2ml) was added. The quartz tubes were then closed with Teflon caps and placed into the sample rack. The holding vessel was filled with a solution of water (300g) containing H_2SO_4 (5g) that served as the absorption liquid. After the autoclave was loaded with argon to a pressure of 40 bar, the samples were heated to $260 \text{ }^\circ\text{C}$, and this temperature was maintained for 40min. The digests were then diluted (10ml)

with Milli-Q water in 10ml polypropylene tubes. The acidified sample solutions were measured using ICPMS.

The standards for external calibration were prepared from a standard stock multi-element solution in the same acid concentration as the samples. Total trace metal concentrations in these digest solutions were determined with an Agilent ICPMS 7500ce equipped with an ISIS (Integrated Sample Introduction System), an ASX-500 auto-sampler with a Microflow PFA-100 nebulizer, and using 1.02mm ID and 0.89 mm ID tubing (Ismatec, Glattbrugg, Switzerland). Before measurement, the ICPMS was tuned with a 10 µg L-1 solution of Li, Y, Tl (m/z/ 7, 89, 205) for maximum sensitivity.

The total trace element concentration was determined by external calibration, and ⁷²Ge and ¹¹⁵In were used as internal standards. The accuracy of total trace metal determinations was checked by analyzing certified reference material Dorm-2 and Dolt-3. Table 1 shows the standards measured and certified concentrations for the elements measured.

Geukensia demissa and Mytilus edulis Total Element Analysis

As stated previously total element concentration analysis was run using an Agilent 7500 inductively coupled plasma absorption spectrometry (ICPMS) for 30 trace metals listed in Table 2. All values are given in dry mg/kg concentrations. It can be seen that the *Mytilus edulis* mussel has a greater concentration of metals than the *Geukensia demissa* which could be due to longer exposure time to the sea surface microlayer or due to the size difference (1 ½ inch *Geukensia demissa* and ¼ inch *Mytilus edulis*). Both organisms feed by filtering and do not have drastically different biology's.

Spartina alterniflora and core sample

Spartina alterniflora metal concentrations for leaf and root show the root sample in most cases has a slightly higher metal concentration than the leaf. The only large difference between the two is the concentration of Cu in the root is two fold greater than that of the leaf. The root when compared to soil concentrations is more highly enriched in all elements.

Core results down to 25cm show a large concentration of most metals located in the 10-15cm range. Depth profiles of individual trace metals are shown in figure C2. All of the trace metal concentrations are normalized to Al in order to remove the lithogenic effect on trace metal mobility. However, note that the normalization did not change the general trend with depth for each of the plotted profiles.

Figure C3 shows a comparison of from two other studies conducted in Delaware salt marshes throughout the years. The Pb/Al figure shows an increase in Pb at 5cm which corresponds to a date of about 1978. The Kim data shows a maximum ²¹⁰Pb value between 11-13cm (1930's), which he attributes to a significant nongasoline source of Pb, deposited onto the salt marsh. He also

describes that Cu and Zn sources at this depth also show maximum peaks and attribute these values to similar sources as the Pb.

Sea Surface Microlayer

As predicted the SML is highly enriched in metals, Table C5. The sample was measured without freezing drying “wet”, freeze dried “dry” and the sieve portion of the sample, which was done in order to separate large particles out of the sample. All values are in mg/kg. Large concentrations of Rb, Pb, As and Sr were found in these samples.

Once total concentrations of trace metals were found for all samples the viability of speciation experiments was determined. After concentrations were determined it was decided due to large amounts of previous work that only the surface microlayer samples will be utilized for Se and As speciation experiments. The total concentration of Se and As in the surface microlayer was Se $0.879 \text{ mg/kg} \pm .05$ and As $12.44 \pm .07 \text{ mg/kg}$ dry while the wet concentrations were $0.252 \text{ mg/kg} \pm .002$ and $0.015 \text{ mg/kg} \pm .001$ which fall into reported values of previous studies (Wildgust, M. et al., 1998).

Based off of the concentration of sample 0.2 grams of homogenized freeze-dried SML and 4ml of “wet” SML was added to a 10mL polypropylene vial and 5mL of Milli-Q water added. The sample was then agitated for 1hour and the supernatant removed using centrifuge at 3500 rpm for 15min. The extraction procedure was repeated two more times, with the supernatant removed after each centrifugation. A detailed flow chart of extraction results can be seen in the following figures. After the final Milli-Q water extraction the residue pellet was taken and 5mL of Methanol, Acetone and Hexane were also used for extraction utilizing the same procedure. The final residue was then dried.

Triplicates of each extraction and final residue was taken for a total of 15 samples. The methanol, acetone and hexane samples were evaporated and then brought up in 5ml Milli-Q water and 2ml of Nitric acid. 2ml of Nitric acid was added to the other samples then placed in the MLS GmbH ultraclave high performance microwave reactor for digestion. Samples were then run on the ICPMS for Se and As concentration of extract. Figure 2 shows the concentration found for each element for each extraction step. Total extraction recovery of Se was found to be 56% while As was 65% retained. Another extraction was performed due to low yields and utilized only three Methanol extractions. Figure 5 shows the results of this extraction and final yield of As of $107\% \pm 6$ and $111\% \pm 9$ for Se retained during extraction.

The final extraction utilized the “wet” SML, which was not freeze dried. The sample was taken and directly centrifuged with the supernatant removed as H2O extract 01. From that point methanol was used as in previous experiments for extraction. A final yield of As showed $87.7\% \pm 3$ and $89.5\% \pm 5$ Se retained during extraction.

As and Se Speciation Determination: ICPMS-HPLC *Cation exchange column: Ionosphere 5C*

Flow injection found that concentrations were generally lower than expected but extraction samples still included enough As and Se for ICPMS-HPLC. Dry MeOH direct and with added H₂O₂ (Figure C6) both show similar chromatograms which indicate a large peak (t=0.620) directly in the front. This most likely indicates that the arsenic in the sample is anionic. Wet H₂O direct and with added H₂O₂ (figure C7) show a large peak at the front (t=0.610) but then two other peaks at t=1.0 and t=4.50. The direct sample shows low levels of these two peaks but they then grow with the addition of H₂O₂ while the large front peak slightly shrinks. It is most likely that the H₂O₂ is oxidizing species of arsenic. Wet MeOH direct and with added H₂O₂ (figure 8) both show similar chromatograms which indicate a large peak at t=0.600 but a new set of peaks forming at t=2.9 and 3.5. Evaporate samples of Dry MeOH and with added H₂O₂ show similar peaks with a front peak at t=0.600 and at t=3.4. The peak at t=3.4 is similar to that found in Wet MeOH (figure C8). The residue samples treated with 0.1M TFA and 10% H₂O₂ both show similar chromatograms with a very large peak at the front (t=0.600) and two much smaller peaks at t=2.4 and t=3.4.

Anion exchange column: Dionex As14

Building off of the results from the cation exchange Ionosphere column it was determined that most of the Arsenic species were of anionic composition. The Dionex As14 was then chosen in order to identify these species. Dry MeOH direct and with added H₂O₂ shows small levels of arsenic located at t=1.9, t=2.3 and t=4.4. These times most likely correlate to As (III), DMA and As(V) but a spiking experiment is needed to confirm. The H₂O₂ sample shows that oxidation is occurring causing a decrease in the t=2.3 peak and an increase in the t=4.4 peak.

Selenium Species Cation Ionosphere

All of the selenium in each of these samples came off of the column directly in the front denoting that the compound is most likely anionic. No other peaks were seen throughout the entire chromatogram.

Selenium Anion: Dionex As14

For all of the chromatograms either no Se is seen or very small concentration <1 ppb. There are peaks seen at t=8.9 for only ⁸²Se while at t=5.0 ⁷⁷Se constantly shows a peak. Due to the discrepancy between elements these peaks are most likely a form of interference.

Conclusion

Salt Marshes

The retention efficiency of aerosols in salt marshes can be calculated based on a steady state model for the airborne excess of ²¹⁰Pb in sediments compared

with the annual depositional flux of ^{210}Pb in the region. Utilizing the method and constants detailed in Kim (et. al., 2004) it is assumed that 65% of atmospheric aerosols are retained in the Canary Creek salt marsh. Comparing concentrations of trace element cores from the nearby Wolfe Glade salt marsh it is seen that the total inventories of Zn, Pb, and Cu have total inventories higher due to higher fluvial soil components.

Specific activities of ^{238}U and reasons for the net accumulation in salt marshes were hypothesized by Church (et al., 1996), it is thought that uranium scavenging occurs during the process of tidal mixing and attendant flocculation of humic acids and iron oxides. Secondly, uranium extraction occurs at the marsh surface sediments which is favored with an increase in sulfuric acidity at the summer salt marsh surface.

From core samples and comparison with previous data it can be concluded that the Canary Creek Salt marsh has showed signs of “wash-out” of the atmospheric and contaminant sources due to a large natural, fluvial soil input. From ^{210}Pb data it can be seen that during the 1970's the marsh reached its maximum pollution peak. As expected Pb isotopic signature is a useful tracer in coastal sediment studies for determining sedimentation rates and historical Pb sources.

Sea Surface Microlayer

The arsenic species identified are mostly inorganic arsenicals such as As (V) and As (III), other species include Arsenobetaine, Dimethylarsinate and DMAE. In order to confirm the presence of these species a spiking experiment needs to be performed for each. Once spiking experiments can confirm the existence of specific peaks the identification of unknown arsenicals can continue. Though these species make up the majority there are unknown species of cationic form that need to be further studied, specifically peaks at $t=2.6$ and $t=3.5$ found in the Wet MeOH direct and H₂O₂, Dry Evaporate Direct and H₂O₂ samples. The peak at $t=3.5$ has a concentration of about 10ppb while the smaller broader peak at $t=2.6$ is about 7ppb.

As for selenium the picture is much less clear. The cationic ionosphere column shows a small amount of Se which comes off the column instantly, suggesting a compound of anionic makeup. The anionic dionex 14As shows there is either none or less than 1ppb of selenium in the sample. Peaks found at $t=8.9$ (^{82}Se only) and $t=5.0$ (^{77}Se only) seem to indicate some type of interference is occurring. Moving forward with this little bit of data I would recommend a new Se sample be prepared with a higher concentration of Se present, along with specific parameters for Se species identification. Also the use of a different anionic column may provide insight into if the Se was sticking to the column.

Total metal analysis of the two mussel species shows that higher concentration in *Mytilus edulis* may correlate with having a longer contact with the SML compared to *Geukensia demissa*. This is based off the measurements taken at the sight showing the mean high tide and exact location of both species. In order to confirm this hypothesis more tests and samples are needed.

In the absence of major anthropogenic sources on the Canary Creek salt marsh, trace metals are primarily brought by tidal waters flowing through the large creek and are deposited either on the creek bottom or on the marsh mud flat, when

tidal waters percolates over the marsh after filling creeks during high tides. Tidal water being the common source and assumingly similar mobility behavior of individual trace metals would mean that trace metal concentration should not vary over short distances within the depositional zones of Canary Creek. Depth profiles generally show an increase in concentration with depth. While the root and grass of *Spartina alterniflora* show similar metal concentrations.

Moving forward all samples will also be tested for ^{210}Po and ^{210}Pb back in the US in order to confirm if there is a correlation between ^{210}Po and class B metals. Analysis of the SML Se and As species will continue and more SML will be collected and shipped to Graz. A plan should be worked out with Kevin for how to move forward and what experiments should be run in the US to help identify Se species. Other collaborated work is also possible.

References:

Cherry, R.D., Shannon, L.V., 1974. The alpha radioactivity of marine organisms. *Atomic Energy Review* 12, 3e45.

Parfenov, Y., 1974. Polonium-210 in the environment and in the human organisms. *Atomic Energy Review* 12, 75e143.

Turekian KK, Nozaki Y, Benninger LK (1977) Geochemistry of atmospheric radon and radon products. *A Rev Earth Planet Sciences* 5: 227±255
Bruland, K. W. (1983). Trace elements in sea-water. In: *Chemical Oceanography* (Eds J. P. Riley and R. Chester). Academic Press, London, pp. 157–220.

Turner, D. R., M. Whitfield, and A. G. Dickson. (1981). The equilibrium speciation of dissolved components in freshwater and seawater at 25°C and 1 atmosphere pressure. *Geochimica et Cosmochimica Acta*, 45, 855–881.

Cherry, R. D., and M. Heyraud. (1981). Polonium-210 content of marine shrimp; variation with biological and environmental factors. *Marine Biology*, 65, 165–175.

Fisher, N. S., K. A. Burns, R. D. Cherry, and M. Heyraud. (1983). Accumulation and cellular distribution of ^{241}Am , ^{210}Po , and ^{210}Pb in two marine algae. *Marine Ecology Progress Series*, 11, 233–237.

Cherrier, J., W. C. Burnett, and P. A. LaRock. (1995). Uptake of polonium and sulfur by bacteria. *Geomicrobiology Journal*, 13, 103–115.

Stewart, G. M., and N. S. Fisher. (2003a). Experimental studies on the accumulation of polonium-210 by marine phytoplankton. *Limnology and Oceanography*, 48, 1193–1201.

Schwarz, K. (1976). Essentiality and metabolic functions of selenium. *Medical Clinics of North America*, 60, 745–767.

Durand, J. P., F. P. Carvalho, F. Goudard, J. Pieri, S. W. Fowler, and O. Cotret. (1999). ²¹⁰Po binding to metallothioneins and ferritin in the liver of teleost marine fish. *Marine Ecology Progress Series*, 177, 189–196.

Stewart, G. M, J. K. Cochran, J. Xue, C. Lee, S. Wakeham, R. A. Armstrong, P. Masque, and J. C. Miquel. (2007). Exploring the connection between Po-210 and organic matter in the northwestern Mediterranean. *Deep-Sea Research I*, 54, 415–427.

J. Kirby, W. Maher, *J. Anal. At. Spectrom.* 2002, 17, 838.

J. Kirby, W. Maher, M.J. Ellwood, F. Krikowa, *Aust. J. Chem.* 2004, 57, 957.

Germain, P., G. Leclerc, and S. Simon. (1995). Transfer of polonium-210 into *Mytilus edulis* (L.) and *Fucus vesiculosus* (L.) from the Baie de Seine (Channel coast of France). *Science of the Total Environment*, 164, 109–123.

Viarengo A (1989) Heavy metals in marine invertebrates: mechanisms of regulation and toxicity at the cellular level. *Rev aquat Sciences* 1: 295±317

Engel DW, Roesijadi G (1987) *Metallothioneins: a monitoring tool*. University of South Carolina Press, Columbia

Liss PS, Duce RA 2005 *The Sea Surface and Global Change*. Cambridge University Press: UK.

T.C. Stadtman, Selenium biochemistry, *Ann. Rev. Biochem.* 59 (1990)111-127.

G.A. Cutter. Elimination of nitrite interference in the determination of selenium by hydride generation. *Analytical Chemica Acts*, 149 (1983).

G.A. Cutter, K.W. Bruland. The marine biogeochemistry of selenium: a re-evaluation. *Limnology and Oceanography*, 29 (1984).

G.A. Cutter and L.S. Cutter. Source and cycling of selenium in the western and equatorial Atlantic Ocean. *Deep-Sea Research II*, 48 (2001).

C.J. Measures, J.D. Burton. The vertical distribution and oxidation states of selenium in the northeast Atlantic Ocean and their relationship to biological process. *Earth and Planetary Science Letter*, 49 (1980).

H. Ohlendorf. Bioaccumulation and effects of selenium on wildlife. *Agriculture and the Environment*, Soil Science Society of America. (1989).

N.M. Price, P.J. Thampson. Selenium: an essential for growth of coastal marine diatom *Thalassosira pseudonana*. *Journal of Phycology*, 23 (1987).

Zhang, W. Cai, Y., Tu, C. Arsenic speciation and distribution in an arsenic hyperaccumulating plant. *Sci. Total Environment*. 2002.

Cullen, W.R. Reimer, K. Arsenic speciation in the environment. *J. Chem. Rev.* 1989.

Francesconi, K. A. Kuehnelt, D. Determination of arsenic species: A critical review of methods and applications, *Analyst*, 2004.

Francesconi, K.A., Edmond, J.S. Arsenic and marine organisms. *Adv. Inorg. Chem.* 1997.

Schmeisser, E. Raml, R. Francesconi, K.A, Kuehnelt, D. Thio arsenosugars identified as natural constituents of mussels by liquid chromatography mass spectrometry. *Chem Commun.* 2004.

Sirot, V. Guerin, T. Volatier, J.L. Dietary exposure and biomarkers of arsenic in consumers of fish and shellfish from France. *Sci. Total Environ.* 2009

Table C1: Dolt-3 (Dogfish Liver) and Dorm-2 (Dogfish Muscle) were used at reference standards throughout the experiments.

| Element | Reference Dolt-3 | | | | Reference Dorm-2 | | | |
|----------------|-------------------------|---------------|--------------------|------------------------------|-------------------------|---------------|--------------------|------------------------------|
| | Conc. ug/g | Conc RSD % | Certified Conc. | Measured vs. Certified | Conc. ug/g | Conc RSD % | Certified Conc. | Measured vs. Certified |
| Fe | 1494.38 | 0.70 | 1484.00 | 10.38 | 157.37 | 1.28 | 142.00 | 15.37 |
| Ni | 3.75 | 0.86 | 2.72 | 1.03 | 19.10 | 0.65 | 19.40 | -0.30 |
| Cu | 32.52 | 0.53 | 31.20 | 1.32 | 2.30 | 1.47 | 2.34 | -0.04 |
| Cd | 19.78 | 1.84 | 19.40 | 0.38 | 0.06 | 1.13 | 0.04 | 0.02 |
| As | 9.76 | 12.22 | 10.20 | -0.44 | 19.55 | 9.75 | 18.00 | 1.55 |
| Se | 7.92 | 2.59 | 7.06 | 0.86 | 2.14 | 1.69 | 1.40 | 0.74 |
| Ag | 1.24 | 10.45 | 1.20 | 0.04 | 0.05 | 9.68 | 0.04 | 0.01 |
| Pb | 0.31 | 2.01 | 0.32 | -0.01 | 0.14 | 4.19 | 0.07 | 0.07 |

Table C2: Total trace metal analysis for *Geukensia demissa*, and *Mytilus edulis*. Elements with “*” mean that sample concentration was outside of calibration curve range and cannot be confirmed.

| Sample | 7 Li [3] | 9 Be [3] | 11 B [3] | 23 Na [2]* | 24 Mg [2]* |
|--------------------------|------------------|-------------------|------------------|--------------------|------------------|
| <i>Mytilus edulis</i> | 1.622 ± 0.11 | 0.003 ± 0.0007 | 1.989 ± 0.14 | 32064.675 ± 2244.5 | 3829.637 ± 268.1 |
| <i>Geukensia demissa</i> | 0.961 ± 0.07 | 0.001 ± 0.0006 | 1.814 ± 0.13 | 30146.362 ± 2110.2 | 3216.281 ± 225.1 |
| | 27 Al [3]* | 39 K [2]* | 43 Ca [3]* | 51 V [2] | 53 Cr [2] |
| <i>Mytilus edulis</i> | 9264.768 ± 648.5 | 9264.768 ± 648.5 | 3829.132 ± 268.0 | 2.841 ± 0.20 | 2.368 ± 0.16 |
| <i>Geukensia demissa</i> | 7136.480 ± 499.6 | 11928.429 ± 834.9 | 1919.886 ± 134.4 | 1.337 ± 0.09 | 1.365 ± 0.20 |
| | 55 Mn [2] | 56 Fe [2]* | 59 Co [2] | 60 Ni [2] | 65 Cu [2] |
| <i>Mytilus edulis</i> | 21.946 ± 1.54 | 895.885 ± 62.71 | 0.616 ± 0.04 | 1.899 ± 0.13 | 5.741 ± 0.40 |
| <i>Geukensia demissa</i> | 14.336 ± 1.00 | 429.011 ± 30.03 | 0.329 ± 0.02 | 1.539 ± 0.11 | 7.235 ± 0.51 |
| | 66 Zn [3] | 71 Ga [3] | 75 As [2] | 78 Se [1] | 85 Rb [3] |
| <i>Mytilus edulis</i> | 86.461 ± 6.05 | 0.424 ± 0.03 | 7.364 ± 0.52 | 3.633 ± 0.25 | 51.569 ± 3.61 |
| <i>Geukensia demissa</i> | 46.989 ± 3.29 | 0.193 ± 0.01 | 10.912 ± 0.76 | 2.236 ± 0.16 | 45.565 ± 3.19 |
| | 88 Sr [3] | 98 Mo [3] | 107 Ag [3] | 111 Cd [3] | 125 Te [3] |
| <i>Mytilus edulis</i> | 37.003 ± 2.59 | 0.787 ± 0.06 | 0.138 ± 0.01 | 0.463 ± 0.03 | 0.015 ± 0.001 |
| <i>Geukensia demissa</i> | 27.589 ± 1.93 | 0.797 ± 0.06 | 1.187 ± 0.08 | 0.684 ± 0.05 | 0.009 ± 0.001 |
| | 137 Ba [3] | 208 Pb [3] | 209 Bi [3] | 238 U [3] | |
| <i>Mytilus edulis</i> | 11.656 ± 0.81 | 1.346 ± 0.09 | 0.020 ± 0.001 | 0.190 ± 0.01 | |
| <i>Geukensia demissa</i> | 7.452 ± 0.52 | 0.656 ± 0.05 | 0.010 ± 0.001 | 0.076 ± 0.01 | |

Table C3: Total trace metal analysis for *Spartina alterniflora* and core samples.

| Sample | 7 Li [3] | | 9 Be [3] | | 11 B [3] | | 23 Na [2]* | | 24 Mg [2]* | |
|------------------|--------------|----------|--------------|--------|--------------|--------|--------------|--------|--------------|--------|
| | mg/L | ± | mg/L | ± | mg/L | ± | mg/L | ± | mg/L | ± |
| Plant Leaf | 47.49 | 3.32 | 0.12 | 0.01 | 15.58 | 1.09 | 113318.1 | 7932.3 | 21062.9 | 1474.4 |
| Plant Root | 63.22 | 4.43 | 0.19 | 0.01 | 16.57 | 1.16 | 102731.5 | 7191.2 | 20163.3 | 1411.4 |
| Soil around root | 29.42 | 2.06 | 0.08 | 0.01 | 5.01 | 0.35 | 10200.7 | 714.0 | 6494.4 | 454.6 |
| Soil 5-10cm | 31.13 | 2.18 | 0.13 | 0.01 | 5.23 | 0.37 | 18470.0 | 1292.9 | 6723.5 | 470.6 |
| Soil 10-15cm | 33.10 | 2.32 | 0.10 | 0.01 | 4.72 | 0.33 | 12786.5 | 895.1 | 6359.3 | 445.2 |
| Soil 15-20cm | 39.15 | 2.74 | 0.10 | 0.01 | 4.67 | 0.33 | 6554.0 | 458.8 | 5994.6 | 419.6 |
| Soil 20-25cm | 23.74 | 1.66 | 0.08 | 0.01 | 3.39 | 0.24 | 25128.7 | 1759.0 | 5802.4 | 406.2 |
| | 27 Al [3]* | | 39 K [2]* | | 43 Ca [3]* | | 51 V [2] | | 53 Cr [2] | |
| | mg/L | ± | mg/L | ± | mg/L | ± | mg/L | ± | mg/L | ± |
| Plant Leaf | 347037.1 | 24292.6 | 57169.5 | 4001.9 | 18484.6 | 1293.9 | 112.30 | 7.86 | 83.96 | 5.88 |
| Plant Root | 539868.4 | 37790.8 | 45627.3 | 3193.9 | 15236.7 | 1066.6 | 129.74 | 9.08 | 112.52 | 7.88 |
| Soil around root | 305145.8 | 21360.2 | 10675.0 | 747.2 | 4803.5 | 336.2 | 63.43 | 4.44 | 59.38 | 4.16 |
| Soil 5-10cm | 297194.1 | 20803.6 | 10853.7 | 759.8 | 4766.9 | 333.7 | 69.93 | 4.90 | 60.27 | 4.22 |
| Soil 10-15cm | 320368.4 | 22425.8 | 11237.7 | 786.6 | 4214.4 | 295.0 | 73.14 | 5.12 | 63.86 | 4.47 |
| Soil 15-20cm | 385695.6 | 26998.7 | 11925.4 | 834.8 | 3549.6 | 248.5 | 74.67 | 5.23 | 68.65 | 4.81 |
| Soil 20-25cm | 232477.6 | 16273.4 | 8585.9 | 601.0 | 3326.5 | 232.9 | 43.69 | 3.06 | 40.01 | 2.80 |
| | 55 Mn [2]* | | 56 Fe [2]* | | 59 Co [2] | | 60 Ni [2] | | 65 Cu [2] | |
| | mg/L | ± | mg/L | ± | mg/L | ± | mg/L | ± | mg/L | ± |
| Plant Leaf | 5679261.4 | 397548.3 | 37200.9 | 2604.1 | 11.01 | 0.77 | 69.93 | 4.90 | 61.52 | 4.31 |
| Plant Root | 6029831.5 | 422088.2 | 45343.0 | 3174.0 | 13.01 | 0.91 | 42.66 | 2.99 | 128.95 | 9.03 |
| Soil around root | 1165625.0 | 81593.8 | 24762.7 | 1733.4 | 6.37 | 0.45 | 25.26 | 1.77 | 15.08 | 1.06 |
| Soil 5-10cm | 1126953.6 | 78886.8 | 29008.9 | 2030.6 | 6.84 | 0.48 | 23.35 | 1.63 | 20.12 | 1.41 |
| Soil 10-15cm | 1079998.2 | 75599.9 | 26315.6 | 1842.1 | 6.90 | 0.48 | 20.58 | 1.44 | 16.49 | 1.15 |
| Soil 15-20cm | 1037327.0 | 72612.9 | 20938.8 | 1465.7 | 7.35 | 0.51 | 23.86 | 1.67 | 21.37 | 1.50 |
| Soil 20-25cm | 672534.6 | 47077.4 | 15561.9 | 1089.3 | 5.82 | 0.41 | 15.83 | 1.11 | 9.37 | 0.66 |
| | 66 Zn [3] | | 71 Ga [3] | | 75 As [2] | | 78 Se [1] | | 85 Rb [3] | |
| | mg/L | ± | mg/L | ± | mg/L | ± | mg/L | ± | mg/L | ± |
| Plant Leaf | 496.45 | 34.75 | 14.59 | 1.02 | 18.65 | 1.31 | 1.16 | 0.08 | 792.6 | 55.5 |
| Plant Root | 653.00 | 45.71 | 19.72 | 1.38 | 26.73 | 1.87 | 1.64 | 0.11 | 1027.6 | 71.9 |
| Soil around root | 131.36 | 9.20 | 9.64 | 0.67 | 13.51 | 0.95 | 0.70 | 0.05 | 475.9 | 33.3 |
| Soil 5-10cm | 142.54 | 9.98 | 9.25 | 0.65 | 22.05 | 1.54 | 1.20 | 0.08 | 476.5 | 33.4 |
| Soil 10-15cm | 138.23 | 9.68 | 10.13 | 0.71 | 19.42 | 1.36 | 0.86 | 0.06 | 528.7 | 37.0 |
| Soil 15-20cm | 181.73 | 12.72 | 12.03 | 0.84 | 12.73 | 0.89 | 0.80 | 0.06 | 600.2 | 42.0 |
| Soil 20-25cm | 99.02 | 6.93 | 7.18 | 0.50 | 13.94 | 0.98 | 0.55 | 0.04 | 370.0 | 25.9 |
| | 88 Sr [3] | | 98 Mo [3] | | 107 Ag [3] | | 111 Cd [3] | | 125 Te [3] | |
| | mg/L | ± | mg/L | ± | mg/L | ± | mg/L | ± | mg/L | ± |
| Plant Leaf | 234.35 | 16.40 | 8.64 | 0.60 | 2.67 | 0.19 | 1.60 | 0.11 | 0.177 | 0.012 |
| Plant Root | 201.45 | 14.10 | 4.57 | 0.32 | 3.74 | 0.26 | 1.14 | 0.08 | 0.242 | 0.017 |
| Soil around root | 56.01 | 3.92 | 0.38 | 0.03 | 0.37 | 0.03 | 0.18 | 0.01 | 0.056 | 0.004 |
| Soil 5-10cm | 75.16 | 5.26 | 1.01 | 0.07 | 0.35 | 0.02 | 0.31 | 0.02 | 0.082 | 0.006 |
| Soil 10-15cm | 63.69 | 4.46 | 0.75 | 0.05 | 0.29 | 0.02 | 0.23 | 0.02 | 0.088 | 0.006 |
| Soil 15-20cm | 47.15 | 3.30 | 0.63 | 0.04 | 0.47 | 0.03 | 0.46 | 0.03 | 0.079 | 0.006 |
| Soil 20-25cm | 47.50 | 3.33 | 1.25 | 0.09 | 0.32 | 0.02 | 0.17 | 0.01 | 0.073 | 0.005 |
| | 137 Ba [3] | | 208 Pb [3] | | 209 Bi [3] | | 238 U [3] | | | |
| | mg/L | ± | mg/L | ± | mg/L | ± | mg/L | ± | | |
| Plant Leaf | 232.89 | 16.30 | 62.26 | 4.36 | 0.44 | 0.03 | 2.03 | 0.14 | | |
| Plant Root | 343.35 | 24.03 | 85.01 | 5.95 | 0.58 | 0.04 | 3.14 | 0.22 | | |
| Soil around root | 132.47 | 9.27 | 38.28 | 2.68 | 0.22 | 0.02 | 1.14 | 0.08 | | |
| Soil 5-10cm | 134.12 | 9.39 | 62.20 | 4.35 | 0.27 | 0.02 | 1.78 | 0.12 | | |
| Soil 10-15cm | 145.53 | 10.19 | 54.42 | 3.81 | 0.50 | 0.04 | 1.79 | 0.13 | | |
| Soil 15-20cm | 159.82 | 11.19 | 56.03 | 3.92 | 0.64 | 0.04 | 2.05 | 0.14 | | |
| Soil 20-25cm | 102.79 | 7.20 | 23.91 | 1.67 | 0.21 | 0.01 | 1.74 | 0.12 | | |

Table C4: Total trace metal analysis for the SML (mg/kg).

| Sample | 7 Li [3] | 9 Be [3] | 11 B [3] | 23 Na [2]* | 24 Mg [2] * |
|---------|------------------|-------------------|------------------|--------------------|------------------|
| Dry SML | 23.454 ± 1.64 | 0.070 ± 0.005 | 5.531 ± 0.39 | 50940.914 ± 3565.9 | 7920.874 ± 554.5 |
| Wet SML | 0.498 ± 0.03 | 0.002 ± 0.0006 | 0.149 ± 0.01 | 1856.136 ± 129.9 | 245.575 ± 17.2 |
| | 27 Al [3]* | 39 K [2]* | 43 Ca [3]* | 51 V [2] | 53 Cr [2] |
| Dry SML | OR ± 0.0 | 9316.413 ± 652.15 | 4402.219 ± 308.2 | 34.866 ± 2.44 | 29.045 ± 2.03 |
| Wet SML | 4671.101 ± 326.9 | 264.609 ± 18.5 | 127.051 ± 8.89 | 0.834 ± 0.06 | 0.673 ± 0.05 |
| | 55 Mn [2] | 56 Fe [2]* | 59 Co [2] | 60 Ni [2] | 65 Cu [2] |
| Dry SML | 204.407 ± 14.3 | 13119.964 ± 918.4 | 3.937 ± 0.27 | 10.661 ± 0.75 | 7.321 ± 0.51 |
| Wet SML | 5.236 ± 0.37 | 297.748 ± 20.8 | 0.093 ± 0.007 | 264.642 ± 18.5 | 1.719 ± 0.12 |
| | 66 Zn [3] | 71 Ga [3] | 75 As [2] | 78 Se [1] | 85 Rb [3] |
| Dry SML | 67.022 ± 4.7 | 5.977 ± 0.42 | 7.854 ± 0.55 | 0.672 ± 0.05 | 310.577 ± 21.7 |
| Wet SML | 1.400 ± 0.09 | 0.135 ± 0.009 | 0.191 ± 0.01 | 0.013 ± 0.01 | 7.176 ± 0.50 |
| | 88 Sr [3] | 98 Mo [3] | 107 Ag [3] | 111 Cd [3] | 125 Te [3] |
| Dry SML | 73.204 ± 5.1 | 0.755 ± 0.05 | 1.840 ± 0.13 | 0.290 ± 0.02 | 0.031 ± 0.002 |
| Wet SML | 2.109 ± 0.15 | 0.020 ± 0.001 | 0.035 ± 0.002 | 0.005 ± 0.0004 | 0.001 ± 0.0001 |
| | 137 Ba [3] | 208 Pb [3] | 209 Bi [3] | 238 U [3] | |
| Dry SML | 179.610 ± 12.5 | 12.746 ± 0.89 | 0.303 ± 0.02 | 1.207 ± 0.08 | |
| Wet SML | 3.592 ± 0.25 | 0.329 ± 0.02 | 0.006 ± 0.0004 | 0.022 ± 0.002 | |

Table C5: Flow Injection results compared with expected concentrations in extraction samples.

| Sample | 75 As | 82 Se | 77 Se |
|--------------------------|-------|-------|-------|
| | µg | µg | µg |
| Calibration Std | 10.0 | 10.0 | 10.0 |
| Wet MeOH | 50.4 | 190.6 | 38.5 |
| Dry MeOH | 33.8 | 32.0 | 31.9 |
| Wet H2O | 69.8 | 83.8 | 34.6 |
| Wet MeOH w/H2O2 | 41.8 | 190.1 | 269.8 |
| Wet H2O w/H2O2 | 69.4 | 78.1 | 221.0 |
| Dry MeOH w/H2O2 | 29.0 | 29.9 | 95.2 |
| Dry Evaporate | 25.3 | 93.8 | 118.3 |
| Dry Evaporate w/ H2O2 | 21.4 | 5.2 | 2.9 |
| Residue TFA | 172.3 | 3.7 | 6.1 |
| Residue TFA H2O2 | 171.0 | 4.0 | 7.0 |

Table C6: Ionosphere 5C species and sum results from extracts

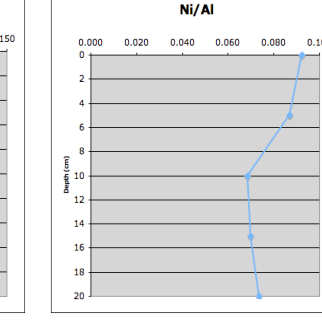
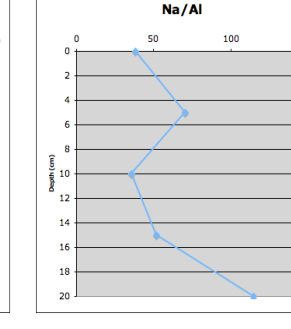
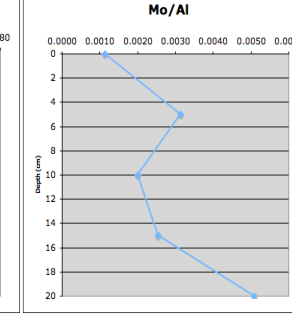
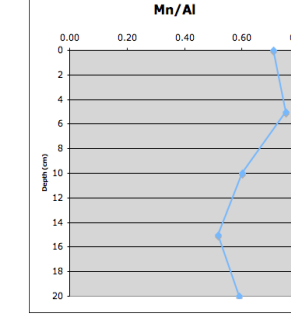
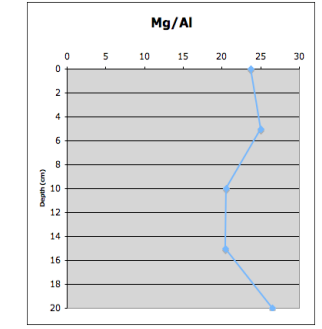
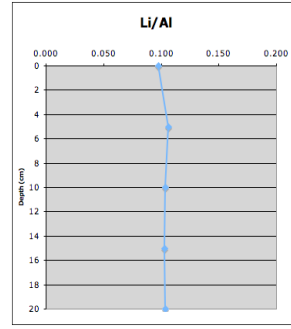
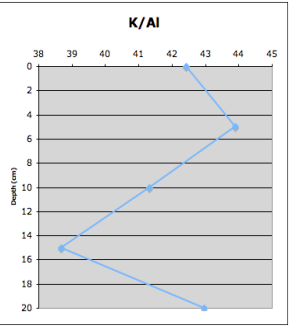
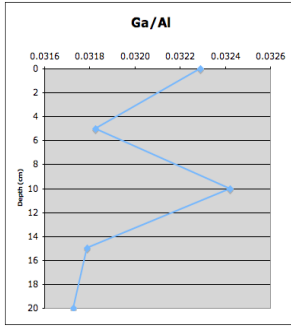
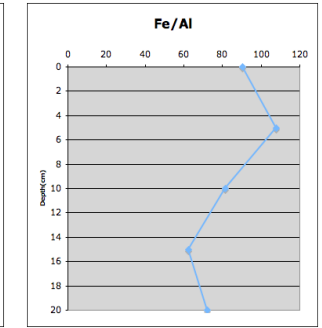
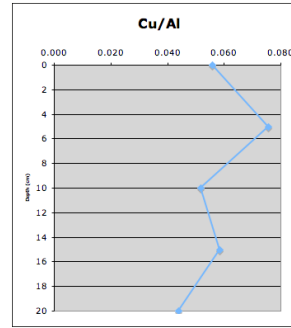
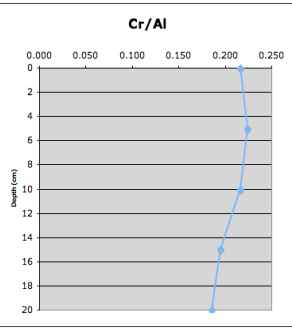
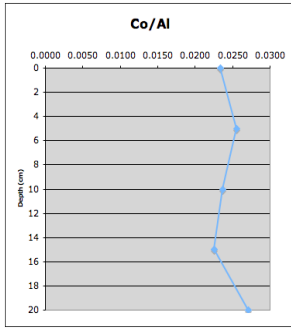
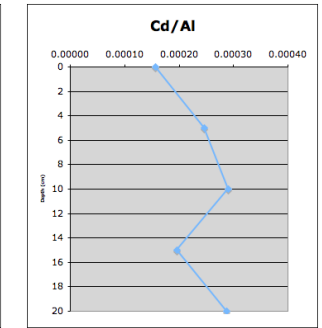
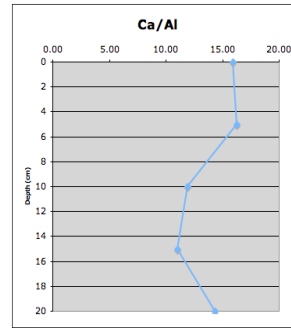
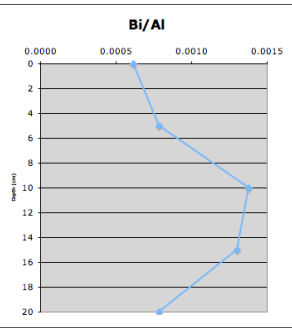
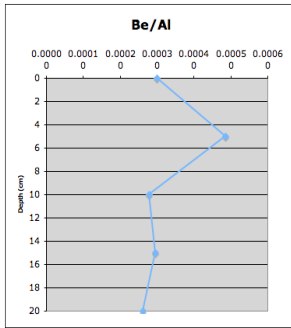
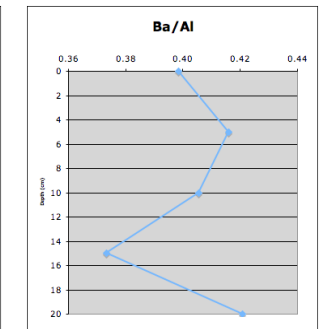
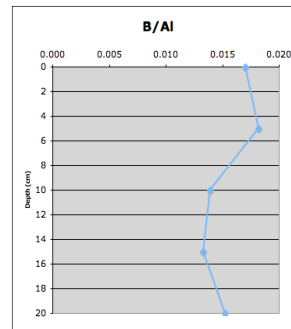
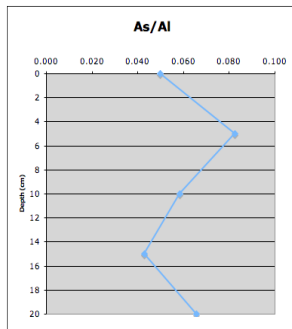
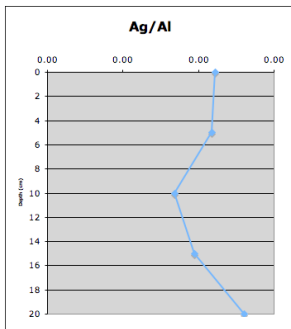
| | 82 Se front | 77 Se front | 75 AB | 75 As? | 75 DMAE | 75 Sum As | 82 Sum Se82 | 77 Se 77 | 82 Se 82 |
|-----------------------|-------------|-------------|-------|--------|---------|-----------|-------------|----------|----------|
| Sample Name | Conc. | Conc. | Conc. | Conc. | Conc. | Conc. | Conc. | Conc. | Conc. |
| 10ppb | 2.6 | | 10.4 | 11.3 | 9.5 | 0.0 | 0.0 | | |
| 50ppb | 50.0 | 50.0 | 49.9 | 49.7 | 50.1 | 81.9 | 0.1 | 50.0 | 50.0 |
| Wet MeOH | 13.8 | 2.8 | | | | 58.9 | 16.5 | | |
| Dry MeOH | | | | | | 30.5 | 2.8 | | |
| Wet H2O | 9.6 | 2.4 | 7.5 | | 1.3 | 94.2 | 10.9 | | |
| Wet MeOH w/H2O2 | 16.8 | 1.3 | | | | 44.6 | 18.8 | | |
| Wet H2O w/H2O2 | 13.2 | 1.2 | 40.3 | | 4.8 | 84.1 | 14.8 | | |
| Dry MeOH w/H2O2 | 7.1 | 4.3 | 2.1 | | | 24.7 | 0.0 | | |
| Dry Evaporate | 13.3 | 2.6 | | | | 41.2 | 0.0 | | |
| Dry Evaporate w/ H2O2 | 15.2 | 1.5 | | | | 25.0 | 0.0 | | |
| Residue TFA | 3.9 | | | 224.9 | | 280.7 | 0.0 | | |
| Residue TFA H2O2 | 6.4 | 4.1 | | 199.4 | | 240.0 | 0.0 | | |

Table C7: Results from the anion exchange column Dionex As14.

| Sample Name | 82 TMS _e | 77 TMS _e | 78 TMS _e | 75 As(III) | 75 DMA | 78 Selenite | 82 Selenite | 77 Selenite | 75 As(V) | 75 As Sum | 78 Se Sum | 82 Se Sum | 77 Selenate | 78 Selenate | 82 Selenate |
|-----------------------|---------------------|---------------------|---------------------|------------|--------|-------------|-------------|-------------|----------|-----------|-----------|-----------|-------------|-------------|-------------|
| | µg | µg | µg | µg | µg | µg | µg | µg | µg | µg | µg | µg | µg | µg | µg |
| 10ppb | 10.2 | 10.0 | 11.3 | 11.1 | 8.9 | 9.6 | 10.4 | 10.5 | 10.0 | 0.0 | 0.1 | 0.0 | 10.1 | 11.4 | 10.1 |
| 50ppb | 52.4 | 49.6 | 50.7 | 54.6 | 46.1 | 52.3 | 50.7 | 50.5 | 50.0 | 0.0 | 0.1 | 0.0 | 50.2 | 50.9 | 50.0 |
| 100ppb | 98.8 | 100.2 | 99.5 | 97.6 | 102.1 | 98.9 | 99.6 | 99.7 | 100.0 | 0.0 | 0.1 | 0.0 | 99.9 | 99.4 | 100.0 |
| Wet MeOH | 0.7 | | | 20.5 | 8.3 | | | | 1.5 | 40.6 | 0.1 | 12.5 | | | |
| Dry MeOH | | | | 0.6 | 8.1 | | | | 1.6 | 23.8 | 0.2 | 7.5 | | | |
| Wet H2O | | | | 14.6 | 21.7 | | | 4.7 | 26.7 | 79.0 | 0.1 | 13.7 | | | |
| Wet MeOH w/H2O2 | | | | 0.2 | 0.7 | | | | 1.1 | 30.1 | 0.0 | 0.0 | | | |
| Wet H2O w/H2O2 | | | | 8.2 | 39.1 | 0.7 | 0.7 | 4.1 | 28.8 | 78.5 | 0.1 | 20.7 | | | |
| Dry MeOH w/H2O2 | | | | 0.5 | | | | | 7.1 | 19.2 | 0.1 | 0.0 | | | |
| Dry Evaporate | | | | 22.7 | | | | | 1.3 | 27.9 | 0.0 | 0.0 | | | |
| Dry Evaporate w/ H2O2 | | | | 19.9 | | | | | 1.3 | 24.5 | 0.1 | 0.0 | | | |
| Residue TFA | | | | 23.7 | 11.3 | | | | 142.4 | 178.2 | 0.1 | 0.1 | | | |
| Residue TFA H2O2 | | | | 3.2 | 3.0 | | | | 106.4 | 147.1 | 0.2 | 0.0 | | | |



Figure C1: Canary Creek Delaware intertidal marsh sampling area. Samples were collected at two sites (Roosevelt Inlet and Canary Creek) over a 12 hour tidal cycle



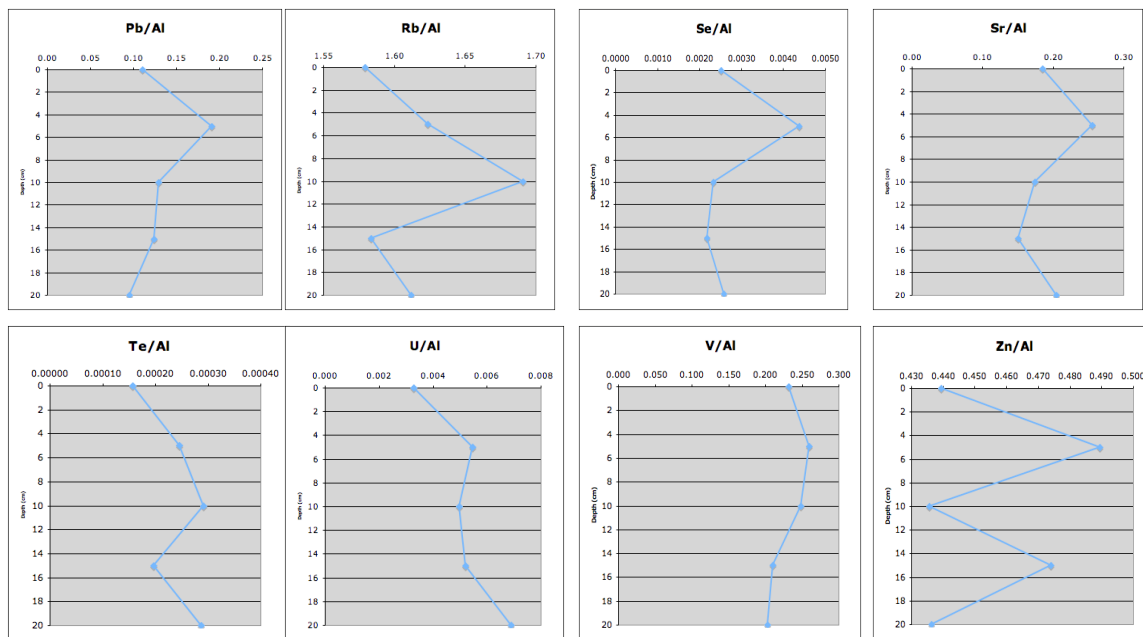


Figure C2: Depth distribution of trace metal content measured from the Canary creek core sample. Trace metal concentrations are normalized to Al to account for the accumulation affected by the variation in the mobility of different trace metals.

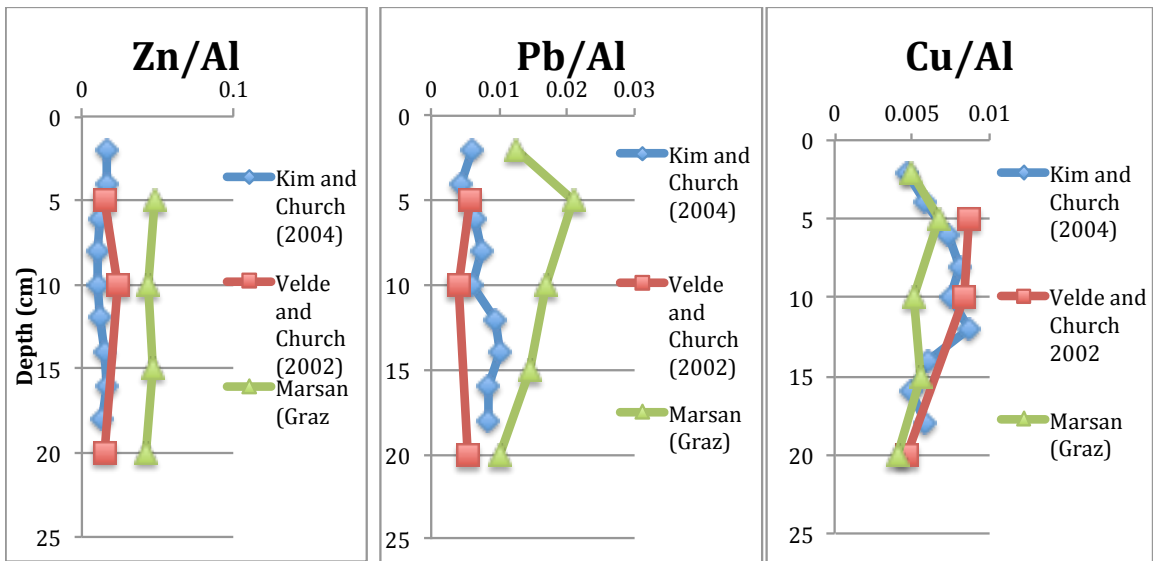


Figure C3: Depth profiles of elements from various Delaware Salt marshes.

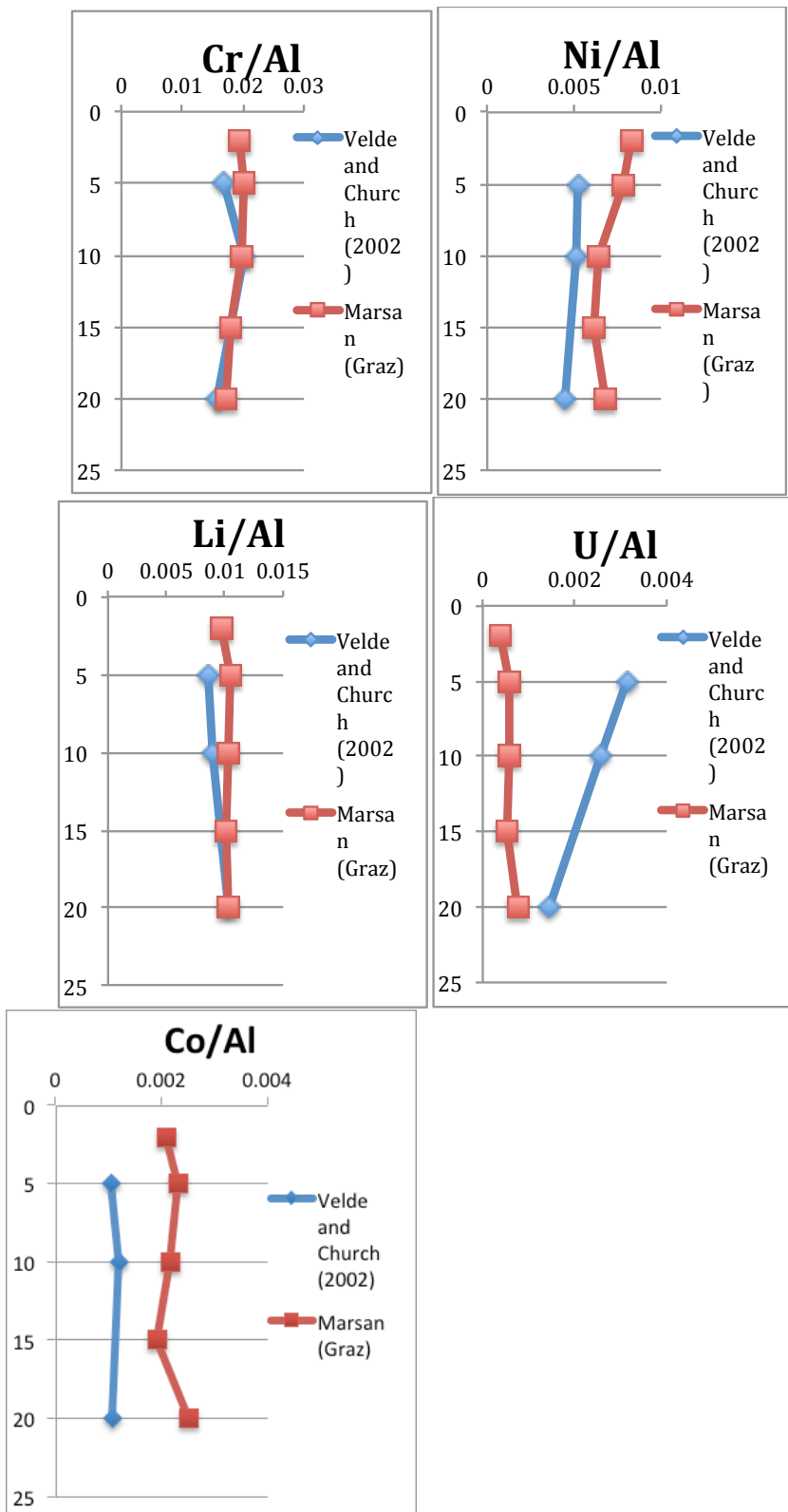


Figure C4: Depth profiles of elements from sediment cores from two Delaware Salt Marshes.

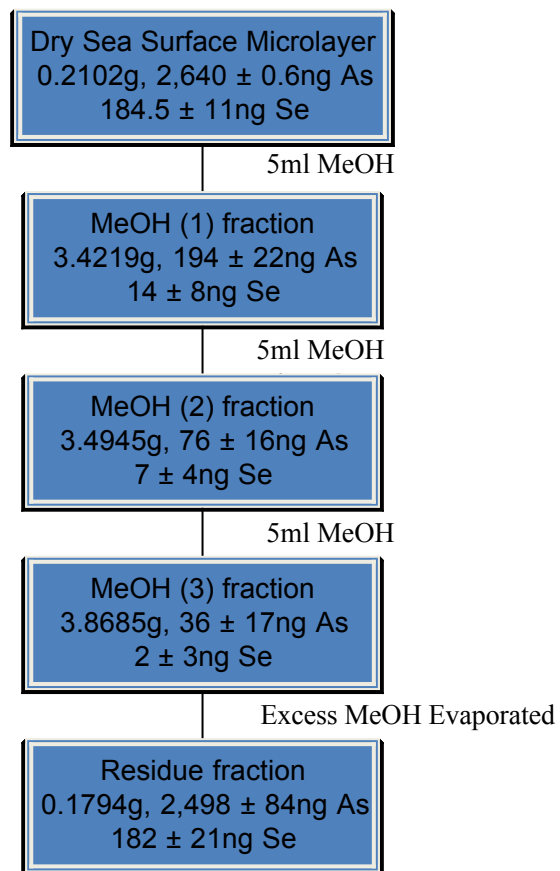


Figure C5: Extraction of As and Se compounds from freeze dried sea surface microlayer

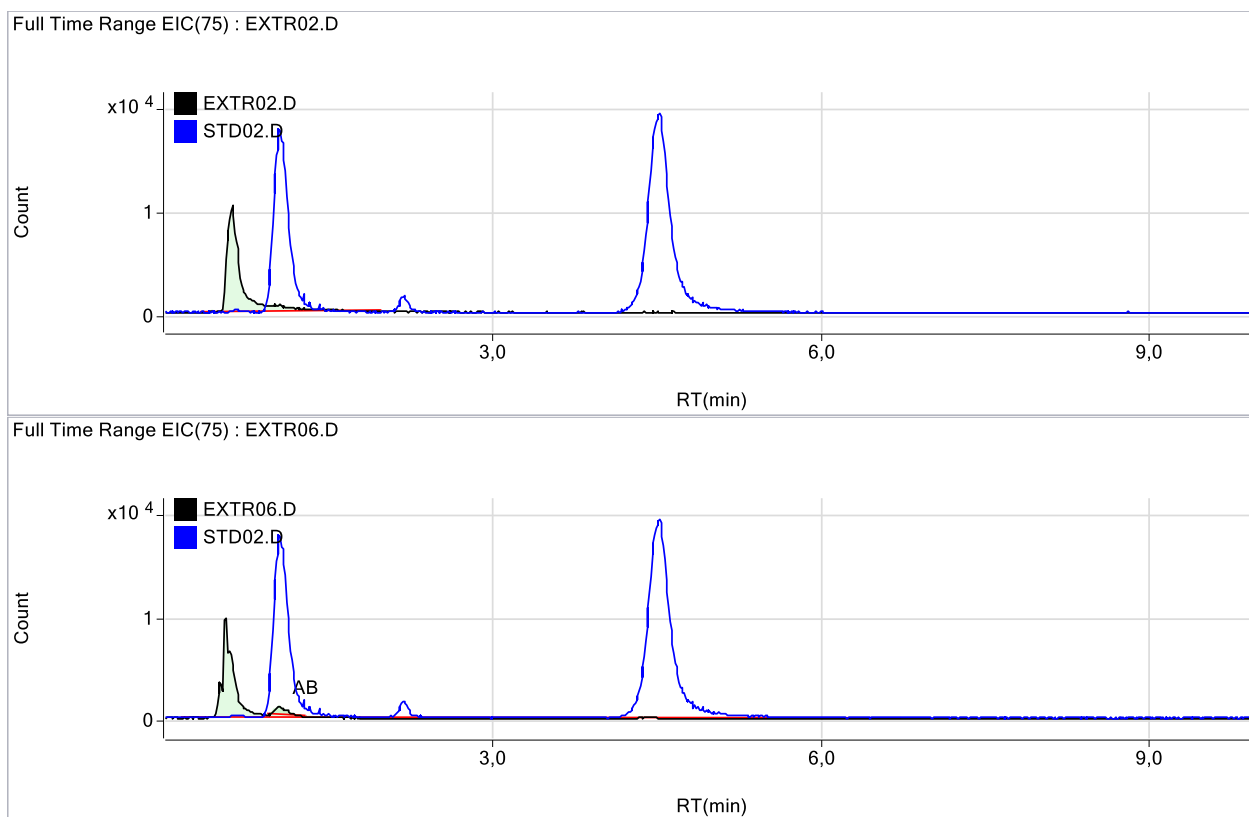


Figure C6: Full time range chromatogram for Arsenic Dry MeOH Direct (a) and Dry MeOH with 10% H₂O₂ (b) added.

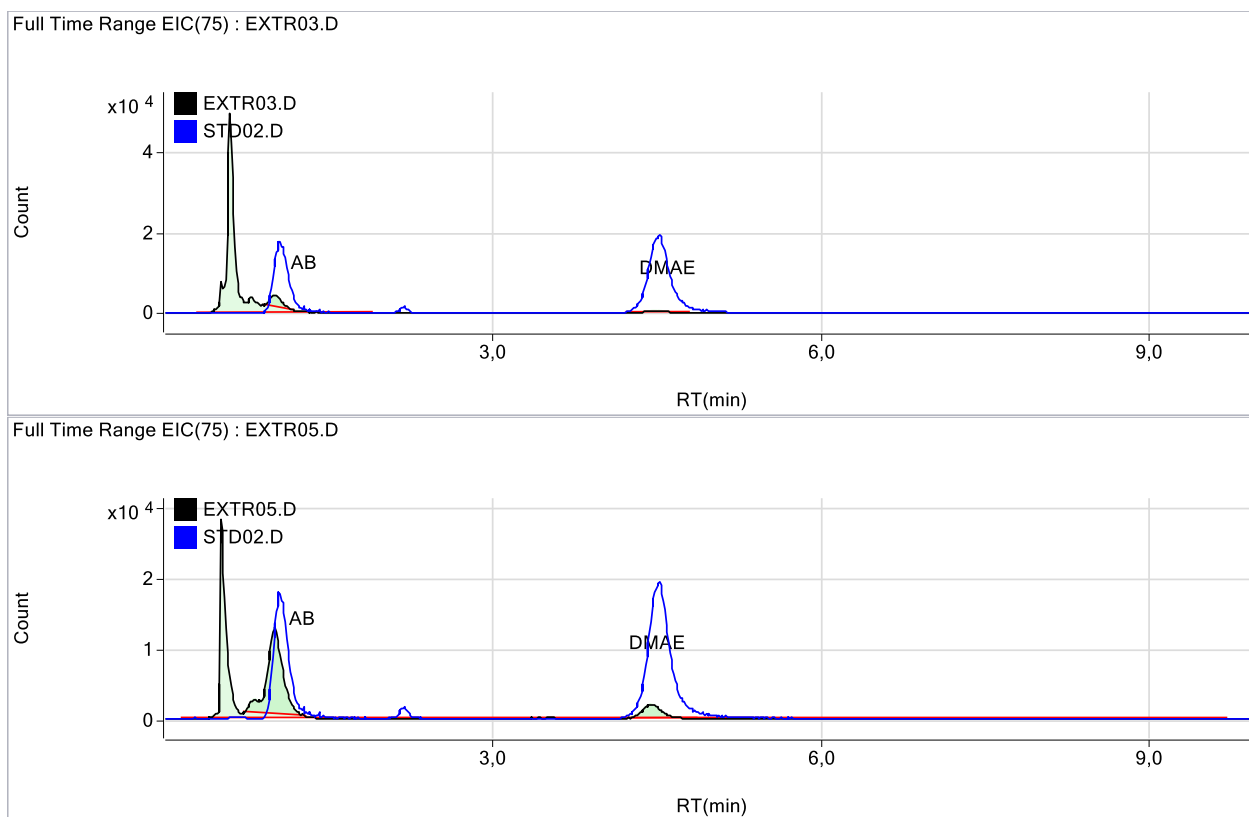


Figure C7: Full time range chromatogram for Arsenic Wet H₂O Direct (a) and Wet H₂O with 10% H₂O₂ (b) added.

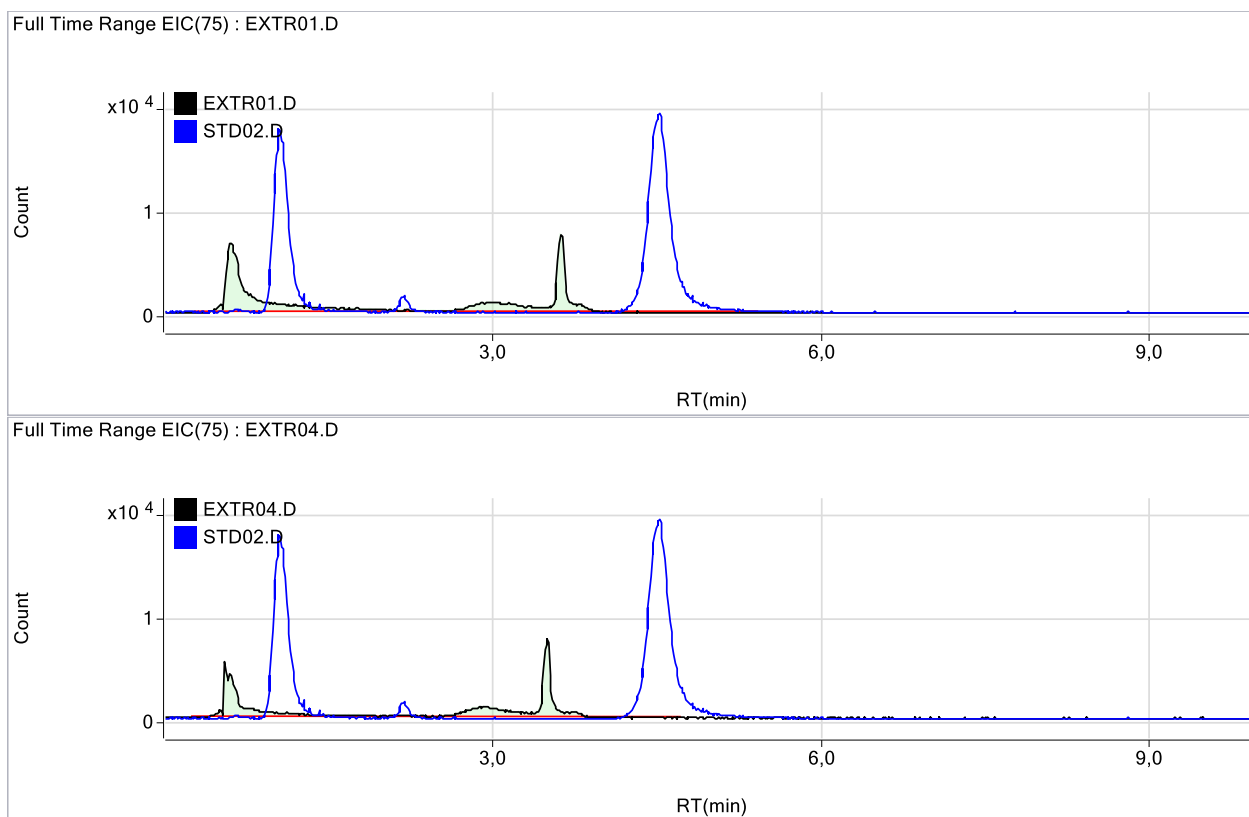


Figure C8: Full Time range chromatogram for Arsenic Wet MeOH Direct (a) and Wet MeOH with 10% H₂O₂ (b) added.

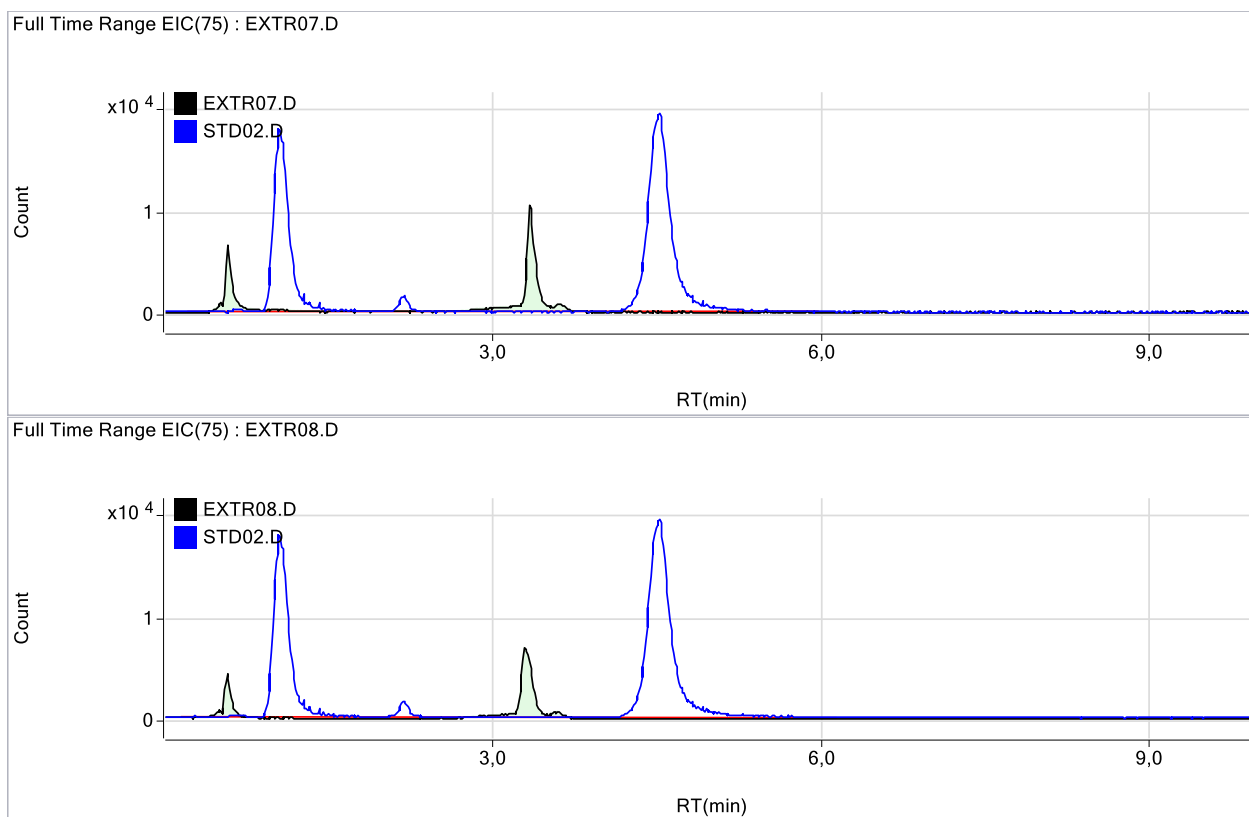


Figure C9: Full time range chromatogram for Arsenic Dry MeOH evaporate direct (a) and Dry MeOH evaporate with 10% H₂O₂ (b) added.

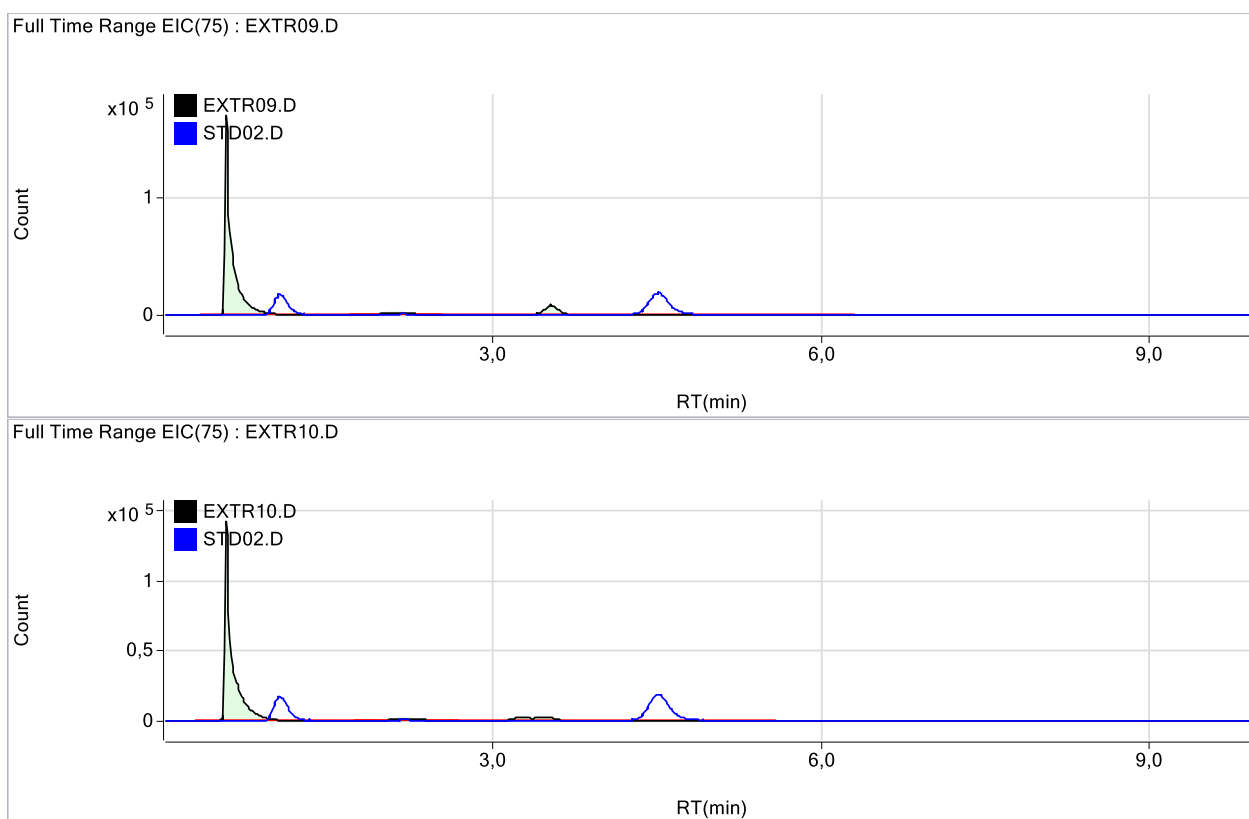


Figure C10: Full time range chromatogram for Arsenic Residue 0.1M TFA direct (a) and Residue 0.1M TFA with 10% H₂O₂ (b) added.

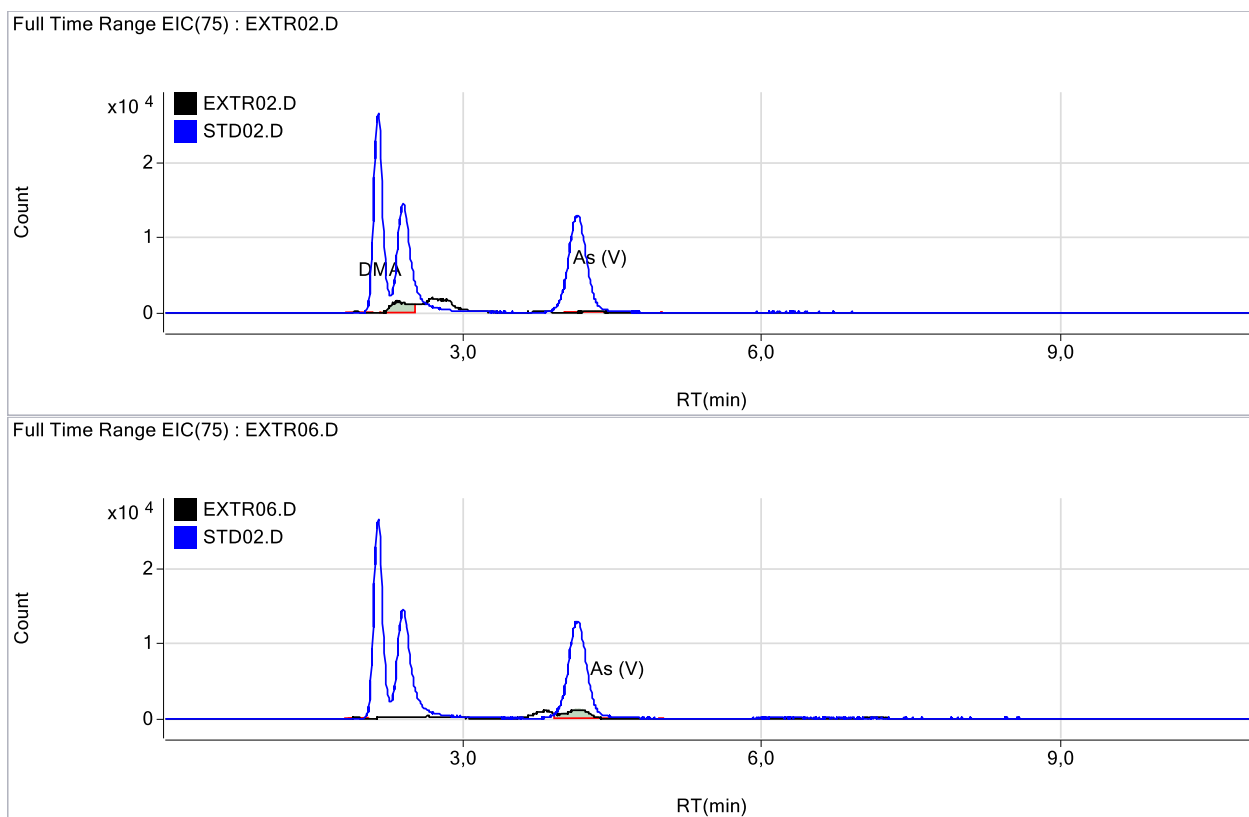


Figure C11: Full time range chromatogram for Arsenic Dry MeOH Direct (a) and Dry MeOH with 10% H₂O₂ (b) added.

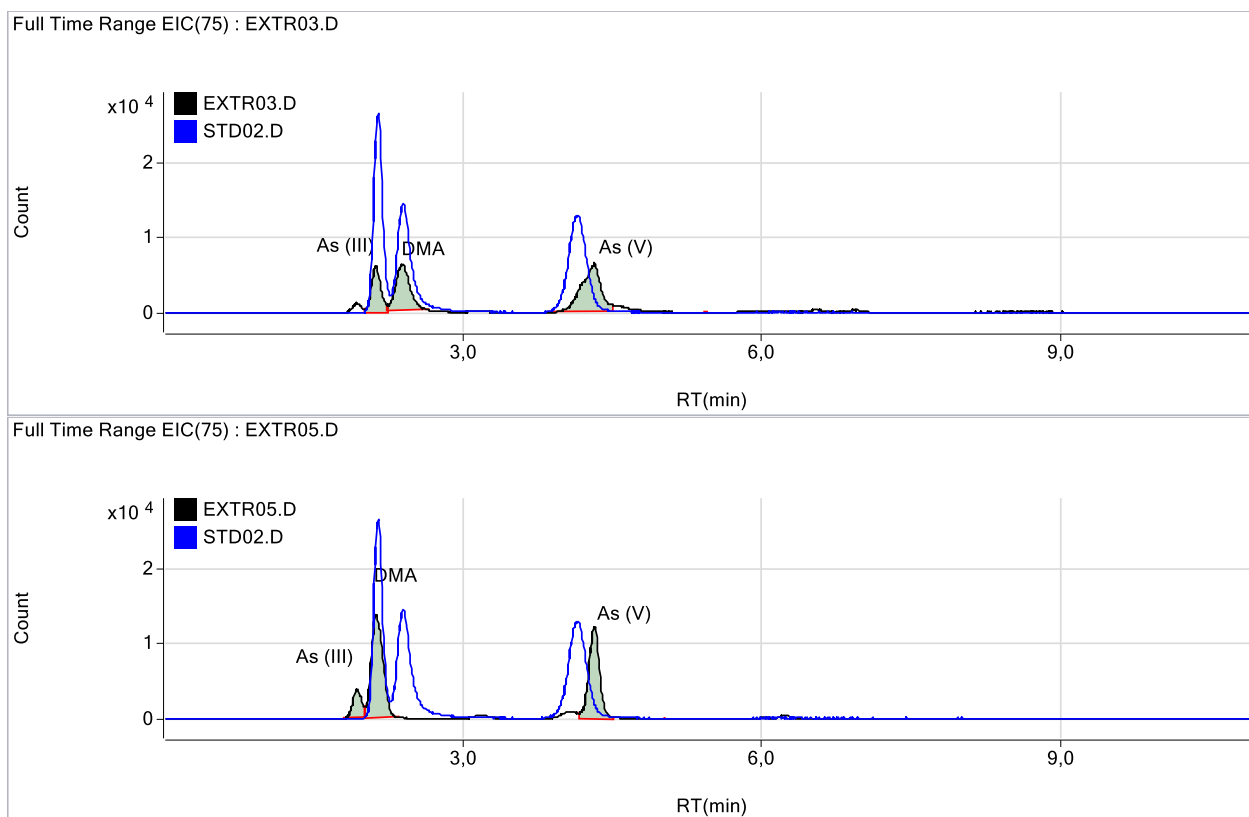


Figure C12: Full time range chromatogram for Arsenic Wet H2O Direct (a) and Wet H2O with 10% H2O2 (b) added.

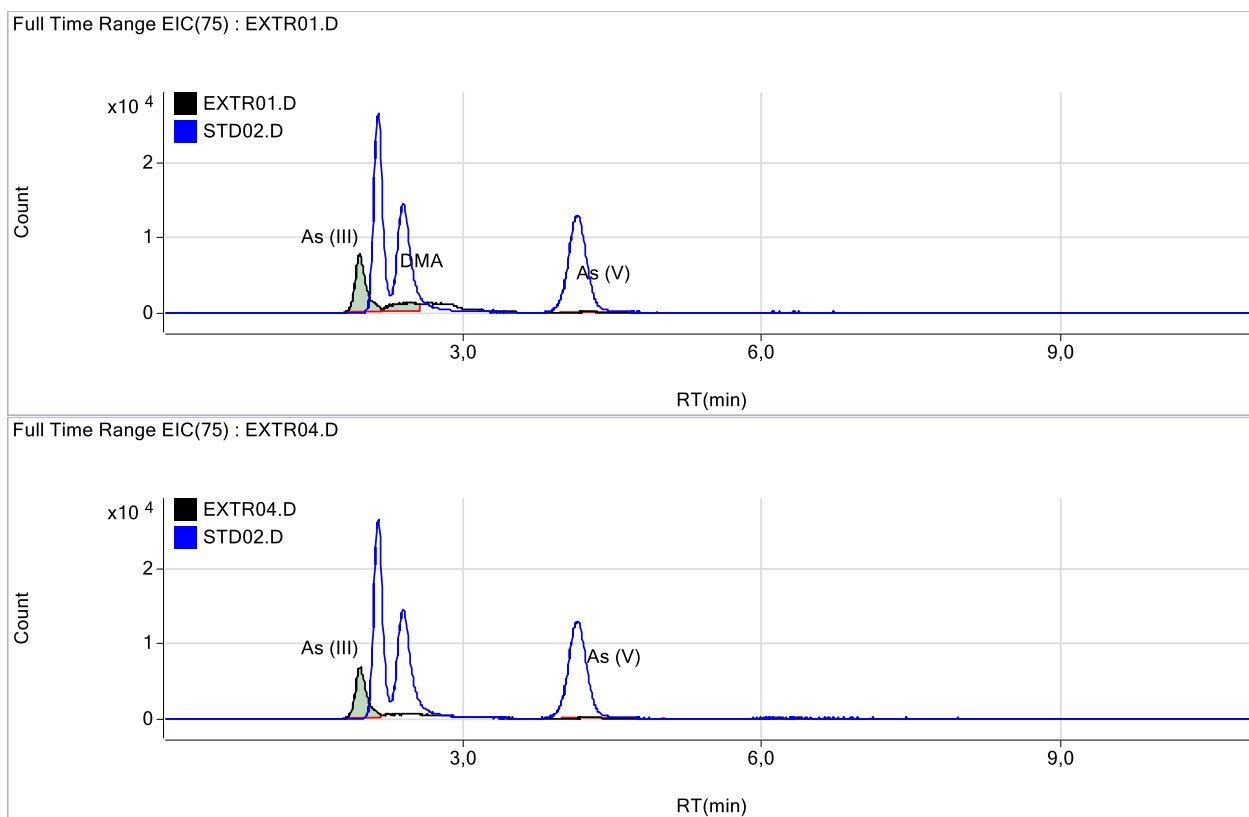


Figure C13: Full Time range chromatogram for Arsenic Wet MeOH Direct (a) and Wet MeOH with 10% H₂O₂ (b) added.

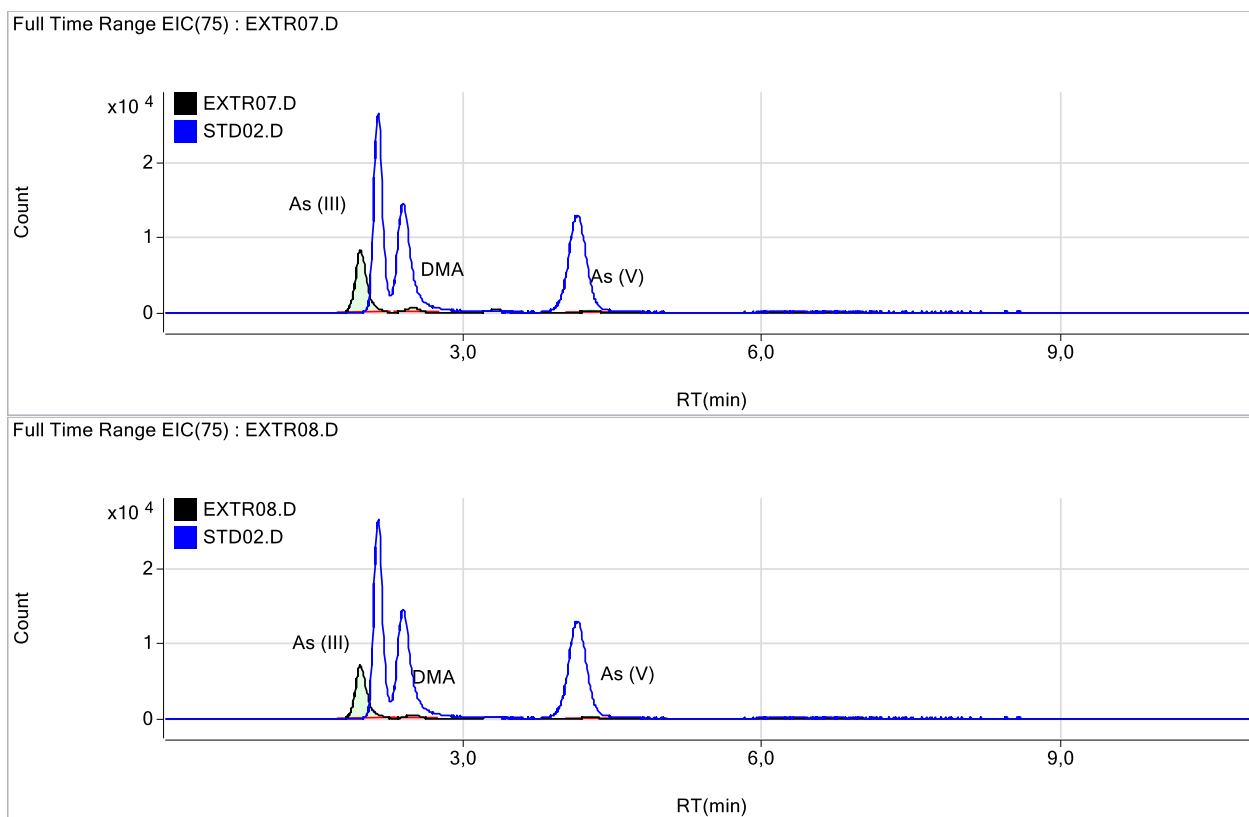


Figure C14: Full time range chromatogram for Arsenic Dry MeOH evaporate direct (a) and Dry MeOH evaporate with 10% H₂O₂ (b) added.

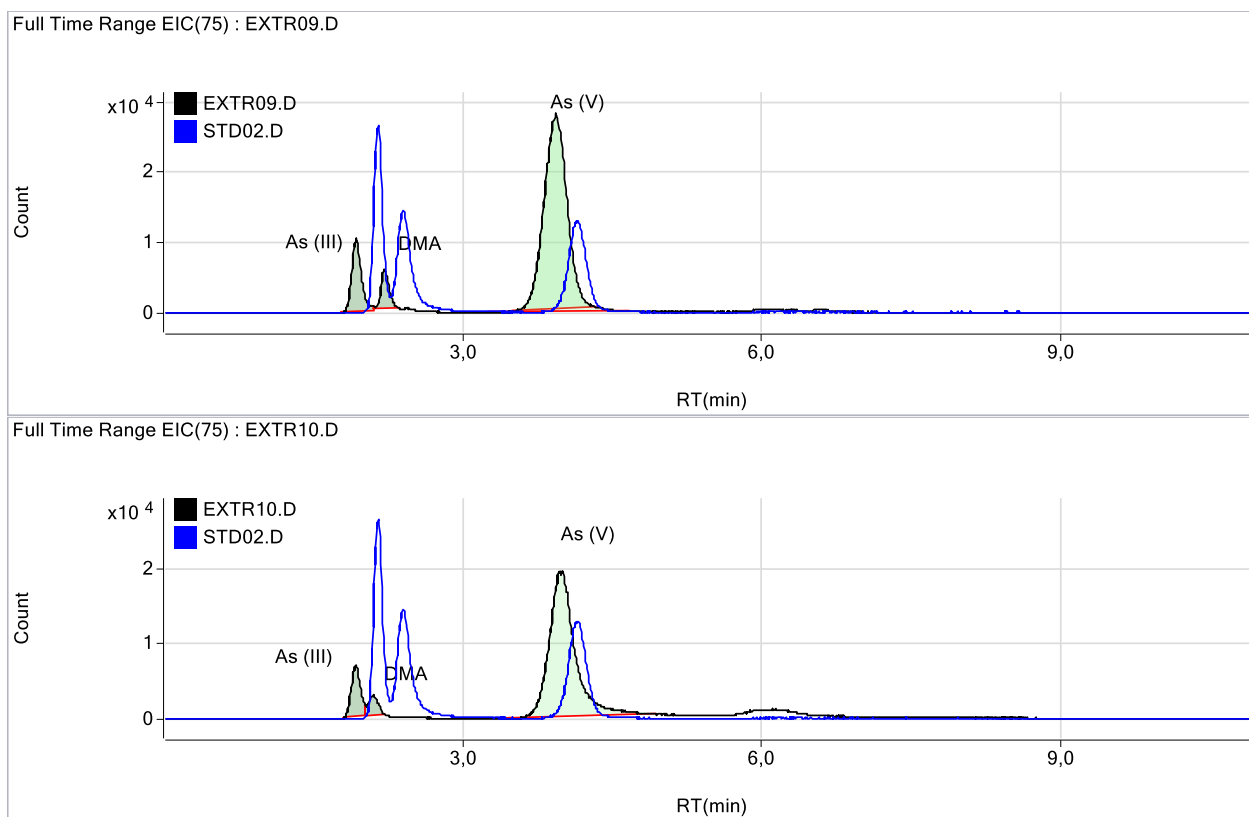


Figure C15: Full time range chromatogram for Arsenic Residue 0.1M TFA direct (a) and Residue 0.1M TFA with 10% H2O2 (b) added.

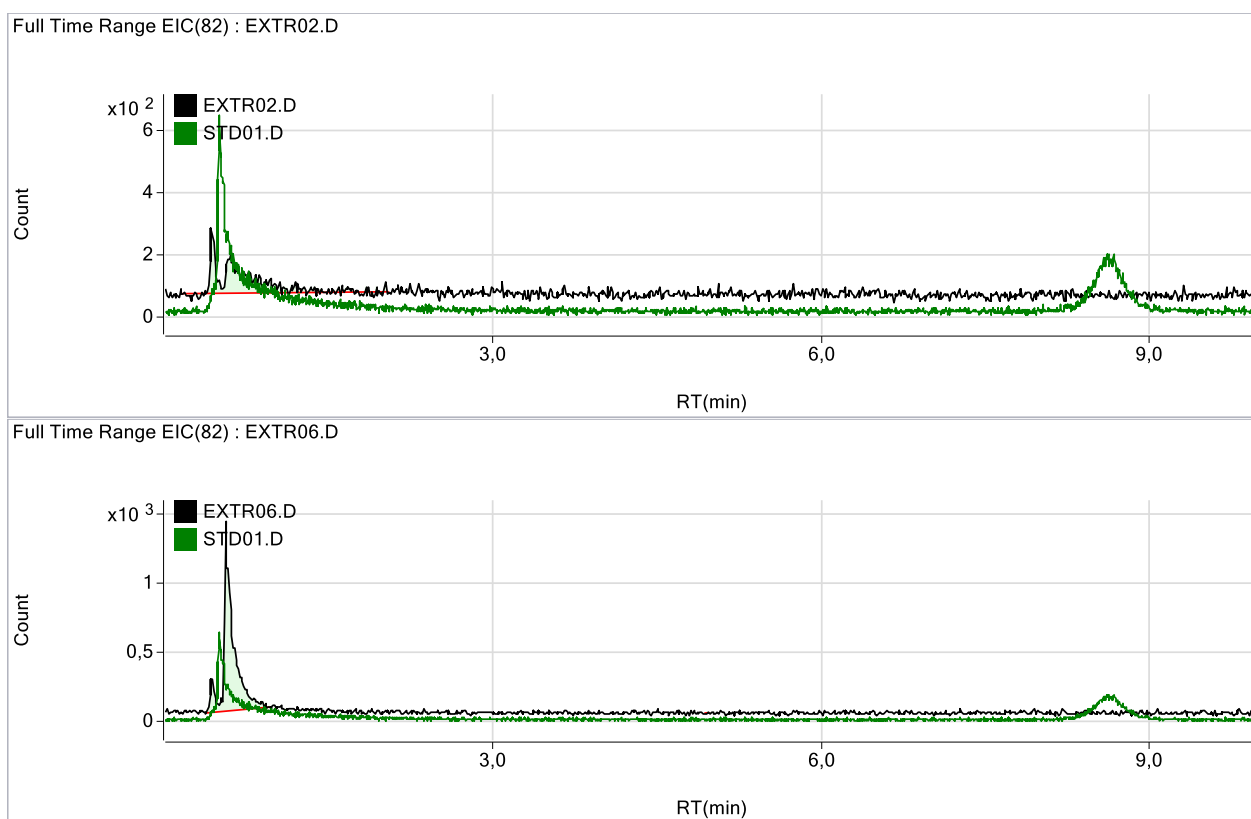


Figure C16: Full time range chromatogram for Selenium Dry MeOH Direct (a) and Dry MeOH with 10% H₂O₂ (b) added.

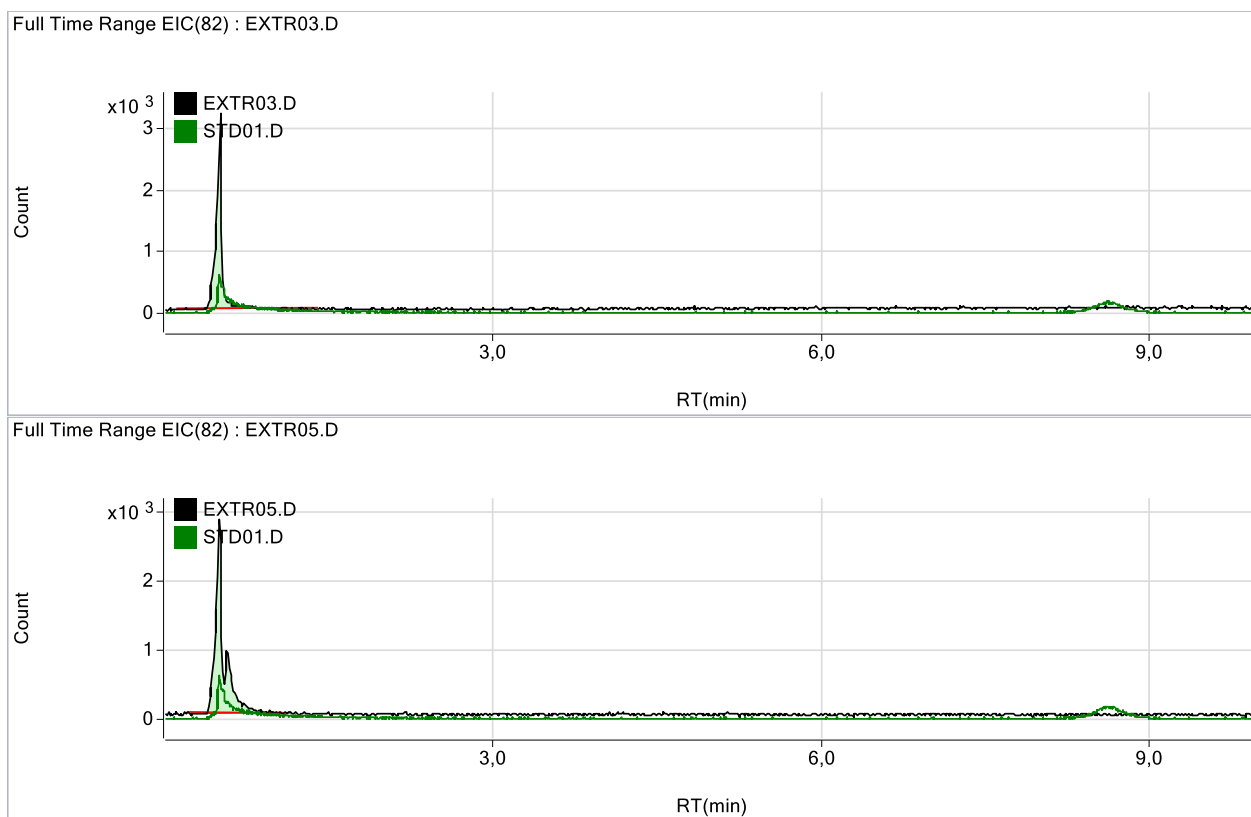


Figure C17: Full time range chromatogram for Selenium Wet H₂O Direct (a) and Wet H₂O with 10% H₂O₂ (b) added.

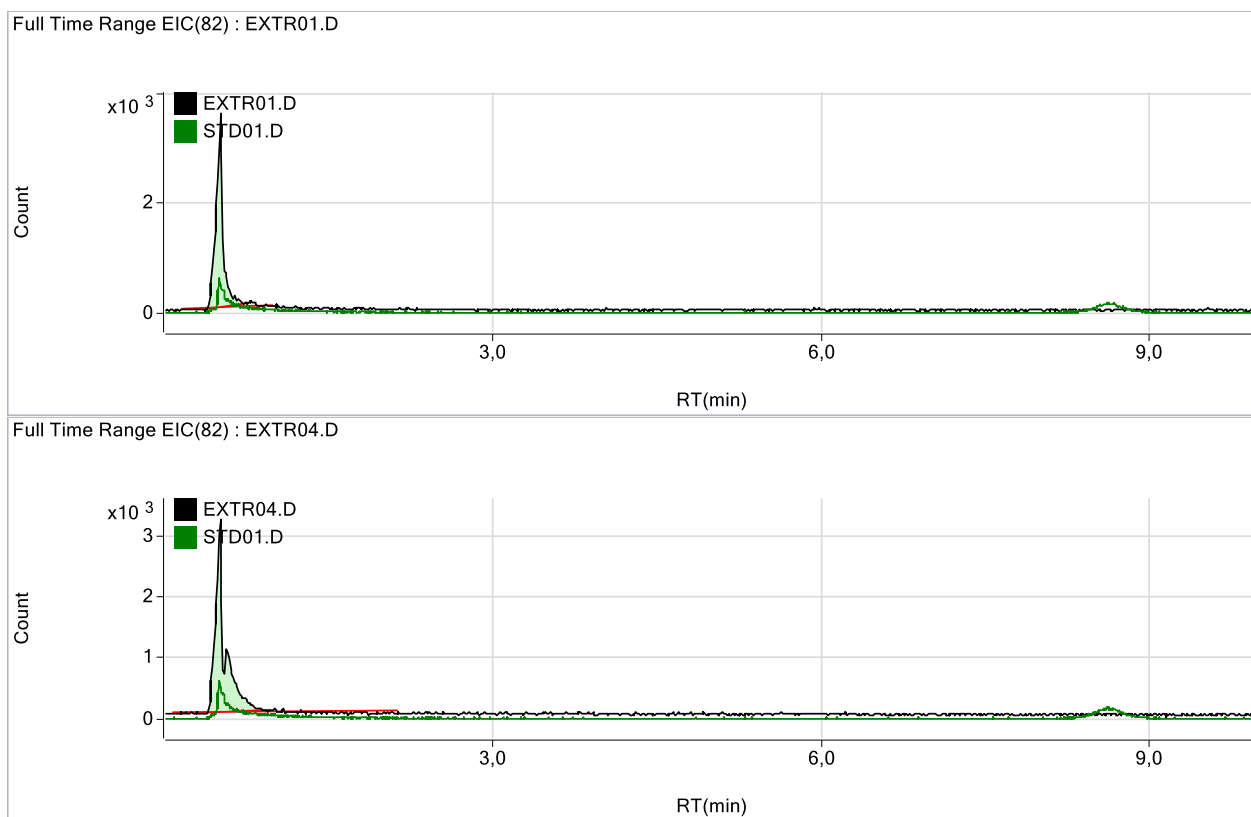


Figure C18: Full Time range chromatogram for Selenium Wet MeOH Direct (a) and Wet MeOH with 10% H2O2 (b) added.

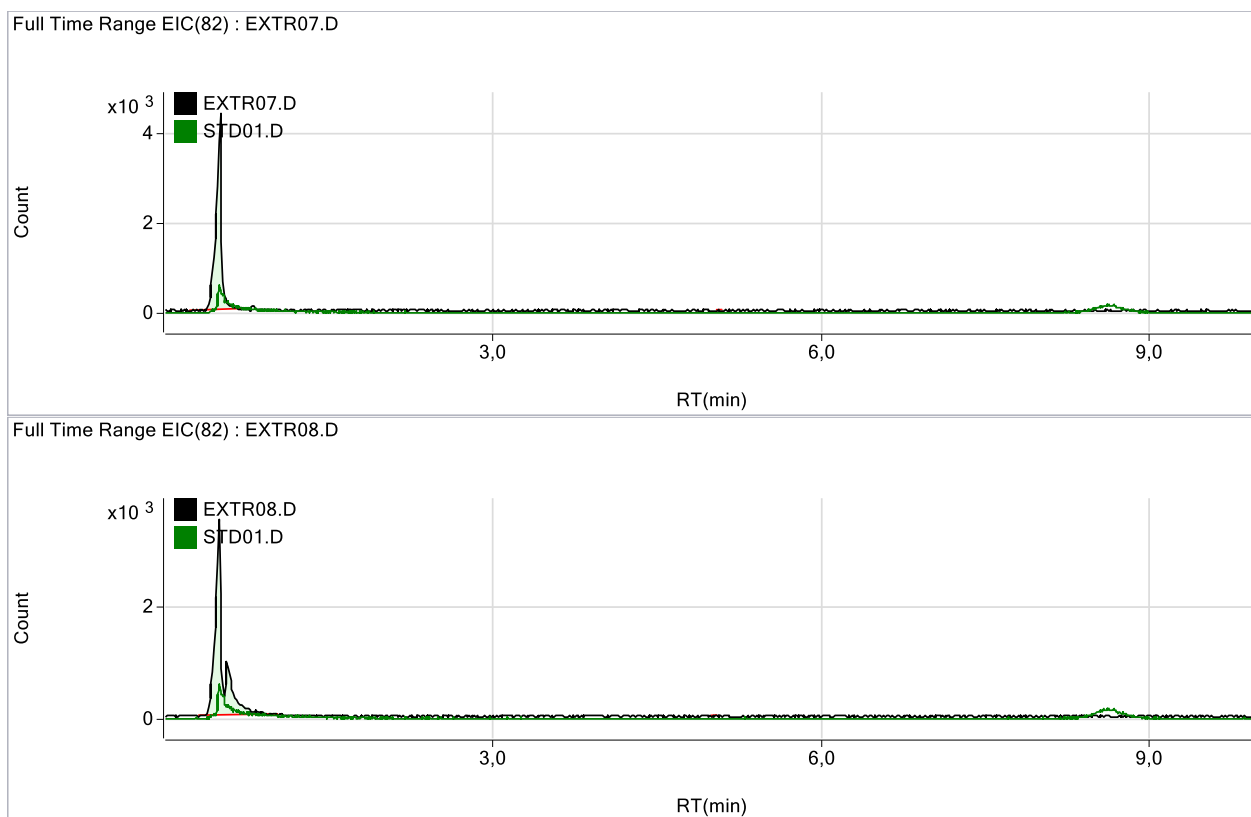


Figure C19: Full time range chromatogram for Selenium Dry MeOH evaporate direct (a) and Dry MeOH evaporate with 10% H₂O₂ (b) added.

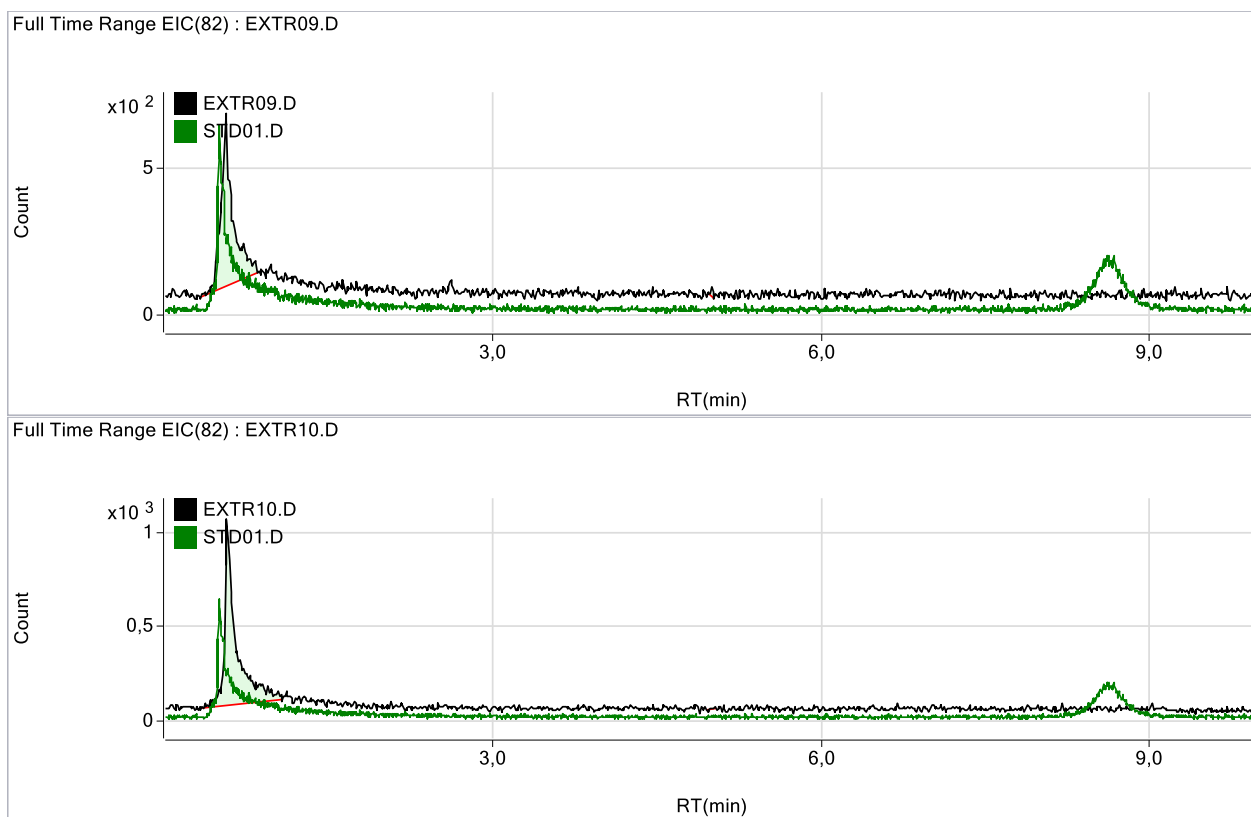


Figure C20: Full time range chromatogram for Selenium Residue 0.1M TFA direct (a) and Residue 0.1M TFA with 10% H₂O₂ (b) added.

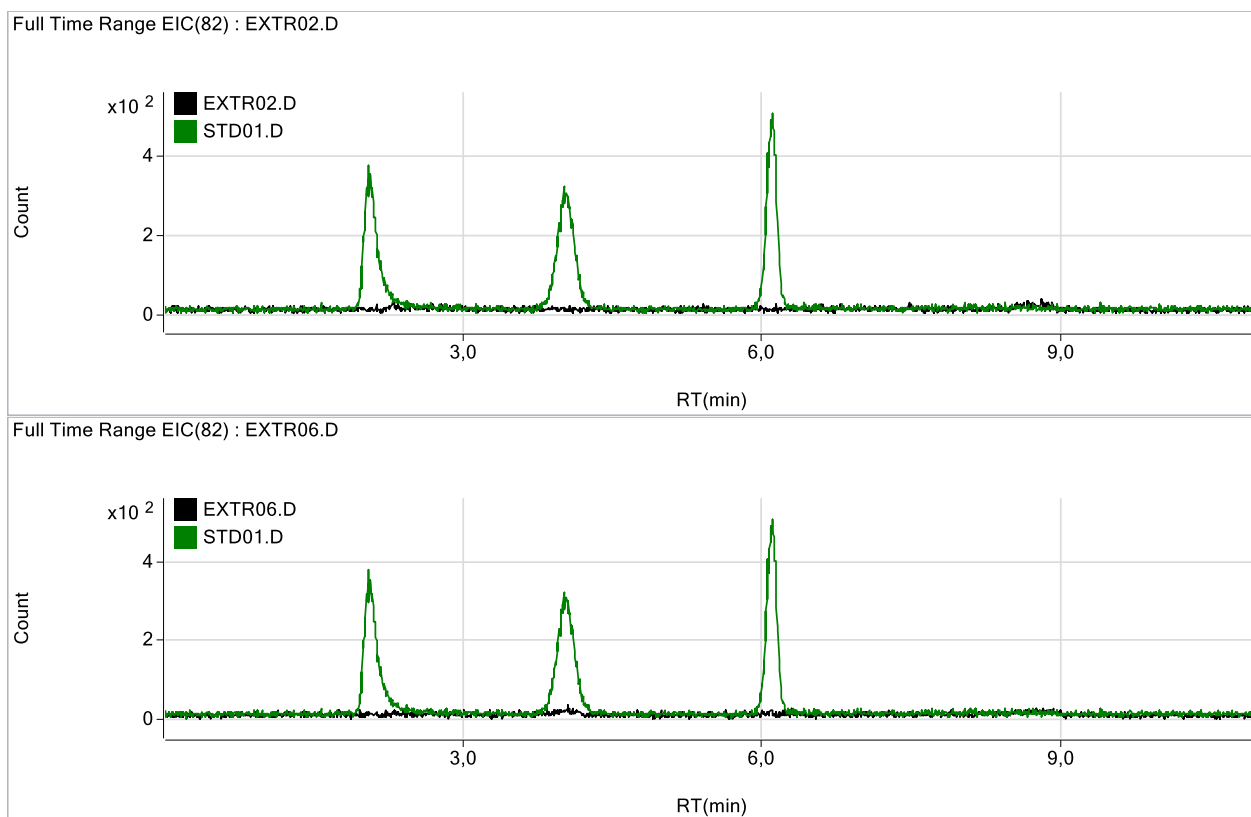


Figure C21: Full time range chromatogram for Selenium Dry MeOH Direct (a) and Dry MeOH with 10% H₂O₂ (b) added.

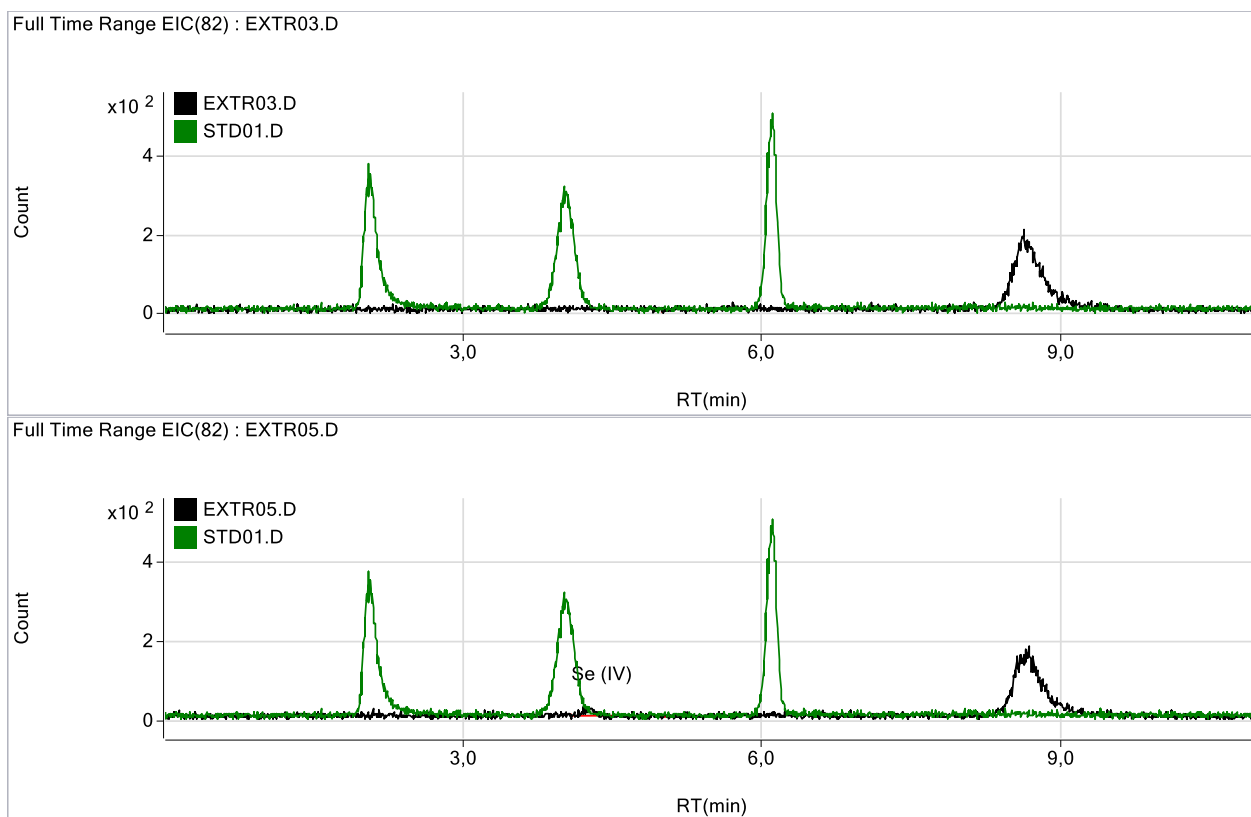


Figure C22: Full time range chromatogram for Selenium Wet H₂O Direct (a) and Wet H₂O with 10% H₂O₂ (b) added.

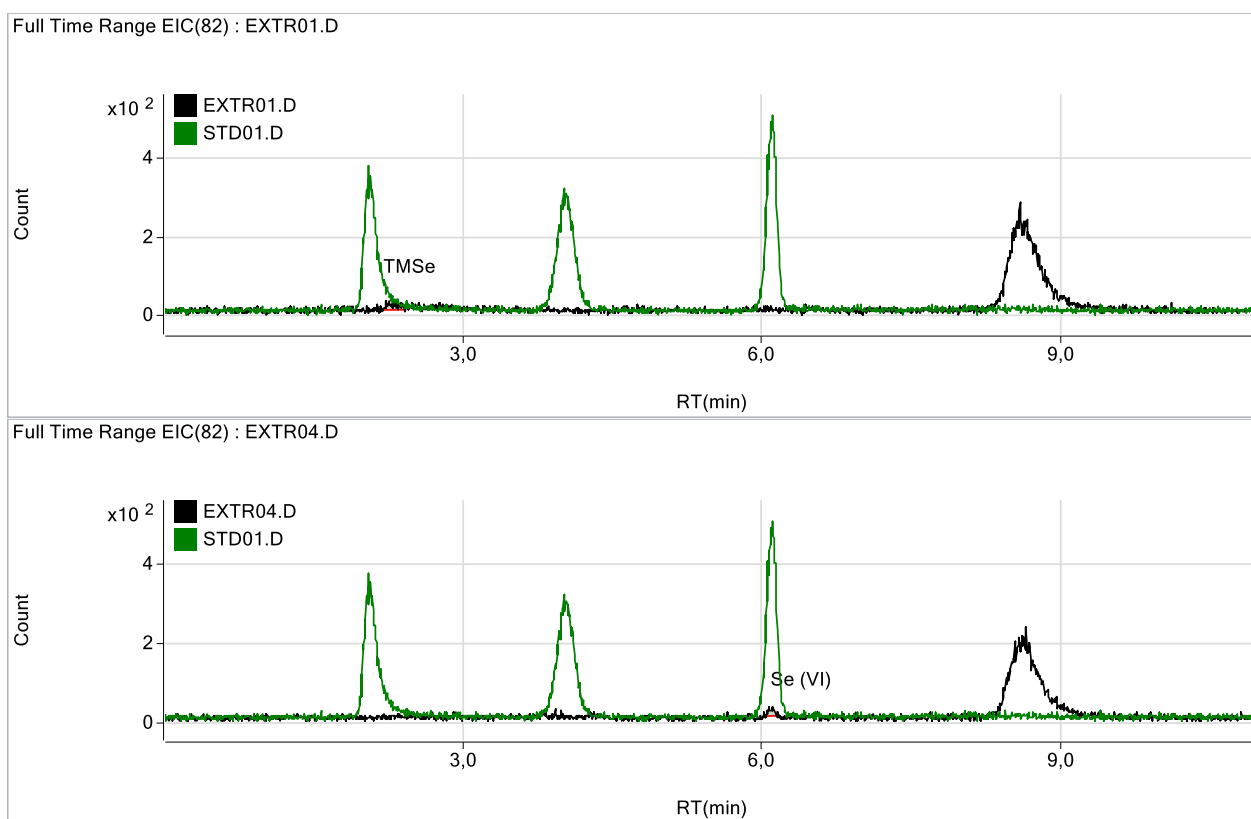


Figure C23: Full Time range chromatogram for Selenium Wet MeOH Direct (a) and Wet MeOH with 10% H₂O₂ (b) added.

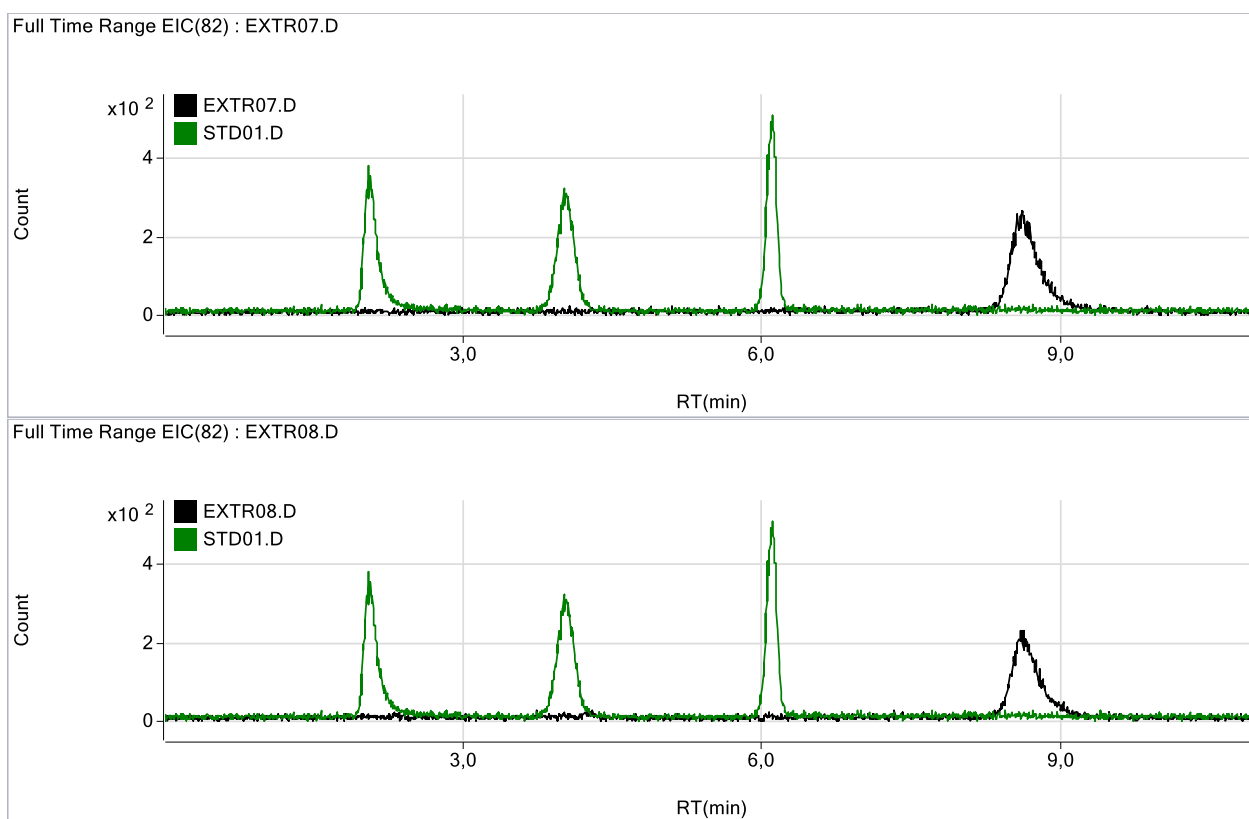


Figure C24: Full time range chromatogram for Selenium Dry MeOH evaporate direct (a) and Dry MeOH evaporate with 10% H₂O₂ (b) added.

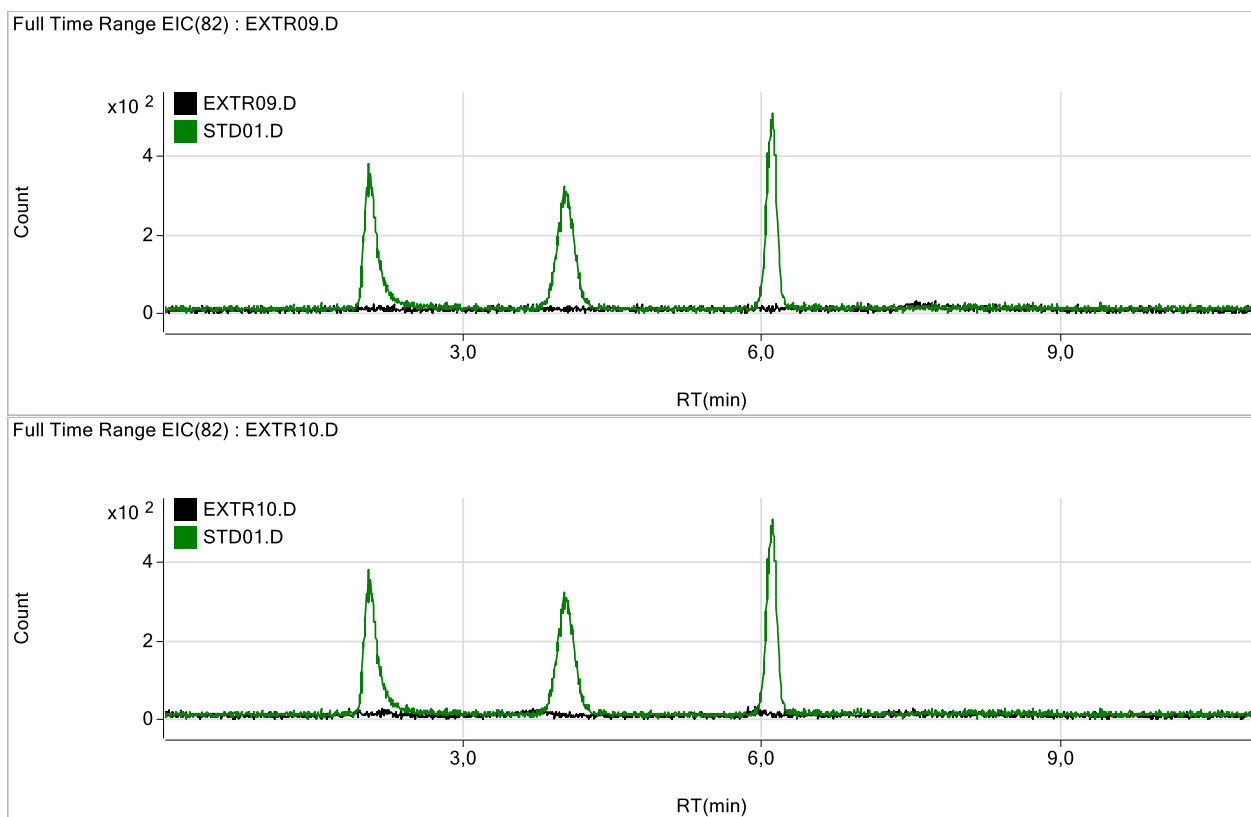


Figure C25: Full time range chromatogram for Selenium Residue 0.1M TFA direct (a) and Residue 0.1M TFA with 10% H₂O₂ (b) added.